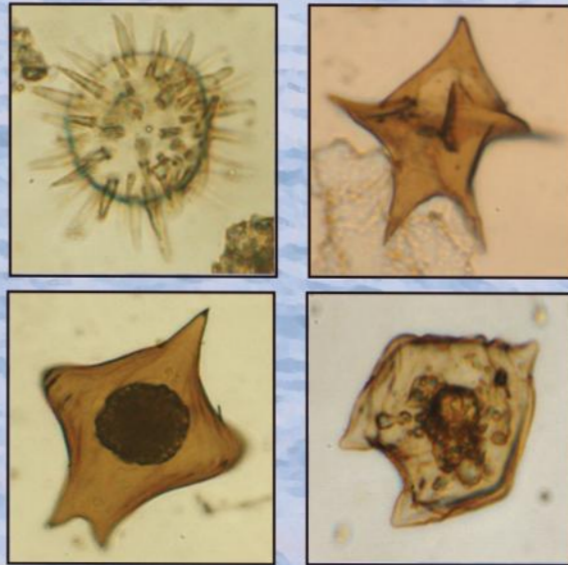


Studies on ecology of cyst forming dinoflagellates from the Northern Indian Ocean



Thesis submitted to the Goa University
for the degree of
Doctor of Philosophy
in
Marine Sciences

Dhiraj Dhondiram Narale

CSIR-National Institute of Oceanography
Dona Paula, Goa - 403 004,
INDIA

2016

**Studies on ecology of cyst forming dinoflagellates from the
Northern Indian Ocean**

A Thesis submitted to
Goa University
for the award of the Degree of
Doctor of Philosophy
in
Marine Sciences

By
Dhiraj Dhondiram Narale
CSIR-National Institute of Oceanography
Dona Paula, Goa – 403004, India

Under the Guidance of
Dr. A. C. Anil
CSIR-National Institute of Oceanography
Dona Paula, Goa – 403004, India

July 2016

“Desire, when it stems from the heart and spirit when it is pure and intense, possesses awesome electromagnetic energy. This energy is released into the ether each night, as the mind falls into the sleep state. Each morning it returns to the conscious state reinforced with the cosmic currents. That which has been imaged will surely and certainly be manifested.....”

-A.P.J. Abdul Kalam (Wings of Fire)

यन्मातापितरौ वृत्तं तनये कुरुतः सदा ।
न सुप्रतिकारं तत्तु मात्रा पित्रा च यत्कृतम् ॥
- रामायण, अयोध्याकाण्ड

*The deeds done by mother and father for their
children constantly..., there is no requital to
these actions performed by the parents.*

-Ramayana, Ayodhya Kand

Dedicated to my parents

Contents	Page
<i>Statement of the Candidate</i>	<i>i</i>
<i>Certificate of the Research Supervisor</i>	<i>ii</i>
<i>Acknowledgements</i>	<i>iii</i>
1. General Introduction	1
1.1. The dinoflagellates	1
1.2. Life cycles stages	2
1.3. Cyst morphology and taxonomy	4
1.4. Cyst function	5
1.4.1 Survival strategy	5
1.4.2 Bloom dynamics	6
1.4.3 Ecological responses	7
1.5 Cyst forming dinoflagellate ecology	7
1.6 Importance of cyst studies in Indian region	8
1.7 Objectives and overviews of thesis	10
2. Inter and intra-annual variation in the cyst forming dinoflagellates in the Bay of Bengal	13
2.1. Introduction	13
2.2. Material and Methods	14
2.2.1 Oceanographic settings of the Bay of Bengal	14
2.2.2 Sampling strategy	17
2.3 Sample collection and processing	18
2.3.1 Water parameters	18
2.3.2 Phytoplankton sample	18
2.3.3 Climatic variables	19
2.3.4 Data analysis	19
2.4 Results	20
2.4.1 Climatic variability	20
2.4.2 Hydrological variability	21
2.4.3 Phytoplankton assemblages	24
2.4.4 Dinoflagellate distribution	26
2.4.5 Effect of climatic variability on cyst forming dinoflagellate	32
2.4.6 Composition of planktonic and cyst assemblages of dinoflagellates	39
2.5 Discussion	39
2.5.1 Dinoflagellate population in the region	
2.5.2 Responses of cyst forming dinoflagellate community to the monsoons	46
2.5.3 Comparison of phytoplankton and cysts assemblage of dinoflagellates	49
2.6 Conclusion	50

3. Distribution of dinoflagellate cyst in recent sediments along the Indian coast	52
3A Dinoflagellate cyst distribution along the south-western Bay of Bengal	52
3A.1 Introduction	52
3A.2 Materials and methods	53
3A.2.1 Description of the study region	53
3A.2.2 Sediment sampling	54
3A.2.3 Sediment preparation, processing and analysis	55
3A.2.4 Data analysis	57
3A.3 Results	57
3A.3.1 Dinoflagellate cyst assemblage	57
3A.3.2 Dinoflagellate cyst distribution	61
3A.3.3 Comparison of dinoflagellate cyst and planktonic dinoflagellates	62
3A.4 Discussion	62
3A.4.1 Comparison of dinoflagellate cyst abundance with different regions	62
3A.4.2 Cyst assemblages along the south-western boundary of the Bay of Bengal	64
3A.4.3 Composition of dinoflagellate cysts and planktonic dinoflagellates	67
3A.5 Conclusion	69
3B Assessing the monsoonal control on dinoflagellate cyst distribution in recent sediments along the north-western Bay of Bengal	70
3B.1 Introduction	70
3B.2 Material and methods	71
3B.2.1 Regional environmental and oceanographic settings	71
3B.2.2 Sediment sampling, processing and analysis	74
3B.2.3 Geochemical analysis	76
3B.2.4 Environmental and hydrographical parameters	76
3B.2.5 Statistical analysis	77
3B.3 Results	78
3B.3.1 Dinoflagellate cyst assemblage	78
3B.3.2 Statistical analysis	79
3B.3.2.1 Spatial distribution of cyst assemblage	79
3B.3.2.2 Species distribution in relation to the monsoonal environmental and oceanographic variability	86
3B.4 Discussion	88
3B.4.1 Transport and preservation	89
3B.4.2 Spatial distribution of dinoflagellate cyst in relation to environmental conditions	90

3B.4.2.1 Coastal assemblage	90
3B.4.2.2 Neritic-oceanic assemblage	92
3B.4.3 Cyst records of potentially harmful species	94
3B.5 Conclusion	95
3C Scenario of dinoflagellate cyst assemblages along the Indian coasts	97
3C.1 Introduction	97
3C.2 Methodology	98
3C.3 Result and discussion	99
4 Dinoflagellate cyst as a proxy of paleo-productivity and climatic variability in the Northern Indian Ocean	104
4A Evolution of productivity and monsoonal dynamics in the eastern Arabian Sea during the past 68 ka	108
4A.1 Introduction	108
4A.2 Climatic and Oceanographic setting	110
4A.3 Material and Methods	112
4A.3.1 Sediment core	112
4A.3.2 Palynological sample preparations and analysis	113
4A.3.3 Statistical analysis	115
4A.4 Results	115
4A.4.1 Dinoflagellate cyst assemblage and abundance	115
4A.4.2 Statistical analysis and dinoflagellate cyst zones	119
4A.5 Discussion	123
4A.5.1 Dinoflagellate cyst preservation and OMZ intensity	123
4A.5.2 Productivity variations in the EAS	126
4A.5.3 Relationship between dinoflagellate cyst assemblage and monsoon variability	128
4A.6 Conclusion	134
4B Late Quaternary productivity and climatic changes in the western Bay of Bengal	136
4B.1 Introduction	136
4B.2 Climatic and Oceanographic setting	136
4B.3 Material and methods	136
4B.3.1 Sediment core	136
4B.3.2 Palynological sample preparations and analysis	136
4B.3.3 Statistical analysis	137
4B.4 Results	137
4B.5 Discussion	141
4B.5.1 Absolute abundance of dinoflagellate cysts	142
4B.5.2 Link between cyst abundance to the climate change	142

4B.5.3 Productivity variability during the Holocene and last glacial period	143
4B.6 Conclusion	145
5 Influence of benthic and pelagic linkages on the distribution of dinoflagellates along the South Andaman region	147
5.1 Introduction	147
5.2 Materials and methods	149
5.2.1 Study area	149
5.2.2 Sampling strategy	150
5.2.3 Water and sediment sample processing	151
5.2.4 Water and sedimentary parameter	151
5.2.5 Environmental data	152
5.2.6 Statistical analysis	152
5.3 Results	153
5.3.1 Climatic variability	153
5.3.2 Hydrological characteristics	154
5.3.3 Planktonic dinoflagellate population	157
5.3.4 Dinoflagellate cyst population	163
5.3.5 Spatio-temporal variation in dinoflagellate population	163
5.3.6 Seasonal cycling and benthic-pelagic linkages	169
5.3.7 Effect of environmental variables on dinoflagellate community structure	172
5.4 Discussion	175
5.4.1 Dinoflagellate community structure	176
5.4.2 Role of monsoonal interventions on dinoflagellate community structure	178
5.4.3 Harmful algal blooms prospective in the South Andaman region	188
5.5 Conclusion	190
6 Summary	192
Bibliography	200
Appendix	235
Publications	

Statement of the Candidate

As required under the University ordinance 0.19.8 (vi), I state that the present thesis entitled "Studies on ecology of cyst forming dinoflagellates from the Northern Indian Ocean" is my original contribution and the same has not been submitted on any previous occasion. To the best of my knowledge, the present study is the first comprehensive work of its kind from the area mentioned.

The literature related to the problem investigated has been cited. Due acknowledgements have been made wherever facilities and suggestions have been availed of.


Dhiraj Dhondiram Narale



सी एस आई आर - राष्ट्रीय समुद्र विज्ञान संस्थान
(वैज्ञानिक एवं औद्योगिक अनुसंधान परिषद)

CSIR - national institute of oceanography
(Council of Scientific & Industrial Research)



Certificate

This is to certify that the thesis entitled "Studies on ecology of cyst forming dinoflagellates from the Northern Indian Ocean", submitted by Mr. Dhiraj Dhondiram Narale for the award of the degree of Doctor of Philosophy in Marine Science is based on his original studies carried out by him under my supervision. The thesis or any part thereof has not been previously submitted for any other degree or diploma in any Universities or Institutions.

*Dr. A. C. Anil
Research Guide
Chief Scientist
Biofouling and Bioinvasion Division
National Institute of Oceanography
Dona Paula-403 004, Goa*

दोना पावला, गोवा 403 004 भारत
DONA PAULA, GOA - 403 004, India

: 91-(0)832-2450 450
fax : 91-(0)832-2450 602/03

e-mail : ocean@nio.org
URL : <http://www.nio.org>

Regional Centres
Mumbai, Kochi, Visakhapatnam

Acknowledgements

Many people have contributed to the existence of this thesis. I wish to express my heartfelt thanks to all those who helped me, during this course of work.

First of all, I would like to thank my supervisor and guru, Dr. A. C. Anil, for many reasons. Thanks for introducing me to the field of “dinoflagellate ecology”, having patience with me and giving motivation for continued efforts.

I would like to express my gratitude towards Dr. V. V. Gopalakrishna for helping and encouraging me throughout my study period in numerous ways.

I express my sincere gratitude to Dr. P. Divakar Naidu for providing the core AAS 1/21 and SK 218/9 samples and guiding me during the paleoecology studies.

I am immensely thankful to Dr. S.S. Sawant, Prof. Dr. Janarthanam, FRC Members, for duly assessing research progress and valuable suggestions during thesis work. I thank Prof. Dr. C. U. Rivonkar, Prof. Dr. G. N. Nayak and Prof. Dr. H. B. Menon, Department of Marine Sciences, Goa University for helping me through various administrative processes.

I sincerely thank Dr. Jagadish Patil for structuring the thesis and encouraging me whenever I feel low. I also thank Dr. Dattesh Desai, for continued support and constructive suggestions during scientific as well as personal difficulties, Dr. Lidita Khandeparker and Dr. Smita Mitbavkar for helping hand at every stage of my work.

Mr. K. Venket has made available his support in a number of ways as and when it was required and for that, I am very thankful to him.

I thank the Director-National Institute of Oceanography (NIO) for giving me an opportunity to carry out this research. I acknowledge Council of Scientific and Industrial Research (CSIR) for providing Senior Research fellowships. A part of this work was supported by the Indian-XBT programme (INCOIS, Ministry of Earth Science) and Global Ballast Water Management Programme (Ministry of Shipping and DG Shipping, India). I thank Department of Science and Technology, New Delhi for providing financial support to attend the training course on identification of Dinophyceae and its cyst, conducted by AWI, Germany. I also acknowledge help provided by Dr. Grenson George, Scientist, CARI, Port Blair for making initial arrangements during field sampling and providing lab facility

I convey my gratitude to Dr. Malte Elbrachter, AWI and Dr. Kenneth Mertens, Ghent University for providing training on the taxonomy of Dinophyceae and their cysts.

I thank in particular to my labmates, Dr. Ravidas Naik, Dr. Priya D'Coasta, Dr. Sahana Hegde, Dr. Shamina D'Silva, for phytoplankton identification work and Dr. Chetan A. Gaonkar, Dr. Sumit Mandal, Dr. Temjensangba Imchen who provided a friendly ear and help at various occasions. I am grateful to my friends, Rajath Chitari and Vinayak Kulkarni for their enormous help and making this journey memorable. I would like to thank my other group members Kirti, Kaushal, Rajaneesh, Lalita, Suchandan, Ranjith, Dayakaran, Apoorva, Majitha, Laxman, Sumit, Noyal, Aseem, Roy, Sathish K., Achutan, Gobardhan, Devdatta and Sangita for their help and support. My special thanks to XBT members for their support.

Thanks and appreciation also go to NIO family members, Shahin, Prachi, Ravi, Sushant, Hrishi, Navnath, Rashmi, Vasuki and my friends Yogesh, Gajanan, Birudev, Guruprasad, Sandip, Shramik, Arvind, Shivraj, Sanjeev for their continuous support and encouragement. My special thanks to Nilofar for her great support and friendship during this tough time.

I have no words to thank my biggest support and source of energy, my family. All this is possible only due to their unconditional love and support. Thank you for continuing to believe in me.

Dhiraj Dhondiram Narale

Chapter 1
General Introduction

Chapter 1 General Introduction

1.1 The dinoflagellates

Dinoflagellates (Dinophyceae) are among the dominant microphytoplankton groups, contributing substantially to eukaryotic production in the marine environment. These diverse flagellated phytoplanktons are having ~2500 extant species from about 300 genera and, at least, the same number of extinct taxa (Hoppenrath et al., 2009). The earliest fossil taxa of dinoflagellate were dated back to about 240 million-year-old Middle Triassic period of the Mesozoic era (Fensome et al., 1993). Indeed throughout the evolution process, they have evolved a tremendous diversity of life forms and biological mechanisms as a resultant of adaptability to a varied environmental niche (Hackett et al. 2004). Dinoflagellates also have developed unique and different feeding strategies. More than half of the dinoflagellate species are autotrophic, have chloroplast. Heterotrophs obtain food by using various mechanisms like ingestion of particulate food (phagotrophy), direct sucking of prey (myzocytosis) (Schnepf and Deichgraber, 1984). Species like *Protoperidinium*, have specialized feeding modes like pallium, peduncle feeding or feeding through complex organelles like nematocyst, ocelloid, and piston (Gaines and Elbrachter, 1987; Schnepf and Elbrachter, 1992). Some autotrophic species use an alternative mechanism like osmotrophy and phagotrophy to meet their nutritional need, called mixotrophs. The mode of nutrition decides the survival strategies of dinoflagellates and their response to surrounding environmental conditions (Taylor and Pollinger, 1987; Smayda and Reynolds, 2003). Similarly, productive and predictive trophic modes enable them as an important component of the food web and nutrient cycle in the marine ecosystem (Jeong et al., 2010). Dinoflagellates are the major contributors

(~75%) in red tides and Harmful Algal Blooms (HABs) producing phytoplankton (Smayda, 1997). Among the modern dinoflagellates, ~84 species are known to be responsible for HABs, causing water discoloration and producing a variety of toxins (IOC-UNESCO Taxonomic Reference List of Harmful Microalgae; Moestrup et al., 2009). Some species have also evolved different life cycle strategies (cyst-formation) to cope with varying environmental conditions (Bravo and Figueroa, 2014), which remain dormant in sediments for a variable time period ranging from a few hours (Garces et al., 2002) and even up to a century (Ribeiro et al., 2011).

1.2 Life cycle stages

Generally, cyst formation in dinoflagellates occurs as the fate of sexuality (Von Stosch, 1973; Steidinger, 1975; Anderson and Wall, 1978) and can be regulated by unfavorable and stressed environmental conditions. Most of the cyst forming species supposed to have similar life history stages (Pfiester and Anderson, 1987), involving the fusion of haploid (n) gametes from parental vegetative cells (Fig. 1.1). This mating further produces diploid ($2n$) planozygotes that ultimately form resting cysts (hypnozygotes). This process of cyst formation also known as 'encystment.' Further, the germination (excystment) and proliferation fate of cyst is controlled by endogenous as well as exogenous factors (cues). Endogenous factors mainly involve cell biological clock, which controls species-specific mandatory dormancy period (Kremp, 2013). This 'dormancy factor' mainly facilitate durable viability of cysts in the sediment. Excystment can be achieved within 'a small window' of exogenously 'favorable factors' like optimum temperature, salinity, oxygen supply, photoperiods, and nutrients (Anderson et al., 1987; Anderson and Taylor, 1987; Bravo and Anderson, 1994; Kremp and Anderson, 2000).

Various cytoplasmic transformation processes like, shrinking of cytoplasmic content, accumulation of lipids and polyhedral bodies (Xiaoping et al., 1989; Binder and Anderson, 1990), accumulation of pigmented bodies (especially in *Alexandrium* species) accompany the encystment process (Bolch et al., 1991; Bravo et al., 2006). Similarly, excystment also involves species-specific physiological responses, among them cell wall enlargement can be observed in many dinoflagellate species e.g. *Lingulodinium polyedrum* (Kokinos and Anderson, 1995).

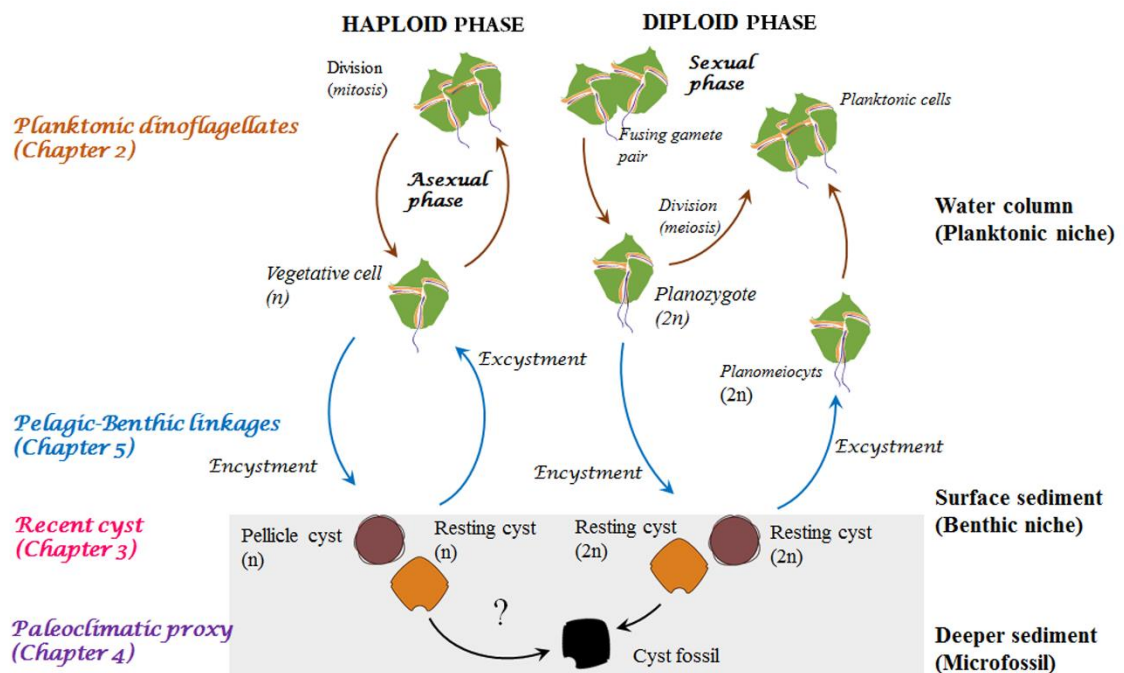


Fig. 1.1 The life cycle of dinoflagellate (as inferred from Bravo and Figueroa, 2014), also representing the objectives and structure of the present research work.

However, in some studies, thin walled cyst (pellicle cyst) formation observed in few dinoflagellate species (Fig. 1.1). These stages are temporary, of short duration and can be a part of asexual e.g. *Scrippsiella hangoei* (Kremp and Parrow, 2006) or sexual e.g. *Alexandrium* species (Bravo et al., 2006; Bravo and Figueroa, 2014) life cycle. Thus, life cycle strategies in dinoflagellate often seem to be ‘plastic’, with the engagement of

different mechanisms and pathways (Fig. 1.1) may be complementary in one and the same species (Kremp, 2013).

1.3 Cyst morphology and taxonomy

Since cyst-forming dinoflagellate species have both, the planktonic and cyst stages, there are two different taxonomic systems in practice for cyst identification and nomenclature (Head, 1996; Matsuoka and Fukuyo, 2000). Biologists follow the planktonic stages based nomenclature system, in which cyst named by their planktonic affinity (e.g., Nehring, 1997; Sonneman and Hill, 1997). In paleontology nomenclature system (fossil) cysts have been classified on the basis of their well-defined morphological characteristics (Lentin and Williams, 1975; Lentin and Williams, 1993; Fensome et al., 1993; Zonneveld and Pospelova, 2015). During the 1960s, paleontologists observed some extant dinoflagellate cysts with same morphology as fossils in planktonic as well as surface sediment samples. These cyst morphotypes further have been classified and described under the paleontological system (e.g. Wall and Dale 1968). Thus, few cyst morphotypes have been classified by two different nomenclature systems and have different scientific names. The present thesis comprises study on ecological aspects of planktonic dinoflagellate (Chapter 2 and 5) and their counterparts from recent (Chapter 3) and Late Quaternary (Chapter 4) sediments. In Chapter 2 and 5 planktonic nomenclatures are used, whereas in Chapter 3 and 4 paleontological names are given to cyst forms. Furthermore to tackle the heterogeneity in nomenclature systems, lists of both paleontological and planktonic names are provided in each chapter.

Dinoflagellates produce species-specific cyst types with different morphological features (Fensome et al., 1993; Matsuoka and Fukuyo, 2000; Zonneveld and Pospelova,

2015). The important cyst morphotypes identification features comprises the shape, colour of cyst, wall structure, paratabulations, ornamentation, and the archeopyle (aperture) structure (Fig. 1.2) through which germlings (germinated cells) protrude out. Further, this morphological characteristic diversity is more in organic-walled cyst morphotypes (*Gymnodinium*, *Gonyaulax*, *Protoperidinium*, *Lingulodinium*) than the calcareous ones (*Ensiculifera*, *Scrippsiella*, *Thoracosphaera*; *Calciodinella*). A general schematic of cyst identification is provided in Fig. 1.3.

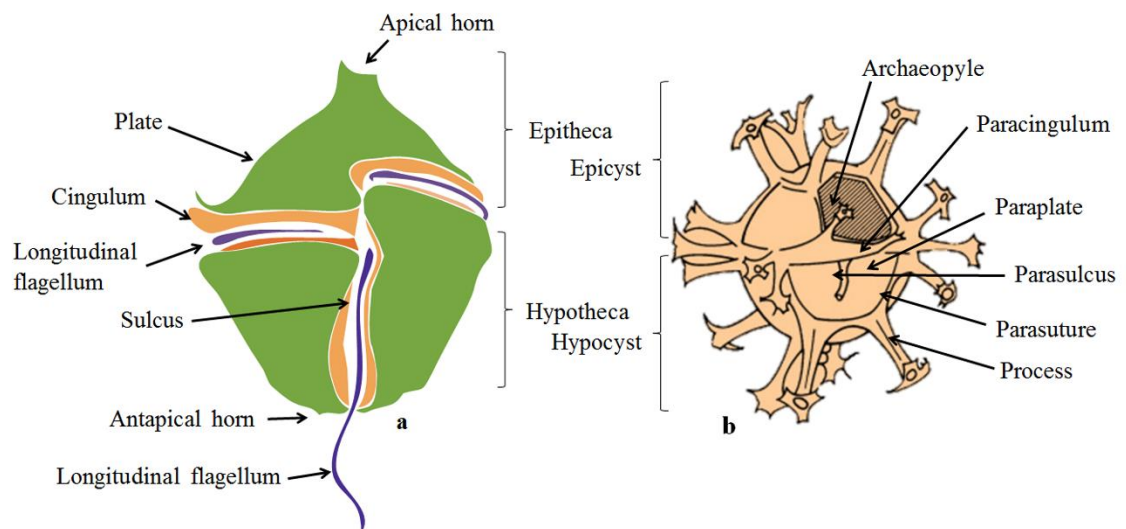


Fig. 1.2 Morphological comparison between a) planktonic dinoflagellate, b) cyst and terminology used in their description.

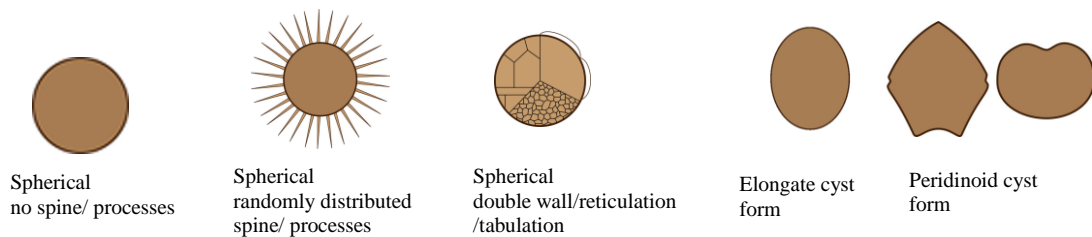
1.4 Cyst functions (Importance of cyst strategies in dinoflagellates)

1.4.1 Survival strategy

Complex cell wall structure of dinoflagellate resting cyst composed of a biomacromolecule, dinosporin, which enables them to resist physical, chemical, biological destruction, and degradation (Fensome et al., 1993; Bogus et al., 2014). This protective adaptation attributes to longer survival, proliferation and dispersion of cyst

population (Dale, 1983; Anderson et al., 1985; Bravo and Figueroa, 2014). Cyst formation can be triggered by stressful environmental conditions (Pfiester and Anderson, 1987). Generally cyst formation can be observed as response to growth limitation factors like phosphate or nitrate limitation (Anderson et al., 1985; Figueroa et al., 2006; Wang et al. 2007), anoxic conditions and/or light limitations (Sgrosso et al., 2001; Figueroa et al., 2006; Rintala et al., 2007; Lundgren and Graneli, 2011). In the case of *Scrippsiella trochoidea* cyst formation can be observed as a survival strategy to reduce grazing or parasitic pressure under laboratory conditions (Chambouvet et al., 2011; Lundgren and Graneli, 2011).

a) Brown coloured cyst



b) Transparent cyst

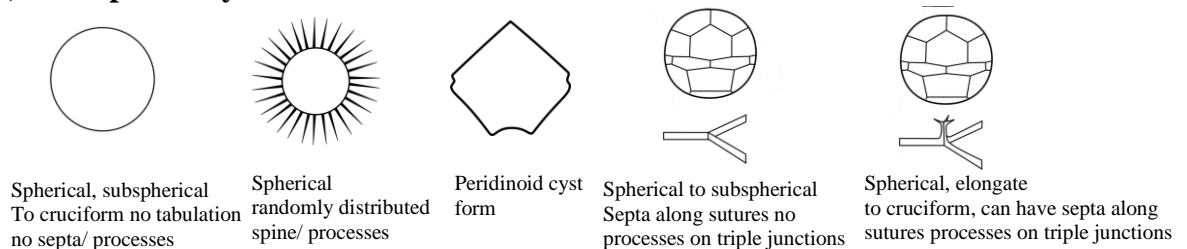


Fig. 1.3 General classification and identification characteristics of dinoflagellate cyst morphotypes (from Zonneveld and Pospelova, 2015)

1.4.2 Bloom dynamics

Cyst functions determine the dinoflagellate species survival and success in the marine environment (Anderson, 1998; Azanza and Taylor, 2001; Dale, 2001a; Anderson

et al., 2012; Bravo and Figueroa, 2014). In the case of toxic species like *Alexandrium*, *Scrippsiella* resting stages control their bloom dynamics in the coastal regions. Newly formed cyst gets deposited in the benthic seed banks. In a turn of favorable conditions, they substantially contribute to the pelagic bloom population. Similarly, higher toxin content in cyst than planktonic forms could also be a potential source of shellfish intoxication (Oshima et al., 1992) in the coastal regions.

1.4.3 Ecological responses

Dinoflagellates have different species-specific environmental requirements for proliferation, hence their cyst distribution in sediments can be well correlated with the environmental, physical and biogeochemical variables in the water column (de Vernal et al., 2001; Marret and Zonneveld, 2003; Pospelova et al., 2008; Zonneveld et al., 2013). Due to this, microfossil records of cyst assemblage present in sediment are an important tool for biostratigraphy and paleoenvironmental reconstruction studies (de Vernal and Pedersen, 1997; Reichart and Brinkhuis, 2003; Pospelova et al., 2006; Radi and de Vernal, 2008; Naidu et al., 2012; Price et al., 2013) as well as for tracing the harmful bloom incidences in the region (Anderson, 1998; Dale, 2001a).

1.5 Cyst-forming dinoflagellate ecology

To understand dinoflagellate life cycle functions, ecological understanding of planktonic and resting stages, factors influencing their geographic distribution and planktonic-benthic transitions is essential (Godhe et al., 2001, Morquecho et al., 2004). However, most of the dinoflagellate distribution studies frequently relate species composition to physicochemical environmental variables in the water column. Similarly,

the majority of cyst distribution studies are focused on the reconstruction of environmental and oceanographic variability. However, the role of different life strategies (resting and planktonic stages), which are important in regulating the species' seasonal dynamics, succession, and dominance are often ignored, in both the cases.

1.6 Importance of cyst studies in the Indian region

The Northern Indian Ocean has two different water masses. A low saline water mass is formed in the Bay of Bengal due to the large freshwater influx, whereas a high saline water mass exists in the Arabian Sea. Although seasonal reversal in the Asian monsoons influences both, the Arabian Sea and the Bay of Bengal, the oceanography and biology differ considerably. In the Arabian Sea variations in temperature is large compared to salinity, but in the Bay of Bengal, a temperature gradient is less throughout the year as compared to salinity (Wyrcki, 1973). Conventionally, the Bay of Bengal is supposed to be a less productive region than its counterpart i.e. the Arabian Sea (Qasim, 1977; Radhakrishna et al., 1978; Prasanna Kumar et al., 2002). Although it receives enormous riverine nutrient influx, nutrient scavenging to deeper sediment (Qasim, 1977), strong stratification (Wyrcki, 1973), high suspended load (Gomes et al., 2000; Prasanna Kumar et al., 2010), absence of strong upwelling and winter convection are some of the reasons for the low primary productivity in the Bay of Bengal. In contrast, strong summer upwelling and winter convection place the Arabian Sea among the most productive regions in the world. In the region, dinoflagellate ecology studies are mainly carried out as part of local as well as regional phytoplankton surveys. Exclusive studies on dinoflagellate ecology including planktonic (Naik et al., 2011; Sahu et al., 2013) and resting cysts are meager (Godhe et al., 2000; Patil, 2003, D'Costa et al., 2008; D'Silva et

al., 2011; D'Silva et al., 2012a; D'Silva et al., 2013). The ecological response of major dinoflagellate groups in the tropical region remains unexplored.

In the Indian region, dinoflagellate cyst studies were initiated during the 1960s (Kumar, 1980). The first catalogue of fossil dinoflagellate cyst in India was published by Anand Kumar (Kumar, 1980). The other pioneer studies in the region include Varma and Dangwal, 1964; Jain and Lantz, 1973; Jain, 1978. Further, Dr. Naresh Mehrotra has a remarkable contribution to fossil dinoflagellate cyst taxonomy and biostratigraphy studies along the Indian region. His publication includes 'Atlas of dinoflagellate cyst from Mesozoic-Tertiary Sediments of Krishna-Godavari Basin' (Mehrotra, 2003) and other research articles (Mehrotra, 1981; Mehrotra et al., 1996; Mehrotra and Sarjeant, 1984a,b, 1986, 1987, 1990, 1998; Mehrotra and Singh, 2003; Mehrotra et al., 2005; Mehrotra et al., 2012), mainly illustrating fossil dinoflagellate taxonomy from Late Jurassic-Cretaceous sediments. In 2006, Birbal Sahni Institute of Palaeobotany, Lucknow has published 'A Catalogue of Dinoflagellate Cysts from India' (Khowaja-Ateequzaman, 2006), which includes taxonomic descriptions fossil dinoflagellates. In regional context, other fossil dinoflagellates studied has been carried out commonly as part of cyst taxonomy (Garg and Jain., 1993; Garg et al., 2011) or part of palynomorphs assemblage (Limaye et al., 2007; Srivastava et al., 2013; Srivastava and Farooqi, 2013) and rarely as part of distribution (Ram et al., 1996). However, the studies illustrating the ecological aspects of cyst-forming species in relation to planktonic and resting stages are meager.

In this thesis, the information on the ecology of cyst-forming dinoflagellate from the Northern Indian Ocean corroborated through extensive, rigorous sampling and

analysis of planktonic as well as sediment samples is provided. The thesis is structured in accordance with the following research objectives.

1.7 Objectives and overview of thesis

1.7.1 Inter and intra-annual variation in the cyst-forming dinoflagellates

Conventionally, the Bay of Bengal is considered as a less productive region than the Arabian Sea (reasons are discussed in Section 1.6). The biological responses to the seasonally varying environmental conditions are still understudied in the Bay of Bengal. Previous phytoplankton and dinoflagellate studies showed that dinoflagellate population is diverse in the region (Madhav and Kondalarao, 2004; Madhu et al., 2006; Naik et al., 2011). However, studies relating to their interaction with the environmental variability in the region is rather limited. In this study, efforts were made to understand the distribution of cyst-forming dinoflagellates in relation with regionally and seasonally changing environmental conditions in the Bay of Bengal (**Chapter 2**).

1.7.2 Dinoflagellate cyst distribution in the sediments

Modern dinoflagellate studies in the region are comparatively new, initiated in the 1990s. The first research article on dinoflagellate cyst distribution was published from the central west coast of India (Mangalore region) by Godhe et al. (2000). In the subsequent years, cyst distribution in surface sediments in the region was documented from the Zuari estuary, Goa (Patil, 2003), Mumbai Port (D'Costa et al., 2008) and west coast of India (D'Silva et al., 2011). History of dinoflagellate cyst assemblage for a couple of centuries along the west coast of India was illustrated by D'Silva et al. (2012). In the Bay of Bengal, information on modern dinoflagellate distribution is only restricted to the

Visakhapatnam harbour (D'Silva et al., 2013). Most of the previous studies in the region were based on the fossil records of the dinoflagellates (Kumar, 1980; Mehrotra et al., 1987). In this study efforts were made to evaluate the modern dinoflagellate cyst assemblage along the south-western and north-western Bay of Bengal (**Chapter 3A and 3B**). Additionally, these results are compared with the earlier published cyst records from the eastern Arabian Sea (Godhe et al., 2000; D'Costa et al., 2008; D'Silva et al., 2011; D'Silva et al., 2012a) to present a scenario of dinoflagellate cyst abundance and assemblage distribution in the seas around India (**Chapter 3C**). Furthermore, to evaluate the cyst abundance and assemblage variability in the Indian region over the Late Quaternary period, two sediment cores from the eastern Arabian Sea (**Chapter 4A**) and the western Bay of Bengal (**Chapter 4B**) were also analyzed.

1.7.3 Influence of benthic and pelagic linkages on distribution of dinoflagellates along the Andaman coast

To understand dinoflagellate life cycle functions, knowledge of planktonic, resting stages, and factors influencing their ecology, geographic distribution, planktonic-benthic transitions is essential (discussed in the introduction). Monsoon seasonality and associated environmental variability influence dinoflagellate population dynamics along both the (west and east) coasts of India (D'Costa et al., 2008; D'Silva et al., 2013).

The Andaman Islands though a part of Indian Territory, experiences different environmental conditions. In the recent years, increased anthropogenic activity has altered the water characteristics of this eco-sensitive region (Jayaraju et al., 2011; Sahu et al., 2013). As a consequence, algal bloom incidences have increased in the Andaman region (Eashwar et al., 2001; Dharani et al., 2004; Sachithanandam et al., 2013; Sahu et

al., 2014, Begum et al., 2015). Recent phytoplankton studies revealed the presence of a diverse population of harmful dinoflagellates in the coastal region (Sahu et al., 2014, Begum et al., 2015). However, the effect of different environmental characteristics on their population dynamics is not known. In this thesis, results of the study elucidating the possible pelagic-benthic coupling on cyst forming dinoflagellate population from the South Andaman region is presented (**Chapter 5**).

Chapter 2
Inter and intra-annual variation in the cyst forming dinoflagellates in the Bay of Bengal

Chapter 2 Inter and intra-annual variation in the cyst forming dinoflagellates in the Bay of Bengal.

2.1 Introduction

The success of phytoplankton population in the marine environment is mainly dependent on their ecological responses and growth characteristics. Among them dinoflagellates have a less nutrient requirement (low K_s value) and possess diverse survival strategies such as mixotrophy, heterotrophy, endosymbiotic association etc., allowing them to inhabit oligotrophic to eutrophic environments. Cyst/resting stage formation also plays a significant role in dinoflagellate existence and proliferation. About 10% out of the ~2500 extant species of living marine dinoflagellates form cysts (Head, 1996), a very small but important proportion of the total (discussed in Chapter 1). Resistant benthic cyst stage in their life cycle is of considerable importance in stratigraphy and HAB studies since they can be preserved in resting as well as fossil forms. Hence to aid in the interpretation of the biostratigraphy, paleoclimatic and HAB development studies in marine environment, understanding the ecology of the planktonic, thecate stages and the conditions under which they survive, proliferate and encysts could be of great value.

In the Bay of Bengal, the planktonic and cyst dinoflagellate assemblage is diverse in both coastal (mesotrophic) and oceanic (oligotrophic) environments (Taylor, 1976; Naik et al., 2011; D'Silva et al., 2013). Changes in the environmental conditions driven by riverine discharges and monsoonal variabilities make the Bay of Bengal a unique ecosystem in the Northern Indian Ocean. However, the information on the influence of the biological (prey availability and competitive stress) and environmental

variables on the abundance and diversity of cyst-forming dinoflagellate groups is lacking.

To understand the effect of monsoonal interventions on phytoplankton community in the Bay of Bengal surface water sampling was carried out at regular intervals for five years. This work is an extension of the Indian Expendable Bathy Thermograph (Indian XBT) programme in which samples were collected by a Ship of Opportunity network along Chennai-Port Blair (CP) and Port Blair-Kolkata (PK) sectors. This sampling approach was found suitable as it offered a spatial and fine temporal scale resolution of the phytoplankton community (Hegde, 2010; Naik, 2010).

In this chapter, data of cyst-forming dinoflagellate population is used to elucidate their community structure variability on inter and intra-annual basis in relation to monsoonal interventions. Furthermore, this data set is compared with the available information on dinoflagellate cyst community to give a glimpse of their diversity in the region.

2.2 Materials and Methods

2.2.1 Oceanographic settings of the Bay of Bengal

The Bay of Bengal experiences a semi-annual reversal of monsoonal winds divides the year into the South West (SW or summer) and North East (NE or winter) monsoons, separated by inter-monsoonal periods (spring and fall inter-monsoon). Strong south-westerly wind blow during the SW monsoon (June-September), which changes the surface East Indian Coastal Current (EICC) flow in a clockwise direction (Shankar et al., 2002; Fig. 2.1). South-westerly wind favors offshore wind-driven Ekman transport, results into weak upwelling along the southeast coast (De Sousa et al.,

1981; Shetye et al., 1991). In the northern region, enormous fresh water supply from the Ganga-Brahmaputra (annual mean 16186 and 11892 m^3s^{-1} respectively), Irrawaddy (13018 m^3s^{-1}), Mahanadi (1710 m^3s^{-1}), Godavari (3180 m^3s^{-1}) and Krishna (1730 m^3s^{-1}) river systems substantially lowers salinity (Varkey et al., 1996) and also reduces the upwelling intensity (Shetye et al., 1991). The warm and low saline surface water strengthen the upper ocean stratification, shallow the mixed layer depth (<10m) (Shetye et al. 1993; Tomczak and Godfrey 1994; Prasanna Kumar et al., 2002; Narvekar and Prasanna Kumar, 2014). The strong winds prevailing during this season is unable to erode the strong stratification (Shenoi et al., 2002; Narvekar and Prasanna Kumar, 2014). In the region, higher fluvial nutrient supply supports the increase in total phytoplankton biomass, whereas moderate levels of the primary production and chlorophyll indicate the possible light limitation due to increased riverine suspended load and cloud cover (Gomes et al., 2000; Madhupratap et al., 2003; Madhu et al., 2006; Prasanna Kumar et al., 2010). In the southern region, the intrusion of the high saline Arabian Sea water and strong winds able to drive wind-driven mixing. However, less nutrient availability does not support primary production. Along the southwest inshore region, shallow nitracline due to river discharge and partly upwelling process (Madhu et al., 2006), controls total phytoplankton abundance and primary production (Radhakrishna et al., 1978; Madhu et al., 2006).

The onset of fall intermonsoon (October) winds over the Bay drastically reduces their speed in the north. Although precipitation strength decreases during this period, overall nutrient and chlorophyll distribution pattern along the region is similar as like the summer monsoon (Narvekar and Prasanna Kumar, 2014).

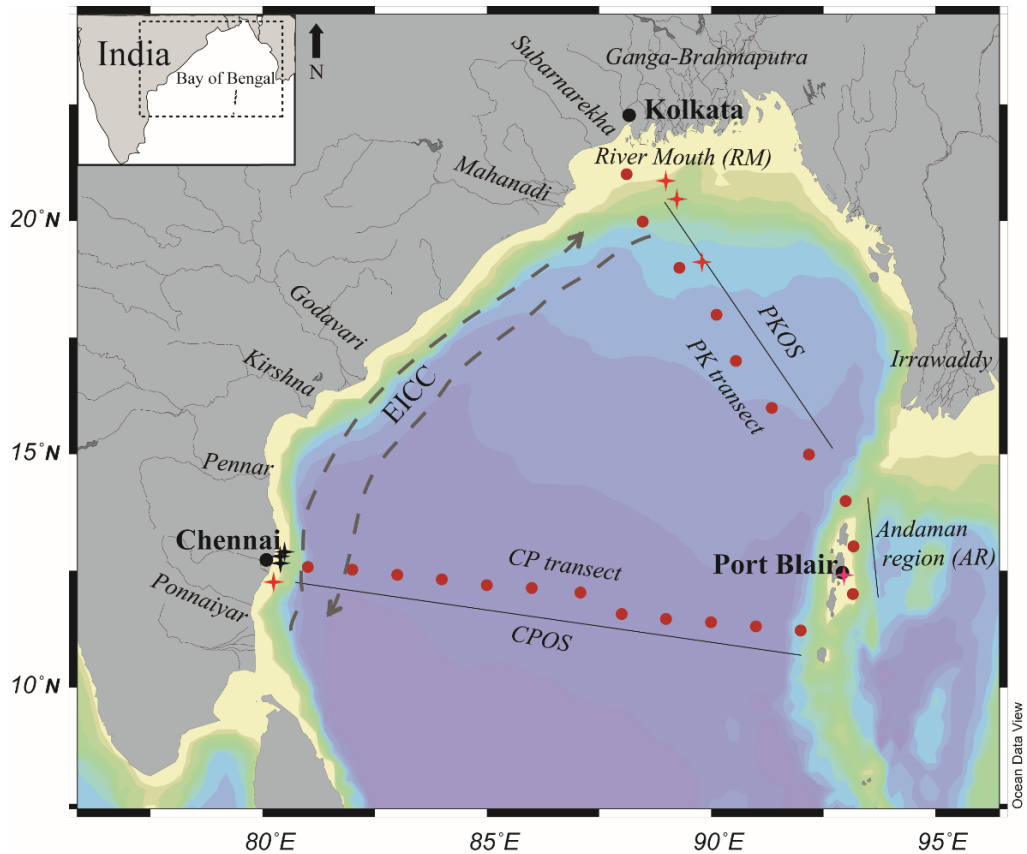


Fig. 2.1 Study area map showing sampling locations (circles) along the Chennai-Port Blair (CP) and Port Blair-Kolkata (PK) transects in the Bay of Bengal.

Note: East Indian coastal current (EICC) during SWM (clockwise) and NEM (anticlockwise); Sediment sampling locations (from Chapter 3A and 3B) along Chennai (during SASU-125, black star and SK-261, red star), Andaman region (pink star) and northern Bay of Bengal (during SK-261, red star).

During the NE monsoon (November-February), winds blow north-easterly. The surface current flows in an anticlockwise direction (Shankar et al., 2002; Fig. 2.1). The net cooling and increased salinity due to high evaporation, lead to a rapid decrease in upper water column thermal stratification along the offshore region. However, intense stratification by the fresh water cap does not allow convective mixing and nutrient supply to upper layers in the northern region (Madhupratap et al., 1996; Gomes et al., 2000). Still, increased nitrate and silicate concentration along with the deep light

penetration in the water column fuel growth of phytoplankton and primary production in the northern and eastern inshore region (Gomes et al., 2000; Madhu et al., 2006; Paul et al., 2008). The peak solar heating strongly stratifies the upper ocean waters during the spring intermonsoon (March-May). The weaker winds are unable to erode the strong stratification and facilitate deep mixing, leading to the formation of shallow mixed layer depth (Narvekar and Prasanna Kumar, 2014). Although increased solar radiation deeper light penetration depth, but nutrient poor water unable to support enough phytoplankton production in the offshore region (Madhu et al., 2006; Paul et al., 2008). However, it increases towards the inshore due to moderate riverine nutrient flux (Gomes et al., 2000; Madhupratap et al., 2003).

2.2.2 Sampling strategy

Surface water samples were collected from 22 stations (separated by one-degree intervals), along CP transect (12 stations) and PK transect (10 Stations) in the Bay of Bengal (Fig. 2.1) on a regular basis, October 2006 to September 2011 (48 months). To study the responses of dinoflagellate community to the monsoons, sampling months are classified accordingly classical monsoonal divisions (Fig. 2.2).

Furthermore, to elucidate the regional environmental variability on dinoflagellate community 22 sampling stations are grouped into 4 regions (Fig. 2.1), Chennai-Port Blair oceanic stations (CPOS, Stations 1 to 12), Andaman Region (AR, Station 13 to 15), Port Blair-Kolkata oceanic stations (PKOS, Stations 15 to 21) and River Mouth (RM, Station 22).

2.3 Sample collection and processing

2.3.1 Water parameters

Sea surface temperature (SST) at sampling stations was obtained from water column temperature profiles recorded by XBT MK21-T7 Probes (SIPPICAN Inc.). Sea surface salinity (SSS) of field samples were determined from conductivity values measured in the laboratory using GUILDLINE AUTOSAL 8400B Salinometer.

For nutrient analysis [dissolved inorganic nitrogen (DIN), dissolved inorganic phosphate (DIP)], 10 ml of seawater samples were collected into cryo-vials, stored in liquid nitrogen. The nutrient samples collected during October 2006 to October 2009 were analyzed using TECHNICON autoanalyzer, whereas SKYLAR SANplus autoanalyser was used for samples from November 2009 to September 2011. For both analyses, standard spectrophotometric procedures were followed (Grasshoff et al., 1983).

2.3.2 Phytoplankton sample

For the enumeration of micro-phytoplankton community, 1-liter surface water sample was fixed using acetic Lugol's iodine solution. These samples were brought back to the laboratory and kept settling for 48 h (Hasle, 1978). Later, the volume was brought down to 100 ml and then to 10 ml final concentration after another 48 h settling period. From this 10-ml final concentration, 3 ml sample was taken in a Petri dish (3.8 cm diameter) and examined under an inverted microscope (OLYMPUS-IX 71) at 100X to 1000X magnification. Phytoplankton cell concentrations were determined in cells per liter (cells L⁻¹) according to the standard method (Hasle, 1978). Identification of the dinoflagellate was carried out to the lowest possible taxonomic level using standard

identification manuals and keys (Subrahmanyam, 1968; Taylor, 1976; Tomas, 1997; Okolodkov, 2005; Hoppenrath et al., 2009). In this chapter, only data of dominant and cyst forming dinoflagellate species is presented (Table 2.1).

Further, to evaluate the potential of cyst formation in these species present dataset is compared with the contemporary cyst distribution studies (respective coastal stations data from Chapter 3A, 3B and 4) from the coastal and neritic regions (Fig. 2.1; Table 2.2) along CPOS (station 1, near Chennai), AR (station 13, near South Andaman), PKOS (station 20 and 21, neritic region of northern Bay of Bengal) and RM (Station 22).

2.3.3 Climatic variables (data adapted from *Chitari et al., Current Science* communicated)

The rainfall and wind speed datasets (grid area of 7°28' N–25°88' N and 77°88' E–97°28' E) were obtained from NOAA Earth System Research Laboratory (<http://www.esrl.noaa.gov/psd/data/gridded/data.unified.daily.conus.html>) and APDRC (Asia-Pacific Data Research Centre, <http://apdrc.soest.hawaii.edu>) respectively. The values of PAR (Photosynthetically active radiation) were extracted from Level 3 MODIS (<http://oceandata.sci.gsfc.nasa.gov>).

2.3.4 Data Analysis

Multivariate statistical analysis performed on cyst forming dinoflagellate data to elucidate their response to the monsoonal variability using CANOCO 4.5 software for Windows (ter Braak and Smilauer, 2002). Detrended Correspondence Analysis (DCA) was used to test the character of variability within the cyst forming species assemblages.

The length of the first DCA gradient is in the range of 1.2 to 1.7 standard deviations in the present dataset (for four different seasons), indicating the species appearance have a linear response to environmental variables. Due to this linear model character of data set, Redundancy analysis (RDA) was performed. Forward selection method was used to reduce the set of variables that could effectively explain the greatest amount of variance (Conditional effect) in the dinoflagellate dataset. The Monte Carlo Test was used to determine the significance of each environmental parameter, based on 499 unrestricted permutations. The significance level of the variables $P < 0.05$ indicates that environmental variables are strongly related to the cyst forming species data.

2.4 Results

2.4.1 Climatic variability

The onset of SWM, the southwesterlies strengthen during June, wind speed reach peak during July-August (Fig. 2.2a and b). Wind speed reduces during September and vanishes by October (SIM) due to the weakening of southwesterlies. During November-February (NEM), northeasterly winds prevail north, turning northwesterly in the south. Wind speed reaches a peak during December and gradually weakens at the end of February. The rainfall pattern showed seasonal and regional differences in precipitation (supplementary data Fig. 2.1). In CPOS, high precipitation was noticed during SWM and NEM, whereas in PKOS it was higher during SWM. In AR rainfall pattern is irregular. However, generally, late NEM months (January-March) are the dry period of the year. Monsoonal interventions like cloud cover and rainfall control the PAR in the Bay of Bengal. The PAR was reduced during the SWM and NEM than SIM and FIM seasons in the study region (Fig. 2.2c and d).

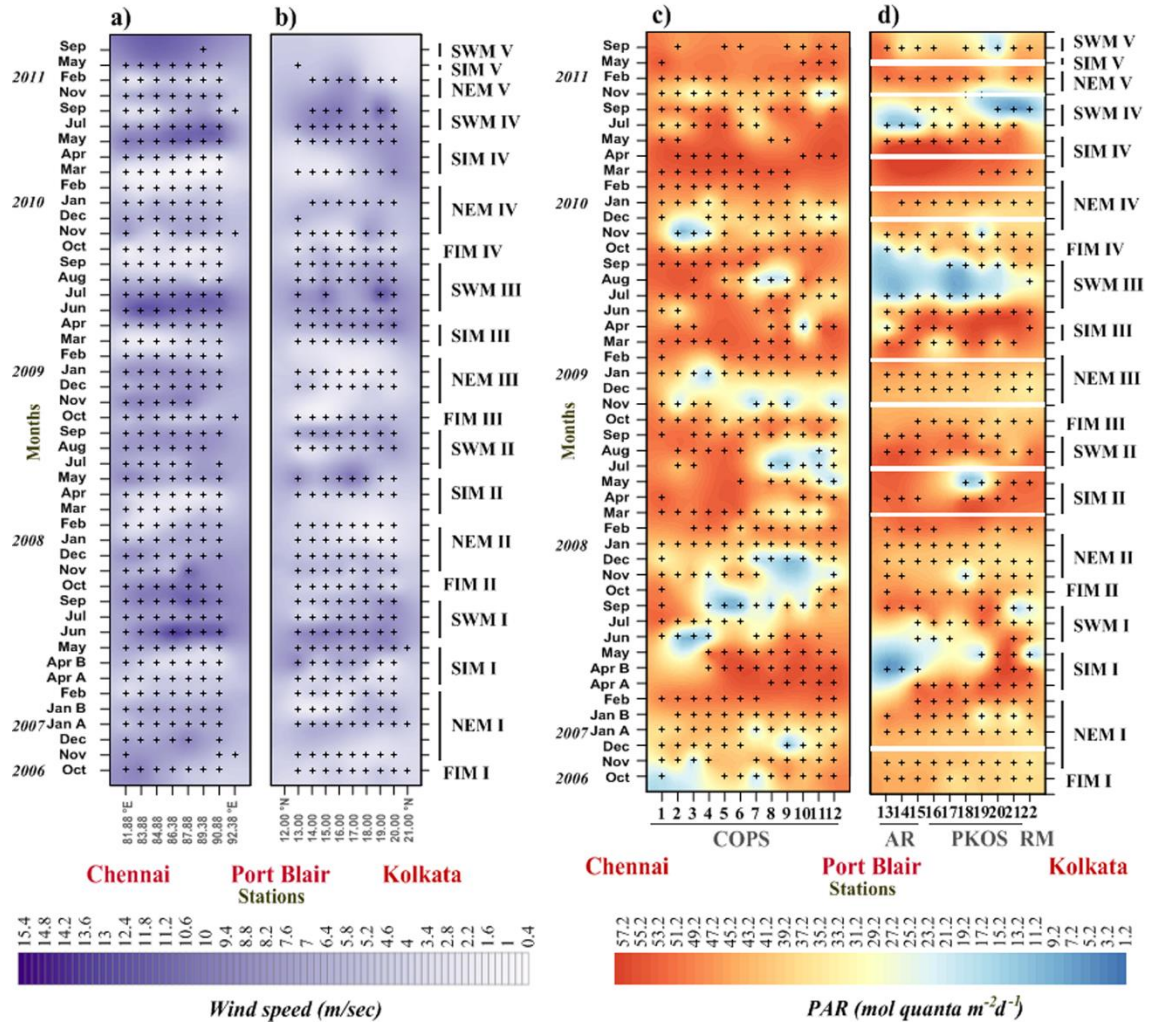


Fig. 2.2 Spatial and temporal variation in wind speed (a and b) and PAR (c and d) along the Chennai-Port Blair and Port Blair-Kolkata transects. Superimposed post map (+) symbols on contours denote the sampling stations for which data is available (data adapted from *Chitari et al., Current Science* communicated). White lines superimposed (Fig. 2.2d) on contours (along Port Blair-Kolkata transect) denotes no sampling months.

2.4.2 Hydrological variability

Monsoonal seasonality controls the regional and seasonal differences in the hydrological characteristics in the Bay. Temporally lower SSTs were observed in both transects during the NEM season, caused due to high evaporation and net cooling (Fig. 2.3a and b). Spatially sampling stations in PK transect were cooler than the CPOS, due

In the regional context, SSS was relatively high in CPOS (29.2 to 34.4 psu) due to evaporation and intrusion of high saline water (Fig. 2.3c and d). Riverine influx mainly governs SSS variations in the RM and PKOS sectors. Lower SSS was observed during the SWM due to increased riverine discharge. Relatively higher SSSs were reported during the SIM and FIM resultant of reduced freshwater influx (Fig. 2.3d).

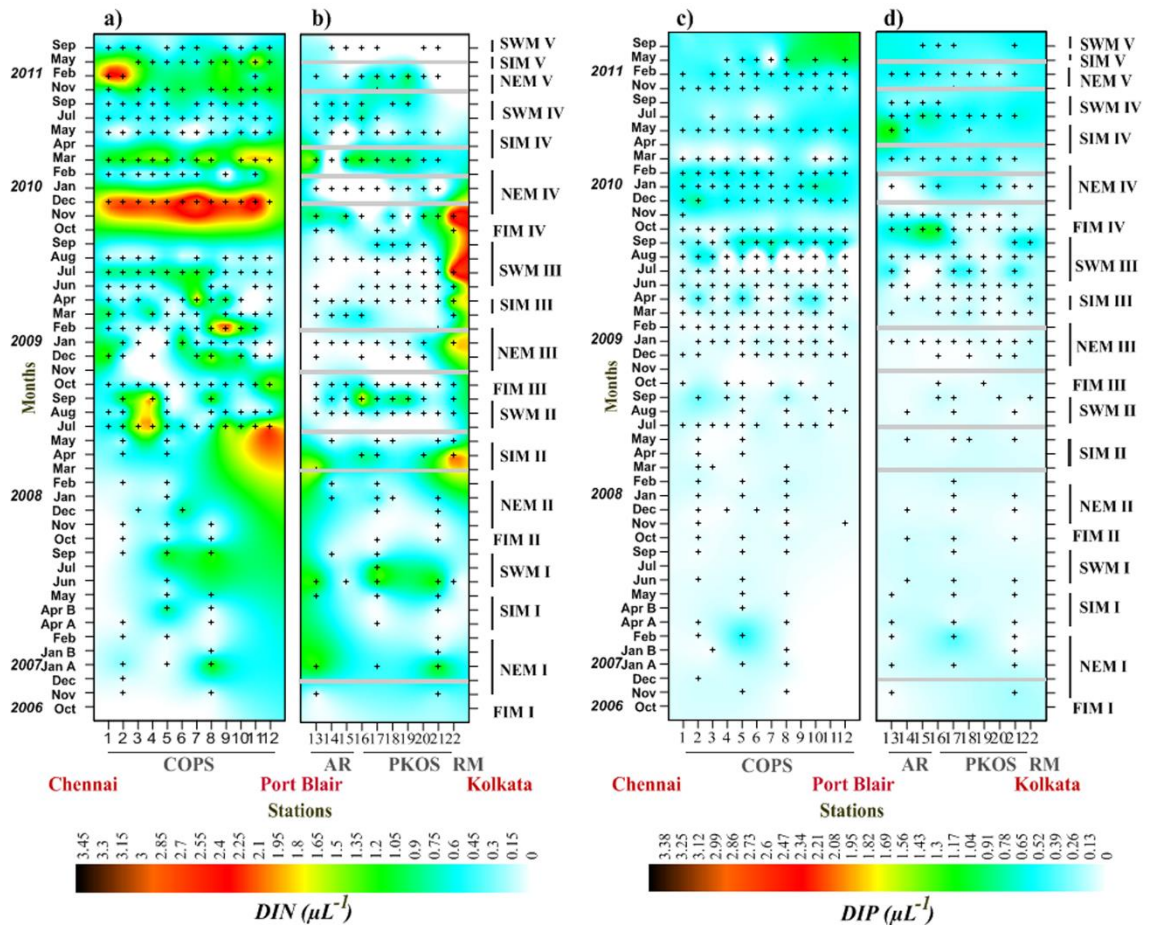


Fig. 2.4 Spatial and temporal variation in nutrients, DIN (a and b) and DIP (c and d) along the Chennai-Port Blair and Port Blair-Kolkata transects. Superimposed post map (+) symbols on contours denote the sampling stations for which data is available. White lines superimposed (Fig. 2.4b and d) on contours (along Port Blair-Kolkata transect) denotes no sampling months.

The surface water nutrient (DIN and DIP) concentrations highlight the oligotrophic nature of the Bay waters (Fig. 2.4a, b, c and d). Over the most of the

sampling months, nutrient concentrations were below detectable range, especially during the SIM and FIM. On a regional basis, higher DIN (up to $4.23 \mu\text{L}^{-1}$) and DIP (up to $3.08 \mu\text{L}^{-1}$) concentrations were reported in the RM and AR during SWM and NEM (Fig. 2.4b and d). A similar trend was observed in the CPOS and PKOS stations, with maximum DIN and DIP concentrations during the SWM (Fig. 2.4a and c).

2.4.3 Phytoplankton assemblages

Four hundred and thirty-two species or genera of phytoplankton were recorded from surface waters of the Bay of Bengal, with absolute abundance ranging from 6.8×10^2 to 3.68×10^5 cells L^{-1} (Chitari et al., unpublished data). Overall phytoplankton community was dominated by diatoms with respect to abundance (1.2×10^2 to 3.66×10^5 cells L^{-1}), whereas dinoflagellate contributes more in species richness (Chitari et al., unpublished data). One hundred and ninety-seven species or genera of diatoms were reported, with *Chaetoceros affinis*, *C. decipiens*, *C. lorenzianus*, *C. peruvianus*, *Chaetoceros* spp., *Thalassionema nitzschioides*, *Lauderia annulata*, *Pseudonitzschia* spp., *P. delicatissima*, *Rhizosolenia* spp. and *Navicula* spp. most abundantly distributed in the study region (Chitari et al., unpublished data).

Dinoflagellate population in the region was diverse with 174 phototrophic and 64 heterotrophic species or genera (supplementary data Table 2.1). *Scrippsiella trochoidea*, *Amphidinium* spp., *Prorocentrum* spp., *Gonyaulax* spp., *Dinophysis caudata* and *Triplos furca* were the most dominant phototrophic dinoflagellate species in the region. Among the heterotrophs, *Protoperdinium* spp., *P. divergens*, *Preperidinium meunieri* and *Gyrodinium* spp. were abundant. Twenty-eight dinoflagellate species, belonging to genus *Alexandrium*, *Diplopsalis*, *Gonyaulax*, *Gymnodinium*,

Lingulodinium, *Pyrophacus*, *Pentapharsodinium*, *Protooperidinium* and *Scrippsiella* were reported in the region are known for cyst formation (Table 2.1).

Table 2.1 List of cyst-forming dinoflagellates and their percentage contribution in surface waters along CPOS, AR, PKOS and RM regions.

Species Name	Abbreviations	CP transect		PK transect	
		CPOS	PKOS	AR	RM
<i>Alexandrium minutum</i>	Amin		0.1		
<i>Alexandrium tamarense</i>	Atam	0.2	0.8	0.4	
<i>Alexandrium</i> spp.	Aspp	8.6	4.5	8.8	4.4
<i>Gonyaulax digitalis</i>	Gdig	0.1	0.1	0.2	
<i>Gonyaulax scrippsae</i>	Gscr	0.8	0.3	1.7	
<i>Gonyaulax spinifera</i>	Gspi	0.8	0.4	1.3	0.5
<i>Gonyaulax</i> spp.	Gspp	10.0	10.6	8.6	1.9
<i>Gymnodinium catenatum</i>	Gcat	0.2			
<i>Lingulodinium polyedrum</i>	Lpol	0.3		0.2	
<i>Pyrophacus horologium</i>	Phor	0.5	0.3	0.4	
<i>Pyrophacus steinii</i>	Pste	0.3	0.1	0.4	
<i>Scrippsiella spinifera</i>	Sspi	0.2			
<i>Scrippsiella trochoidea</i>	Stro	42.8	39.5	36.9	20.7
<i>Scrippsiella</i> spp.	Sspp	6.3	9.1	4.5	2.8
<i>Diplopsalis lenticula</i>	Dlen	0.1	0.6		
<i>Pentapharsodinium tyrrhenicum</i>	Ptyr	0.2			
<i>Protooperidinium claudicans</i>	Pclu	0.2	0.3	0.4	3.3
<i>Protooperidinium conicum</i>	Pcon	0.4	0.4	0.2	4.5
<i>Protooperidinium curvipes</i>	Pcur				2.1
<i>Protooperidinium divergens</i>	Pdiv	2.1	1.4	3.2	9.5
<i>Protooperidinium leonis</i>	Pleo	0.7	1.0	1.1	1.0
<i>Archaeperidinium minutum</i>	Arcmin	1.1	1.1	2.8	4.2
<i>Protooperidinium oblongum</i>	Pobl	0.2		0.2	2.4
<i>Protooperidinium ponticum</i>	Ppon		0.5		
<i>Protooperidinium pentagonum</i>	Ppen	0.4	0.1	1.5	0.3
<i>Protooperidinium subinerme</i>	Psub	0.3	0.1	0.2	0.1
<i>Protooperidinium</i> spp.	P spp	21.3	25.9	25.4	28.9
<i>Preperidinium meunieri</i>	Pmeu	1.8	3.0	1.7	13.0

2.4.4 Dinoflagellate distribution

2.4.4.a CPOS region

Overall phytoplankton abundance in the CPOS region ranged from 10 cells L⁻¹ to 6.3×10⁴ cells L⁻¹ (supplementary data Fig. 2.1). Phytoplankton community varied spatially along the CPOS, diatoms being the dominant planktonic community at the shelfward stations i.e. 1 and 12 (supplementary data Fig. 2.1). The phytoplankton abundance at CPOS region was largely determined by dominant diatom species, *C. curvisetus*, *Chaetoceros* spp., *Coscinodiscus* spp., *Guinardia striata*, *Rhizosolenia* spp., *Thalassiosira* spp., *Navicula* spp. and *Pseudonitzschia* spp. (Chitari et al., unpublished data). Dinoflagellate contribution to phytoplankton community increased towards the oceanic region (station 2 to 11) (Fig. 2.5a). Dinoflagellate community in the region was dominantly represented by phototrophic *Amphidinium* sp., *Alexandrium* spp., *Gonyaulax* spp., *S. trochoidea*, *C. furca*, heterotrophic *Protoperidinium* species and other unidentified thecate dinoflagellates (UTDs) (supplementary data Table 2.1). Temporally, highest phytoplankton abundance (especially diatoms) was observed during the SWM and then NEM along the CPOS (supplementary data Fig. 2.1; Fig. 2.5b). In contrast, dinoflagellate community was abundant during the SIM and FIM, with some exception (Fig. 2.5a). Calcareous cyst forming *S. trochoidea* species dominated planktonic dinoflagellate assemblage along the CPOS region (Fig. 2.6a; 2.7). Other dominant Peridinioides includes *Protoperidinium* spp., *Preperidinium meunieri*, *Archaepridinium minutum*, *P. divergence* and *Scrippsiella* spp. (Table 2.1).

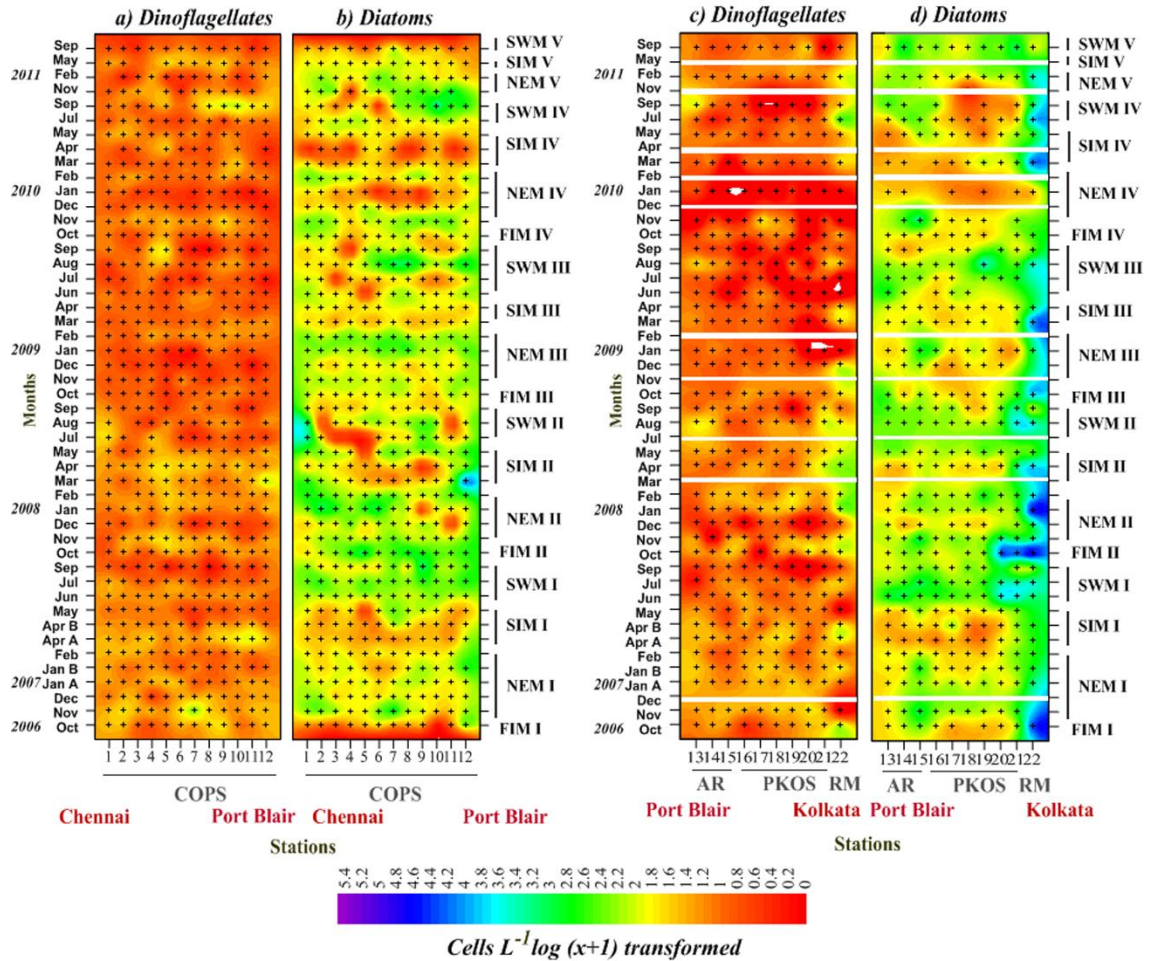


Fig. 2.5 Spatial and temporal variation of dinoflagellates (a and c) and diatoms (b and d), abundance [$\log(x+1)$ transformed] along the Chennai-Port Blair and Port Blair-Kolkata transects. Superimposed post map (+) symbols on contours denote the sampling stations for which data is available. White lines superimposed (Fig. 2.5c and d) on contours (along Port Blair-Kolkata transect) denotes no sampling months.

The dominant phototrophic Gonyaulacoids, *Gonyaulax* species, *G. spinifera*, *G. scrippsae*, *Alexandrium* species and *Gymnodinium* species were substantially contributed to the cyst forming dinoflagellate community (Table 2.1). In the region, cyst forming dinoflagellate population exhibits inter- and intra-annual variation in the population dynamics (Fig. 2.7a-d). The abundance of dominant cyst forming species, especially, *S. trochoidea* was observed during the early SIM (March and April)

followed by late SWM (September) (up to 450 and 280 cells L⁻¹ respectively) (Fig. 2.6a, 2.7a,d). The predominance of cyst-forming *Preperidinium* species was observed during SWM (up to 115 cells L⁻¹) followed by NEM (Fig. 2.8, 2.9a). Phototrophic *Pyrophacus steinii* that was rare in occurrence in the Bay was observed during the SWM along the CPOS region.

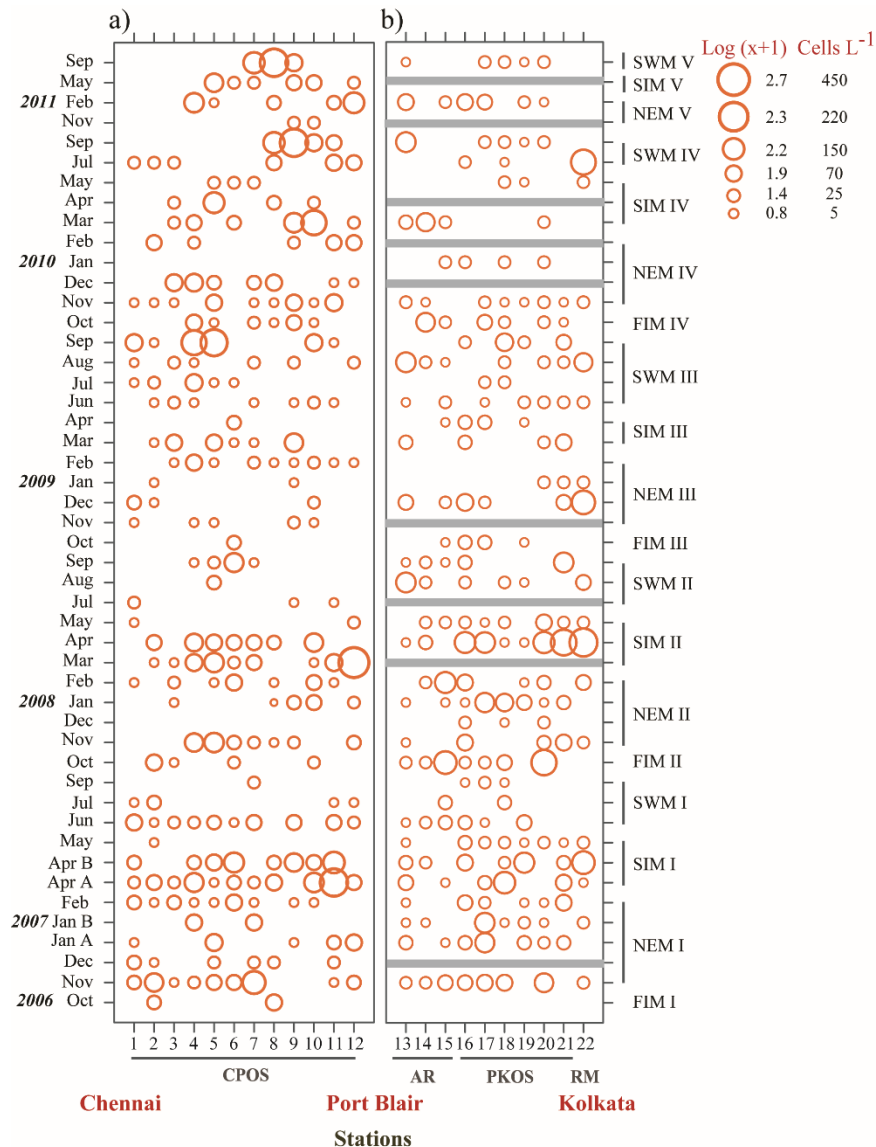


Fig. 2.6 Spatial and temporal variation in *S. trochoidea* abundance along the Chennai-Port Blair and Port Blair-Kolkata (a and b) transect. Circles indicate the log (x+1) transformed and corresponding absolute abundance values. White lines superimposed (Fig. 2.6b) on contours (along Port Blair-Kolkata transect) denotes no sampling months.

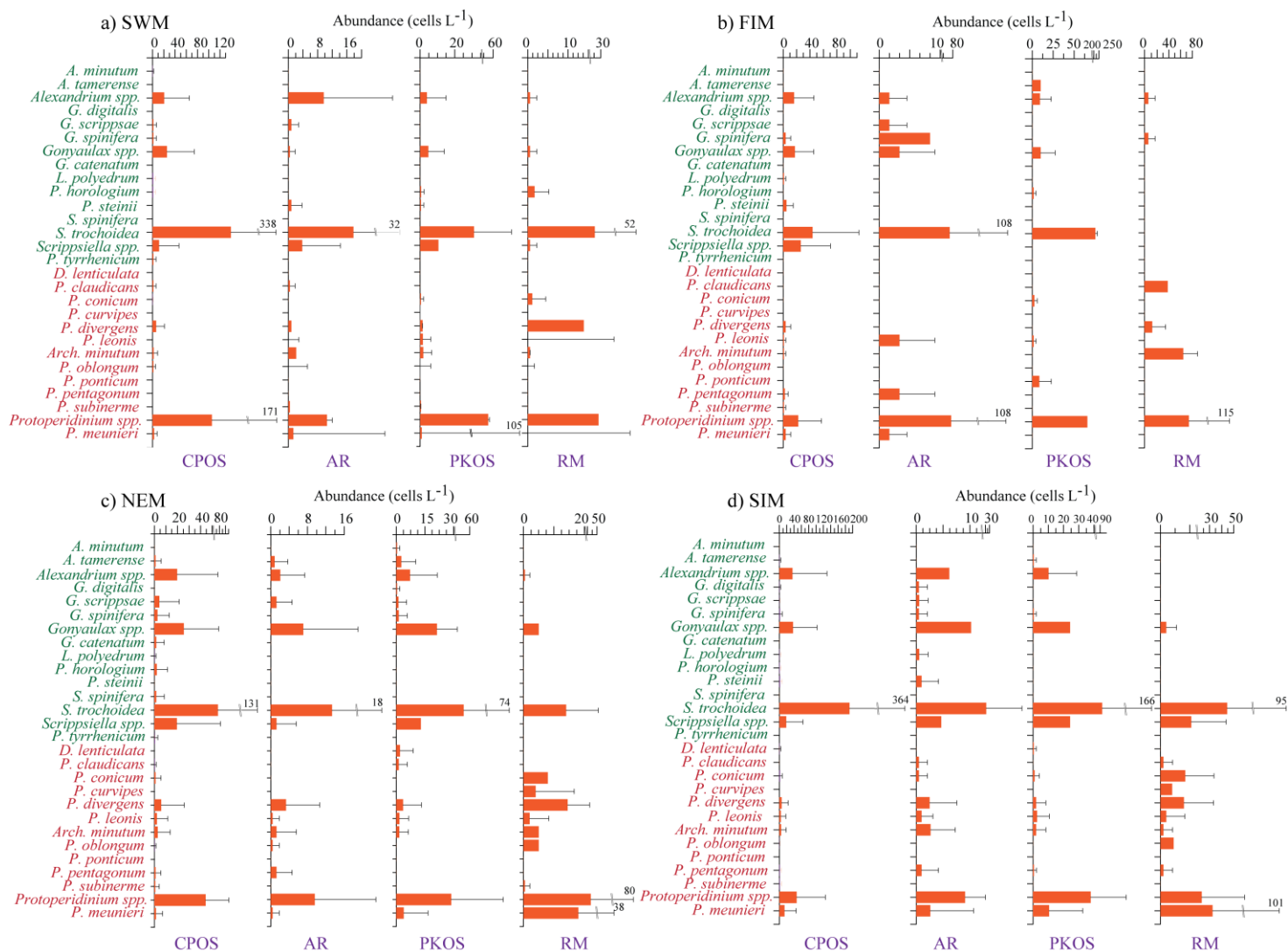


Fig. 2.7 Variation in cyst forming dinoflagellate population during (a) SWM, (b) FIM, (c) NEM and (d) SIM seasons along the CPOS, AR, PKOS and RM regions in the Bay of Bengal. Horizontal bars represents abundance (cells L⁻¹) of cyst-forming species (seasonal and station average) along with error bars representing the standard deviation (sd) from the mean. For broken error bars, maximum values of sd are given at the cap. Phototrophic and heterotrophic species represented in green and red colour respectively.

2.4.4.b PK transect

Phytoplankton community was higher along the PK transect, especially at RM sector (30 to 2.7×10^5 cells L⁻¹) and PKOS (10 to 5.1×10^4 cells L⁻¹) than the CPOS (supplementary data Table 2.1). Dominant diatom species, *Chaetoceros* spp., *C. curvisetus*, *Thalassinema nitzschoides*, *Pseudonitzschia delicatissima*, *C. lorenzianus*, *Pseudonitzschia* spp., *C. peruvianus*, *C. decipiens* and *C. affinis* contributes substantially to the phytoplankton community in the PK transect. Their higher abundance was observed in the RM sector (Chitari et al., unpublished data). As like the CPOS region, diatom population was abundant in the coastal region (RM and then AR), whereas dinoflagellate population contributes substantially to the total phytoplankton community in the PKOS region (Chitari et al., unpublished data). In the PK transect, phototrophic dinoflagellates species, *S. trochoidea*, *Amphidinium* spp. and heterotrophic *Protoperidinium* species together with UTDs were abundant in dinoflagellates (supplementary data Table 2.1). Temporally, highest dinoflagellate abundance was observed during the end of the NEM (January and February), and then SIM, FIM (October) along the PKOS regions (Fig. 2.5c).

Calcareous cyst forming *S. trochoidea* (up to 300 cells L⁻¹) dominated dinoflagellate assemblage in the PK sector, irrespective of the regions (Fig. 2.6a). Other Gonyaulacoids, *Alexandrium* spp., *Gonyaulax* species including *G. spinifera* and *G. scrippsae* were abundant in PKOS (Table 2.1). Protoperidinoid species including *P. conicum*, *P. claudicans*, *P. divergens*, *P. leonis*, *Archaepridinium minutum*, *P. pentagonum* and *Preperidinium meunieri* were abundant in the region, especially at RM during NEM and SIM seasons (Fig. 2.7c and d). Along transect temporal variation in

cyst forming dinoflagellate population and their distribution was observed. *S. trochoidea* was dominant in the water column throughout the sampling seasons, especially during SIM. However, lowest abundance was observed during the SWM season (Fig. 2.6b). Similarly, an abundance of other phototrophic species belonging to Gonyaulacoids was lower during the SWM season (Fig. 2.7a). Heterotrophic Protoperidinioid species were relatively dominant throughout the year in the RM region (Fig. 2.7; 2.8b).

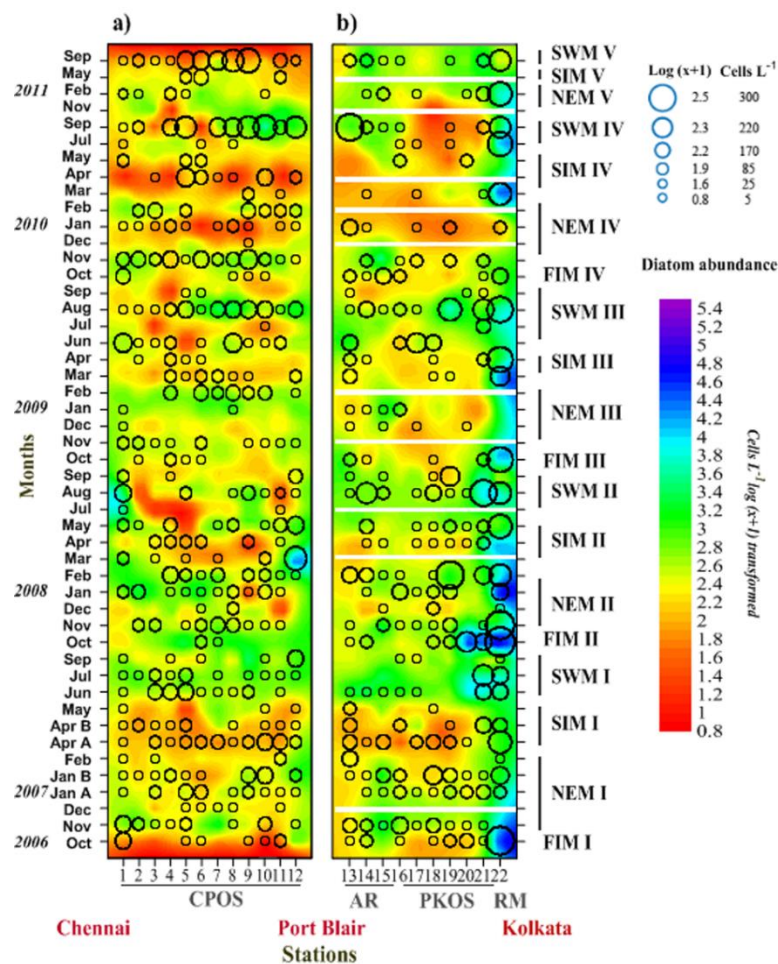


Fig. 2.8 Spatial and temporal variation in cyst forming *Protoperidinium* species abundance (circles) along the Chennai-Port Blair and Port Blair-Kolkata (a and b) transect, superimposed on diatom distribution plot (colour counters). White lines superimposed (Fig. 2.8b) on contours (along Port Blair-Kolkata transect) denotes no sampling months. Note: Circles indicate the $\log(x+1)$ transformed and corresponding absolute abundance of *Protoperidinium* species, values given in the figure.

However, in the PKOS their dominance was observed especially during the SWM and FIM (Fig. 2.7a and b). The abundance of other cyst forming Protopteridinioids was negligible, except *P. curvipes*, which was abundant towards RM during NEM and SIM seasons (Fig. 2.7c and d).

2.4.5 Effect of climatic variability on cyst forming dinoflagellate

The RDA provides the further comprehensive relationship between cyst forming dinoflagellate population and environmental variability. In the RDA, using the selected environmental (SST, SSS, wind speed, PAR, DIP, DIN) and biological variables (diatom abundance), the eigenvalues for first two dominant axes explain the cumulative variance in the species data (Fig. 2.9a to 2.12a). Orientations of the sampling stations on an RDA biplot reflect their species assemblage and association to the environmental variables. Further, the length and orientation of environmental vectors indicate their relative importance and approximate relations to the RDA axes.

The RDA analysis for cyst forming dinoflagellates assemblage during the SWM reveals the first two RDA axis (RDAs 1 and 2) are dominant and represent 55% total cumulative variance (Fig. 2.9a). Diatom abundance (diatoms) correlated with the RDA 1 ($R^2 = 1.4473$), whereas SST is linked to RDA 2 ($R^2 = 1.1797$ and 1.5056) (supplementary data Table 2.2a). Diatoms and SST play an important role when analyzed separately (Marginal effects) (Fig. 2.9a). However together with other variables, diatoms and DIN explains the major and significant part of the data variation ($p < 0.05$) (conditional variable). RDAs 1 is defined by a positive score of *Protopteridinium* spp., *P. conicum*, *P. divergence*, *Pyrophacus horologium*, *S.*

trochoidea, *Archaepridinium minutum*, whereas RDAs 2 is characterized by *P. leonis*, *Preperidinium meunieri* (Fig. 2.9a; supplementary data Table 2.2b).

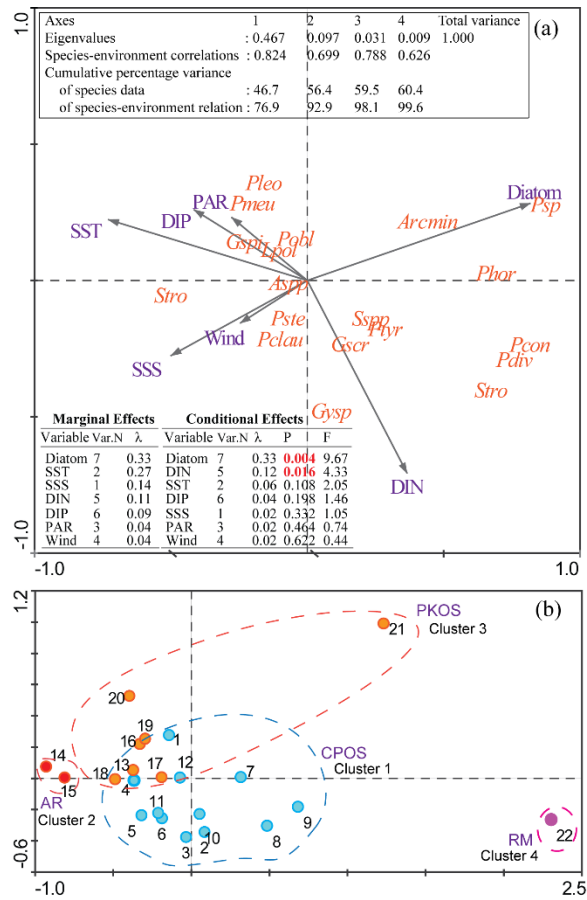


Fig. 2.9 Redundancy analysis (RDA) ordination diagram of (a) species and (b) sampling stations in relation to the environmental variability during the SWM. For species abbreviations please refer Table 2.2. Abbreviations of environmental parameters: SSS, sea surface salinity; SST, sea surface temperature; DIN, dissolved inorganic nitrogen; DIP, dissolved inorganic phosphate; PAR, Photosynthetically active radiation; Diatoms, diatom abundance.

The station ordination diagram defines four distinct clusters (Fig. 2.9b). Sampling stations from the CPOS region corresponds to cluster 1, which is characterized by species like, *S. trochoidea*, *Gymnodinium* spp., *P. claudicans*, *G. scrippsae*, *Scrippsiella* spp., *P. tyrrhenicum*. Cluster 2 represented stations from the PKOS region. Cyst-forming species, *Alexandrium* spp., *L. polyedrum*, *G. spinifera*, *P.*

oblongum, *Preperidinium meunieri*, *P. leonis* were characterized these stations. Stations from AR are grouped in cluster 3, which are differentiated due to the presence of *Archaepridinium minutum*. Cluster 4 comprises stations 22 from the RM region, whereas station 21 from PKOS region is also oriented towards it. *Protoperidinium* spp. and *Archaepridinium minutum* reaches their maximum abundance in these two stations. However, the comparative dominance of *P. divergens* and *S. trochoidea* at station 22 differentiate it from station 21.

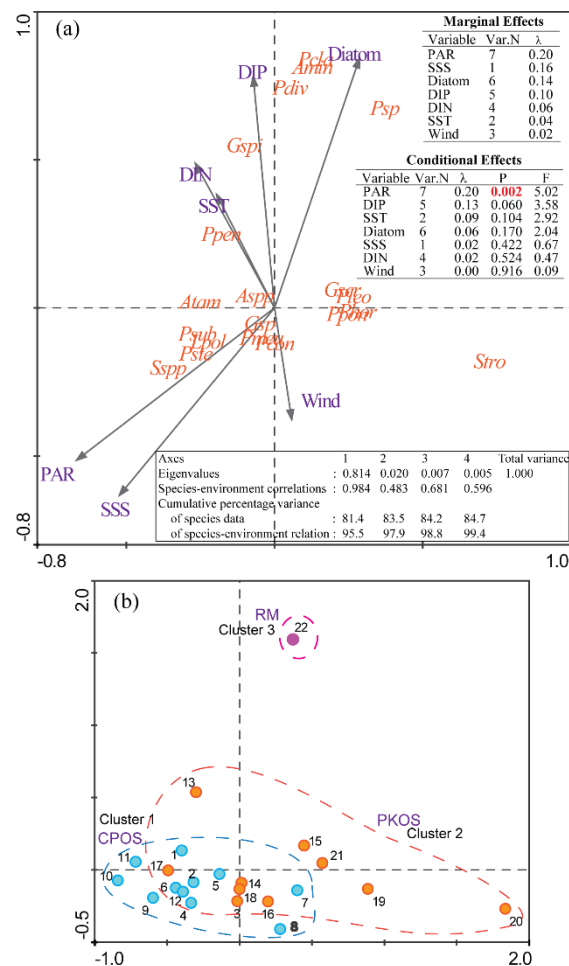


Fig. 2.10 Redundancy analysis (RDA) ordination diagram of (a) species and (b) sampling stations in relation to the environmental variability during the FIM. For species and environmental variable abbreviations please refer Table 2.2 and legends of Fig. 2.9 respectively.

During the FIM, RDA results showed that diatoms were positively correlated with RDAs 1 ($R^2= 0.4845$). In addition to diatoms ($R^2= 0.5737$), SST and DIP also corresponds to RDAs 2 ($R^2= 0.4300$ and 0.3522 respectively) (supplementary data Table 2.3a). PAR, SSS and diatoms are important role when analyzed separately (Marginal effects) (Fig. 2.10a). However PAR and DIP explains a significant part of the data variation ($p<0.05$) when analyzed together with other variables (conditional variable). *S. trochoidea*, *Protoperidinium* spp., *P. ponticum* and *P. horologium* show positive score with the RDAs 1 (supplementary data Table 2.3b). RDAs 2 is described by a positive score of *Archaepridinium minutum*, *P. divergence*, *Protoperidinium* spp. and *G. spinifera*. Three different assemblages of cyst-forming species are reflected in sampling stations ordination (Fig. 2.10b). Cluster 1 represents stations from the CPOS region, with an abundance of *Scrippsiella* spp., *Gonyaulax* spp (Fig. 2.10a and b). Whereas species like *L. polyedricum*, *P. steinii*, *P. subinermis*, *Preperidinium meunieri* are present only in COPS region with low abundance. Cluster 2 comprised of sampling stations PKOS and AR regions, which are mainly characterized by the presence of *S. trochoidea*. Other species, *A. tamarense*, *G. scrippsae*, *P. conicum*, *P. leonis*, *P. ponticum* and *P. horologium* are present only in this region with less abundance. *G. spinifera*, *P. claudicans*, *P. divergens*, *Archaepridinium minutum* and *Protoperidinium* spp. are comparatively abundant at RM. Phototrophic *Alexandrium* species, are widely distribute species does not fall in any particular cluster.

During the NEM, the RDAs 1 and 2 explain respectively 81% and 20% of the total variance (Fig. 2.11a). Diatoms positively correlated with the RDAs 1 ($R^2= 1.4473$), whereas DIN corresponds with RDAs 2 ($R^2 = 1.1797$ and 1.5056)

(supplementary data Table 2.4a). Diatoms, SST, and SSS are an important role (Marginal effects) (Fig. 2.11a). However, diatoms explain a significant part of the data variation ($p < 0.05$) when analyzed together with other variables.

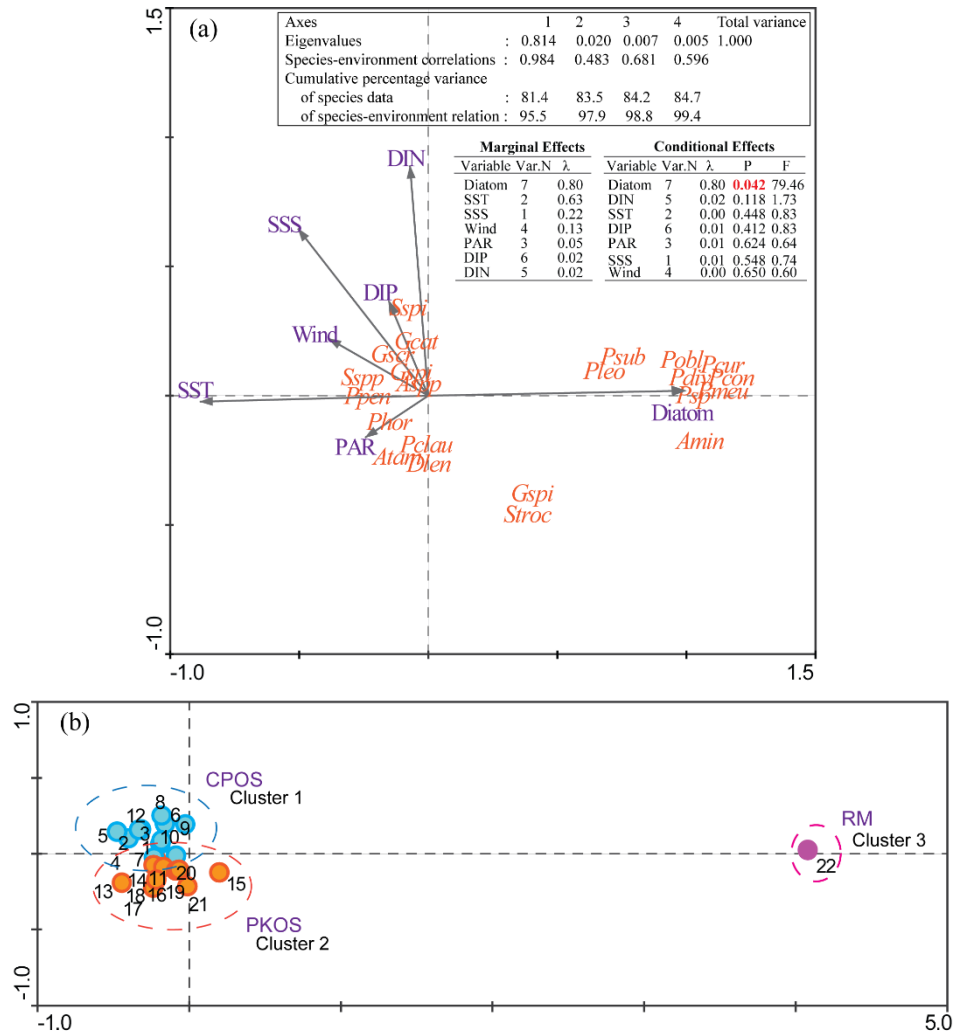


Fig. 2.11 Redundancy analysis (RDA) ordination diagram of (a) species and (b) sampling stations in relation to the environmental variability during the NEM. For species and environmental variable abbreviations please refer Table 2.2 and legends of Fig. 2.9 respectively.

Heterotrophic Protozooids, *P. conicum*, *P. curvipes*, *P. divergence*, *Archaepridinium minutum*, *P. oblongum*, *Protozooidium* spp., *P. subinermis*, *P. leonis* and *Preperidinium meunieri* showed positive score with the RDAs 1 (supplementary data Table 2.4b). RDAs 2 is described by a positive score of *Scrippsiella* spp., *P. subinermis* and a negative score of *S. trochoidea* and *G. spinifera*. Sampling stations ordination represents three different assemblages (Fig. 2.11b). Sampling stations from the CPOS region corresponds to cluster 1. Cyst-forming species, *Alexandrium* spp., *S. spinifera*, *Scrippsiella* spp., *G. scrippsae*, *G. spinifera* are comparatively abundant at COPS region, whereas and *G. catenatum* were exclusively in this region (Fig. 2.7c). Cluster 2 comprised of sampling stations PKOS and AR regions, which are mainly characterized by the presence of *P. claudicans*, *D. lenticulatum* and *P. horologium* (Fig. 2.7c). *P. curvipes*, *P. conicum*, *P. divergence*, *P. oblongum*, *Protozooidium* spp., *Preperidinium meunieri* were comparatively abundant at RM region (cluster 3). Phototrophic species, *G. spinifera* and *S. trochoidea*, the abundant and widely distribute species does not fall in any particular cluster.

Diatoms were positively correlated with RDAs 1 ($R^2= 0.9883$) during the SIM, whereas DIN ($R^2= 0.7835$), SSS ($R^2= 0.5133$) and wind speed ($R^2= 0.3194$) corresponded to RDAs 2 (supplementary data Table 2.5a). Diatoms explained a significant part of the data variation ($p<0.05$) when analyzed together with other variables (conditional variable) (Fig. 2.12a). *P. oblongum*, *P. divergence*, *P. conicum*, *P. curvipes*, *Protozooidium* spp., *Preperidinium meunieri* were associated with the RDAs 1 (Fig. 2.12a; supplementary data Table 2.5b). Species like *S. spinifera*, *G. scrippsae*, and *P. subinermis* shows positive score with RDAs 2, whereas *S. trochoidea*

2.4.6 Comparison of planktonic and cyst assemblages of dinoflagellates

Comparison of the present (planktonic) cyst forming species data with (surface sediment) cyst distribution studies from the region revealed heterogeneity in both the assemblages. Dinoflagellate cyst population in the all three regions was diverse than the planktonic population (Table 2.2). At station 1 (near Chennai), 21 and 14 species were observed in the sediment and water column respectively. Further assemblage differences were intense in the northern Bay of Bengal (35 cyst and 20 planktonic species) and Andaman region (44 cyst and 14 planktonic species). Assemblage differences mainly observed in the *Gonyaulax*, *Scrippsiella* and *Protoperidinium* species, their population was diverse in the sediment than the water column in all three regions (Table 2.2). Furthermore, Protoperidinoid species, *P. divergence* present in the water column was not observed in the cyst forms (Table 2.2).

2.5 Discussion

2.5.1 Dinoflagellate population in the region

The biological processes in the Bay of Bengal are mainly controlled by the seasonality in the monsoonal pattern and resultant river inputs from the peninsular riverine systems. Freshening of surface waters due to riverine discharge and rains into the Bay leads to low saline cap formation with low SSS over a large area (Shetye et al. 1993). Thus, river discharge and precipitation over evaporation lead to (low E-P) strongly stratified upper layers (Shetye et al. 1993; Narvekar and Prasanna Kumar, 2014). This eventually hinders the atmospheric, sea surface and sub-surface interactions, which subsequently affect the biological and biogeochemical processes (Ittekkot et al. 2003).

Table 2.2 Comparison of cyst-forming dinoflagellates (planktonic forms) observed in the present study (Pre stu) with the cysts (resting stages) recorded from the coastal and shelf region of Bay of Bengal. Note: Here occurrence of planktonic dinoflagellates from station 1 (near Chennai), 13 (Andaman region) and 20, 21, 22 (northern Bay of Bengal region, NBOB) compared with cyst records from respective regions i.e Chennai (Chapter 3A and 3B), Andaman region (Chapter 4) and NBOB (Chapter 3B). Asterisks (*) represents presence of species.

Thecate dinoflagellate affinity (Biological Name)	Dinoflagellate cyst (Paleontological Name)	Chennai		NBOB		Andaman region	
		3A & 3B	Pre Stu	3B	Pre Stu	4	Pre Stu
<i>Alexandrium catenella</i>	-					*	
<i>Alexandrium tamarensense</i>	-		*	*			
<i>Alexandrium pseudogonyaulax</i>	-					*	
<i>Alexandrium</i> spp.	<i>Alexandrium</i> spp.	*	*	*	*	*	*
<i>Gonyaulax</i> sp.	<i>Bitectatodinium spongium</i>	*		*		*	
<i>Cochlodinium polykrikoides</i>	-					*	
<i>Gonyaulax digitalis</i> , <i>G. spinifera</i> complex	<i>Spiniferites bentorii</i>	*		*		*	
<i>Gonyaulax scrippsae</i> , <i>G. spinifera</i> complex	<i>Spiniferites bulloideus</i>	*	*	*		*	*
<i>Gonyaulax scrippsae</i> , <i>G. spinifera</i> complex	<i>Spiniferites ramosus</i>	*		*	*		*
<i>Gonyaulax mirabilis</i> , <i>G. spinifera</i> complex	<i>Spiniferites mirabilis</i>	*		*		*	
<i>Gonyaulax mirabilis</i> , <i>G. spinifera</i> complex	<i>Spiniferites hyperacanthus</i>	*		*			
<i>Gonyaulax membranaceus</i> , <i>G. spinifera</i> complex	<i>Spiniferites membranaceus</i>	*		*		*	
<i>Gonyaulax</i> sp.	<i>Spiniferites delicatus</i>	*		*			
<i>Gonyaulax spinifera</i> , <i>G. spinifera</i> complex	<i>Spiniferites pachydermus</i>					*	
<i>Gonyaulax</i> sp.	<i>Spiniferites</i> sp.				*	*	*
<i>Gyrodinium impudicum</i>	<i>Gyrodinium impudicum</i>			*		*	
<i>Gonyaulax</i> sp.	<i>Impagidinium paradoxum</i>			*			
<i>Gonyaulax</i> sp.	<i>Impagidinium sphaericum</i>					*	
<i>Gonyaulax</i> sp.	<i>Impagidinium</i> sp.					*	
<i>Gonyaulax spinifera</i>	<i>Nematosphaeropsis labyrinthus</i>					*	
<i>Lingulodinium polyedrum</i>	<i>Lingulodinium machaerophorum</i>	*	*	*		*	
<i>Pentapharsodinium dalei</i>	-					*	

Continued....

Table 2.2....Continued....

Thecate dinoflagellate affinity (Biological Name)	Dinoflagellate cyst (Paleontological Name)	Chennai 3A & B	Pre Stu	NBOB 3B	Pre Stu	Andaman region 4	Pre Stu
<i>Pyrophacus horologium</i>	-				*		
<i>Pyrodinium bahamense</i>	<i>Polysphaeridium zoharyi</i>			*		*	
<i>Protoceratium reticulatum</i>	<i>Operculodinium centrocarpum</i>	*				*	
<i>Scrippsiella lachrymosa</i>	-					*	
<i>Scrippsiella trochoidea</i>	-		*	*	*	*	*
<i>Scrippsiella spinifera</i>	-			*			
<i>Scrippsiella</i> spp.	-		*		*		*
<i>Pyrophacus stenii</i>	<i>Tuberculodinium vancampoae</i>			*		*	*
<i>Archaeoperidinium minutum</i>	<i>Archaeoperidinium minutum</i>		*	*	*	*	*
-	<i>Echinidinium transparantum</i>			*		*	
-	<i>Echinidinium</i> sp.			*		*	
<i>Diplopsalis lebourae</i>	-				*		
<i>Diplopsalis lenticula</i>	-				*		
<i>Protoperidinium americanum</i>	-			*		*	
<i>Protoperidinium avellanum</i>	<i>Brigantedinium cariacense</i>	*		*		*	
<i>Protoperidinium denticulatum</i>	<i>Brigantedinium irregulare</i>			*		*	
<i>Protoperidinium conicoides</i>	<i>Brigantedinium simplex</i>			*		*	
<i>Protoperidinium</i> spp.	<i>Brigantedinium</i> spp.	*		*		*	
<i>Protoperidinium claudicans</i>	<i>Votadinium spinosum</i>				*	*	*
<i>Protoperidinium conicum</i>	<i>Selenopemphix quanta</i>		*	*	*	*	*
<i>Protoperidinium curvipes</i>	-		*				
<i>Protoperidinium divergens</i>	-		*		*		*
<i>Protoperidinium nudum</i>	<i>Selenopemphix quanta</i>			*			
<i>Protoperidinium latissimum</i>	-	*		*		*	
<i>Protoperidinium leonis</i>	<i>Quinquecuspis concreta</i>	*	*	*	*	*	*

Continued....

Table 2.2....Continued....

Thecate dinoflagellate affinity (Biological Name)	Dinoflagellate cyst (Paleontological Name)	Chennai 3A & B	NBOB			Andaman region	
			Pre Stu	3B	Pre Stu	4	Pre Stu
<i>Protoperidinium oblongum</i>	<i>Votadinium calvum</i>	*	*	*	*	*	
<i>Protoperidinium ponticum</i>	-			*			
<i>Protoperidinium pentagonum</i>	<i>Trinovantedinium applanatum</i>	*	*	*	*	*	*
<i>Protoperidinium steidingerae</i>	-			*		*	
<i>Protoperidinium stellatum</i>	<i>Stelladinium stellatum</i>	*		*		*	
<i>Protoperidinium thrianum</i>	-	*					
<i>Protoperidinium</i> species	<i>Stelladinium robustum</i>			*		*	
<i>Protoperidinium</i> spp.	<i>Lejeunecysta</i> spp.			*			
<i>Protoperidinium subinermis</i>	<i>Selenopemphix nephroides</i>			*	*	*	
<i>Preperidinium meunieri</i>	<i>Dubridinium caperatum/ Zygabikodinium lenticulatum</i>		*		*		*
<i>Peridinium quinquecorne</i>	-					*	
<i>Protoperidinium</i> sp. Type. 1	-	*	*	*	*	*	*
<i>Protoperidinium</i> sp. Type 2	-	*					

Stratified water column, with characteristic oligotrophic conditions, tend to promote stasis of the resident dinoflagellate population, rather than promoting growth or blooms (Smayda, 2002). Dinoflagellate abundance observed in this study was generally within the range of 5-2160 cells L⁻¹ (average 322 cells L⁻¹) in RM region and 10-1050 cells L⁻¹ (average 73 cells L⁻¹) in oceanic regions. Even though the surface waters of the Bay of Bengal are stratified and nitrate-deficient, supports relatively diverse dinoflagellate community (Naik et al., 2010; Chitari et al., unpublished data; supplementary Table 2.1).

Planktonic dinoflagellate population in the Bay of Bengal was characterized by the dominance of mixotrophic dinoflagellates, *S. trochoidea*, *Prorocentrum* spp., *P. micans*, *T. furca* and *D. caudata* and *Triplos furca* (Chitari et al., unpublished data). Mixotrophy is an important adaptive survival strategy of dinoflagellates, increases access to growth limiting nutrients, carbon, and other growth factors through phagotrophy and autotrophy (Stoecker, 1999; Bockstahler and Coats, 1993; Jeong et al., 2010). Mixotrophic “K-selection” protists are ‘generalists’ with less efficiency of converting food to energy compared to ‘specialists’ (heterotrophs and autotrophs) (Raven, 1997; Flynn and Mitra, 2009), and dominate in more mature systems from eutrophic to oligotrophic (Mitra et al., 2014, Jones, 2000, Burkholder et al., 2008). The dual capacity of mixotrophic dinoflagellates to utilize dissolved and particulate organic substances efficiently and/or availability of prey organisms could enable them to proliferate in the water column (discussed in Chapter 5, Section 5.4.1).

In the region, about 10% dinoflagellate species are known for cyst formation capacity. Calcareous cyst forming *S. trochoidea*, a mixotrophic dinoflagellate species

well distributed in the region (Fig. 2.6a and b). *S. trochoidea* is C-strategist (competitors, opportunistic colonists; Smayda and Reynolds, 2003) well-known inhabitant from a wide variety of environmental conditions (Kim and Han, 2000). This mixotrophic species can feed on the other phytoplankton species (Jeong et al., 2005). Bloom and red tides of *S. trochoidea* have been reported in Japan, Korea and China (Ishikawa and Taniguchi, 1996; Wang et al., 2004; Qi et al., 2004). However in the natural environment, bloom dynamics of *S. trochoidea* is not directly driven by nutrient changes (Yin et al. 2008). Recent laboratory culture studies highlighted the decline in planktonic *S. trochoidea* population due to nutrient deficiency (Cao et al., 2006). Similar high irradiance positively influences *S. trochoidea* cell density (Zhuo-Ping et al. 2009). Light deficiency facilitates temporary cyst formation in *S. trochoidea* (Lundgren and Graneli, 2011). In the study region, *S. trochoidea* was abundant during SIM along the PK sector (Fig. 2.6b and 2.7d), whereas additional dominance was observed along the CP sector during declining phase of SWM i.e. September (Fig. 2.6a). Similarly, results of RDA reveals that population density does not show any relation with the nutrient concentration. *S. trochoidea* population in the region reaches to its minimum abundance during active SWM months i.e. June to August (Fig. 2.6a and b). Elevated shear stress associated with SWM could enforce the *S. trochoidea* migrate towards the subsurface regions. Additionally, ultimate survival strategies like temporary resting stages formation and mixotrophy could facilitate the *S. trochoidea* to maintain static in the Bay waters during adverse conditions. Start to come up only during September, when monsoonal rainfall declines and cloud cover reduces (Naik et al., 2010). *S.*

trochoidea population proliferates during the SIM season, with a clear sky and no rainfall (Fig. 2.6a and b).

Heterotrophic Protopteridinioid species dominated dinoflagellate assemblage in the study region. Heterotrophic Protopteridinioid species considered as ‘generalist’, feeding on diversified feeding habits ranging from larger diatoms (*Skeletonema*, *Fragilidium*, *Chaetoceros*, etc.) to autotrophic dinoflagellates (Jacobson and Anderson, 1992; Naustvoll, 2000; Jeong et al., 2010). It has been reported that some *Protopteridinium* species feed on copepod eggs and nauplii or their detritus, some even prefer cannibalism (at least in culture), if other food resources are inadequate (Jeong and Latz, 1994; Naustvoll, 2000). Studies have shown that *Protopteridinium* consumes prey through a unique mechanism. The specialized pseudopodia-like structure, called the ‘pallium’ enables them to feed on prey organisms and digestion occurs external to the *Protopteridinium* cell (Jacobson and Anderson, 1992). This feeding adaptation enables *Protopteridinium* to consume prey as large as or larger than themselves (including chain-forming diatoms) (Naustvoll, 2000), and thus they can compete with mesozooplankton for food resources (within the trophic level). Several field studies have confirmed that the availability of prey organisms is the main controlling factor for the dominance of *Protopteridinium* species and their cysts along the various eutrophic and productive upwelling regions, and plays important role in trophic dynamics (Kjaeret et al., 2000; Matsuoka et al., 2003; Gribble et al., 2007; Kim et al., 2009) Additionally Protopteridinioids have comparatively faster-swimming rates (Lombard and Cappon, 1971; Jeong and Latz, 1994), which enable them to capture the prey organisms as well as vertical migration to escape from temporary unfavorable conditions like turbidity,

turbulence, etc. (Smayda, 2002). Laboratory feeding experiments demonstrated species specific-prey selection strategies in *Protoperidinium* species. *P. pallidum* prefers diatoms, while *P. steinii* feed better on both diatoms and dinoflagellates (Naustvoll, 2000). *P. crassipes* can feed on phototrophic dinoflagellates (Jeong and Latz, 1994) whereas *P. conicum* prefer to feed on *Ditylum brightellii* (Menden-Deuer et al., 2005). Species like *P. divergens* can have specific prey preference (to *P. micans*), which response negatively to change in feeding organisms (Kjaeret et al., 2000). This type of prey-predator relationship in case of *Protoperidinium* is difficult to establish in the natural ecosystem (Kjaeret et al., 2000; Gribble et al., 2007). However, in the natural ecosystem food availability considerably important than other environmental variables in regulating population growth and distribution of *Protoperidinium* species (Dodge, 1994; Kjaeret et al., 2000). In the Study region, abundance and diversity of *Protoperidinium* was higher during the SWM and FIM in the PK transect, whereas in CP transect during SWM and NEM. This trend in *Protoperidinium* coincides well with the diatom distribution pattern (Fig. 2.5b and d; 2.8a and b) in the Bay of Bengal (discussed in next section).

2.5.2 Responses of cyst-forming dinoflagellate community to the monsoons

The orientation of dinoflagellate assemblage together with different environmental variables in the RDAs emphasizes seasonal and geographical differences in the distribution of dinoflagellate population in the region. Seasonal monsoonal interventions also play an important role in the distribution of cyst-forming dinoflagellates assemblage in the Bay of Bengal. The Protoperidinoids dominated dinoflagellate population at the northernmost RM station (22) throughout the sampling

period. Generally during the SWM heavy rainfall into the catchment area brings a heavy load of nutrient enriched freshwater inflow in the northern Bay region. This supports the increased production in this region. Similarly, the EICC carries these nutrient enriched waters towards the offshore region in the northern Bay. The RDA orientation of station 21 towards RM region during the SWM suggests the availability of diatoms fueled by nutrient enrichment supports regional Protoperidinoids dominance (Fig. 2.9a and b). At RM, an abundance of phototrophic species, *Gonyaulax* and *Alexandrium* spp. was comparatively higher during the NEM, FIM and SIM (Fig. 2.7 b, c, d). These phototrophic species have an optimum light requirement for growth (Prezelin et al., 1986; Lim et al., 2006; Susek, 2005). Thus, increased light intensity due to reduced suspended load during these seasons could support their increased abundance in the surface waters.

Regional differences in cyst forming dinoflagellate population were prominent in the PKOS and AR region, mainly influenced by the seasonally varying riverine influx. In the PKOS region moderately influenced by the riverine influx at the northern side (stations 21), especially during SWM (discussed in the previous paragraph), whereas oceanic conditions prevail along the southern stations (Stations 20, 19, 18, 17 and 16). Similarly in the AR region station 14 and 15 clustered together in stations RDA ordination (Fig. 2.9b). During the SWM, these stations receive Irrawaddy rivers runoff, which eventually supports primary production in this region. The abundance of Protoperidinoids, especially *Archaepridinium minutum* in this region could be resultant of diatom availability. However in the rest of seasons, oceanic conditions prevail along PKOS and AR regions. These regional differences in physical and resultant biological

changes well reflected in the RDA analysis. During NEM, SIM and FIM seasons, the AR stations were generally clustered with the PKOS stations (Fig. 2.10b, 2.11b, and 2.12b), which highlight the prevalence of oceanic conditions. In the northern PKOS region, the dominance of *P. leonis* and *Preperidinium meunieri* in SWM season and *P. claudicans*, *D. lenticulatum* during the NEM emphasize the availability of food material. The presence of phototrophic *G. spinifera*, *L. polyedrum* during the SWM and *P. horologium*, *A. tamarensis* during the NEM and FIM along the southern part highlight prevalence of light availability.

The sampling stations in the CPOS region experiences oligotrophic conditions except during the NEM season. Cyst-forming dinoflagellate assemblage in this region was characterized by the presence of phototrophic *Gonyaulax* species, *G. spinifera*, *G. scrippsae* and *Gonyaulax* spp. These species can grow in diversified environments, with low to moderate nutrient concentration and elevated temperatures (discussed in Chapter 4A, Section 4.5.2). The presence of these species highlights the warmer oligotrophic conditions in the CPOS region. The prevailing winds trigger weak water mixing during the NEM, which supports moderate nutrient advection and in turn phytoplankton abundance in the surface water. Influence of these physical and resultant biological forces was observed on the cyst forming dinoflagellate species, which was dominated by phototrophic *Alexandrium* spp., *Scrippsiella* spp., *G. scrippsae*, *S. spinifera* and *G. catenatum*. Increased light condition during this period together with moderate nutrient concentration could facilitate their growth in CPOS region. Heterotrophic species like *P. claudicans* and *Preperidinium meunieri* were abundant in the coastal stations during the SWM and during the NEM over the entire region.

Clusters of sampling stations observed in the RDA ordination during the SWM, NEM and FIM were not characterized during the SIM (except RM station) (Fig. 2.12b). Moreover, dinoflagellate population of dominant phototrophic and heterotrophic species was abundant and well dispersed in the region during SIM. The weaker winds are unable to facilitate deep mixing and erode the strong stratification, which eventually leads to the shallow mixed layer depth and oligotrophic conditions. This condition can be observed over a large area of the Bay, except the northern part, where moderate riverine nutrient flux supports phytoplankton production (Madhu et al., 2006; Paul et al., 2008; Gomes et al., 2000; Madhupratap et al., 2003). During this season reduced water mixing, turbulence due to stratified water mass and oligotrophic surface waters with more light availability could facilitate the growth of dinoflagellates (*C* and *S*-strategist) (Smayda and Reynolds, 2003). However in the northern region, sustainable diatom population supports the growth of predatory *Proto-peridinium* population.

2.5.3 Comparison of planktonic and cysts assemblages of dinoflagellates

Comparison of coastal and neritic planktonic dinoflagellate assemblages in the present study with their resting counterparts from sediments (cysts) reveals that cyst population is diverse than planktonic ones (Table 2.2). This type of heterogeneity can be observed in the occasional and/or seasonal samplings (Dale, 1983; Moscatello et al., 2004). However, it is interesting that these assemblage differences are also visible in the long term, regular monitoring (time series) studies like the present one. These differences can be resultant of the practical difficulties like, i) sample preservation technique, which sometimes alters the morphology of planktonic cells, ii) light microscopy limitations in identification of naked/unarmored and small thecate

planktonic dinoflagellates (Orlova et al., 2004). Furthermore, recent molecular studies revealed that the dinoflagellates have high-level intraspecific genetic diversity (Lin et al., 2009). These changes further highlighted in recent cyst-theca relationship and genetic studies in cyst forming dinoflagellate species like *S. trochoidea* species complex, *Protoperidinium* and *Gonyaulax spinifera* member species (Montresor et al., 2003; Gottschling et al., 2005; Gribble and Anderson, 2007; Morquecho et al., 2009). These species possess ‘heterospory’, where single planktonic species from different cyst morphotypes (Head, 1996). This intraspecific heterogeneity can be distinguished up to a large extent in the cyst morphological studies. Therefore, studies including plankton and sediment sampling strategies provide better information on dinoflagellate assemblage (Dale, 1983, Hesse et al., 1996, Satta et al., 2013) and are very much essential in phytoplankton ecology and harmful algal bloom monitoring programs.

2.6 Conclusion

In the Bay of Bengal, seasonal monsoonal interventions play an important role in the distribution of cyst-forming dinoflagellates assemblage. A small portion of planktonic dinoflagellates (~10%) have cyst-formation capability but substantially contributes to the dinoflagellate flora in the surface waters. In the region, stratified and nitrate-deficient waters, promote stasis of the resident cyst-forming dinoflagellate population. The predominance of *S. trochoidea* and Protoperidinoids emphasize feeding adaptability (mixotrophy and heterotrophy) are important survival strategies in this oligotrophic waters. Additionally, the prevalence of mixotrophic, *S. trochoidea* during SIM and late SWM highlight the light availability with a clear sky and no rainfall

facilitate their proliferation. The dominance of *Protooperidinium* in the region, especially at embayment suggests food availability (mainly diatoms) support their distribution.

Regional and seasonal variances in phototrophic dinoflagellates prevalence illustrate the effect of possible niche differentiation on their distributions. Increased light, temperature, reduced rainfall and suspended load with low to moderate nutrient concentrations during the NEM, FIM and SIM facilitate the growth of Gonyaulacoid species in the region. Further, the comparison of cyst-forming species data with coastal cyst mapping studies emphasizes that the intraspecific heterogeneity can be distinguished up to a large extent in the cyst morphological studies. Therefore, both planktonic and sediment sampling strategies can provide an illustration of dinoflagellate population in the coastal region.

Appendix

Supplementary data associated with Chapter 2 can be found in Appendix I

Chapter 3
Distribution of dinoflagellate cyst in recent
sediments along the Indian coast

3A Dinoflagellate cyst distribution along the south-western Bay of Bengal

3A.1 Introduction

Dinoflagellates form organic-walled or calcareous cysts (e.g. Wall and Dale, 1968; Head, 1996; Matsuoka and Fukuyo, 2000) as a part of sexual (Steidinger, 1975; Anderson and Wall 1978) or occasionally asexual reproduction (e.g. Figueroa et al., 2008). Approximately 200 marine dinoflagellate species are known to form resting cysts (Head, 1996) as part of their life cycle. Cysts get preserved in sediments for several years (Dale, 1983) and even up to a century (Ribeiro et al., 2011), and serve as potential seed banks that can be important to dinoflagellate bloom dynamics and species dispersal (Anderson et al., 1995; Anderson et al., 1998; Dale, 2001). They remain viable in a ship's ballast tank sediment and biofilms, subsequently transported to different regions by shipping (Drake et al., 2005). Additionally, resting cysts may be introduced to new locations through shellfish transplantation (Anderson and Wall, 1978). The sediments store resting stages produced by the planktonic species present in the region, thus providing a historical archive at different temporal resolutions (Dale, 2001a). Cyst mapping of harmful dinoflagellate species assemblages can provide information about the mechanism of recurrence and spread of HAB species (Anderson et al., 1998). Moreover, by studying the cysts in a specific region, it is possible to record dinoflagellate species whose pelagic stages are rarely observed and difficult to identify (Hesse et al., 1996).

In spite of the importance of dinoflagellate cysts in understanding the population dynamics of vegetative stages, information from the seas around the Indian subcontinent is very limited and mainly restricted to the west coast of India (Godhe et al., 2000; D'Costa et al., 2008; D'Silva et al. 2011). Recently, dinoflagellate cyst assemblage has been studied from surface sediments of Visakhapatnam harbour

(D'Silva et al., 2013). To date, information on modern cyst assemblages and their distributions from other parts of the western boundary of the Bay of Bengal is lacking. This study of dinoflagellate cyst distribution is the first of its kind from the south-western Bay of Bengal (south-east coast of India). The aims of this study are i) to evaluate the spatial variation of dinoflagellate cyst assemblages in surface sediments along the western boundary of the Bay of Bengal, ii) its comparison with planktonic dinoflagellate records, and iii) to compare the cyst abundance in the present study with that of other regions.

3A.2 Materials and methods

3A.2.1 Description of the study region

The sampling stations are located on the Indian continental shelf, in the vicinity of the south-western boundary of the Bay of Bengal. The physical oceanography of the area is controlled by the monsoons. Forming part of the seasonally reversing monsoon-current system, the East Indian Coastal Current (EICC) changes direction twice a year (Shankar et al., 2002). The summer monsoon (May-September) begins in May with strong winds blowing towards the south-west. The clockwise surface current develops in summer, flows in a south-westward direction with a velocity of $\sim 0.2 \text{ m s}^{-1}$. During the winter monsoons (November-February), winds blow north-eastwards. The surface current flows in an anticlockwise direction. The current velocity reaches 0.5 m s^{-1} .

The south-east continental shelf of India is a river-dominated shelf system characterized by inputs of fresh water, suspended sediment and nutrients from the rivers Krishna-Godavari, Cauvery, Ponnaiyar, and Penner. The surface water tends to be rich in silicate, supporting the predominance of diatoms throughout the year (Madhu et al., 2006). Weak, localized wind-driven upwelling has been reported in this

area during the summer monsoon (Shetye et al., 1991). Oceanographic features like sea surface salinity (SSS) and sea surface temperature (SST) are influenced mainly by the reversing EICC and riverine runoff. The average SSS and SST ranges from 27.3 to 30.0 and 25.6 to 34.5°C respectively.

The characteristics of the shelf sediments vary from north to south. The south is dominated by silty-sand, whereas clayey-silt and silty-clay are present in the north (Musale and Desai, 2010). The sediments along the continental shelf are thought to be fresh owing to the high sedimentation through riverine input.

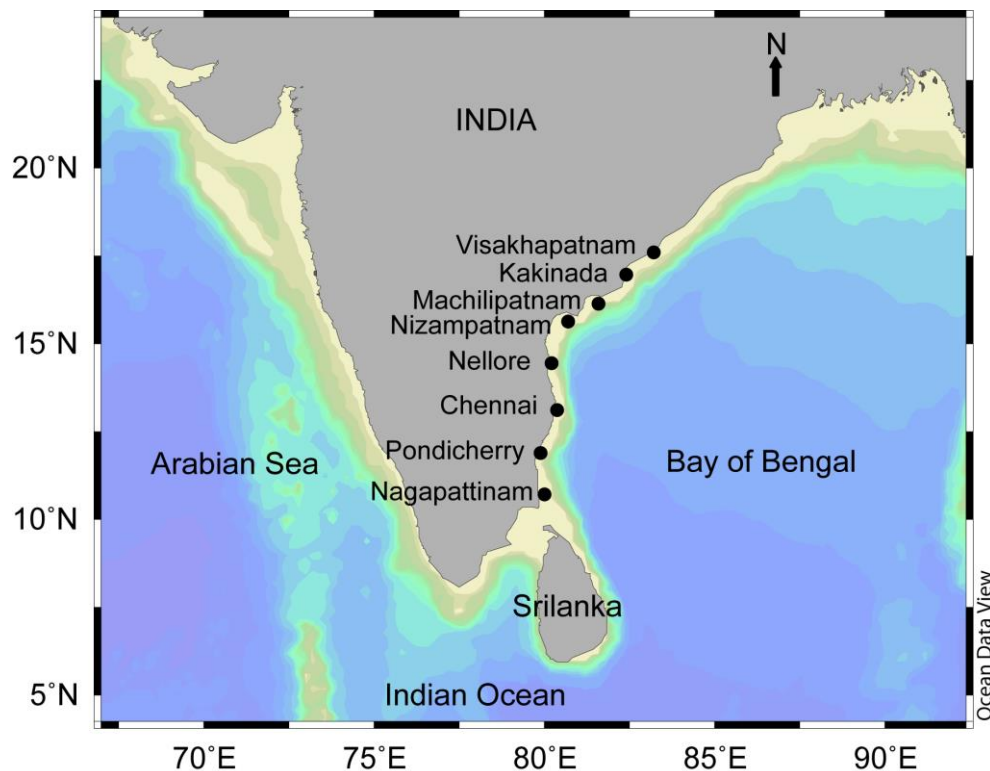


Fig. 3A.1 Location of sampling stations along the south-western Bay of Bengal

3A.2.2 Sediment sampling

Surface sediments were collected from 8 stations (covering a distance of 63 nautical miles) along the western boundary of the Bay of Bengal (off the south-east coast of India) (Fig. 3A.1, Table 3A.1) during the Sagar Sukti cruise (SASU 125) in the winter

monsoon (December 2006). At each station (except Visakhapatnam) sediment sampling was carried out at 2-3 different sites at intervals of 2 nautical miles. Surface sediment samples were collected using a modified van Veen grab (grabbing area 0.04 m²) equipped with flaps on the top, enabling cores of surface sediments to be collected. Duplicate sediment cores (PVC cores, 25 cm long, inner diameter of 2.5 cm) were obtained with the grab. At Visakhapatnam, a sample was collected at only one position with a gravity corer (1 m length, inner diameter 5 cm). All sediment cores (PVC and gravity) were sectioned at 2 cm intervals, mixed well and stored in airtight plastic bags at 4°C in the dark.

Table 3A.1 Geographical coordinates and cyst abundance (cysts g⁻¹) at the sampling stations along the south-western Bay of Bengal. Note: data on sediment characteristics for the stations marked with an asterisk was obtained from Musale and Desai (2010).

Station Name	Latitude (°N)	Longitude (°E)	Water depth (m)	Samples analysed	Cyst abundance	Sediment characteristics (%)		
						Sand	Silt	Clay
Visakhapatnam	17.58	83.23	31	6	331	0.7	41.2	58.1
Kakinada*	16.95	82.41	30	10	128	0.8	42.5	56.7
Machilipatnam*	16.15	81.58	27	12	89	1.4	50.0	48.6
Nizamapatnam*	15.61	80.66	20	10	59	1.6	67.5	30.9
Nellore*	14.45	80.23	24	8	83	61.5	19.3	19.1
Chennai	13.10	80.40	30	8	45	80.5	13.3	6.2
Pondicherry*	11.91	79.91	27	8	29	79.8	12.4	7.8
Nagapattinam	10.70	80.03	25	4	63	81.8	11.7	6.5

3B.2.3 Sediment preparation, processing, and analysis

Sediment samples from the upper 0-2 cm sections of each sediment core were treated using a palynological method (Matsuoka and Fukuyo, 2000) with some modifications (D'Costa et al., 2008). A known weight (2-3 g) of wet sediment was repeatedly washed with distilled water to remove salts. The salt-free sample was treated with 7 ml 10% HCl to dissolve calcareous minerals and then with 30% HF to dissolve silicate materials. Each chemically treated sample was rinsed 3-4 times with

distilled water to remove the acid. Subsequently, the acid-free slurry was sieved through a tier of two different meshes (120 and 20 μm) to remove coarse and fine material. The residue accumulated on the 20 μm mesh was then suspended in 10 ml distilled water and stored in a vial. For the quantification of calcareous cysts, 2-3 g of wet sediment samples were rinsed with distilled water only and sieved through 120 and 20 μm meshes without any acid treatment. The sieved sample (10 ml) was then stored in a vial until further analysis.

For microscopic identification of dinoflagellate cyst, an aliquot of the processed sample was diluted to a total volume of 2 ml in a transparent Petri dish (3.8 cm diameter), mixed well and placed on the microscope stage. After the sample had settled, the entire Petri dish was scanned under an inverted microscope (Olympus IX 71), equipped with a digital camera Olympus CAMEDIA C-4040ZOOM) at 100 and 400X magnifications. Depending on the volume of the aliquot, the processed sample was counted in duplicate or a higher number of replicates, such that a total of 2 ml was analysed. Dinoflagellate cysts were identified on the basis of the published literature (Wall and Dale, 1968; Sonneman and Hill, 1997; Matsuoka and Fukuyo, 2000).

A known weight (1 g) of wet sediment sample was dried at 70°C for 24 h to estimate the water content (Matsuoka and Fukuyo, 2000). Cyst concentration was calculated as the number of cysts per gram of dry sediment (cysts g^{-1}) using the formula $N/W (1-R)$, where N-number of cysts, W-weight of sediment and R-proportion of water in the sediment.

The percentage grain size composition of the sediment (sand, silt, and clay) was determined by standard wet sieving (for sand) and pipette analysis (for silt and clay) (Buchanan, 1984). In this study, sediment samples from three stations

(Visakhapatnam, Chennai, and Nagapattinam) were analysed for grain size composition, while data from other stations and the same period were obtained from Musale and Desai (2010). The size classification used was sand ($> 62 \mu\text{m}$), silt ($62\text{-}3.9 \mu\text{m}$) and clay ($< 3.9 \mu\text{m}$).

To assess the distribution of cyst-producing dinoflagellate species in the study area, the information collected from previous studies (Madhav and Kondalarao, 2004) on the distribution of dinoflagellate planktonic cells during different seasons from the same study region is presented together with cyst data (present study; Table 3A.1). Although several reports on phytoplankton distribution are available, we selected for comparison only those in which dinoflagellates from the sampling region were identified down to species level.

3A.2.4 Data analysis

The abundance of dinoflagellate cysts was converted into a lower triangular similarity matrix using the Bray-Curtis coefficient. This similarity matrix was then subjected to cluster analysis by the group average method to evaluate the spatial variation. All the analyses were carried using PRIMER software 5.

3A.3 Results

3A.3.1. Dinoflagellate cyst assemblage

A total of 24 dinoflagellate cyst morphotypes were recorded in the sediment samples collected along the south-western Bay of Bengal (Table 3A.2; Fig. 3A.2). 20 of these 24 cyst types were identified to species level and 2 to genus level (*Protoperidinium* sp. type 1 (PpS1) and *Protoperidinium* sp. type 2 (PpS2); Table 2, Fig. 3m-n). The remaining 2 cyst morphotypes (Fig. 3A.3o-p) could not be identified as they lacked identifying structures and germination were not successful. Hence,

depending on their morphology, they are characterized as dinoflagellate cyst type 1 (DC1) or dinoflagellate cyst type 2 (DC2). Furthermore, cysts belonging to the *Gonyaulax spinifera* species complex, i.e. *Spiniferites mirabilis* and *S. membranaceus*, are recorded as *Gonyaulax spinifera* complex in this study. The light microscopy photomicrographs of dinoflagellate cysts recorded are provided in Figure 3A.3.

Table 3A.2 List of cyst-forming dinoflagellates from the south-western Bay of Bengal compiled from earlier published planktonic data (PBOB) and dinoflagellate cysts recorded previously along the southeastern Bay of Bengal (SBOB). References indicated as superscript numbers: ¹ Madhav and Kondalarao, 2004; ^U Unpublished XBT-project data. [†] Potentially harmful species; ^{††} red-tide-forming species; [#] calcareous cyst species. ^{\$}Unidentified cyst morphotypes recorded in the present study.

Planktonic dinoflagellate (Biological name)	Dinoflagellate cyst (Paleontological name)	Species code	PBOB	SBOB
Autotrophic				
<i>Alexandrium</i> sp.			• ¹	
<i>Gonyaulax diacantha</i>			• ^U	
<i>Gonyaulax digitalis</i> , <i>G. spinifera</i> complex	<i>Spiniferites bentori</i>	Sben	• ¹	•
<i>Gonyaulax scrippsae</i> , <i>G. spinifera</i> complex	<i>Spiniferites ramosus</i>	Sram		•
<i>Gonyaulax spinifera</i> complex [†]	<i>Spiniferites mirabilis</i>	Smir		•
<i>Gonyaulax membranaceus</i> , <i>G. spinifera</i> complex	<i>Spiniferites membranaceus</i>			
<i>Gyrodinium impudicum</i>	-	Gyrl		•
<i>Lingulodinium polyedrum</i> [†]	<i>Lingulodinium machaerophorum</i>	Lmac		•
<i>Protoceratium reticulatum</i> [†]	<i>Operculodinium centrocarpum</i>	Ocen		•
<i>Pyrophacus steinii</i>			• ^U	
<i>Scripsiella trochoidea</i> ^{††#}			• ^U	
<i>Scripsiella</i> sp.			• ^U	
Heterotrophic				
<i>Diplopsalis lenticula</i>			• ¹	
<i>Protoperidinium avellana</i>	<i>Brigantedinium cariacense</i>	Bcar		•
<i>Protoperidinium cf. avellana</i>	-	CBcar		•
<i>Protoperidinium claudicans</i>	<i>Votadinium spinosum</i>	Vspi	• ¹	•
<i>Protoperidinium compressum</i>	<i>Stelladinium stellatum</i>	Sste		•
<i>Protoperidinium conicum</i>	<i>Selenopemphix quanta</i>	Squa	• ¹	•
<i>Protoperidinium excentricum</i>			• ¹	
<i>Protoperidinium grandii</i>			• ¹	
<i>Protoperidinium latissimum</i>	-	Plat		•
<i>Protoperidinium leonis</i>	<i>Quinquecuspis concreta</i>	Qcon	• ¹	•
<i>Protoperidinium nudum</i>	-	Pnud		•
<i>Protoperidinium oblongum</i>	<i>Votadinium calvum</i>	Vcal	• ¹	•
<i>Protoperidinium pentagonum</i>	<i>Trinovantedinium applanatum</i>	Tapp	• ¹	•
<i>Protoperidinium subinermis</i>	<i>Selenopemphix nephroides</i>		• ¹	
<i>Protoperidinium thorianum</i>	-	Ptho		•
<i>Protoperidinium</i> sp.	<i>Lejeunecysta</i> sp.	Leje		•
<i>Protoperidinium</i> sp.	<i>Stelladinium robustum</i>	Srob		•
<i>Zygabikodinium lenticulatum</i> / <i>P. meunieri</i>	<i>Dubridinium caperatum</i>	Dcap		•
<i>Protoperidinium</i> sp. Type 1 ^{\$} -		PpS1		•
<i>Protoperidinium</i> sp. Type 2 ^{\$} -		PpS2		•
Dinoflagellate cyst type 1 ^{\$} -		DS1		•
Dinoflagellate cyst type 2 ^{\$} -		DS2		•



Fig. 3A.2 Dinoflagellate cyst abundance (cysts g⁻¹) of each species in the surface sediments at 8 sampling stations along the south-western Bay of Bengal. The error bar represents the standard deviation from the mean. Cluster grouped four stations are shown by grey shaded horizontal bars. For the species code, please refer Table 3A.2.

The dinoflagellate cyst assemblage was dominated by heterotrophic Protoperidinioid species, *Quinquecuspis concreta* (*P. leonis*, 13%), *Trinovantedinium applanatum* (*P. pentagonum*, 11%), and *Stelladinium stellatum* (*P. stellatum*, 8.5%) (Fig. 3A.2). Phototrophic dinoflagellates consisted of six species (Fig. 3A.2). Among them *Operculodinium centrocarpum*, (*Prorocentrum reticulatum*, 10%), *Spiniferites mirabilis* and *S. membranaceus* complex (*G. spinifera* species complex, 9%) and *Lingulodinium machaerophorum* (*L. polyedrum*, 8%) were abundant.

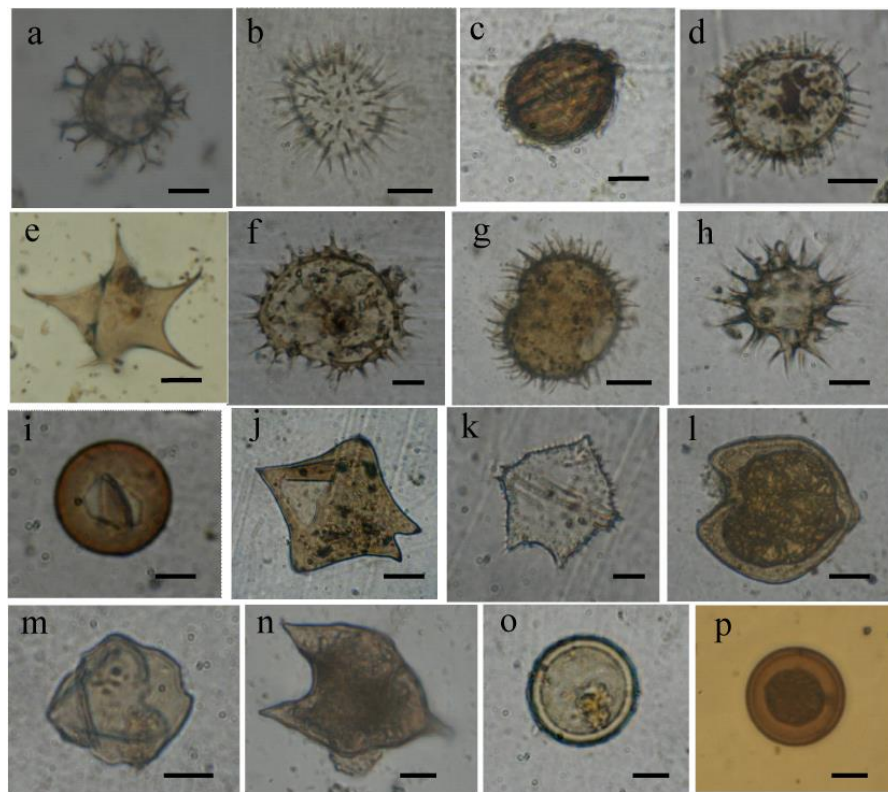


Fig. 3A.3 Photomicrographs of dinoflagellate cysts recorded from the recent sediments along the south-western Bay of Bengal: (a) *Gonyaulax spinifera* complex, (b) *Lingulodinium machaerophorum*, (c) *Zygabikodinium lenticulatum*, (d) *Operculodinium centrocarpum*, (e) *Stelladinium stellatum*, (f) *Selenopemphix quanta*, (g) *Votadinium spinosum*, (h) Cyst of *Protoperidinium nudum*, (i) *Brigantedinium cariacense*, (j) Cyst of *Protoperidinium latissimum*, (k) *Trinovantedinium applanatum*, (l) *Votadinium calvum*, (m) *Protoperidinium* sp. 1, (n) *Protoperidinium* sp. 2, (o) Dinoflagellate cyst type 1, (p) Dinoflagellate cyst type 2. All scale bars 20 μm .

3A.3.2. *Dinoflagellate cyst distribution*

The dinoflagellate cyst abundance ranged from 29 to 331 cysts g^{-1} , and their numbers increased from southern (Nagapattinam) to northern (Visakhapatnam) stations (Fig. 3A.4a, Table 3A.1). Cyst abundance was influenced by the sediment characteristics. Cyst abundance was higher in fine-grained (silt-clay dominated) sediments than in sandy sediments (Table 3A.1). Cluster analysis of the sampling stations based on the dinoflagellate cyst assemblage at the 50% similarity level revealed one group of four stations (Machilipattinam, Kakinada, Nellore, and Nizampatnam) and four ungrouped stations (Fig. 3A.5). The grouped stations had a higher cyst abundance (59 to 128 cysts g^{-1}). Among the four ungrouped stations, the cyst abundance (331 cysts g^{-1}) was the highest at Visakhapatnam and lower at the other three stations (Nagapattinam, Chennai, and Pondicherry; Fig. 3A.4a, Table 3A.1).

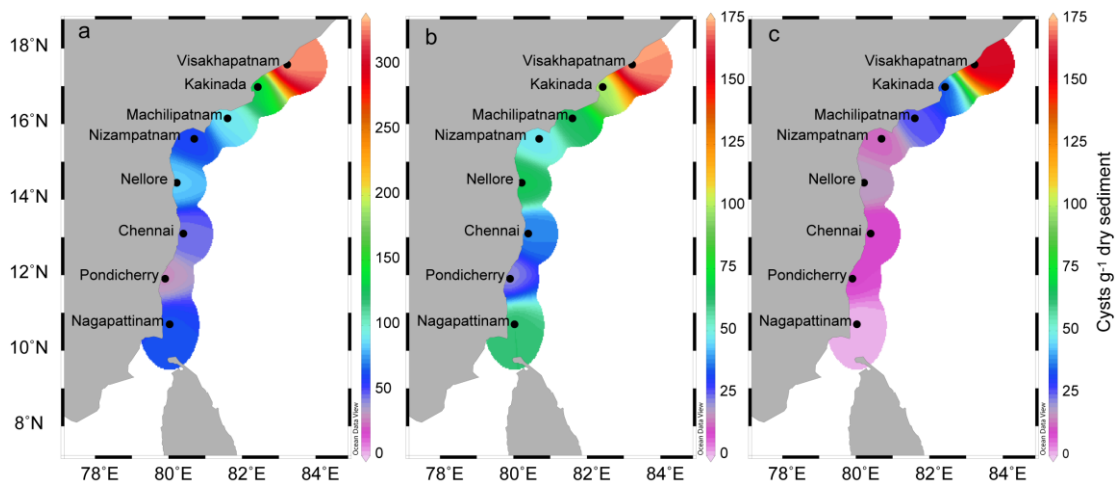


Fig. 3A.4 Spatial distribution of (a) total dinoflagellate cysts, (b) heterotrophic dinoflagellate cysts and (c) phototrophic dinoflagellate cysts.

3A.3.3. Comparison of dinoflagellate cysts and planktonic dinoflagellates

Comparison of the present data with the collated information on the cyst-forming species revealed that 14 cyst-producing dinoflagellate species present in the sediments (cysts) had not been previously identified in planktonic samples (Table 3A.2). Among these, the *Gonyaulax spinifera* complex (*S. membranaceus* and *S. mirabilis*), *L. machaerophorum* and *O. centrocarpum* dominated the cyst assemblage and had not been previously recorded in the planktonic form. Furthermore, 8 cyst-producing dinoflagellate species previously recorded in the planktonic samples were not observed in their cyst forms (Table 3A.2). Cysts of calcareous species were not observed in the sediment sample treated without acid.

3A.4. Discussion

3A.4.1. Comparison of dinoflagellate cyst abundance with different regions

Zonneveld et al. (2013) summarized the global distribution of dinoflagellate cysts from recent sediments and their relationship to environmental conditions. The compilation presented here includes data sets on the dinoflagellate cyst distribution from this study region that were not published in any earlier compilation. The global distribution of dinoflagellate cyst abundance as collated from the literature and the present study is given in Table 3A.3. For this comparison, studies that used similar sample processing (acid treatment) and cyst abundance presentation methods (cysts g^{-1}) are considered. The present compilation revealed that the cyst abundance recorded in this study was low (29 to 331 cysts g^{-1}) as compared to sub-tropical and temperate coastal regions (Table 3A.3). However, the cyst abundance recorded is on a par with that of other tropical regions (Table 3A.3), such as the coasts of south-east Asia (Furio et al., 2012) and the west coast of India (Godhe et al., 2000; D'Costa et al., 2008; D'Silva et al., 2011).

Table 3A.3 Records of dinoflagellate cysts abundance from different parts of the world.

Study areas	Cyst abundances	References
A Offshore southeast Greenland	102-7920	Boessenkool et al., 2001
b Mediterranean Sea	177-929	Elshanawany et al., 2010
Izmir Bay (Aegean Sea, Eastern Mediterranean)	41-3292	Aydin et al., 2011
c North Canary Basin, NW Africa	192-13147	Targarona et al., 1999
Benguela upwelling, off SE Africa	139-38580	Holzwarth et al., 2007
Offshore NW Iberia	15000- >75000	Sprangers et al., 2004
d Chinese Coastal waters	154-113483	Wang et al., 2004
Yellow China sea	114-20828	Hwang et al., 2011
Geoje Island, Korea	528-2834	Shin et al., 2007
Tokyo bay, Japan	240-8380	Matsuoka et al., 2003
e Southern Ocean (eastern Atlantic sector)	74-8714	Esper and Zonneveld, 2002
f Eastern Australia	100-20000	McMinn, 1990
g Sabah, Malaysia	2-411	Furio et al., 2006*
Northwestern and Central Philippines	30-580	Furio, et al., in press*
Northwestern Philippines	43-1940	Baula et al., 2008*
h MPT and JNPT Mumbai, India	36-262	D'Costa et al., 2008
Zuari estuary, India	150-570	Patil (Unpublished)
West coast of India	6-1076	D'Silva et al., 2011
Sediment core	71-19880	D'Silva et al., 2012
i Visakhapatnam harbour, India	15-1218	D'Silva et al., 2013
Southeast coast of India	29-331	Present study
South Andaman Region	21-355	Present study (Chapter 5)

The abundance of dinoflagellate cysts (139 to 75,000 cysts g^{-1}) along the western boundaries of the African subcontinent (Table 3A.3), has been related to intensive upwelling (Targarona et al., 1999; Sprangers et al., 2004; Holzwarth et al., 2007). A high dinoflagellate cyst abundance (100 to 25,000 cysts g^{-1}) is also recorded in the Arctic and Atlantic confluence (Table 3A.3). In sub-polar regions with highly variable nutrient supplies and environmental conditions (Solignac et al., 2009), opportunistic species with higher growth rates are favoured, resulting in a lower species richness (Barton et al., 2010). In the Mediterranean Sea (Table 3A.3) the high cyst abundance is influenced mainly by river plumes and eutrophic waters in coastal regions (Elshanawany et al., 2010; Aydin et al., 2011). Another region where high cyst numbers are reported embraces the waters around China, Korea, and Japan (Table

3A.3); this has been related to eutrophication (Matsuoka et al., 2003; Shin et al., 2007). Furthermore, a high abundance (in thousands) of dinoflagellate cysts has been recorded in sediment traps in the western Arabian Sea upwelling region (Zonneveld and Brummer, 2000). Compared to these numbers, the dinoflagellate cyst abundance reported in recent sediments along the coasts of India is low (Table 3A.3), even though the west coast of this subcontinent is influenced by upwelling and the south-west monsoon. The present regional cyst abundance comparison highlight that, though different sets of environmental parameters influence cyst formation in different parts of Indian region (discussed in Chapter 3C), however, cyst abundance does not reveal the much regional difference. Further intensive studies are needed to investigate the reason for the small numbers of dinoflagellate cysts in the region.

3A.4.2. Cyst assemblages along the south-western Bay of Bengal

Along the study region, the cyst abundance decreased from north to south (Fig. 3A.4a). It has been observed that the differences in cyst abundance and assemblage composition between areas are caused primarily by differences in the abundance of vegetative cells and their cyst production efficiencies, and/or by differences in the hydrology and the sedimentary regime (Anderson et al., 1995; Dale, 1983; Joyce et al., 2005). Dinoflagellate cysts are believed to have the hydrodynamic characteristics of fine silt-sized particles (Dale, 1983; Kawamura, 2004) and can be transported by water currents. In the study area, the abundance of dinoflagellate cysts can be correlated with the texture of the sediment, i.e. silt and clayey sediment. A high cyst abundance was encountered in the fine-grained (silt and clayey) sediments as compared to the sandy sediments (Table 3A.1). The southern stations (Chennai, Pondicherry and Nagapattinam, 3 ungrouped stations, Fig. 3A.5) contain a high percentage of sand, which is not suitable for cyst deposition (Dale, 1983), while the

sediments at the northern stations (Nellore, Nizampatnam, Machilipattinam, Kakinada, and Visakhapatnam) are characterized by high percentage of silt-clay and a high cyst abundance (Table 3A.1). These results indicate that sediment grain size plays a major role in determining the cyst distribution in this area.

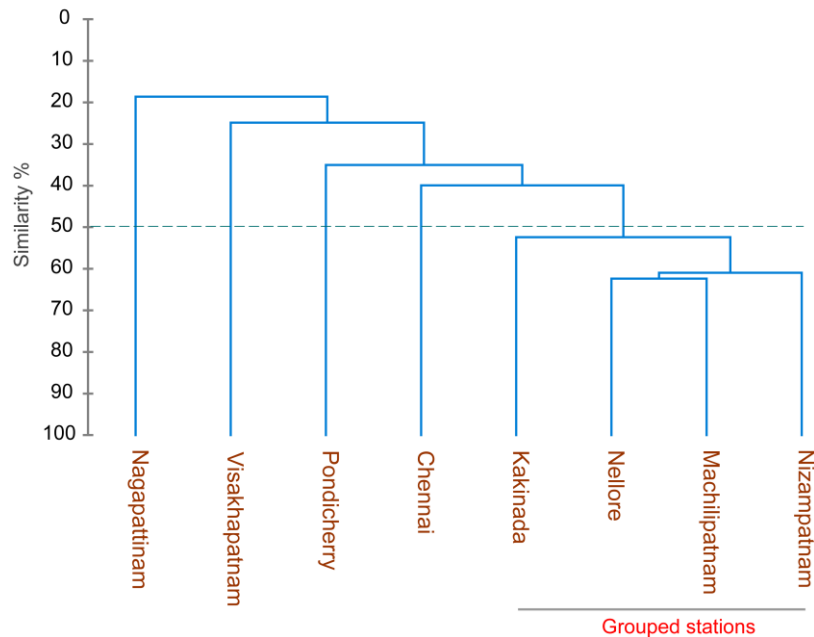


Fig. 3A.5 Cluster dendrogram of sampling stations relationship using the Bay Curtis similarity coefficient and group average method.

Apart from this, other processes, like bio- and oxidative degradation, benthic predation, and bioturbation, also influence the cyst assemblage and distribution in the sediments (Zonneveld et al., 1997a; Persson and Rosenberg, 2003). A contemporaneous study investigating the macrobenthic community along the south-east coast of India (Musale and Desai, 2010) indicated the dominance of burrowing and subsurface deposit-feeding polychaetes (e.g. *Magelona cincta*, *Cirratulus* sp., *Capitella capitata* etc.), and bivalves in the silty-clayey sediments at the northern stations (Nellore, Nizampatnam, Machilipattinam and Kakinada), where cyst abundance was comparatively higher. At Pondicherry, the loose sandy sediment harboured only a few surface feeding polychaetes (*Prionospio* spp., *Amphiarete* sp.)

and the cyst abundance was low. It has been reported that *Protoperidinium* cysts are more susceptible to degradation by the activity of deposit-feeding animals than the cysts of phototrophic species such as *O. centrocarpum*, *L. machaerophorum*, and *Spiniferites* spp. (Persson and Rosenberg, 2003). However, in this study, Protoperidinoid cysts were dominant, indicating that bioturbation and predation by benthic fauna are unlikely to be the major factors determining the composition of the cyst assemblages.

Another study from the west coast of India (D'Silva et al., 2011) reported the dominance of heterotrophic forms (*Protoperidinium* spp.). Their dominance is generally attributed to i) elevated nutrient concentrations and high productivity (Harland et al., 2006), ii) availability of prey organisms such as diatoms (Matsuoka et al., 2003; Godhe and McQuoid, 2003), iii) reduced light intensity (Dale 2001b) and iv) the smaller production of phototrophic dinoflagellates (Dale, 2001b). As in any other tropical coastal environment, the high nutrient supply through the riverine material, the dominance of diatoms (Madhu et al., 2006) and the low light penetration due to suspended riverine loads could be the governing factors ensuring the dominance of heterotrophic dinoflagellates over phototrophic dinoflagellates in this coastal region.

At Visakhapatnam station, phototrophic species mainly *O. centrocarpum*, *L. machaerophorum* and *Spiniferites* species contributed significantly to the total cyst abundance (Figure 3A.2). Earlier studies indicated that the dominance of phototrophic forms can be influenced by variable salinity regimes, nutrient inputs and sediment texture (Dale, 2000; Godhe and McQuoid, 2003; Kawamura 2004). The dominance of *O. centrocarpum* in Visakhapatnam harbour has also been correlated with elevated nutrient inputs (D'Silva et al., 2013). The present sampling station at Visakhapatnam

is part of the mesotrophic environment (Tripathy et al., 2005) in the vicinity of Visakhapatnam harbour and is influenced by a varying salinity (range 17 to 35) that is due to terrestrial runoff and the current circulation pattern (Vijaykumaran, 2005). It is possible that a high nutrient input and varying salinity regimes could be the reason for the dominance of phototrophic forms. Cysts of *Alexandrium affine*, *A. minutum*, *Cochlodinium* sp., *Pentapharsodinium dalei*, *Pyrophacus steinii*, *Diplopelta parva*, *Protoperidinium denticulatum* and *P. subinermis*, reported from Visakhapatnam harbour (D'Silva et al., 2013), were not observed at this station (Table 3A.2), which is located approximately 4 km away from the harbour.

3A.4.3. Comparison of dinoflagellate cysts and planktonic dinoflagellates

Studies including plankton and sediment sampling provide better information on dinoflagellate species composition in a given area, since this sampling strategy allows, i) recognition of both mobile and cyst stages (Dale, 1983), ii) identification of rare dinoflagellate species whose planktonic stages are rare and difficult to identify (Hesse et al., 1996), iii) provides a glimpse of seasonally and annually varying dinoflagellate community in a given area (Dale, 1983; Moscatello et al., 2004) and, iv) facilitates detection of harmful species not previously reported in the region (Satta et al., 2013). Thus, generally the number of dinoflagellate species in a study area increases when information on cysts is included in the study (Persson and Rosenberg, 2003; Orlova et al., 2004; Satta et al., 2010).

Fourteen cyst-forming dinoflagellate species not previously identified in planktonic samples were detected in the sediments analysed in this study (Table 3A.2). This may be due to the sample preservation technique, which sometimes alters the morphology of planktonic cells. Particularly, the light microscopic identification of naked/unarmoured vegetative dinoflagellates is more difficult in the preserved state

than of their cyst forms. The small size thecate *Gonyaulax* (*Spiniferites*) species like *G. spinifera* and *G. scrippsae* are very difficult to differentiate in poorly preserved samples. Apart from this, the identification of small thecate dinoflagellates is difficult without an exhaustive thecal plate analysis (Orlova et al., 2004). Consequently, some taxa of the genera *Protoperidinium*, *Gonyaulax*, *Gymnodinium*, and *Gyrodinium* are usually identified only to generic level. These identification difficulties affect the comparative taxonomic analysis. Seasonal cycles in the occurrence of vegetative cells and benthic cysts could be another factor for the mismatch.

On the other hand, the eight cyst-forming dinoflagellate species observed in planktonic form were previously not recorded in recent sediments (Table 3A.2). This may be attributed to i) the low production of cysts in the water column, which is insufficient to produce a detectable quantity of cysts; ii) the acids used in the palynological method of sediment preparation, which dissolves the calcareous cyst wall and/or cyst. Hence calcareous cyst-forming *S. trochoidea* and other *Scripsiella* spp. may be overlooked in such samples (Montresor et al., 1998). This could result in an underestimation of the total dinoflagellate cyst abundance. To resolve this, microscopic analysis of untreated, distilled water cleaned and sieved sediment samples was carried out. The absence of these species in an untreated sediment sample highlights the undetectable quantity of cysts production rather than the methodology used for sediment preparation.

Cysts of potential yessotoxin producing (YTXs) *Protoceratium reticulatum* (*O. centrocarpum*), *Lingulodinium polyedrum* (*L. machaerophorum*) and *Gonyaulax spinifera* complex (*Spiniferites* species analogs) have been reported from the surface sediments of the south-western Bay of Bengal. Since from this region yessotoxin

toxicity incidences have not been reported, the potential of these YTXs species to produce toxicity event is unknown and need further study.

3A.5 Conclusion

The present study of the dinoflagellate cyst distribution along the southwestern Bay of Bengal recorded a southward decrease in cyst abundance that was influenced mainly by sediment texture (a high cyst abundance in silt-clay and a low one in sandy sediments). Fourteen cyst-forming dinoflagellate species including three potentially harmful ones (*G. spinifera*, *O. centrocarpum* and *L. machaerophorum*), not previously reported in planktonic samples, were recorded for the first time. The abundance of autotrophs along with heterotrophic dinoflagellate at Visakhapatnam region highlight effect of anthropogenic nutrient inputs on dinoflagellate population. Cyst abundance along the study region is low compared to subtropical and temperate coastal regions but is similar to that in other tropical regions, including the west coast of India and South Andaman region.

3B Assessing the monsoonal control on dinoflagellate cyst distribution in recent sediments along the north-western Bay of Bengal

3B.1 Introduction

The Bay of Bengal (the Bay) has a uniquely connected system of climatic, oceanographic and biological processes controlled by the seasonality in monsoon and resultant freshwater-sediment influx through the Ganga-Brahmaputra and other Indian rivers. Conventionally the Bay is supposed to be less productive region than its counterpart i.e. the Arabian Sea (Qasim, 1977; Radhakrishna et al., 1978; Prasanna Kumar et al., 2002). Although the Bay receives enormous riverine nutrient influx, their supply is thought to be scavenged to the deeper sediments due to the narrow shelf (Qasim, 1977). Large seasonal freshwater influx and precipitation makes the surface layers less saline and stratified, which also hampers nutrient advection to the surface layers. Similarly, high suspended load and cloud cover reduce light availability to the phytoplankton growth and productivity during the active riverine influx (Gomes et al., 2000; Prasanna Kumar et al., 2010). To assess the influence of monsoon variability on the biological production and phytoplankton distribution only a few in-situ observations has been carried out in the region (e. g. Gomes et al., 2000; Madhu et al., 2006; Paul et al., 2008; Naik et al., 2011). Still the response of different functional groups of phytoplankton to monsoonal variability and productivity changes are not well studied in the region.

Dinoflagellates represent a portion of the eukaryotic production in the marine region. Dinoflagellate species have different species-specific environmental requirements, hence their cyst distribution in sediments can be well correlated with the environmental (light penetration), physical (salinity, temperature) and biogeochemical (nutrients, feed, oxygen) variables in the water column (Marret and

Zonneveld, 2003; Zonneveld et al., 2013). Due to this dinoflagellate cyst assemblage in sediment presents important tool for paleoenvironmental and paleoceanographic reconstruction studies (Zonneveld and Brummer, 2000; Pospelova et al., 2006; Radi and de Vernal, 2008; Price et al., 2013) as well as tracing the HABs incidences in the region (Anderson et al., 1995; 1998; Dale, 2001a).

In the Bay of Bengal, very few studies have been carried out to address the modern dinoflagellate cyst distribution in surface sediments and are mainly restricted to the Visakhapatnam Harbour (D'Silva et al., 2013). However, the north-western part of the Bay where influx riverine control oceanographic and biological settings remains unexplored. In this study, we analysed modern dinoflagellate cyst assemblage variation in surface sediment samples from the north-western Bay. The aim of the study is to investigate the environmental control on the dinoflagellate cyst assemblage and distribution in recent sediments.

3B.2 Material and methods

3B.2.1 Regional environmental and oceanographic settings

The bay experiences a semi-annual reversal of monsoonal winds, divides the year into the Southwest (SW or summer) and Northeast (NE or winter) monsoons, separated by inter-monsoonal periods (spring and fall inter-monsoon). Strong south-westerly wind blow during the SW monsoon (June-September), which changes the surface East Indian Coastal Current (EICC) flow in a clockwise direction (Shankar et al., 2002; Fig. 3B.1). South-westerly wind favours offshore wind-driven Ekman transport, results into weak upwelling along the southeast coast (De Sousa et al., 1981; Shetye et al., 1991). In the northern region, enormous fresh water supply from the Ganga-Brahmaputra (annual mean runoff 11892 and 16186 m³s⁻¹ respectively) and Mahanadi River (1710 m³s⁻¹) systems substantially lowers salinity (Varkey et al.,

1996) and also reduces the upwelling intensity (Shetye et al., 1991). The warm and low salinity surface water strengthen the upper ocean stratification (Prasanna Kumar et al., 2002; Narvekar and Prasanna Kumar, 2014). The strong winds prevailing during this season is unable to erode the strong stratification, shallow the mixed layer depth (<10m) (Narvekar and Prasanna Kumar, 2014). In the region, higher fluvial nutrient supply supports the increase in total phytoplankton biomass, whereas moderate levels of the primary production and chlorophyll indicates the possible light limitation due to increased riverine suspended load and cloud cover (Gomes et al., 2000; Madhupratap et al., 2003; Madhu et al., 2006; Prasanna Kumar et al., 2010; Narvekar and Prasanna Kumar, 2014). Along the southwest inshore region, shallow nitracline due to river discharge and partly upwelling process (Madhu et al., 2006), controls total phytoplankton abundance and primary production (Radhakrishna et al., 1978; Madhu et al., 2006).

With the onset of fall intermonsoon, winds over the bay drastically reduce their speed in the north. Although precipitation strength decreases during this period, overall nutrient and chlorophyll distribution pattern along the region is similar as like the summer monsoon (Narvekar and Prasanna Kumar, 2014).

During the NE monsoon (November-February), the surface current flows in an anticlockwise direction (Shankar et al., 2002; Fig. 3B.1). The net cooling and increased salinity due to high evaporation, lead to a rapid decrease in upper water column thermal stratification along the offshore region. However, intense stratification by the fresh water cap does not lead to convective mixing and nutrient supply to upper layers in the northern region (Gomes et al., 2000). Still, increased nitrate and silicate concentration along with the deep light in the water column fuel

growth of phytoplankton and primary production in the shore region (Gomes et al., 2000; Madhu et al., 2006; Paul et al., 2008).

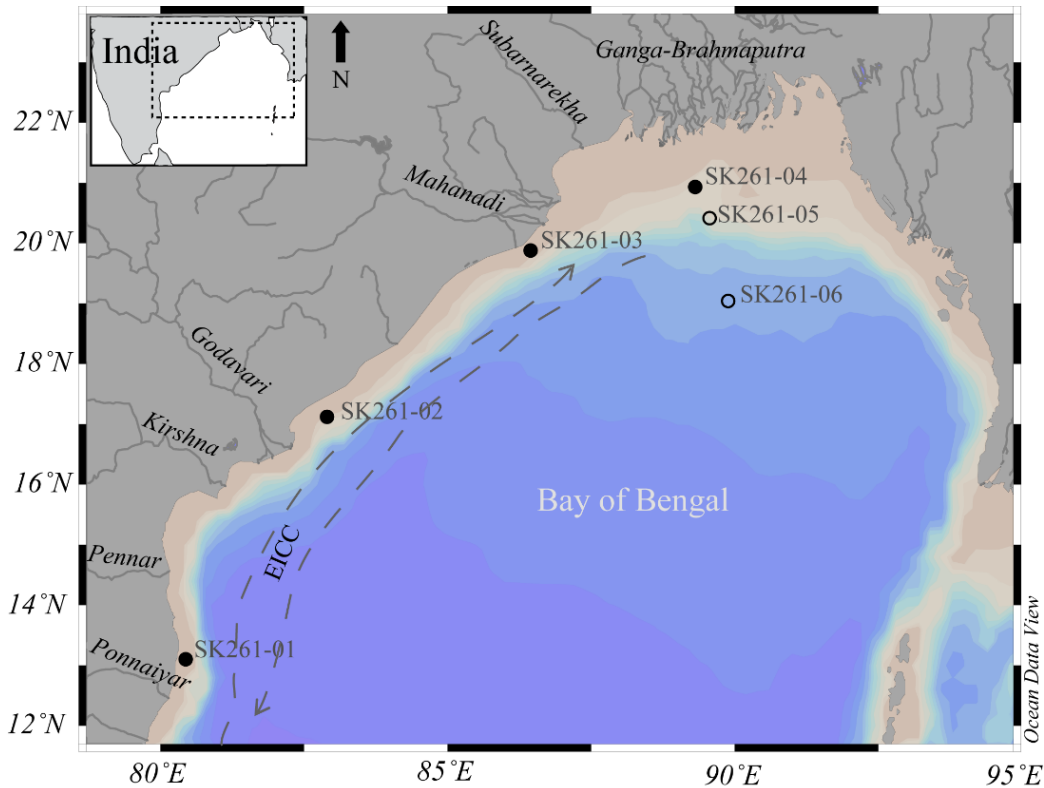


Fig. 3B.1 Map of study area illustrating sampling sites along with the sea-surface East Indian Coastal Current (EICC) during the SW monsoon (clockwise), NE monsoon (anticlockwise), major and minor rivers draining along the north-western Bay of Bengal. Note: filled circles- Coastal stations; empty circle- Neritic-Oceanic stations.

The peak solar heating strongly stratifies the upper ocean waters during the spring intermonsoon. The weaker winds are unable to erode the strong stratification and facilitate deep mixing, leading to the formation of shallow mixed layer depth (Narvekar and Prasanna Kumar 2014). Although increased solar radiation deeper light penetration depth, but nutrient poor water unable to support enough phytoplankton production in the offshore region (Madhu et al., 2006; Paul et al., 2008). However, it increases towards the inshore due to moderate riverine nutrient flux (Gomes et al., 2000; Madhupratap et al., 2003).

3B.2.2 Sediment sampling, processing, and analysis

Sediment sampling was carried out at the stations located on the Indian continental shelf along the north-western region of the bay during the ORV Sagar Kanya Cruise (SK-261), July-August 2009. Surface sediment samples were collected with box core at a water depth ranging from 56 to 154 m (Table 3B.1).

Table 3B.1 Geographical coordinates, water depth and sediment texture at the sampling sites. Coastal and Neritic-oceanic stations presented in orange and blue coloured text.

Stations	Latitude (°N)	Longitude (°E)	Depth	Sediment texture	
SK261-01	13.099	80.334	56	Sandy silt	
SK261-02	17.123	82.903	62	Silty clay	Coastal stations
SK261-03	19.876	86.451	86	Silty clay	
SK261-04	20.933	89.316	108	Clayey	
SK261-05	20.503	89.51	135	Clayey	Neritic-oceanic stations
SK261-06	19.027	89.903	154	Clayey	

Triplicate sediment cores (PVC cores, inner diameter 3.2 cm) were obtained from the grab. All sediment core were sectioned (2 cm interval), mixed well and stored in air tight polycarbonate bottles at 4°C in the dark until further processing. Surface sediment samples (0-2 cm) from each core were processed according to the palynological method (Matsuoka and Fukuyo, 2000) with some modifications. A known weight of wet sediment (7-8 g) was repeatedly washed with distilled water to remove salts, sonicated (30 sec.) and sieved through 120 µm and 10 µm meshes to remove coarse and fine particles. The slurry accumulated on 10 µm was treated with HCL (10%) for 10 h and HF (30%) for 3 h (refer Chapter 3A, Section 3A.2.3 for details of sample processing protocol). For observation, aliquots of processed sample were used. Observations were carried out under an inverted microscope (Olympus IX 71) at a magnification of 200 and 1000 times.

For estimation of the dry weight of wet sediment and cyst concentration refer to chapter 3, section 3A.2.3

Dinoflagellate cysts were identified based on published morphological descriptions (Fensome et al., 1993; Lewis et al., 1999; Matsuoka and Fukuyo, 2000; Rochon et al., 2009; Radi et al., 2013; Sarai et al., 2013; Mertens et al., 2015) and modern dinoflagellate cyst determination key by Zonneveld K.A.F. and Pospelova, V. (2015) (online version: https://www.marum.de/en/Modern_Dinocyst_Key.html). The nomenclature used in this study is in accordance with Head (1996), Zonneveld (1997b) and Zonneveld et al. (2013).

Prior to statistical analysis, some dinoflagellate species were grouped together on the basis of morphological similarity (Table 3B.2). *Spiniferites* species, *S. ramosus*, and *S. bulloideus* were grouped together as *S. ramosus* because of very slight interspecific morphological variation in size and processes thickness. Similarly, *S. mirabilis* and *S. hyperacanthus* have morphological similarities with the exception of the absence of crown process in *S. hyperacanthus*, hence grouped as *S. mirabilis* (Radi and de Vernal, 2008; Rochon et al., 2009). *Echinidinium transparantum* and *Echinidinium* sp. grouped as *Echinidinium* spp. to avoid confusion in identification due to marginal morphological differences. *Brigantedinium* spp. represent all spherical brown cysts. Intraspecific differentiation is difficult in *Brigantedinium* species without observing the archeopyle; sometimes cyst folding also hides the archeopyle structure (Pospelova et al., 2010). *Selenopemphix quanta* and cyst of *P. nudum* have similar morphology with some variation in size and number of process, hence considered as *S. quanta*. Furthermore, species with minimum occurrence (less than 2 stations) and less relative abundance in the study region were excluded from the statistical analysis. These include *Spiniferites delicatus*, *Gymnodinium impudicum*, *Polysphaeridinium zoharyi* and cyst of *Protopteridinium steidingeriae*.

3B.2.3 Geochemical analysis

Total carbon (TC) content measurements of dried, homogenized sediment samples were carried out using an NC soil element analyzer (FLASH 2000, Thomas scientific). The accuracy of analysis was 0.02% using BBOT [2,5-Bis (5-tert-butyl-benzoxazol-2-yl) thiophenol] standard. The total inorganic carbon (TIC) content was measured through CO₂ coulometer (CM5015, UIC Inc.) following acidification of the samples (in acidification module, CM5230, UIC Inc.). The accuracy of the analysis was 2% for standard CaCO₃. The total organic carbon (C_{org}) content was calculated as the difference between total carbon and total inorganic carbon (C_{org}= TC-TIC) (supplementary data).

3B.2.4 Environmental and hydrographical parameters

Present-day sea surface temperature (SST), sea surface salinity (SSS), nitrate, phosphate and silicate concentrations were extracted from the World Ocean Atlas (WOA) 2009 dataset [National Climatic Data Centre (NCDC), <https://www.nodc.noaa.gov/OC5/SELECT/woaselect/woaselect.html>]. For multivariate analysis only annual average SST and SSS was used, whereas in the case of nutrients seasonal mean was calculated from the respective monthly data (supplementary data). Annual mixed layer depth (MLD) was calculated from monthly values obtained from Monterey and Levitus, 1997 (<https://www.nodc.noaa.gov/OC5/WOA94/mix.html>). Satellite-derived surface chlorophyll *a* (Chl_a) data was extracted from SeaWiFS (http://gdata1.sci.gsfc.nasa.gov/daac-bin/G3/gui.cgi?instance_id=ocean_month). Here we used seasonal Chl_a concentrations calculated from respective monthly values, which have been obtained from Chl_a data for the period of 9 years (June 1999 to October 2008; supplementary data). All environmental parameter values were interpolated with Ocean Data View version 4 (ODV 4.6.5; Schlitzer, 2014). Also, C_{org}

and water depth at each station (Table 3B.1) were also used in the multivariate analysis to see their influence of cyst distribution in the study region (supplementary data Table 3B.1).

3B.2.5 Statistical analysis

The abundance of dinoflagellate cyst was subjected to calculate univariate measures, Shannon-Weaver diversity index (i.e. species diversity- H'), species richness and evenness using the software PRIMER 6. Further, a cluster analysis based on the Bray-Curtis similarity index was performed on dinoflagellate cyst abundance data. A similarity profile (SIMPROF) test was carried out to detect the different station groups using 1,000 permutations (for the mean similarity profile) and 999 permutations (for the simulated profile) with 0.05 significance level. A similarity percentage analysis (SIMPER) was carried out to determine the higher contribution of cyst taxa into cluster group formation. Before statistical analysis, dinoflagellate cyst data was logarithmically transformed ($\log x+1$) to minimize the dominance of few abundant species and increases the weight of less abundant species, which could thrive in the narrow ecological niche.

Further, the multivariate statistical analysis was performed on logarithmically transformed relative abundance data of dinoflagellate cyst using CANOCO 4.5 software for Windows (ter Braak and Smilauer, 2002). Detrended Correspondence Analysis (DCA) was performed to determine the species that are likely to have similar geographical distribution. In DCA, the length of the first gradient axis was 2.5 standard deviations (sd) unit indicate a unimodal variation (ter Braak and Smilauer, 2002) in the cyst assemblage distribution. Due to the unimodal character of data set a multivariate direct gradient analysis, Canonical Correspondence Analysis (CCA) was performed to correlate the cyst distribution with environmental parameters. The

conditional effect, the amount of variability explained by only one particular variable (eliminating covariance), is calculate through forward selection. The Monte Carlo testing was used to determine the significance of each environmental parameter, based on 499 unrestrained permutations (supplementary data Table 3B.2).

3B.3 Results

3B.3.1 Dinoflagellate cyst assemblage

A total of 39 taxa belonging to 21 groups were identified from surface sediment samples collected from the north-western Bay. Among 39 cyst morphotypes, 34 were identified up to species level, 5 up to genus level. Benthic domain assemblage consisted cysts of 20 heterotrophic and 19 phototrophic dinoflagellates, including 1 calcareous cyst forming mixotrophic taxa, *Scrippsiella trochoidea* (Table 3B.2). The most prominent heterotrophic taxa were *Brigantedinium* spp. (5-29%), *Trinovantedinium applanatum* (up to 26%), *Quinquecuspis concreta* (up to 19%), *Selenopemphix quanta* (up to 12%) and *Protoperidinium latissimum* (up to 14%). The dominant constituents of the phototrophic assemblage were *Bitectatodinium spongium* (up to 28%), *Impagidinium sphaericum* (up to 22%), *Spiniferites mirabilis* (up to 9%), *S. ramosus* (up to 5%), *S. membranaceus* (up to 6%) and *Lingulodinium machaerophorum* (up to 6%) (Fig. 3B.2).

The dinoflagellate cyst abundance in sediment varied between 27 to 298 cysts g^{-1} . Cyst abundance was comparatively less (27 cysts g^{-1}) at the southern station (SK261-01), whereas a gradual increase is observed towards the northern stations (90 to 298 cysts g^{-1}). Highest cyst abundance was observed at the offshore stations (SK261-06; 298 cysts g^{-1}), which further decreased shelfward (up to 218 cysts g^{-1}) (Fig. 3B.2). Cyst assemblage towards the offshore was dominated by cyst produced by phototrophic species, which was the reason for the decreased H/A ratio towards

offshore (from 3.1 to 0.9; Fig. 3B.2). Within the coastal ambiance heterotrophic species dominated cyst assemblage and their dominance increased northward, shown by increased H/A ratio (0.8 to 4.1; Fig. 3B.2).

The species diversity (H') varied from 2.09 to 2.68. Cyst assemblage at the offshore station was less diverse (2.09) than the shelfward assemblage (2.18 to 2.68), which was further represented by less species richness (Fig. 3B.2). Species evenness also showed a similar trend with reduced evenness towards offshore (0.92 to 0.82). Along the coastal stations, dinoflagellate cyst assemblage was more diverse (2.68) at SK261-02 with highest species richness (4.2).

3B.3.2 Statistical analysis

3B.3.2.1 Spatial distribution of cyst assemblage

Cluster analysis of the Bray-Curtis similarity matrix based on cyst abundance grouped sampling stations into two grouped and one separate station (SIMPROF test $p < 0.005$; Fig. 3B.3). Group 1 stations (SIMPROF similarity 67.22 %) comprised of the coastal sampling sites with shallow water depths (SK261-02, SK261-03, and SK261-04). Group 2 (SIMPROF similarity 46.54%) comprised sampling stations located at the northern part of the bay with deeper water depths (SK261-05 and SK261-06). The relative contribution (%) of each species to the similarity in each group was determined by SIMPER analysis (Table 3B.3). *Brigantedinium* spp. dominated the cyst association in both the groups, hence their percentage contribution along with other cyst taxa could be a discriminating factor between both groups. The most conspicuous trend was observed in heterotrophic cysts, which dominate species assemblage at group 1 (coastal) stations. Cyst assemblage at these stations was dominated by, *T. applanatum*, *S. quanta*, *Bitectodinium spongium*, *S. robustum*, *P. latissimum*, *Archaepridinium minutum*, *S. remosus*, *L. machaerophorum* and *Echinidinium* spp. (Fig. 3B.2; Table 3B.3).

Table 3B.2 Dinoflagellate cyst species identified in surface sediment samples along the north-western Bay of Bengal, with abbreviations and thecate dinoflagellate affinity.

Dinoflagellate cyst (Biological Name)	Abbreviations	Thecate dinoflagellate affinity (Paleontological Name)	Group
Phototrophic			
<i>Alexandrium</i> sp.	Aspp	<i>Alexandrium</i> sp.	
<i>Bitectatodinium spongium</i>	Bspo	–	
<i>Spiniferites bentorii</i>	Sben	<i>Gonyaulax digitalis</i> , <i>G. spinifera</i> complex	
<i>Spiniferites bulloideus</i>	–	<i>Gonyaulax scrippsae</i> , <i>G. spinifera</i> complex	<i>Spiniferites ramosus</i>
<i>Spiniferites ramosus</i>	Sram	<i>Gonyaulax scrippsae</i> , <i>G. spinifera</i> complex	<i>Spiniferites ramosus</i>
<i>Spiniferites mirabilis</i>	Smir	<i>Gonyaulax spinifera</i> complex	<i>Spiniferites mirabilis</i>
<i>Spiniferites hyperacanthus</i>	–	<i>Gonyaulax spinifera</i> complex	<i>Spiniferites mirabilis</i>
<i>Spiniferites membranaceus</i>	Smem	<i>Gonyaulax spinifera</i> complex	
<i>Spiniferites delicates</i>	Sdel	<i>Gonyaulax spinifera</i> complex	
<i>Spiniferites pachydermus</i>	Spac	<i>Gonyaulax spinifera</i> complex	
–	Gimp	<i>Gymnodinium impudicum</i>	
<i>Impagidinium paradoxum</i>	Ipar	<i>Gonyaulax</i> sp.	
<i>Impagidinium sphericum</i>	Ispe	<i>Gonyaulax</i> sp.	
<i>Impagidinium</i> sp.	Isp	<i>Gonyaulax</i> sp.	
<i>Lingulodinium machaerophorum</i>	Lmac	<i>Lingulodinium polyedrum</i>	
<i>Polysphaeridium zoharyi</i>	Pzoh	<i>Pyrodinium bahamense</i>	
<i>Operculodinium centrocarpum</i>	Ocen	<i>Protoceratium reticulatum</i>	
<i>Tuberculodinium vancampoe</i>	Tvan	<i>Pyrophacus stenii</i>	
–	Stro	<i>Scripsiella trochoidea</i>	
Heterotrophic			
–	Amin	<i>Archaepridinium minutum</i>	
<i>Echinidinium transparantum</i>		<i>Protoperidinium</i> sp.	<i>Echinidinium</i> sp.
<i>Echinidinium</i> sp.	Echi	<i>Protoperidinium</i> sp.	<i>Echinidinium</i> sp.

Continued...

Table 3B...Continued...

Dinoflagellate cyst (Biological Name)	Abbreviations	Thecate dinoflagellate affinity (Paleontological Name)	Group
–	Pame	<i>Protoperidinium americanum</i>	
<i>Brigantedinium cariacense</i>		<i>Protoperidinium avellana</i>	<i>Brigantedinium</i> spp.
<i>Brigantedinium irregulare</i>		<i>Protoperidinium denticulatum</i>	<i>Brigantedinium</i> spp.
<i>Brigantedinium simplex</i>		<i>Protoperidinium conicoides</i>	<i>Brigantedinium</i> spp.
<i>Brigantedinium</i> spp.	Bspp	<i>Protoperidinium</i> sp.	<i>Brigantedinium</i> spp.
<i>Votadinium spinosum</i>	Vspi	<i>Protoperidinium claudicans</i>	
<i>Selenopemphix quanta</i>	Squa	<i>Protoperidinium conicum</i>	<i>Selenopemphix quanta</i>
–	–	<i>Protoperidinium nudum</i>	<i>Selenopemphix quanta</i>
–	Plat	<i>Protoperidinium latissimum</i>	
<i>Quinquecuspidata concreta</i>	Qcon	<i>Protoperidinium leonis</i>	
<i>Votadinium calvum</i>	Vcal	<i>Protoperidinium oblongum</i>	
<i>Trinovantedinium applanatum</i>	Tapp	<i>Protoperidinium pentagonum</i>	
–	–	<i>Protoperidinium steidingeriae</i>	
<i>Stelladinium stellatum</i>	Sste	<i>Protoperidinium stellatum</i>	
<i>Stelladinium robustum</i>	Srob	<i>Protoperidinium robustum</i>	
<i>Selenopemphix nephroides</i>	Snep	<i>Protoperidinium subinerme</i>	
<i>Lejeunecysta</i> spp.	Leje	<i>Protoperidinium</i> sp.	

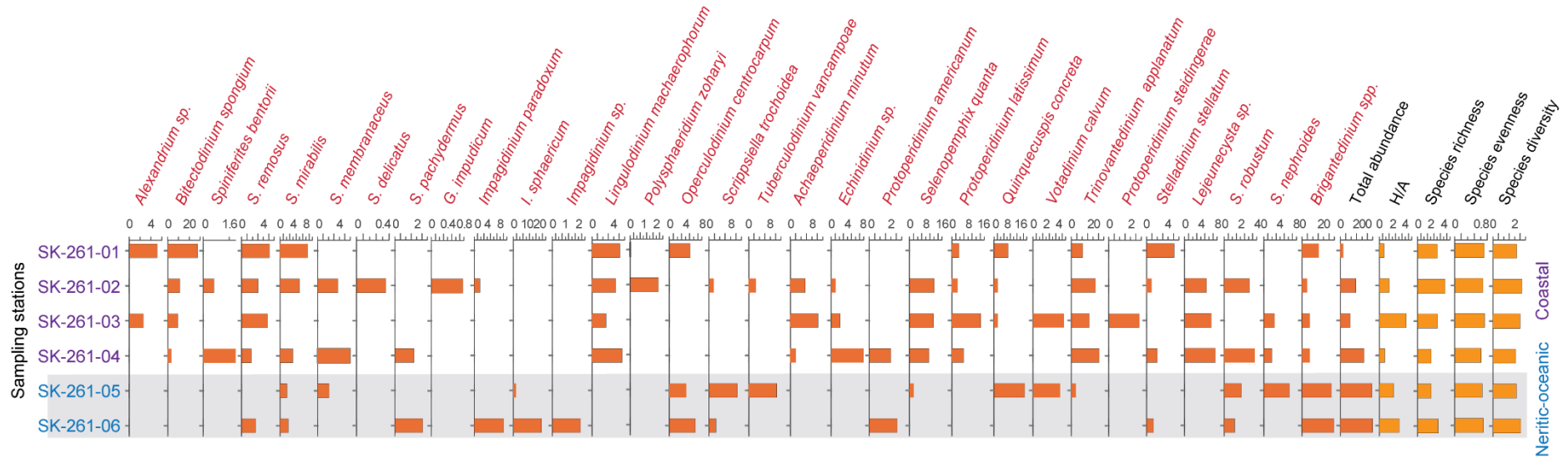


Fig. 3B.2 Relative abundance and distribution of cyst taxa along with total cyst abundance (cysts g^{-1}), the heterotrophic and phototrophic ratio (H/A), species richness, evenness and Shannon-Weaver diversity index (H') in surface sediment along the north-western Bay of Bengal. The horizontal grey box highlights the Neritic-Oceanic stations.

At group 2 (neritic-oceanic) stations, although *Brigantedinium* spp. and *S. nephroides* contribute 25% and 19% respectively in group formation, but overall percentage contribution of these heterotrophic species was 40.5%, whereas the contribution of phototrophic and mixotrophic species *O. centrocarpum*, *S. mirabilis*, *I. sphaericum* and *S. trochoidea* increased to 50.35 % (Table 3B.3).

The DCA station score biplot illustrated the spatial variation within dinoflagellate cyst associations between the sampling stations (Fig. 3B.4). The distribution of the station score discriminate the groups identified in the SIMPROF analysis (Fig. 3B.3). The DCA axis 1 (DCA 1) describes the largest part of the variation and represents a shelfward gradient of sampling stations (Oceanic-neritic to the coastal ambiance). The oceanic-neritic (group 2) stations distributed towards axis whereas coastal (group 1) stations bundled towards the forward extremities. DCA 2 explained spread within the neritic-oceanic and coastal stations by separating station SK261-01 (SIMPROF ungrouped station) from the coastal stations group and station SK261-05 from SK261-06 within neritic-oceanic ambiance.

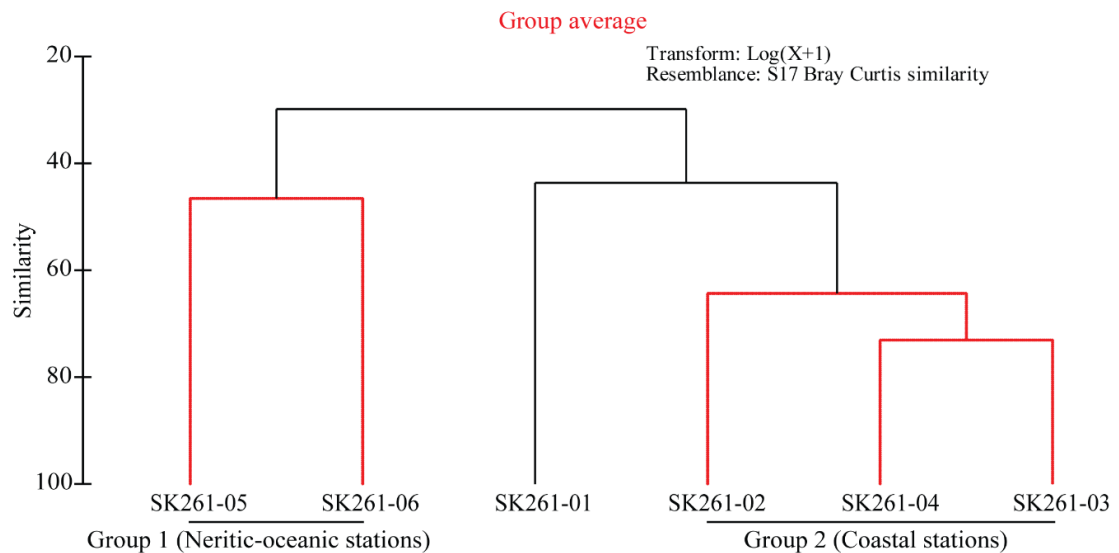


Fig. 3B.3 Cluster dendrogram of sampling station relationship on the basis of Bray-Curtis similarity matrix and similarity profile (SIMPROF) test. The main groups of stations can be identified by dark black lines.

Table 3B.3 Result of SIMPER analysis

Ambiance	Species	Abbreviations	Abundance	Similarity	Contribution (%)	Cumulative (%)
Coastal stations (Group 1) Avg. similarity 67.22	<i>T. applanatum</i>	Tapp	3.44	8.86	13.17	13.17
	<i>S. quanta</i>	Squa	2.82	7.69	11.44	24.62
	<i>B. spongium</i>	Bspo	2.43	6.55	9.74	34.36
	<i>S. robustum</i>	Srob	2.33	5.97	8.88	43.24
	<i>Brigantedinium</i> spp.	Bspp	2.29	5.95	8.85	52.10
	<i>P. latissimum</i>	Plat	2.30	5.82	8.65	60.75
	<i>A. minutum</i>	Amin	2.08	5.55	8.25	69.00
	<i>S. ramosus</i>	Sram	1.65	4.80	7.15	76.14
	<i>L. machaerophorum</i>	Lmac	1.93	4.27	6.35	82.49
	<i>Echinidinium</i> spp.	Echi	1.66	2.98	4.44	86.93
	<i>S. mirabilis</i>	Smir	1.51	1.97	2.93	89.85
	<i>S. membranaceus</i>	Smem	1.50	1.61	2.39	92.25
	Neritic-Oceanic stations (Group 2) Avg. similarity 46.54	<i>Brigantedinium</i> spp.	Bspp	4.44	11.87	25.50
<i>O. centrocarpum</i>		Ocen	2.79	6.98	15.00	40.50
<i>S. undulatum</i>		Sund	3.07	6.98	15.00	55.51
<i>S. trochoidea</i>		Stra	2.80	5.84	12.55	68.05
<i>S. mirabilis</i>		Smir	2.06	5.30	11.40	79.45
	<i>I. sphaericum</i>	Ispe	3.07	5.3	11.40	90.85

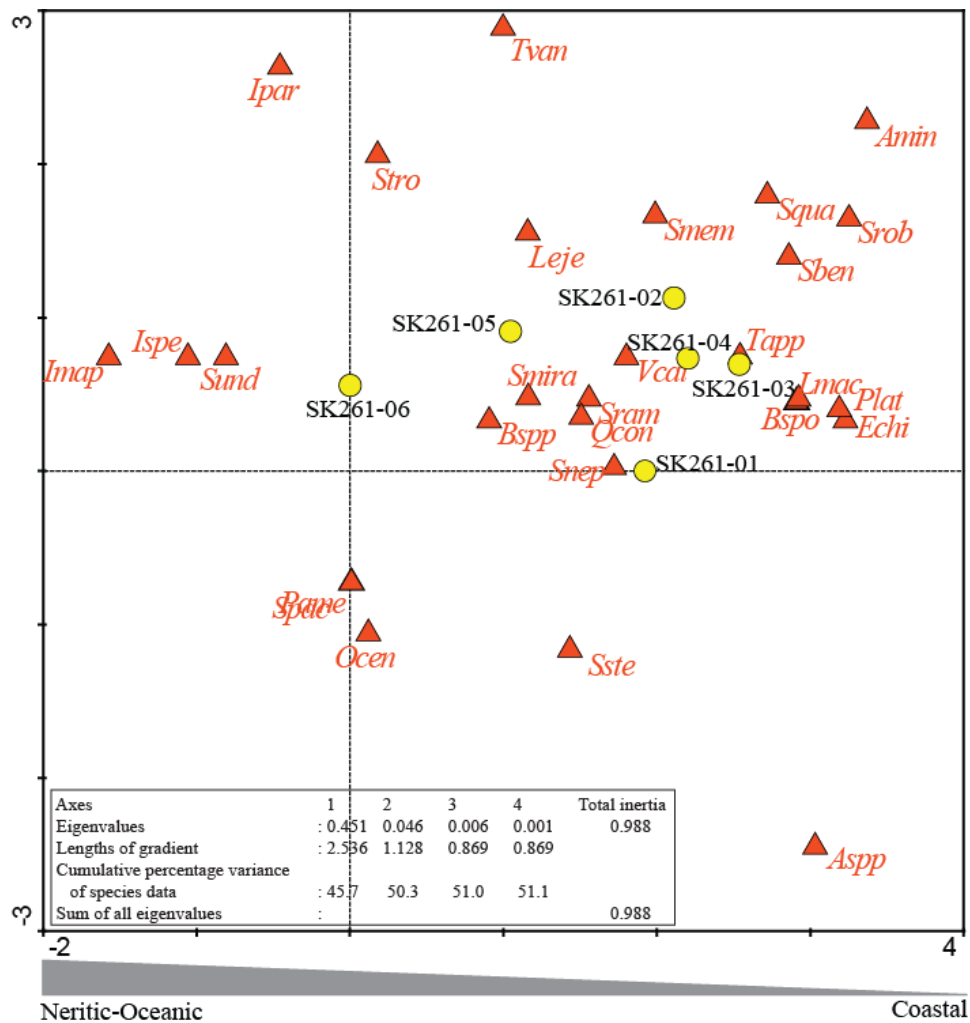


Fig. 3B.4 Detrended corresponding analysis (DCA) biplot illustrates the cyst assemblage variation between coastal and neritic-oceanic sampling sites in the north-eastern Bay of Bengal. Abbreviations of species name: Aspp, *Alexandrium* sp.; Bspo, *Bitectatodinium spongium*; Sben, *Spiniferites bentorii*; Sram, *S. ramosus*; Smir, *S. mirabilis*; Smem, *S. membranaceus*; Spac, *S. pachydermus*; Ipar, *Impagidinium paradoxum*; Ispe, *I. sphaericum*; Ispp, *Impagidinium* sp.; Lmac, *Lingulodinium machaerophorum*; Ocen, *Operculodinium centrocarpum*; Tvan, *Tuberculodinium vancampoae*; Stro, *Scrippsiella trochoidea*; Amin, *Archaepridinium minutum*; Echi, *Echinidinium* sp.; Pame, *Protoperidinium americanum*; Bsp, *Brigantedinium* spp.; Squa, *Selenopemphix quanta*; Plat, *P. latissimum*; Qcon, *Quinquecuspis concreta*; Vcal, *Votadinium calvum*; Tapp, *Trinovantedinium applanatum*; Sste, *Stelladinium stellatum*; Srob, *Stelladinium robustum*; Snep, *Selenopemphix nephroides*; Leje, *Lejeunecysta* spp.

The distribution of DCA species scores biplot illustrated affinities with respect to shelfward environmental gradient (Fig. 3B.4). Cyst belonging to genera

Impagidinium (*I. paradoxum*, *I. sphaericum* and *Impagidinium* spp.), *S. pachydermus*, *O. centrocarpum* and *P. americanum* plotted towards the negative scale of the DCA 1, whereas cysts of other phototrophic and heterotrophic taxa distributed towards the positive extremities. Most of the cyst species associated with cosmopolitan distribution were scored towards positive scale of DCA axis 2.

3B.3.2.2 Species distribution in relation to the monsoonal environmental and oceanographic variability.

A CCA performed on the logarithmically transferred relative abundance data of dinoflagellate cyst reveals the first two CCA axis (CCA 1 and 2) are dominant and represent 45.13% and 21.45% of variances respectively, with total cumulative variance 66.58% (Fig. 3B.5). The CCA reveals that water depth, Chla (NEM, SIM, and FIM), MLD annual, phosphate (SWM) and nitrate (FIM) explain a large part of data variance (marginal effect; supplementary data). After the correcting for covariance between variables, water depth, nitrate (SWM and SIM) and MLD annual are significantly in relation to the CCA axis ($F > 1$), explain the main part of the data variation (conditional effect; supplementary data).

CCA biplot illustrated the factors responsible for the homo- and heterogeneity in the cyst assemblage at the SIMPROF cluster grouped stations (Fig. 3B.5; Supplementary data). The CCA 1 revealed contrast between cyst assemblages at coastal and neritic-oceanic stations. The coastal stations are ordinated at the negative side of the CCA 1 while neritic-oceanic stations are plotted at the positive side (Fig. 3B.5). Cyst assemblage plotted at the negative side (coastal stations) was influenced by seasonality in nutrients (mainly phosphate and nitrite) and Chla concentration, whereas at positive side CCA 1 is well correlated with water depth, C_{org} and MLD (Fig. 3B.5). The negative correlation between MLD and nutrient concentration could reveal; cyst

assemblage changes associated with MLD variations are most likely due to nutrient variability rather than MLD itself. The seasonality in MLD represents the stratification and nutrient variation in the upper water column. The CCA biplot illustrates species responsible for the coastal station group, *B. spongium*, *S. remosus*, *L. machaerophorum*, *A. minutum*, *Echinidinium* spp., *S. quanta*, *P. latissimum*, *T. applanatum* and *S. robustum* shows a positive correlation with seasonal nutrient and Chla concentration (Fig. 3B.5). At the positive side of CCA 1, C_{org} influenced small variation in cyst assemblage, cyst of heterotrophic species, *T. vancampoae*, *V. calvum* and *Q. concreta* shows a strong correlation with it. Similar but less pronounced correlation of *I. sphaericum*, *I. paradoxum*, *Impagidinium* spp., *S. pachydermus*, cyst of *P. americanum* with annual MLD and *S. nephroides*, *O. centrocarpum*, *S. trochoidea* with water depth also been observed.

The CCA 2 reveals that C_{org} and MLD explain a large part of the data set variation. At positive side cyst species *T. vancampoae*, *V. calvum* *Q. concreta*, and *Brigantedinium* spp. strongly correlated with C_{org} and show the highest abundance at Station SK261-05. Similarly cyst species like *I. sphaericum*, *I. paradoxum*, *Impagidinium* spp., *S. pachydermus* and *P. americanum* which have the highest abundance at oceanic station SK261-06 and are strongly influenced by MLD annual. Thus, the results of CCA 2 illustrate the heterogeneity within the cluster group 2 stations (SIMPROF), differentiating station SK261-05 and SK261-06 as neritic and oceanic ambiance respectively.

Other cyst species *S. membranaceus*, *S. mirabilis*, *Lejeunecysta* sp. and *S. stellatum* are ordinated at the central part of the diagram. These species either have random distribution or occurrence in the study area.

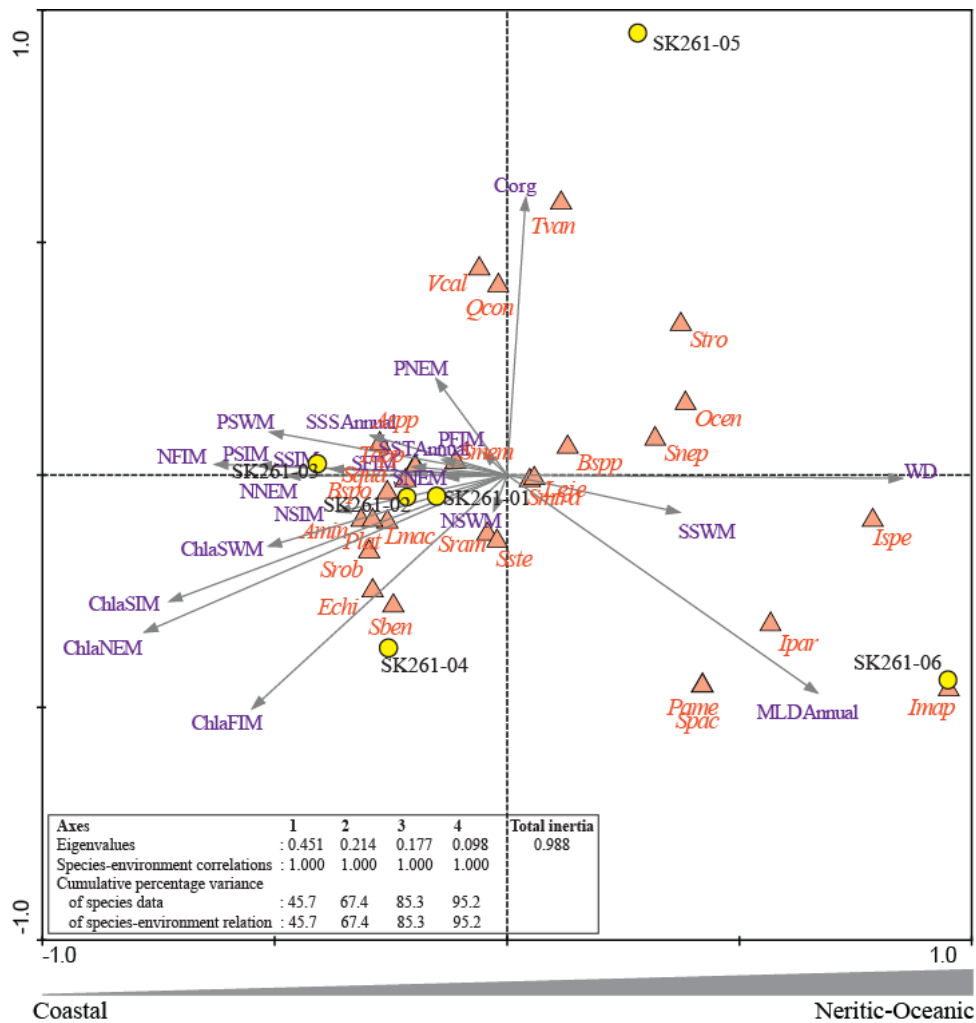


Fig. 3B.5 Canonical Corresponding analysis (CCA) biplot illustrates dinoflagellate cyst species relation to environmental parameters (grey arrows) at the different sampling station. For abbreviations of species please refer captions of Table 3B.2 and Fig. 3B.4. Abbreviations of environmental variables: SSS, salinity; SST, temperature; MLD, mixed layered depth; Chla, chlorophyll *a* concentration at the surface; P, Phosphate; N, Nitrate; S, silicate; C_{org}, total organic carbon; WD, water depth. SWM, Southwest monsoon; FIM, fall intermonsoon; NEM, Northeast monsoon; SIM, summer intermonsoon.

3B.4 Discussion

For the first time, cyst assemblage distribution from recent surface sediments along the north-western Bay of Bengal has been analysed. The geographic distribution of the cyst assemblage and their ordination in the multivariate analysis illustrate monsoonal influence on cyst assemblage distribution in the north-western Bay.

3B.4.1 Transport and preservation

Dinoflagellate cyst distribution in the marine sediments may be misinterpreted due to the possible effect of lateral transport and oxidative degradation during and/or after sedimentary deposition (Zonneveld and Brummer, 2000; Dale 2001a; Zonneveld et al., 2007). Dinoflagellate cyst behaves like silt particles and might easily be transported by ocean currents during their sinking process and after deposition (Anderson et al., 1995). However, long scale dispersal of cyst due to natural process is rare (Zonneveld and Brummer, 2000; Giannakourou et al., 2005; Zonneveld et al., 2009). In the northern bay, surface water current plays an important role in the transport of suspending particle influx discharged by the riverine system to southwards (Shetye et al., 1991). However, lighter clay minerals settle close to riverine flux in clay dominant sediment (Murty and Shrivastava, 1979; Rao et al., 1988). Along the northern stations sediment characteristic as clayey with compact sediments (Table 3B.1) indicating higher sedimentation and less winnowing effect. Further evidence for negligible lateral transport in the northern region is the good match between cyst abundance of coastal and neritic-oceanic sediments (Fig. 3B.2). In the southern station, sediment texture was silty-clay (except SK261-01), and cyst abundance was lesser compared to the northern stations. However, cyst assemblage was similar to the northern coastal station SK261-04 (Fig. 3B.2; Table 3B.3), which indicate the minimal effect of post-depositional lateral transport on cyst assemblage.

The overall preservation of dinoflagellate cyst is affected by the pre- and post-depositional processes in the water column as well as in sediments (Zonneveld and Brummer, 2000; Versteegh and Zonneveld, 2002; Zonneveld et al., 2007). In particular, cyst produced by *Protoperidinium* species are supposed to be vulnerable to oxidative degradation (Versteegh and Zonneveld, 2002; Zonneveld et al., 2007) (discussed in

Chapter 4A, Section 4A.5.1). In the northern bay, the waters have very low (<5 µM) dissolved oxygen content at intermediate depths resulting in a pronounced oxygen minimum zone (Sardessai et al., 2007). Bottom waters below the river plume are characterized by low oxygen concentrations and episodes of anoxia are common features in this region (Sarma et al., 2013). The Higher relative abundance of oxidative degradation-susceptible species, *Q. concreta*, *S. robustum*, *S. nephroides*, *T. applanatum*, *Brigantedinium* spp. and *Echinidinium* spp. (Marret and Zonneveld, 2003; Zonneveld et al., 2007; Zonneveld et al., 2013) in the present study region, suggests less derivative stress and better preservation state.

3B.4.2 Spatial distribution of dinoflagellate cyst in relation to environmental conditions

3B.4.2.1 Coastal assemblage

In the coastal region cyst assemblage was dominated by heterotrophic Protoperidinioid species, *T. applanatum*, *S. quanta*, *S. robustum*, *Brigantidium* spp., *P. latissimum*, *A. minutum*, and *Echinidinium* spp. (Fig. 3B.2; Table 3B.3). In recent sediment, these species dominate cyst assemblage in the nutrient-rich coastal upwelling regions and eutrophic systems (Marret and Zonneveld, 2003; Limoges et al., 2010; Zonneveld et al., 2013). *Protoperidinium* species are known for their diversified feeding ranging from diatoms, phototrophic dinoflagellates (Naustvoll, 2000) to eggs, earlier naupliar stages and adult metazoans (Jeong et al., 2010). Their abundance in recent sediments reflects the availability of prey organisms and in turn the primary production in the overlying water column (Matsuoka, 2003; Holzwarth et al., 2007; Bockelmann and Zonneveld, 2007; Hessler et al., 2013; Zonneveld et al., 2013 and references therein). In the study area, although weak summer monsoon upwelling is prevalent in the southern region (De Sousa et al., 1981; Shetye et al., 1991), the

productivity is primarily controlled by the fluvial nutrient input (Gomes et al., 2000; Madhu et al., 2006; Paul et al., 2008). The CCA ordination in the present study indicates that dominance of these species well correlates with the Chla, silicate and nitrate concentrations towards the coastal ambience (Fig. 3B.5). Similarly, the silicate is an essential element for the cell wall synthesis and growth in diatoms and is not used by dinoflagellate for growth. Hence, the relation of dinoflagellate with silicate concentration along the coastal ambience (Fig. 3B.5) can be related to the availability of diatom in the water column.

The higher abundance of phototrophic, *B. spongium*, *S. remosus* and *L. machaerophorum* was characteristic of the cyst assemblage within the coastal ambience (Fig. 3B.2). In recent sediments, an abundance of *B. spongium* and *L. machaerophorum* has been observed in the coastal upwelling sites with elevated nutrients (Marret and Zonneveld, 2003; Zonneveld et al., 2013). Similarly, *L. machaerophorum* characteristically contributes to cyst assemblage deposited in the vicinity of the riverine or estuarine system (Zonneveld et al., 2009 and references therein). Cyst production is typically observed during the upwelling relaxation or in riverine plume with more fresh nutrients and reduced turbidity (Pospelova et al., 2008; Zonneveld et al., 2009). In *B. spongium*, cyst production was observed during active upwelling (Zonneveld and Brummer, 2000; Susek et al., 2005; Vasquez-Bedoya et al., 2008). In the western Arabian Sea, its increased flux can be influenced by higher SST and nutrient concentrations during the SW monsoon (Zonneveld, 1997a; Zonneveld and Brummer, 2000). The CCA ordination of *B. spongium* and *L. machaerophorum* associated to nitrate and Chla (NEM) vector (Fig. 3B.5) could indicate the effect of nutrient availability and light intensity on their growth (Fig. 3B.5). In the Bay, during the NE monsoon reduced riverine plume, increased irradiance along with fresh nutrient supply

facilitate primary production in the coastal region (Gomes et al., 2000; Madhu et al., 2006; Paul et al., 2008), which could also support the growth of *B. spongium* and *L. machaerophorum*. The abundance of *S. ramosus* as observed in the coastal region, suggests the upper water salinity conditions can be reduced permanently or seasonally by river discharge (Zonneveld et al., 2013).

3B.4.2.2 Neritic-oceanic assemblage

In the study area *Brigantedinium* spp., *S. nephroides*, *S. trochoidea*, *I. sphaericum* and *O. centrocarpum* were observed in deeper sediments (Table 3B.3) where oceanic conditions prevail during the NE and spring inter-monsoons. The abundance of *Brigantedinium* spp. and *S. nephroides* is mainly controlled by phytoplankton production during nutrient enrichment events like active upwelling, eutrophication and/or increased riverine flux (Zonneveld and Brummer, 2000; Pospelova et al., 2008; Zonneveld et al., 2009). Higher abundance of these heterotrophic species in this region could be resultant of higher diatom abundance, controlled by riverine nutrient influx (Madhu et al., 2006; Paul et al., 2008). *O. centrocarpum* often dominates water masses characterized by extreme seasonality or environmental instability where shelf and oceanic waters meet (Dale et al., 2002). Nutrient enriched conditions during the NE monsoon influence its high flux in the western Arabian Sea region (Zonneveld, 1997a). Along the East Indian coast, elevated nutrient inputs and salinity variation controls the high abundance of *O. centrocarpum* (D'Silva et al., 2013, Narale et al., 2013). It is possible that abundance of phototrophic *O. centrocarpum* in the neritic-oceanic ambiance can be associated with seasonally varying salinity, light, and nutrient availability. Calcareous cysts of *S. trochoidea* are well distributed in the sediments along the Indian region (Godhe et al., 2000; D'Costa et al., 2008; D'Silva et al., 2013). The dominance of planktonic *S. trochoidea* in the

Bay surface water was observed during the spring intermonsoon (Naik et al., 2011; discussed in Chapter 2; section 2.5.1). In the present study, the reason for increased abundance of *S. trochoidea* cyst in the deeper stations is not clear.

The occurrence of *T. vancampoe*, *V. calvum*, and *Q. concreta* in high abundance differentiate station SK261-05 as neritic from SK261-06 within neritic-oceanic ambiance (Fig. 3B.5). The abundance of heterotrophic *V. calvum* and *Q. concreta* within cyst assemblage, as observed at this station, indicate higher productivity and availability of diatom in the water column (Marret and Zonneveld, 2003; Zonneveld et al., 2013), controlled by fluvial nutrient supply. Phototrophic taxa, *T. vancampoe* commonly associated with the nutrient-rich coastal upwelling sites (Zonneveld, 1997a; Marret and Zonneveld, 2003; Hessler et al., 2013). The abundance of *T. vancampoe* suggests the nutrient availability along with increased light availability (Zonneveld and Susek, 2006) during the NE monsoon may favor its growth in the shelf region.

At station SK261-06 *Impagidinium* species, including *I. sphaericum*, *I. paradoxum*, *Impagidinium* spp. along with *S. pachydermus* and cyst of *P. americanum* were dominant cyst forms. Phototrophic *Impagidinium* species are classified as outer neritic to oceanic species (Mudie and Harland, 1996), dominating cyst assemblage in the oceanic regions with saline, stratified and oligotrophic waters (Zonneveld, 1997b; Zonneveld and Brummer, 2000; Marret and Zonneveld, 2003; Hessler et al., 2013; Zonneveld et al., 2013). These observations agree with multivariate analysis (CCA 2) results of our study (Fig. 3B.5). Increased SST, oligotrophic conditions due to thermal stratification (shallow MLD) and reduced riverine influx during the spring intermonsoon in the region support *Impagidinium* species abundance. *S. pachydermus* and cyst of *P. americanum* are typically dominant in the active upwelling coastal region

(Marret and Zonneveld, 2003; Zonneveld et al., 2013). Stable water condition with elevated nutrients favours the greatest flux of *S. pachydermus* during the end of SW monsoon upwelling in the Somalian region (Zonneveld and Brummer, 2000). In the northern bay, more stable water conditions with less turbidity, increased light penetration, nutrient, and higher salinity could favor the growth of *S. pachydermus* during the NE monsoon. Cyst production of heterotrophic *P. americanum* was observed during active upwelling with more prey availability (Zonneveld et al., 2009). In the northern bay, an abundance of *P. americanum* cyst in surface sediment can be supported by availability of prey organisms resultant of riverine nutrient influx. Co-occurrence of oceanic *Impagidinium* species along with the coastal-neritic *S. pachydermus* and cyst of *P. americanum* at SK261-06 indicate large inter-annual variability in the trophic state of the upper waters, which is mainly influenced by monsoonal variability in the region.

3B.4.3 Cyst records of potentially harmful species

In the north-western Bay, cysts of potentially harmful yessotoxin (YTX) producing species *Gonyaulax spinifera* (*Spiniferites* species analogs), *Protoceratium reticulatum* (*O. centrocarpum*), *Lingulodinium polyedrum* (*L. machaerophorum*) and paralytic shellfish toxin (PST) producing *Pyrodinium bahamense* (*P. zoharyi*) (Fig. 3B.6) were identified. Along with these, potentially red-tide-forming *S. trochoidea* also showed presence in the study area. Although not all *Gonyaulax spinifera* members produce YTXs, but their population was more diverse (species) and dominated cyst assemblage in the region. In the region, no harmful events due to bloom of these species have been reported earlier.

Pyrodinium bahamense is one of the most important paralytic shellfish poisoning (PSP) producing dinoflagellate in the tropical region (Usup et al., 2012). *P. bahamense* was thought to be is monospecies with two varieties, namely var.

compressum and var. *bahamense* (Steidinger et al. 1980). Recently, Martens et al. (2015) recommended ceasing to use these varieties on the basis of both theca and cyst morphological features, biogeographic distribution pattern. Harmful bloom incidences and paralytic shellfish poisoning (PSP) episodes of *P. bahamense* are more frequent and widely spreading along the Southeast Asian region (e.g. Fukuyo et al., 2011; Usup et al., 2012) and had caused adverse socio-economic problems for more than 3 decades (Fukuyo et al., 2011). Similarly, its cyst occurs along most of the Southeast Asian maritime states (Furio *et al.*, 2012; Usup et al., 2012). Considering the increasing incidences of harmful bloom and PSP spread of *P. bahamense* along the adjacent Southeast Asian region, this report of its cysts (*P. zoharyi*) occurrence in the coastal sediments of the north-western Bay of Bengal is noteworthy.



Fig. 3B.6 Micrographs of *Polysphaeridium zoharyi*, (a and b) distally bifurcated, hollow processes (arrow); (c) processes fused at their base (arrow). Scale bare 20 µm.

3B.5 Conclusion

This study showed the utility of cyst population in demarking pelagic events in the Bay of Bengal, which is influenced by seasonality in monsoon and resultant riverine flux. The coastal ambiance was dominated by Protoperidinoid cysts supported by prey availability. The phototrophic forms such as *B. spongium*, *L. machaerophorum*, and *S. ramosus* were exclusively observed in the coastal region influenced by fluctuation in

water turbidity, light intensity, salinity and nutrient availability. The dominance of *Brigantedinium* spp., *S. nephroides* the neritic-coastal ambiance was facilitated by the nutrient supply and prey availability. Whereas seasonal variability in salinity, light and nutrient availability controlled the distribution of *O. centrocarpum*, *V. calvum*, *Q. concreta* and *T. vancampoae* exclusively found in a location interspaced between coastal and oceanic stations indicating possible seasonal variation in coastal and oceanic conditions. The offshore station was dominated by *Impagidinium* species suggesting low nutrient oceanic conditions. The occurrence of *P. zoharyi* along with other potentially harmful species highlight use of dinoflagellate cyst mapping studies.

Appendix

Supplementary data associated with Chapter 3B can be found in Appendix II

3C Scenario of dinoflagellate cyst assemblages along the Indian coasts

3C.1 Introduction

In recent years, consequences of harmful algal blooms (HABs) are increasing globally (Anderson et al., 2012). Approximately 7% of the estimated phytoplankton species have been reported to produce red tides and HABs (Sournia, 1995) with dinoflagellates being the major contributors (Smayda, 1997). Among the modern dinoflagellates ~84 species are known to be responsible for HABs, causing water discoloration and producing a variety of toxins (Moestrup et al., 2009 onwards; IOC-UNESCO Taxonomic Reference list of harmful microalgae, web: <http://www.marinespecies.org/HAB/dinoflag.php>, accessed 29 April 2015). About, 200 extant dinoflagellate species are known to produce dormant resting stages (cysts and/or hypnozygote) as part of commonly sexual or uniquely asexual reproduction (discussed in Chapter 1). In certain harmful species (e.g. *Alexandrium* spp.), cyst formation strategy regulates bloom initiation as well as termination (Dale, 2001) and eventually the bloom dynamics in the coastal regions (Anderson et al., 2012). These dormant life stages facilitate the species dispersion and spread of HABs in previously unaffected areas (Anderson et al., 2012). For example, benthic cyst banks act as seedbeds for bloom dynamics and paralytic shellfish poisoning events (PSPs) of *A. fundyense* in the Gulf of Maine (Anderson et al., 2005). In the South Asian region, *Pyrodinium bahamense* uses the temporary as well as resting cyst stages as a strategy to maintain the stock population for initial and regional spread of HABs and PSPs (Onda et al., 2014; Azanza and Taylor, 2001). Higher toxin content in cysts than planktonic forms could also be a potential source of shellfish intoxication to the benthic biota (Schwinghamer et al., 1994) in the coastal regions. In this context,

mapping the distribution of harmful species in the water column and sediments would improve the understanding of HABs (GEOHAB, 2001).

Along the Indian Coast, algal bloom incidents have been increasingly reported since the 1950s (D'Silva et al., 2012b). Bloom incidences in this region are known to be initiated and developed due to monsoonal influence, riverine discharge and seasonal upwelling (D'Silva et al., 2012b). In the regional context, dinoflagellate bloom incidences of *Noctiluca scintillans*, *Cochlodinium polykrikoides*, *Dinophysis* sp., *Gonyaulax polygramma*, *Gymnodinium* spp., *Karenia brevis*, *K. mikimotoi* and *Prorocentrum micans* were reported along the Indian coast (D'Silva et al., 2012b and references therein). Along the central west coast of India (Mangalore), a toxin profile of the clams from the PSP affected region corresponded to a strain of *A. tamiyavanichii* isolated from Thailand (Karunasagar et al., 1990). Subsequent occurrence of *A. cf tamiyavanichii* cyst has also been reported along the Mangalore coast (Godhe et al., 2000). Cyst occurrence of *A. cf tamiyavanichii* may suggest the potential of cyst survival strategies in regional HABs transport. Bloom incidences of *C. polykrikoides* and resultant fish mortality incidences were reported along the Goa coast and Kerala coast (D'Silva et al., 2012b). Along the Goa coast, cyst of *C. polykrikoides* potentially inoculated blooms in subsequent seasons (October 2001) (Patil and Anil, 2011). Considering the history of cyst strategy in bloom initiation and regional spread of HABs and toxic events, this section provides a comprehensive view of regional cyst mapping studies with an emphasis on potentially harmful species.

3C.2 Methodology

In order to evaluate the dinoflagellate cyst composition and identify the harmful and potentially harmful species in the Indian region, the cyst assemblage of the east coast of India and Port Blair Bay, South Andaman region (D'Silva et al. 2013;

present study, Chapter 3A and 3B) are compared with that of the west coast of India (Godhe et al. 2000; D'Costa et al. 2008; D'Silva et al. 2011) (Fig. 3C.1) and presented in Table 3C.1.

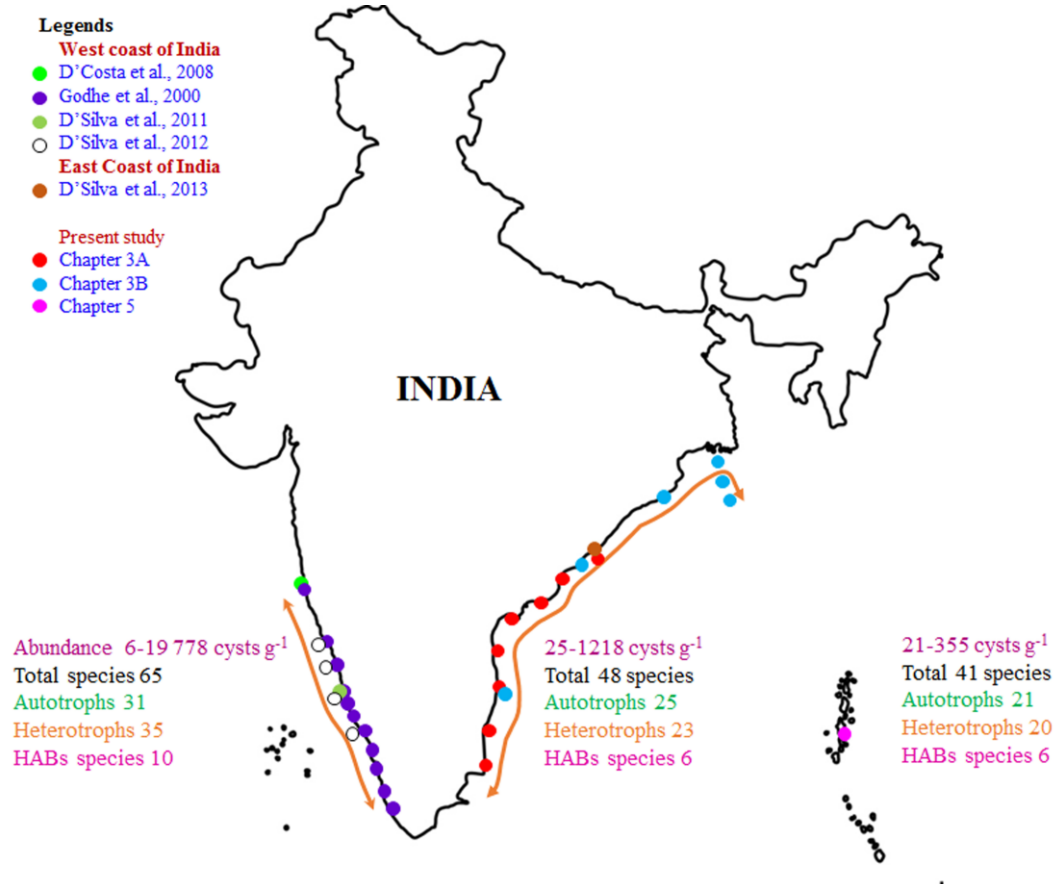


Fig. 3C.1 Modern dinoflagellate cyst mapping studies along the Indian region. Regional differences in cyst assemblages highlighted in the coloured text.

3C.3 Result and discussion

Dinoflagellate cyst abundance in recent sediments from Indian region i.e. the west, east coasts of India and South Andaman region was low, but within comparable range as compared to sub-tropical and temperate coastal regions (refer Chapter 3A, Section 3A.4.1). Exceptionally high cyst abundance (up to 19,778 cysts g⁻¹) in the region was observed along the Mangalore region in core dated back ~1962 due to *Gonyaulax membranacea* bloom (D'Silva et al., 2012b). Taxonomic comparison of the

dinoflagellate cyst data from the east coast and South Andaman region with the cyst mapping studies from the west coast of India (Godhe et al. 2000, D'Costa et al. 2008, D'Silva et al. 2011; D'Silva et al. 2013) emphasises regional differences in species composition along the Indian coast (Table 3C.1). Cysts belonging to the heterotrophic *Protoperidinium* species dominated the cyst assemblage over phototrophic species along the Indian region (D'Costa et al., 2008; D'Silva et al., 2011; D'Silva et al., 2013). However, the total number of cyst-forming species phototrophic and heterotrophic species is higher along the west coast (26 phototrophs and 33 heterotrophs) than the south-east coast (22 phototrophs and 23 heterotrophs) and South Andaman region (21 phototrophs and 20 heterotrophs) (Table 3C.1).

Comparison of the data sets also showed a number of potentially toxic PSPs and red-tide-forming species were low along the east coast and South Andaman region (6 species) than the west coast (10 species) of India (Fig. 3C.1; Table 3C.1). Cysts of potentially harmful PSPs causing species, *A. minutum*, *A. tamarense*, *A. cf. tamiyavanichii*, *Gymnodinium catenatum* and *Pyrodinium bahamense* var. *compressum* (Fraga, S., (ed) 2015; IOC-UNESCO Taxonomic Reference list of harmful microalgae, the web: <http://www.marinespecies.org/HAB./dinoflag.php>) recorded from the surface sediments of the west coast of India (Table 3C.1). Similarly, cyst of yessotoxin (YTXs) producing *G. spinifera*, *P. reticulatum* and *L. polyedrum*; red-tide-forming *A. affine* and *S. trochoidea* (Garate-Lizarraga et al. 2001, Su-Myat and Koike, 2013) also observed along this region. Sediment core analyses from the west coast of India have reported the presence of *A. affine*, *A. minutum*, *G. spinifera*, *L. polyedrum*, *P. reticulatum* and *S. trochoidea* since the early 1900s (D'Silva et al. 2012a).

Table 3C.1 Dinoflagellate cyst assemblage records in surface sediments along the India region. Refer EIC as the east coast of India; SAR as South Andaman Region and WCI as the west coast of India. References indicated as superscript numbers: ¹ Present study, Chapter 3A; ² Chapter 3B; ³ D'Silva et al., 2012a; ⁴ Present study, Chapter 5; ⁵ Godhe et al., 2000; ⁶ D'Costa et al., 2008; ⁷ D'Silva et al., 2011; ⁸ D'Silva et al., 2013. † Potentially harmful species; †† red-tide-forming species; # calcareous cyst species.

Planktonic dinoflagellates (Biological Name)	Dinoflagellate cyst (Paleontological Name)	Regional occurrence		
		EIC	SAR ⁴	WCI
Phototrophs				
<i>Alexandrium affine</i> ††	-			*6,7,8
<i>Alexandrium</i> cf. <i>affine</i>	-	*3		*6
<i>Alexandrium minutum</i> †	-	*3		*7,8
<i>Alexandrium</i> cf. <i>minutum</i>	-			*5,6
<i>Alexandrium tamarensis</i> †	-			*7
<i>Alexandrium</i> cf. <i>tamarensis</i>	-			*7
<i>Alexandrium</i> cf. <i>tamiyavanichi</i> †	-			*6,7
<i>Alexandrium pseudogonyaulax</i> †	-		*	
<i>Alexandrium</i> sp.	-	*2,3	*	*5,7
<i>Bitectatodinium spongium</i>	-		*	
<i>Cochlodinium</i> cf. <i>polykrikoides</i>	-		*	*6,7,8
<i>Cochlodinium</i> sp.	-	*3		*7,8
<i>Gonyaulax digitalis</i> , <i>G. spinifera</i> complex	<i>Spiniferites bentori</i>	*1,2,3	*	*5,6,7,8
<i>Gonyaulax scrippsae</i> , <i>G. spinifera</i> complex	<i>Spiniferites bulloideus</i>	*1,2,3		*5,6,7,8
<i>Gonyaulax verior</i>	-			*5
<i>Gonyaulax spinifera</i> complex †	<i>Spiniferites mirabilis</i>	*1,2,3	*	*5,6,7
<i>Gonyaulax membranaceus</i> , <i>G. spinifera</i> complex	<i>Spiniferites membranaceus</i>	*2	*	*5,6,7,8
<i>Gonyaulax scrippsae</i> , <i>G. spinifera</i> complex	<i>Spiniferites ramosus</i>	*2	*	*5,6,7
<i>Gonyaulax spinifera</i> complex	<i>Spiniferites hypercanthus</i>	*2		
<i>Gonyaulax spinifera</i> complex	<i>Spiniferites delicatus</i>	*2		
<i>Gonyaulax ellegaardiae</i> , <i>G. Spinifera</i> complex	<i>Spiniferites pachydermus</i>	*2	*	
<i>Gonyaulax</i> sp.	<i>Impagidinium paradoxum</i>	*2		
<i>Gonyaulax</i> sp.	<i>Impagidinium sphericum</i>	*2		
<i>Gonyaulax</i> sp.	-	*1,2,3	*	*7
<i>Gymnodinium impudicum</i>	-	*1,2,3	*	*7
<i>Gymnodinium catenatum</i> †	-			*5
<i>Gymnodinium</i> cf. <i>catenatum</i>	-			*6,7
<i>Lingulodinium polyedrum</i> †	<i>Lingulodinium machaerophorum</i>	*1,2,3	*	*5,6,7,8
<i>Pentapharsodinium dalei</i>	-	*3	*	*5,6,7,8
<i>Pheopolykrikos hartmannii</i>	-			*5,6,7,8
<i>Protoceratium reticulatum</i> †	<i>Operculodinium centrocarpum</i>	*1,2,3	*	*5,6,7,8
<i>Pyrodinium</i> cf. <i>bahamense</i>	<i>Polysphaeridium zoharyi</i>			*6
<i>Pyrodinium bahamense</i>	<i>Polysphaeridium zoharyi</i>	*2	*	*7
<i>Pyrophacus steinii</i>	<i>Tuberculodinium vancampoeae</i>	*2,3	*	*5,6,7,8
<i>Pyrophacus</i> sp.	-			*7
-	<i>Echinidinium transparantum</i>	*2	*	
-	<i>Echinidinium</i> sp.	*2	*	
<i>Scrippsiella lachrymosa</i> #	-		*	
<i>Scrippsiella</i> cf. <i>precaria</i> #	-		*	
<i>Scrippsiella trochoidea</i> ††#	-	*2,3	*	*5,6,7,8
<i>Scrippsiella</i> sp.	-	*3		*7,8
<i>Scrippsiella trifida</i> #	-			*7,8

Continued...

Table 3C.1...Continued...

Plaktonic dinoflagellates (Biological Name)	Dinoflagellate cyst (Paleontological Name)	Regional occurrence		
		ECI	SAR ⁴	WCI
Heterotrophs				
<i>Archaeperidinium minutum</i>	-	* ²	*	
<i>Diplopelta parva</i>	-			* ^{5,6,7,8}
<i>Diplopsalis lenticula</i>	-	* ³		* ^{5,6,7}
<i>Diplopsalis cf. lebourae</i>	-		*	
<i>Diplopsalis</i> sp.	-		*	
<i>Lebouraia minuta</i>	-			* ^{7,8}
<i>Lebouraia cf. minuta</i>	-			* ⁶
<i>Polykrikos kofoidii</i>	-			* ⁷
<i>Polykrikos cf. kofoidii</i>	-			* ⁶
<i>Polykrikos schwartzii</i>	-			* ^{5,7}
<i>Polykrikos cf. schwartzii</i>	-			* ⁶
<i>Polykrikos</i> sp.	-			* ^{7,8}
<i>Peridinium quinquecorne</i>	-		*	
<i>Protoperidinium americanum</i>	-	* ²	*	* ⁵
<i>Protoperidinium avellana</i>	<i>Brigantedinium cariacense</i>	* ^{1,2}	*	* ⁵
<i>Protoperidinium cf. avellana</i>	-			* ⁵
<i>Protoperidinium claudicans</i>	<i>Votadinium spinosum</i>	* ^{1,2,3}	*	* ^{5,6,7,8}
<i>Protoperidinium compressum</i>	<i>Stelladinium stellatum</i>	* ^{1,2,3}	*	* ^{5,6,7,8}
<i>Protoperidinium conicoides</i>	<i>Brigantedinium simplex</i>	* ²	*	* ^{6,7}
<i>Protoperidinium conicum</i>	<i>Selenopemphix quanta</i>	* ^{1,2,3}	*	* ^{5,6,7,8}
<i>Protoperidinium denticulatum</i>	<i>Brigantedinium irregulare</i>	* ²	*	* ^{5,6,7,8}
<i>Protoperidinium divaricatum</i>	<i>Xandarodinium variable</i>			* ^{6,7}
<i>Protoperidinium excentricum</i>	-			* ⁵
<i>Protoperidinium latissimum</i>	-	* ^{1,2,3}	*	* ^{5,6,7,8}
<i>Protoperidinium leonis</i>	<i>Quinquecuspis concreta</i>	* ^{1,2,3}	*	* ^{6,7,8}
<i>Protoperidinium minutum</i>	Cyst of <i>Archaeperidinium minutum</i> ?	* ²		* ^{5,8}
<i>Protoperidinium cf. minutum</i>	Cyst of <i>Archaeperidinium minutum</i> ?			* ⁵
<i>Protoperidinium nudum</i>	-	* ^{1,2}		* ⁵
<i>Protoperidinium oblongum</i>	<i>Votadinium calvum</i>	* ^{1,2,3}	*	* ^{5,7,8}
<i>Protoperidinium pentagonum</i>	<i>Trinovantedinium applanatum</i>	* ^{1,2,3}	*	* ^{6,7,8}
<i>Protoperidinium cf. pentagonum</i>	<i>Trinovantedinium capitatum</i>			* ^{5,6,7,8}
<i>Protoperidinium pentagonum</i>	<i>Brigantedinium majusculum</i>			* ⁵
<i>Protoperidinium subinermis</i>	<i>Selenopemphix nephroides</i>	* ^{2,3}	*	* ^{5,6,7,8}
<i>Protoperidinium steidingeriae</i>	-	* ^{1,2}	*	
<i>Protoperidinium thorianum</i>	-	* ¹	*	
<i>Protoperidinium</i> sp.	<i>Lejeunecysta</i> sp.	* ¹		* ⁷
<i>Protoperidinium</i> sp.	<i>Lejeunecysta concreta</i>	* ³		* ^{6,8}
<i>Protoperidinium</i> sp.	<i>Stelladinium robustum</i>	* ^{1,2}	*	* ^{6,7,8}
<i>Protoperidinium</i> sp.	<i>Trinovantedinium palidifuvum</i>			* ⁷
<i>Protoperidinium</i> sp.	<i>Brigantedinium</i> sp.	* ^{1,2,3}	*	* ^{6,7,8}
<i>Zygabikodinium lenticulatum</i> /P. <i>meunieri</i>	<i>Dubridinium caperatum</i>	* ^{1,3}		* ^{6,7,8}

Incidences of HABs and outbreaks of paralytic shellfish poisoning (PSPs) have also occurred along the west coast of India (Godhe et al. 2000). Compared to this, YTXs-producing species *G. spinifera*, *P. reticulatum* and *L. polyedrum* have been observed in the surface sediments of the south-east coast of India and South Andaman region (Table 3C.1). However, only three *Alexandrium* species, *A. affine*, *A. minutum* and *Alexandrium* sp. have been reported from

Visakhapatnam harbour (D'Silva et al. 2013). Cyst of potentially HABs causing *A. pseudogonyaulax* species was exclusively observed in the South Andaman region. However, so far no HABs or PSPs produced by these species have been reported in the region. Oceanographic features like intensive coastal upwelling and anthropogenic input influence the dinoflagellate cyst composition along the west coast of India (D'Silva et al. 2011; Patil, 2003). Furthermore, D'Costa et al. (2008) observed the potential of the south-west monsoon to influence the seasonal cycling between planktonic dinoflagellates in the water column and cysts in the sediments. Along the western Bay of Bengal, climatic and oceanographic events brought through the monsoonal seasonality influence planktonic and cyst assemblage of dinoflagellates (D'Silva et al., 2013; refer Chapter 3B). However, the regional oceanographic and biological differences, like i) less nutrient availability due to stratification, nutrient scavenging to deeper waters, lack of upwelling and convective mixing, ii) competitive stress for light and nutrient scarcity and iii) reduced biological production could be the reasons for the low species diversity in the Bay of Bengal (discussed in Chapter 3B, Section 3B.1, 3B.2). These regional differences in cyst assemblage and diversity were consistent throughout the Late Quaternary period (discussed in Chapter 4B).

In the Indian region, algal bloom incidents have increased in the recent years. Although the number of PSPs and HABs are comparatively less to the western, eastern world, and mainly restricted to the west coast of India. However, the increasing coastal anthropogenic activities make this region susceptible towards the HABs initiation and development. Considering the history of initiation and spread of HAB species along previously known pristine habitats, these resilient dinoflagellate forms have potential candidature for the future blooms.

Chapter 4
Dinoflagellate cyst as a proxy of paleo-
productivity and climatic variability in the
Northern Indian Ocean

Chapter 4 Dinoflagellate cyst as a proxy of paleo-productivity and climatic variability in the Northern Indian Ocean

4.1 Why to study the Ocean paleoproductivity variability?

Ocean productivity, the uptake and sequestration of dissolved inorganic carbon into organic compounds by marine primary producers (through biological fixation) is a fundamental process in regulating carbon exchange between the ocean and atmosphere. This is an essential step in the Biological carbon pump (the oceans' carbon sequestration from the atmosphere to the deep oceans). The Ocean holds approximately 50 times more carbon than the atmosphere (Schmitt, 2008), and 20 times more as the territorial biosphere (Chen and Tsunogi, 1998). There is a continuous exchange between the ocean surface and atmosphere in the form of CO₂. The sequestration of carbon at depths results in a lower partial pressure of CO₂ of the surface water, thus also lowering atmospheric CO₂. Ocean productivity fluctuations influence climate by altering the atmospheric concentrations of CO₂. A slight change in the amount of deeply sequestered carbon content can have a substantial impact on the atmospheric CO₂ inventory. At a longer time scale of the global carbon cycle, a fraction of the organic matter exported from the surface ocean (marine fluxes) survives its passage through the water column and sediment/water interface and gets buried in the accumulating sediments, thereby removing carbon from the ocean/atmosphere system. The marine fluxes transport substantial amount of carbon into the deep ocean sediment reservoir for the timescale of millions of years.

The Ocean-atmosphere interaction evolves through the timescale of the millions of years. The marine sedimentary records (Paleoproxies) reveal temporal coincidence between millennial-scale variations of CO₂ and changes in the ocean's circulation and

biological productivity. Sedimentary archives also provide information of transition phases between different climatic states, abrupt events, which occurred on timescales of millions of years to a few centuries (IPCC, 2013). They inform about multi-centennial to millennial baseline variability, against which the recent changes can be compared to assess whether or not they are unusual. Studies of paleoproductivity proxies are therefore important because they place constraints on past ocean circulation, nutrient distribution and on the history of the oceanic carbon cycle (Gonzalez et al., 2008). Ocean paleoproductivity studies document past changes in the biological production of organic matter and skeletal material. These studies provide insight into the causes of such fluctuations, the consequences for biogeochemical cycles within the ocean, and their correspondence to climatic variability. In addition, paleoclimatic studies enable understanding of the Earth system responses on larger time scales, more than a few centuries, which cannot be estimated from short instrumental records (IPCC, 2013).

4.2 Scenario of the Northern Indian Ocean

The Asian Monsoon system has a strong bearing on the biological productivity of the Northern Indian Ocean i.e. the Arabian Sea and the Bay of Bengal. However, due to different characteristics of surface water masses, the hydrographical and resultant biological characteristics of the Arabian Sea and the Bay of Bengal differ widely. A low salinity water mass is formed in the Bay of Bengal by excess precipitation and abundant river runoff. A high salinity water mass is formed in the Arabian Sea. In most oceanic areas variations in temperature are large compared to salinity, but in the Bay of Bengal temperature gradient throughout the year is less as compared to salinity (Wyrтки, 1973). During the SW monsoon, high precipitation in the Bay of Bengal and freshwater

discharge from the Ganges, Brahmaputra, Irrawaddy, and Godavari lead to strong stratification preventing the entrainment of nutrients into the surface waters all through the year resulting in low primary productivity. Biological features such as chlorophyll, primary productivity, phytoplankton abundance and mesozooplankton are lower in the Bay of Bengal as compared to Arabian Sea (Gauns et al., 2005).

In the regional context, various proxies such as, such as abundance of planktonic foraminifera, coccolithophore, organic carbon, carbon and nitrogen isotopic records have been used to evaluate the paleoproductivity and oceanographic variability in the Arabian Sea (Ivanochko, 2004; Singh et al., 2006, 2011; Cabarcos et al., 2014; Naidu et al., 2014). However, in the Arabian Sea, productivity proxies behave differently in different regions, leading to contradictory conclusions on the past productivity variability over the last Quaternary period (discussed in Chapter 4A). In the eastern Arabian Sea, earlier findings revealed high productivity during interglacials due to strong SW monsoon and low productivity during glacials as a result of poor SW monsoon strength (Naidu, 1991; Ganeshram et al., 2000; Pattan et al., 2003; Shetye et al., 2014). A Recent study reveals that the productivity in the eastern Arabian Sea was higher during the glacials than the interglacials and was mainly controlled by the winter monsoon convection (Banakar et al., 2005; Singh et al., 2006, 2011; Cabarcos et al., 2014). Thus, still debate on whether productivity in the Arabian Sea was higher during Holocene or in last glacial period is ongoing.

As an archive for past productivity and oceanographic variability records, the Bay of Bengal is comparatively less sampled than the Arabian Sea. Only a few studies have been carried out in the region to evaluate paleo-monsoon conditions using terrigenous

flux proxies and organic geochemical proxies (Colin et al., 1998, Fontugne and Duplessy, 1986; Ponton et al., 2012), SST and SSS proxies (Prell et al., 1980; Cullen, 1981; Naidu and Govil, 2010; Govil and Naidu, 2011; Rashid et al., 2011). However, past productivity variability in the region have been estimated using proxies like redox-sensitive trace metals, organic carbon, total nitrogen, carbon and nitrogen isotopic, CaCO_3 and SiO_3 (Pattan et al., 2013; Shetye et al., 2014; Phillips et al., 2014).

In the present study, we used dinoflagellate cyst records to evaluate the paleoproductivity variability and the monsoonal dynamics in the in the eastern Arabian Sea and the western Bay of Bengal.

4A Evolution of productivity and monsoonal dynamics in the eastern Arabian Sea during the past 68 ka

4A.1 Introduction

The Asian Monsoon system has a strong bearing on the biological productivity of the Arabian Sea. The present-day climatic and oceanographic conditions predominating in the Eastern Arabian Sea (EAS) are influenced by both the South West (SW or summer) and North East (NE or winter) monsoon systems. The EAS experiences moderate upwelling and high precipitation along the entire margin during summer and winter vertical mixing in the northern part, and freshwater inflow during winter from the Bay of Bengal in the south (Banse et al., 1987; Bhattathiri et al., 1996; Prasanna Kumar et al., 2000; Gerson et al., 2014). These regional climatic and oceanographic features could also play a significant role in the evolution of productivity variation in the EAS during the Late Quaternary Period. The paleoclimatological and paleoceanographic records have provided detailed information on the late Quaternary climate variability and paleoproductivity variations in the region. Studies from the western Arabian Sea (WAS) revealed productivity was lower during the last glacial period due to a weaker SW monsoon and reduced upwelling (Naidu and Malmgren, 1996; Ivanochko et al., 2005). On the contrary, high productivity during the last glacial period was reported in the northern Arabian Sea (NAS), with an intensified NE monsoon resulting in intense deeper water mixing and increased advection of nutrient-rich subsurface water (Reichart et al., 1998; Luckge et al. 2001; Ivanova et al., 2003).

In the EAS recent studies using paleoproductivity proxies, such as abundance of planktonic foraminifera, coccolithophore, organic carbon, carbon and nitrogen isotopic

records infer that productivity was higher during the Last Glacial Maximum (LGM) than in the Holocene (Ivanochko, 2004; Singh et al., 2006, 2011; Cabarcos et al., 2014; Naidu et al., 2014). In this context, the present study used dinoflagellate cyst records over the last 68 ka to contribute further to the existing paleoclimatic and paleoceanographic information in the EAS.

Dinoflagellate is one of the dominant group of the primary producers in the marine ecosystem and has a complex life cycle which includes cyst (resting stage) formation. The rigid cell wall of dinoflagellate cyst comprises of a biomacromolecule, dinosporin (Fensome et al., 1993; Bogus et al., 2014) which enable them to resist physical, chemical and biological destruction and degradation. Thus, cyst records provide the more reliable paleoceanographic information where other calcareous and siliceous microfossil taxa, such as foraminifera, diatoms, and radiolarian, are subject to dissolution (Pospelova et al., 2006). In the recent years, various paleoceanographic studies have demonstrated the use of dinoflagellate cyst assemblages to reconstruct paleoenvironmental conditions on a centennial as well as millennial time scale (Shaozhi and Harland, 1993; de Vernal and Pederson, 1997; Marret et al., 2001; Mudie et al., 2002; Matthiessen et al., 2005; Pospelova et al., 2006; Price et al., 2013). Dinoflagellates have species-specific differential environmental and growth requirements, thus, their cyst distribution in sediments can portray surface water conditions (Dale, 2001b; Marret and Zonneveld, 2003; Zonneveld et al., 2013). Higher abundance of autotrophic species in sediments reveals stable water conditions with increased light penetration and ample nutrient supply, whereas increased abundance of heterotrophic species cysts reveals availability of prey organisms and productivity

changes (Zonneveld, 1997a; Marret and Zonneveld, 2003; Kim et al., 2009; Zonneveld et al., 2013). In recent surface sediments, dinoflagellate cyst distribution patterns have shown correlation with regionally varying surface water masses, physicochemical (temperature, salinity, dissolved oxygen, nutrients) and biological (food availability, productivity) factors (Marret and Zonneveld, 2003; Zonneveld et al., 2013).

This study presents dinoflagellate cyst abundance and assemblage records at a millennial resolution in the EAS over the last 68 ka. The focus of the present study is to better understand the marine primary productivity changes and seasonal monsoonal dynamics in relation to past climatic variability in the EAS over the late Quaternary period.

4A.2 Climatic and Oceanographic setting

Semi-annual reversal of the SW and NE monsoon winds divides the year into the SW monsoon and NE monsoon seasons respectively, separated by the two inter-monsoonal periods (spring and fall). The environmental changes induced by the monsoonal variability strongly influence oceanographic and climatic features in the Arabian Sea. Strong SW winds develop during the SW Monsoon (May-September) as a result of differential heating of the continental and oceanic regions, leading to a low atmospheric pressure above the Asian Plateau and high atmospheric pressure over the relatively cool southern Indian Ocean. In response to this, strong wind induces offshore Ekman transport, which results in intense upwelling off the Somali and Oman regions (Wyrski, 1973; Clemens et al., 1991; Morrison et al., 1998). During this period, the West Indian coastal current (WICC) develops in the NAS and flows towards the equatorward (Shankar et al., 2002; Fig. 4A.1). The offshore divergence (Ekman

transport) alongshore wind stress component leads to moderate coastal upwelling and sea surface temperature (SST) cooling by 2.5°C along the central west coast of India (Shetye et al., 1985; Naidu and Malmgren, 1999). In the EAS, SW Monsoon precipitation from the Western Ghats drains into the Arabian Sea through rivers and streams, which develops low saline plume towards offshore (Sarkar et al., 2000). As a result, increased thermal stratification reduces mixed layer depth (MLD) and nutrient advection to the euphotic layers (Gerson et al., 2014). Along the coastal regions, the supply of nutrient from upwelled bottom water and terrestrial runoff increases the primary production (Bhattathiri et al., 1996).

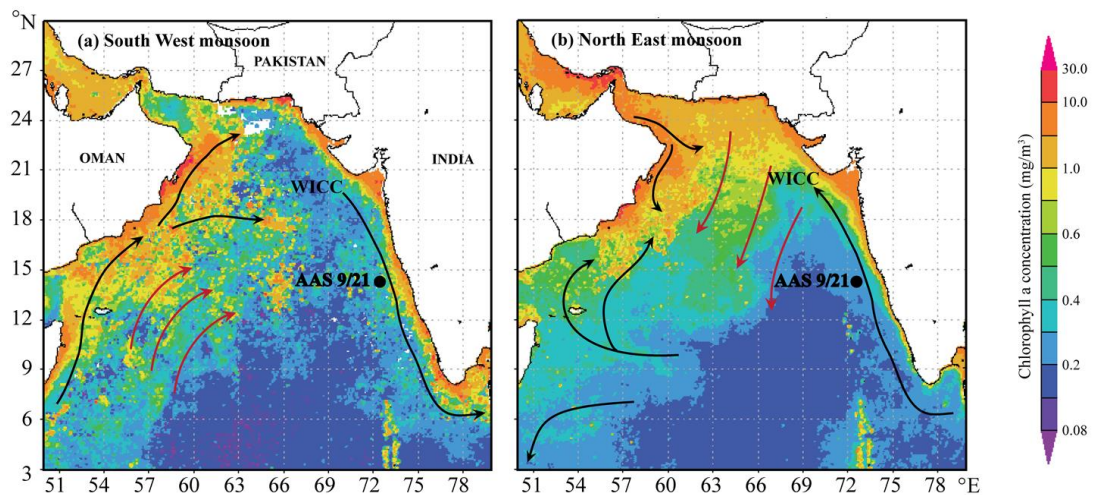


Fig. 4A.1 Core AAS 9/21 sampling site and schematic representation of the ocean circulation (black lines) and dominant wind directions (red lines) in the Arabian Sea during the monsoons (as inferred from Shankar et al., 2002; Schott et al., 2009; Cabarcos et al., 2014). The map indicates chlorophyll concentration (source NASA/ Sea WiFS) during a) the South West monsoon and b) the North East monsoons. WICC=West Indian Coastal Current.

During the NE monsoon (November-February), the wind pattern over the basin reverses to northeast due to the development of high-pressure gradient over the Tibetan Plateau and Central Asia, resulting inflow of cold and dry winds over the Arabian Sea.

This change in wind pattern reverses the direction of the WICC northwards (Shankar et al., 2002; Fig. 4A.1). During NE monsoon about 6 Sv of low saline water of the Bay of Bengal intrudes into the Arabian Sea (Shankar et al., 2002). The dry NE winds generally enhance the evaporation in the NAS, subsequently cooling and convective mixing injects nutrients into the surface layers from the thermocline region, which in turn increases productivity (Banse, 1987; Madhupratap et al., 1996), whereas in the EAS also, deep convective winter mixing supports moderate increase in productivity (Bhattathiri et al., 1996; Prasanna Kumar et al., 2000; Gerson et al., 2014) and biogenic particle flux (Haake et al., 1993) in the open ocean region.

4A.3 Material and methods

4A.3.1. Sediment core

A 4.2 m gravity sediment core AAS 9/21 was collected from the continental slope off Goa, in the EAS (14°30.539'N, 72°39.118'E; water depth 1807) during the A.A. Sidorenko cruise 9 (Fig. 4A.1). The sedimentary sequence consists of a mixture of terrigenous and biogenous material. The terrigenous material comprises clay and silt, whereas the biogenous material consists of planktonic and benthic foraminifera and traces of pteropods and diatoms (Govil and Naidu, 2010).

The Chronology of the core AAS 9/21 up to 310 cm depth was established based on six Accelerator Mass Spectrometry (AMS) ¹⁴C dates (Table 4A.1). Below, the chronology was established by correlating $\delta^{18}\text{O}$ of *Globigerinoides ruber* record with the low-latitude global isostack curve of Martinson et al. (1987) (refer Govil and Naidu, 2010). Sedimentation rate varies from 4.6 to 13.6 cm ka⁻¹ at the core location (Fig. 4A.2; Govil and Naidu, 2010).

Table 4A.1 Age model for core AAS 9/21

Depth (cm)	Radiocarbon age*	Calibrated Calendar years BP**
0	850±25	512±9
53	9540±80	10343±326
110	12770±80	14529±326
148	16070±115	18965±240
213	21290±180	24980±458
310	42660±2500	46282±2283

*AMS 14C dating was performed on monospecific samples of the planktonic foraminifera *G. ruber* using the Tandem Accelerator at Leibniz-Labor für Altersbestimmung und Isotopenforschung, Christian-Albrechts-Universität, Kiel, Germany. **Measured 14C ages were converted to sediment ages using the online CalPal version QuickCal 2005 version 1.4 (Weninger et al., 2006) [adopted from Govil and Naidu, 2010].

4A.3.2 Palynological sample preparation and analysis

The core was cut into 3 cm-thick slices, out of which samples from alternative sections were used for dinoflagellate cyst analysis. Seventy-five samples covering a span of ~68 ka were processed using the palynological method (Matsuoka and Fukuyo, 2000) with some modifications. A known weight of dry sediment (7-8 g) was repeatedly washed with distilled water to remove salts, sonicated (30 sec.) and sieved through 120 µm and 10 µm meshes to remove coarse and fine particles. The slurry accumulated on 10 µm was treated with HCl (10%) for 10 hrs and HF (30%) for 36-48 hrs to dissolve calcareous and silicate materials. Each chemically treated sample was washed with distilled water to remove acid, sonicated for 30 sec. Later, the slurry was sieved through 10 µm to remove fine material. The residue accumulated on the 10 µm mesh was then suspended in 10 ml distilled water and kept in a vial. For observation, aliquots of processed sample were counted in duplicate or a higher number of replicates, such that a minimum of 250 cysts were counted per sample. However, in some samples (representing ages ~8.3, 1.0, 1.67, 11.11 and 11.92 ka) only 150 to 160 cysts were

counted. Dinoflagellate cyst abundance was estimated per gram dry weight sediment (cysts g⁻¹).

Dinoflagellate cysts were identified by using inverted microscope (Olympus IX 71) at 200X and 1000X magnifications based on published morphological descriptions (Fensome et al., 1993; Zonneveld, 1997b; Lewis et al., 1999; Matsuoka and Fukuyo, 2000; Rochon et al., 2009; Radi et al., 2013) and modern dinoflagellate cyst determination key by Zonneveld and Pospelova, (2015) (online version: https://www.marum.de/en/Modern_dinoflagellate_cyst_determination_key.html). The nomenclature used for this study is in accordance with Head (1996), Zonneveld (1997b), Fensome and Williams (2004).

On the basis of morphological similarity, some dinoflagellate species have been grouped together prior to statistical analysis. *Spiniferites* species, *S. ramosus*, and *S. bulloideus* were grouped together as *S. ramosus* because of very slight interspecific morphological variation in size and processes thickness. Similarly, *S. mirabilis* and *S. hyperacanthus* have morphological similarities with the exception of the absence of crown process in *S. hyperacanthus*, hence grouped together as *S. mirabilis* (Radi and de Vernal, 2008; Rochon et al., 2009). *S. quanta* and cyst of *P. nudum* have similar morphology with some variation in size and number of process, hence considered as *S. quanta*. *Stelladinium* species, *S. stellatum*, and *S. reidii* were grouped as *S. stellatum*. *Brigantedinium* spp. represent all smooth walled, spherical brown cysts. In the absence of archeopyle intraspecific differentiation is difficult in these morphotypes, whereas sometimes cyst folding also hides the archeopyle structure (Pospelova et al., 2006).

4A.3.3 Statistical analysis

The abundance of dinoflagellate cyst was further subjected to calculate species diversity (Shannon-Wiener diversity index i.e. H'), species richness and evenness using the software PRIMER (version 6).

Further, the multivariate statistical analysis was performed on relative abundance data of dinoflagellate cyst using CANOCO 4.5 software for Windows (ter Braak and Smilauer, 2002). Prior to statistical analysis, dinoflagellate cyst data were logarithmically transformed ($\log x+1$) to minimize the dominance of few abundant species and increase the weight of less abundant species, which could thrive in the narrow ecological niche. To determine the variability within data set Detrended Correspondence Analysis (DCA) was performed. The length of the first gradient axis was 1.7 standard deviation unit (sd) indicate linear variation (ter Braak and Smilauer, 2002) in cyst assemblage within the core sections. Due to linear character of data set a Principle Component Analysis (PCA) was performed, which can reduce the dimensionality of the data set and summarize it by extracting the smallest number components that account for most of the variation in the original multivariate data (Hair et al., 1992).

4A.4 Results

4A.4.1. Dinoflagellate cyst assemblage and abundance

A total of 29 dinoflagellate cyst species were identified from 75 sediment sample intervals analysed in the core AAS 9/21, covering a time span of ~68 ka (MIS 1-4) (Table 4A.2). The number of species varied from 4 to 17. Cysts of autotrophic Gonyaulacoid species were the most dominant and mainly represented by *Spiniferites*

group, *Spiniferites ramosus* (up to 54%), *S. membranaceus* (up to 45%), *S. bentori* (up to 40%), *S. mirabilis* (up to 38%), *Impagidinium sphaericum* (up to 37%) and *Spiniferites* sp. 1 (up to 21%) (Fig. 4A.2). Other dominant autotrophic species were *S. pachydermus* (up to 17%) and *Operculodinium centrocarpum* (up to 8%).

Table 4A.2 List of dinoflagellate cyst species identified in sediment samples from the Core AAS 9/21 with abbreviations and thecate dinoflagellate affinity.

Dinoflagellate cyst (Paleontological Name)	Abbreviations	Thecate dinoflagellate affinity (Biological Name)
Autotrophic		
<i>Bitectatodinium spongium</i>	Bspo	–
<i>Impagidinium aculeatum</i>	Iacu	<i>Gonyaulax</i> sp.
<i>Impagidinium paradoxum</i>	Ipar	<i>Gonyaulax</i> sp.
<i>Impagidinium sphaericum</i>	Isph	<i>Gonyaulax</i> sp.
<i>Lingulodinium machaerophorum</i>	Lmac	<i>Lingulodinium polyedra</i>
<i>Nematosphaeropsis labyrinthus</i>	Nlab	<i>Gonyaulax spinifera</i> complex
<i>Operculodinium centrocarpum</i>	Ocen	<i>Protoceratium reticulatum</i>
<i>Polysphaeridium zoharyi</i>	Pzoh	<i>Pyrodinium bahamense</i>
<i>Spiniferites bentorii</i>	Sben	<i>Gonyaulax digitalis</i> , <i>G. spinifera</i> complex
<i>Spiniferites bulloideus</i>	–	<i>Gonyaulax scrippsae</i> , <i>G. spinifera</i> complex
<i>Spiniferites hyperacanthus</i>	–	<i>Gonyaulax spinifera</i> complex
<i>Spiniferites membranaceus</i>	Smem	<i>Gonyaulax spinifera</i> complex
<i>Spiniferites mirabilis</i>	Smir	<i>Gonyaulax spinifera</i> complex
<i>Spiniferites pachydermus</i>	Spac	<i>Gonyaulax spinifera</i> complex
<i>Spiniferites ramosus</i>	Sram	<i>Gonyaulax scrippsae</i> , <i>G. spinifera</i> complex
<i>Spiniferites</i> sp. 1	Ssp.1	<i>Gonyaulax</i> sp. complex
Heterotrophic		
<i>Brigantedinium</i> spp.	Bsp.	<i>Protooperidinium</i> spp.
–	Pkof	<i>Polykrikos kofoidii</i>
–	Plat	<i>Protooperidinium latissimum</i>
<i>Echinidinium transparantum</i>	Etra	<i>Protooperidinium</i> sp.
<i>Quinquecuspis concreta</i>	Qcon	<i>Protooperidinium leonis</i>
<i>Selenopemphix nephroides</i>	Snep	<i>Protooperidinium subinerme</i>
<i>Selenopemphix quanta</i>	Squa	<i>Protooperidinium conicum</i>
–	–	<i>Protooperidinium nudum</i>
<i>Stelladinium robustum</i>	Srob	<i>Protooperidinium</i> sp.
<i>Stelladinium stellatum</i>	Sste	<i>Protooperidinium stellatum</i>
<i>Stelladinium reidii</i>	–	<i>Protooperidinium</i> sp.
<i>Trinovantedinium applanatum</i>	Tapp	<i>Protooperidinium pentagonum</i>
<i>Votadinium calvum</i>	Vcal	<i>Protooperidinium oblongum</i>

Among heterotrophic species, *Selenopemphix nephroides* (up to 13%), *Brigantedinium* spp. (up to 8%) and *Trinovantedinium applanatum* (up to 7%) were dominant.

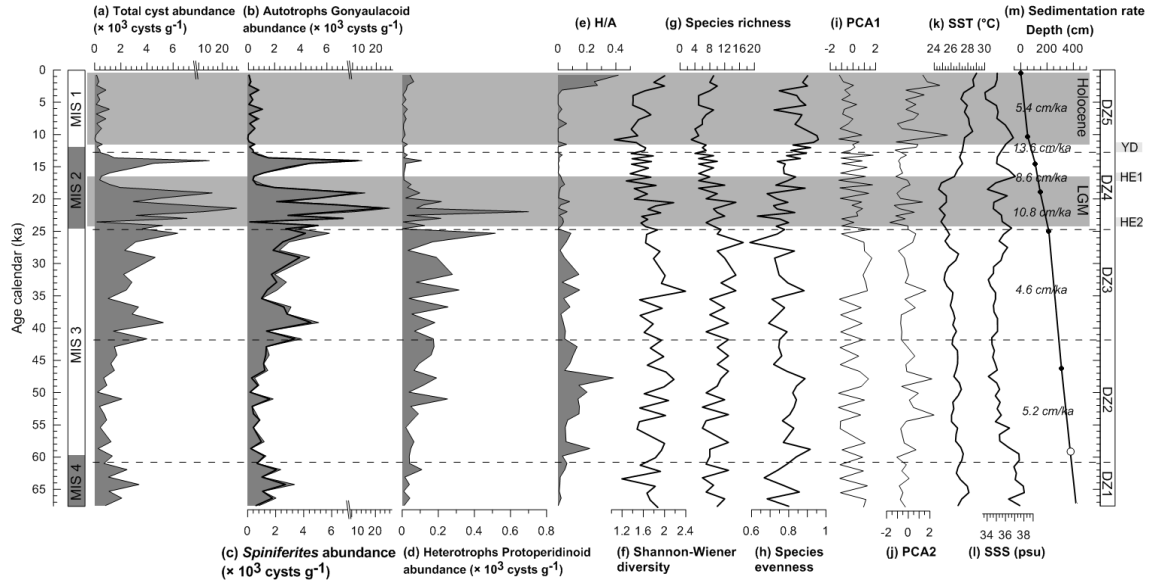


Fig. 4A.2 Relative abundances (%) of selected dinoflagellate cyst taxa and a plot of age-depth along with sedimentation rates (cm ka^{-1}) corresponding between two tie points. AMS ^{14}C dates calibrated to calendar age (filled circles) and isotope stage boundary of MIS 3 and 4 (unfilled circle) [Govil and Naidu, 2010]. For cyst abbreviation please refer Table 4A.2. Dinoflagellate cyst zones (DZ) are separated by dashed lines. The Holocene and LGM are shown by grey shaded horizontal bars. Heinrich events (HE 2 and HE1) and the Younger Dryas (YD) are highlighted in grey.

Dinoflagellate cyst abundance varied down-core from ~ 140 to $26000 \text{ cysts g}^{-1}$, averaging $3000 \text{ cysts g}^{-1}$ (Fig. 4A.3a). Cyst abundance was higher (~ 260 to $3390 \text{ cysts g}^{-1}$, avg. $1470 \text{ cysts g}^{-1}$) in MIS 4 than in early MIS 3 (~ 222 to $2081 \text{ cysts g}^{-1}$, avg. 987 cysts g^{-1}), whereas approximately twofold increase was observed in late MIS 3 (~ 41.67 to 25.3 ka) (~ 1030 to $6350 \text{ cysts g}^{-1}$, avg. $3210 \text{ cysts g}^{-1}$). The cyst abundance was two folds higher during MIS 2 (~ 1500 to $26000 \text{ cysts g}^{-1}$, avg. $5450 \text{ cysts g}^{-1}$), including the LGM (19 to 21 ka), than in MIS 3. In the Holocene, cyst abundance decreased about

three folds than the preceding LGM (Fig. 4A.3a). Over the last 68 ka autotrophic Gonyaulacoid species were dominant (avg. 2400 cysts g^{-1}), than heterotrophic Protoperidinooid species (avg. 80 cysts g^{-1}) (Fig. 4A.3b and d). Although the absolute abundance of heterotrophic cyst taxa was less, their relative abundance was comparatively more during MIS 3 and in the late Holocene (from ~3 ka onwards) (Fig. 4A.3d).

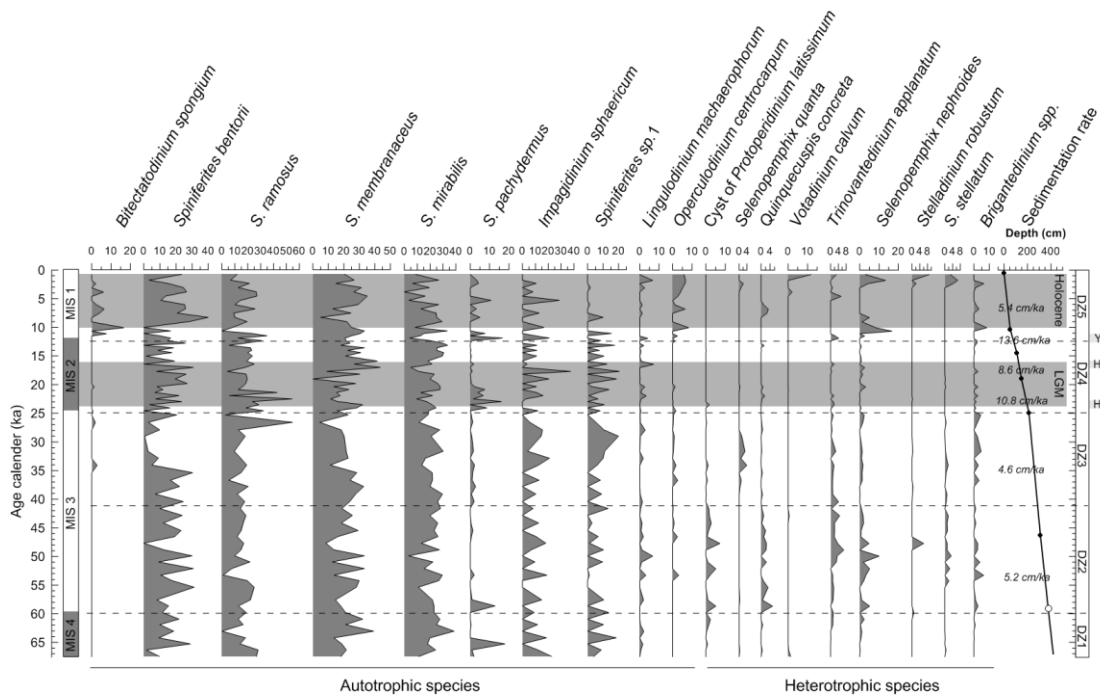


Fig. 4A.3 (a) Total cyst abundance along with (b) Autotrophic (c) Spiniferites (dark line) and (d) Heterotrophic cyst species; (e) Ratio of autotrophic to heterotrophic cysts (A/H); diversity indices (f) Shannon-Wiener diversity index, (g) Species richness, (h) Species evenness; sample score for (i) PCAs 1, (j) PCA 2 and (k) Sea surface temperature (SST) and (l) Salinity (SSS) estimated using Mg/Ca and $\delta^{18}O_w$ of *Globigerinoides ruber* respectively (Govil and Naidu, 2010), (m) Plot of age-depth along with sedimentation rates ($cm\ ka^{-1}$) corresponding between two tie points. AMS ^{14}C dates calibrated to calendar age (filled circles) and isotope stage boundary of MIS 3 and 4 (unfilled circle) [Govil and Naidu, 2010]. Dinoflagellate cyst zones (DZ) are separated by dashed lines. The Holocene and LGM are shown by grey shaded horizontal bars. Heinrich events (HE 2 and HE1) and the Younger Dryas (YD) are highlighted in grey.

The heterotrophic (H) and autotrophic (A) dinoflagellate cyst ratio (H/A) decreased during MIS 4, MIS 2 and the early Holocene (Fig. 4A.3e). An abrupt increase in H/A ratio towards the late Holocene and large variation during MIS 3 was due to the contribution of Protoperidinoid species (Fig. 4A.3d and e).

The Shannon-Wiener, a species diversity index (H') varied from 1.05 to 2.39. It was highest from ~35 to 25 ka and since ~3 ka, and the lowest was observed during the LGM to early Holocene (Fig. 4A.3f). Species richness also followed similar trends as that of species diversity index (Fig. 4A.3g). However, species evenness varied from 0.59 to 0.95, cyst assemblage was more even in MIS 1 (avg. 0.86) (Fig. 4A.3h).

4A.4.2 Statistical analysis and dinoflagellate cyst zones

A Principle Component Analysis (PCA) performed on the logarithmically transformed relative abundance data of dinoflagellate cyst, reveals four principal components axis (1-4 PCs) accounting 28.4%, 11.5%, 8.8% and 7.3% of variances respectively, with a total cumulative variance of 56%. Graphical representation of the same, a PCA biplot, shows ordination of each species and samples along first two most dominant PCs, PCA1 and PCA2 (Fig. 4A.4). Samples similar in species composition are located close to each other in the PCA biplot. Based on sample score for PCA1, PCA2 and relative abundance of dinoflagellate cyst, five dinoflagellate cyst zones (DZ1-5) were established. All dinoflagellate cyst zones were characterized by the dominance of *Spiniferites* species. Apart from this, the characteristic species composition of each zone is presented below.

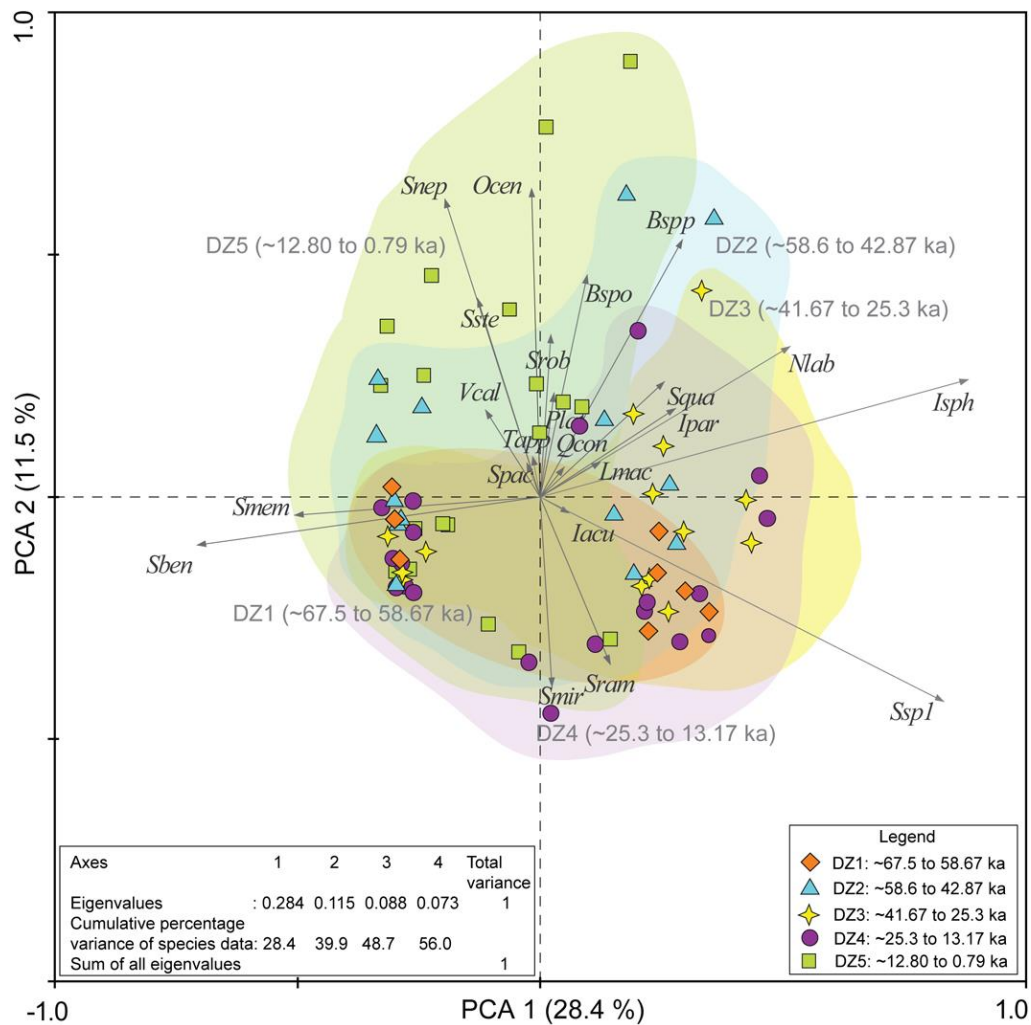


Fig. 4A.4 Principle Component Analysis (PCA) biplot diagram indicate dinoflagellate cyst species (grey arrows) in relation with sediment sample ordination (coloured symbols; diamond, triangle, star, circle, square). Species abbreviations are as given in Table 4A.2.

4A.4.2.1. DZ1 (~67.5 to 58.67 ka)

This zone was dominated by autotrophic *Spiniferites* species, *S. membranaceus* (avg. ~23.2%), *S. mirabilis* (avg. 23.4%), *S. ramosus* (avg. 16.8%) and *S. bentorii* (avg. 13.9%), and relatively less contribution of Protoperidinoid species (avg. 0.03%), which results into lesser Shannon-Wiener diversity index, species richness and evenness (Fig.

4A.2 and 4A.3e, f, g). This zone corresponds to MIS 4 and is characterised by fluctuating values of PCA1 and negative values of PCA2 (Fig. 4A.3i and j).

4A.4.2.2. DZ2 (~58.60 to 42.87 ka)

Approximately two-fold decrease in the absolute cyst and Gonyaulacoid cyst abundance was observed in DZ2 than the preceding DZ1 (Fig. 4A.3a and b). Increased relative abundance of Protoperidinoid species, *Brigantedinium* spp., *S. nephroides*, *S. stellatum*, *Q. concreta*, cyst of *P. latissimum* and *T. applanatum* was observed during this period, which could also be responsible for the increase in the H/A ratio and Shannon-Wiener diversity index (Fig. 4A.2 and 3e, f).

4A.4.2.3. DZ3 (~41.67 to 25.30 ka)

DZ3 extend from mid to late MIS 3 and is distinguished by mostly positive PCA1 and PCA2 values (Fig. 4A.3i and j). Relative abundance of *S. mirabilis* (avg. 21.91%), *S. membranaceus* (avg. 21.3%), *S. ramosus* (avg. 16.6%) and *S. bentorii* (avg. 12.09%) increased during this period, whereas heterotrophic taxa *S. quanta* (avg. ~0.8%) appeared during ~34.09 to 29.04 ka (Fig. 4A.2).

4A.4.2.4. DZ4 (~24.6 to 13.17 ka)

DZ4 coincides with MIS 2, including the LGM. Absolute cyst and autotrophic species abundance showed large fluctuation with numerous spikes (Fig. 4A.3a and b), whereas heterotrophic species abundance was highest during the LGM. An abrupt decrease in absolute cyst, autotrophic and *Spiniferites* species abundance was observed during early MIS2 (23.54 and 20.39 ka) and from 17.03 to 16.45 ka (Fig 3a, b, and c). Changes in cyst assemblage and abundance were also reflected in fluctuating values of

PCA1, whereas most of the PCA2 values were negative (Fig. 4A.3i and j). Relative abundance of *S. membranaceus* (avg. ~22%), *S. ramosus* (avg. 21.54%) and *S. mirabilis* (avg. 21.36%) reached to its maximum during the LGM whereas it was declined in case of heterotrophic taxa *Brigantedinium* spp. (avg. ~0.7%), *Selenopemphix quanta* (avg. ~0.02%), *Quinquecuspis concreta* (avg. ~0.2%) and *Trinovantedinium applanatum* (avg. ~0.4%) (Fig. 4A.2). Absolute abundance of heterotrophic species was lowest during this period than preceding MIS 3 which negatively influenced H/A ratio (Fig. 4A.3e). Fluctuating values of species indices also support the variability in cyst assemblage during this period. Overall decreasing trend in Protoperidinioid taxa reflected in decreased Shannon-Wiener index, species richness whereas increasing species evenness could be supported by increased abundance of Gonyaulacoid species (Fig. 4A.3).

4A.4.2.4. DZ5 (~12.80 to 0.79 ka)

An abrupt increase in a cyst of autotrophic taxa, *Bitectatodinium spongium*, *S. pachydermus* and *O. centrocarpum* were the characteristic feature of this zone (Fig. 4A.2). *S. bentori*, *S. membranaceus* and *S. mirabilis* relatively dominate cyst assemblage especially during 12.36, 9.4, 6.07 and 3.1 ka, in the Holocene (Fig. 4A.2). Relative abundance of heterotrophic species, *S. stellatum*, *S. robustum* and *V. calvum* and *S. nephroides* increased during the late Holocene (~3 ka), which in turn increases H/A ratio, species richness and evenness (Fig. 4A.2 and 4A.3e, f, g). Shannon-Wiener diversity index was lowest during the entire Holocene and increased since ~3 ka due to the appearance of heterotrophic species. PCA1 values were positive whereas PCA2 values were negative in DZ5 (Fig. 4A.3i and j).

4A.5 Discussion

Dinoflagellate cyst production in the marine environment is mainly influenced by physicochemical factors such as SST, sea surface salinity (SSS) and nutrients, thus cyst abundance and assemblages in sediments have been used to reconstruct climatic and oceanographic variability in the geological past (de vernal et al., 2001; Dale, 2001; Mudie et al., 2002; Morquecho and Lechuga-Deveze, 2004; Pospelova et al., 2008; Zonneveld et al., 2013). Recent sediment trap and cyst distribution studies in the Arabian Sea revealed the monsoon influence on cyst production and assemblage (Zonneveld, 1997a; Zonneveld and Brummer, 2000; D'Costa et al., 2008). The present study demonstrates the use of dinoflagellate cyst abundance as a paleoceanographic proxy to understand the monsoonal productivity and OMZ variations in the EAS (Table 4A.3).

4A.5.1. *Dinoflagellate cyst preservation and OMZ intensity*

Dinoflagellate cyst can be affected by oxidative degradation similar to the organic matter, especially cysts of *Protoperidinium* species, which appears to be more sensitive to oxidative degradation than Spiniferites species (Zonneveld et al., 1997a). Poor preservation of *Protoperidinium* in sediment can be linked to aerobic decay in oxygenated bottom water and weak intensity of the OMZ (Zonneveld et al., 1997a, 2007; Reichart and Brinkhuis, 2003), therefore high abundance of *Protoperidinium* species could indicate the increased productivity and good preservation state in the OMZ sediments (Reichart and Brinkhuis, 2003; Zonneveld et al., 2007; Zonneveld et al., 2013). Reichart and Brinkhuis (2003) used *Protoperidinium* cyst as a proxy for paleoproductivity in the NAS, where comparison of *Protoperidinium* cyst abundance

within and outside the OMZ settings highlighted their degradation during paleoclimatic events where bottom waters were oxic. In the core AAS 9/21, absolute abundance of *Protoperidinium* varies over last 68 ka with maximum abundance in MIS 3 and late Holocene (Fig. 4A.3e). This increase in *Protoperidinium* cyst abundance could be facilitated by their better preservation due to reduced oxygen supply and increased denitrification resultant of intense OMZ, an inference supported by several lines of evidence. First, higher $\delta^{15}\text{N}$ and C_{org} value during MIS 3 and late Holocene reveal the increased denitrification and better organic matter preservation in the Core AAS 9/21 sediments (Godad, 2014). Second, increased Mo concentration highlights the low oxygen condition and intensified OMZ during this period (Godad, 2014). Since *Protoperidinium* cysts can be used as productivity proxy, we could expect higher *Protoperidinium* cyst abundance during MIS 4 than in MIS 3, because in the EAS productivity was higher during glacials than interglacials (Ivanochko, 2004; Banakar et al. 2010; Kessarkar et al., 2010; Singh et al., 2011). The sedimentary $\delta^{15}\text{N}$ and Mo records in the core AAS 9/21 reveal weak OMZ due to less denitrification and oxic conditions during the glacials (MIS 4 and MIS 2) (Godad, 2014). This is further supported by other studies in the EAS, which reveals OMZ was less intense and water column denitrification declined during the glacial periods (Ivanochko et al., 2005; Kessarkar et al., 2010). In this context, the variation in *Protoperidinium* cyst abundance can be used as a biological proxy to reconstruct the OMZ variation (Table 4A.3), similar to other geochemical proxies in the late Quaternary sediments along the EAS, in particular, species like *Q. concreta*, *S. stellatum*, *S. nephroides*, *T. applanatum* and *Brigantedinium* sp. which are more susceptible to oxidative degradation and observed in

higher concentrations in anoxic or hypoxic sediments (Zonneveld et al., 1997a, 2007; Zonneveld et al., 2013).

Table 4A.3 Schematic presentation of variation in productivity, OMZ, monsoon and dinoflagellate cyst assemblage in the eastern Arabian Sea during the four Marine Isotopic Stages (MIS 1-4).

<p>MIS 1 Strong summer Monsoon Increased rainfall Increased SST + decreased SSS Stratified water Cloud cover + low light penetration</p>	<p>DZ5 (~12.8 to 0.79 ka) Total cyst abundance (↓) Gonyaulacoid species (↓) Protoperidinoid species (↓) Reduced productivity</p>
<p>MIS 2 Strong winter monsoon Reduced SST + fluctuating SSS Less turbulence + deeper light penetration</p>	<p>DZ4 (~24.6 to 13.17 ka) Abrupt changes in total cyst abundance Fluctuation in Gonyaulacoid and Protoperidinoid abundance High productivity</p>
<p>MIS 3 Increased strength of winter monsoon Decreasing SST + increasing SSS Increased winter convection Increased light penetration</p>	<p>DZ3 (~41.67 to 25.3 ka) Total cyst abundance (↑) Gonyaulacoid species (↑) Protoperidinoid species (↑) Increase in productivity Intense OMZ</p>
<p>Strong summer monsoon Increased rainfall Reduced SST + SSS Stratified water + shallow MLD Cloud cover + reduced light penetration</p>	<p>DZ2 (~58.6 to 42.87 ka) Total cyst abundance (↓) Gonyaulacoid species (↓) Protoperidinoid species (↑) Increasing OMZ intensity</p>
<p>MIS 4 Moderate winter monsoon convection High SST + SSS Less turbulence + deeper light penetration</p>	<p>DZ1 (~67.5 to 58.67 ka) Total cyst abundance (↑) Gonyaulacoid species (↑) Protoperidinoid species (↓) Increased productivity</p>

Cyst produced by Gonyaulacoid species, *L. machaerophorum*, *O. centrocarpum* and *Spiniferites* species including *S. bentori*, *S. mirabilis*, *S. pachydermus* and *S. ramosus* are proven to be moderately sensitive, whereas *Impagidinium* species (*I.*

aculeatum and *I. paradoxum*) and *N. labyrinthus* are resistant to the oxidative degradation (Zonneveld et al., 1997a, 2007). Reichart and Brinkhuis (2003) reported that in surface sediments within and outside the OMZ in the WAS, where fluxes in the productive sea-surface layer were identical, concentrations of most Gonyaulacoid species were similar in all sediments, whereas the OMZ samples were relatively enriched in *Protoperidinium* cysts. The effect of post-depositional species-selective oxidative degradation was minimal on the preservation of Gonyaulacoid species than *Protoperidinium* (Reichart and Brinkhuis, 2003). In the core AAS 9/21, autotrophic Gonyaulacoid species dominated cyst assemblage, with peaks in MIS 4, late MIS 3 and MIS 2 (Fig. 4A.3b). Increased absolute abundance of Gonyaulacoid species, in particular, *Spiniferites* species during these periods reflects the variability in the primary productivity and monsoon in the EAS (Table 4A.3).

4A.5.2 Productivity variations in the EAS

Dinoflagellate cyst assemblage composition reflect surface productivity and their fossil assemblages were used for the reconstruction of the paleoproductivity during the Late Quaternary period in the Santa Barbara Basin (Pospelova et al., 2006), Guaymas Basin (Price et al., 2013), Gulf of Alaska (de Vernal and Pederson, 1997; Marret et al., 2001), Arctic region (Matthiessen et al., 2005), Black sea (Mudie et al., 2002) and south China Sea (Shaozhi and Harland, 1993). In the WAS, relative abundance of dinoflagellate cyst was used for the reconstruction of the SW monsoon variability during the Late Quaternary (Zonneveld, et al., 1997b), whereas in the Bay of Bengal variation in cyst abundance and species assemblage was implicated to study the Late Quaternary productivity and climatic variability (Chapter 4B). In Core AAS 9/21,

the temporal variation observed in Gonyaulacoid species, *Spiniferites* species, in particular, provide valuable information about the millennial time scale productivity variations in the EAS region and is discussed below.

The high absolute abundance of Gonyaulacoid species, *Spiniferites* species in particular, during MIS 2 and MIS 4, indicate biological productivity increase during the glacials (Fig. 4A.3c,d and Table 4A.3). *Spiniferites* cysts belong to autotrophic *Gonyaulax* species, which can sustain in a wide range of environmental variables (mainly salinity, temperature, and nutrients) (Zonneveld et al., 2013). Higher abundance of *Spiniferites* species during the glacials suggest nutrient supply from deeper waters due to vertical winter convection resultant of the strong NE Monsoons, whereas reduced strength of the SW Monsoon decreases cloud cover and supply of low saline terrestrial runoff. This reduces turbidity and increases light penetration into euphotic layers which in turn favours the growth of *Spiniferites* species. Zonneveld and Brummer (2000), also observed high flux of *Spiniferites* species in the sediment trap along the Somalian region during the end of the SW monsoon when water conditions were relatively stable with high nutrient concentrations and reduced turbulence. Furthermore, interpretation of the NE monsoonal control on glacial productivity in the EAS gets support from CaCO₃ data in the present core (Godad, 2014) and recent planktonic foraminifera, coccolithophore and geochemical productivity proxy data from other core studies in the region (Rostek et al., 1997; Ivanochko, 2004; Singh et al., 2006, 2011; Cabarcos et al., 2014). The planktonic foraminiferal species and geochemical proxy records in the core MD76-131 and SK 17 increased two-fold during the glacials and has been attributed to productivity increase due to nutrient enrichment resultant of the NE Monsoon-induced

winter mixing (Singh et al., 2006, 2011; Naidu et al., 2014). The strong, cold and dry NE winds during the glacial would have resulted in enhanced evaporation, resulting an increase of SSS (Govil and Naidu, 2010) and convective upward winter mixing in the EAS (Singh et al., 2011; Rostek et al., 1997; Cabarcos et al., 2014). Above mentioned cores (MD76-131 and SK 17) were from the present OMZ regions. Thus, comparison of cyst abundance records in the core AAS 9/21 with the productivity trends observed in OMZ cores supports that *Spiniferites* species abundance in the present core can be a good indicator of productivity changes during the glacial and interglacial periods in the EAS.

In glacials, *Spiniferites* species abundance was comparatively lower during the MIS 4 than MIS 2 (Fig. 4A.3b), which could reveal the productivity variability during the MIS 4 and MIS 2. This could attribute to the comparatively decreased strength of the NE Monsoon during the MIS 4 than MIS 2 as observed in salinity proxy ($\delta^{18}\text{O}_w$) records in the core AAS/9-21 (Govil and Naidu, 2010). Furthermore, geochemical paleoproductivity proxy records in OMZ also suggest higher productivity during the MIS 2 than MIS 4 due to the strongest NE monsoon (Banakar et al., 2010).

4A.5.3 Relationship between dinoflagellate cyst assemblage and monsoon variability

The MIS 4 was dominated by *Spiniferites* species, mainly *S. bentorii*, *S. ramosus*, *S. membranaceus* and *S. mirabilis* (Fig. 4A.2 and 3b). In modern sediments, these *Spiniferites* species can found in the eutrophic to oligotrophic waters, whereas their high relative abundance can be observed in the nutrient elevated waters within well-mixed surface waters as well as outside the upwelling cells (Zonneveld et al., 2013). *S. bentorii*, *S. membranaceus*, and *S. mirabilis* are warm-water species. In

addition *S. bentorii* and *S. miribilis* can tolerate high SSS as well (Marret and Zonneveld, 2003; Zonneveld et al., 2013). A Higher proportion of *Spiniferites* taxa has also been suggested to reflect the warmer water in the southern Californian region (Prauss, 2002). In the EAS increased the abundance of *Spiniferites* species during MIS 4 could be attributed to comparatively warm, hypersaline (Fig. 4A.1, 2) and stable water mass. This interpretation could be supported by previous paleo-salinity reconstructions on this Core AAS 9/21 (Govil and Naidu, 2010), which reveals that during MIS 4, variation in SST and SSS was higher (Fig. 4A.3k and l), indicating the warmer and saline water as a result of increased evaporation and decreased precipitation due to the relatively stronger NE monsoon.

Absolute cyst abundance decreased from MIS 4 to early MIS 3 (~58.61 to 42.87 ka). A similar shift has been observed in *Spiniferites* species, whereas *Protoperidinium* cyst abundance increased in MIS 3 compared to MIS 4 (Fig. 4A.3c and d). This interval characterised by *Q. concreta*, *S. nephroides*, cyst of *P. latissimum*, *T. applanatum*, and *Brigantedinium* spp. (Fig. 4A.2). This increase in *Protoperidinium* species abundance could be due to their better preservation in the anoxic sediments as discussed in section 5.1. During most of the deglaciation, the winter monsoon winds were weak, resulting in reduced vertical mixing. However, the strong SW monsoon and associated river discharge into the EAS enhance nutrients supply in surface layers, which fuel the growth of primary producers, mainly diatoms. However, reduced light penetration due to increased turbidity and cloud cover during the prevalent SW monsoon as well as competition with diatom for nutrients could be the reasons for the suppressed growth of *Spiniferites* species during early MIS 3.

The upper section of MIS 3 (~41.67 to 25.3 ka) was characterised by increased abundance of autotrophic *Spiniferites* species (Fig. 4A.3b). In the Santa Barbara Basin, elevated relative abundance of *Spiniferites* species was related to the enhanced input of nutrient enriched water (Pospelova et al., 2006). In core AAS 9/21, increasing relative abundance of *Spiniferites* species, especially *S. membranaceus*, *S. miribilis* and *S. remosus* during late MIS 3 could be due to elevating nutrient concentrations resultant of the strong winter convection and more availability of light due to less cloud cover, especially from ~34.09 to 26.62 ka. Cysts of other autotrophic species like *I. sphaericum* and *Spiniferites* sp. 1 increased greatly during this period, which highlights elevated SSS (Fig. 4A.2 and 3k), resultant of increased evaporation due to the strong NE monsoon dry and cold winds. This conclusion is in part supported by the increasing SSS due to lower precipitation during late MIS 3 (Fig. 4A.3l). Increasing abundance of *Protoperdinium* species, especially *S. quanta* reveals a decrease in oxidative degradation due to intense OMZ (refer section 5.1).

A shift from relatively stable to largely fluctuating dinoflagellate cyst abundance characterizes a shift from MIS 3 to MIS 2 (Fig. 4A.3a). Abrupt change in total cyst abundance is the characteristic feature of the MIS 2, including LGM period. Samples from DZ4 are more dispersed in the PCA biplot, demonstrating greater variation in cyst assemblages during MIS 2. Since dinoflagellates respond to their surrounding environmental conditions, high variation in cyst abundance during MIS 2 indicate variability in the climatic and oceanographic conditions was more complex. Absolute abundance of autotrophic species indicate higher productivity, but largely fluctuating cyst abundance values emphasize the productivity changes were not constant

throughout MIS 2. This fluctuation in the cyst abundance could be due to the varying cyst flux, which can be influenced by variation in sedimentation rate during MIS 2 in the present core (Fig. 4A.3). The increased abundance of Gonyaulacoid species, especially *S. ramosus*, *S. membranaceus*, *S. mirabilis*, *S. pachydermus*, and *Spiniferites* sp. 1 during this period suggest strong winter mixing due to the prevalence of the strong NE monsoon winds. Reduced stratification and deeper MLD facilitate vertical advection of nutrients into upper photic layers, which in turn supports the growth of autotrophic dinoflagellates.

Dinoflagellate records showed the sudden decrease in total cyst abundance, *Spiniferites* species abundance and relative abundance of all dominant species during stadial periods (Northern hemisphere cold periods), the Heinrich events (HE2 and HE1) and Younger Dryas (YD) (Fig. 4A.2 and 3a). The reduction in the NE monsoon wind-flow could lead to reducing the winter deep convective mixing and/or upwelling along the EAS, leading to the higher SST (Govil and Naidu, 2010) and decreased production (Anand et al., 2008; Singh et al., 2011). Although the *Spiniferites* species responds well to warmer SST, a rapid switch to stratified, oligotrophic water due to decreased strength of the NE monsoon control their growth in the EAS region. Similar, drastic fluctuations in cyst abundance during the deglaciation caused due to rapid SST fluctuations (Govil and Naidu, 2010).

The dinoflagellate cyst abundance and assemblages document an abrupt change during the transition from MIS 2 to MIS 1 (Fig. 4A.2 and 3a). Absolute cyst abundance declined from about 12.8 to 10 ka, could be resultant of decreased winter mixing due to the weak NE monsoon winds during deglaciation period. This result coincides with the

sharp decrease in foraminiferal records in the Core SK 17, which suggest low productivity during deglaciation in the EAS (Singh et al., 2011). The most important change in cyst assemblage during this period was the presence of *O. centrocarpum*, *B. spongium* and *S. pachydermus* (from about ~11 ka). *O. centrocarpum* reached its maximum abundance during MIS 1 (Fig. 4A.2). These autotrophic cosmopolitan species tolerate a wide range of salinity and temperature (Zonneveld et al., 2013), and commonly associated with unstable waters at the coastal oceanic boundary (Dale et al., 2002). In recent sediment, *B. spongium* are typical to warmer tropical-subtropical marine settings with salinity range 31.9 to 38.3 psu, whereas higher abundance can be an observer in regions where SST >20°C (Zonneveld et al., 2013). *S. pachydermus* are strictly restricted to temperate to equatorial regions (Zonneveld et al., 2013) and able to tolerates SSS 27.8 to 39 psu (Zonneveld et al., 2013). This shift in species assemblage along with increased species diversity could support the increased SST and moderate SSS during the early Holocene (Fig. 4A.3k and l). In the WAS, *B. spongium* and *S. pachydermus* are typically dominant during the SW monsoon upwelling (Zonneveld, 1997a; Zonneveld and Brummer, 2000). The presence of these species during the early Holocene in AAS 9/21 strengthens the belief that the SW monsoon evolved during this period in the Holocene. Furthermore, increase in SST and decreased trend of $\delta^{18}\text{O}_w$ values and SSS represents increased strength of the SW monsoon during ~10.5 to 3 ka in the present core (Fig. 4A.3; Govil and Naidu, 2010).

Since 3 ka, a major shift in the cyst assemblage was observed. Cyst assemblage was characterised by the appearance of *Protoperidinium* species, *S. stellatum*, *S. robustum*, *S. nephroides* and *V. calvum* (Fig. 4A.2). In modern sediments, a high

relative abundance of *S. robustum* and *S. stellatum* is found in warm, hypersaline waters in mesotrophic to eutrophic regions. Among this *S. robustum* is endemic to the Indian Ocean (Zonneveld et al., 2013). The occurrence of these species suggests an increase in SSS and SST around 3 ka (Fig. 4A.3k and l), which could be due to the weak SW monsoon (Govil and Naidu, 2010). Increased abundance of Protoperidinoid species could be due to, better preservation state in sediment with less oxidative stress and increased denitrification (Godad, 2014). However, moderate increase in productivity has been observed in the fertile foraminiferal species records between ~3-1 ka in the core SK 17 (Singh et al., 2011; Cabarcos et al., 2014) which also reveals presence of food material and organic matter, whereas this increase in productivity was not evidenced in autotrophic coccolithophore (productivity factor) records in the same core (Cabarcos et al., 2014). In the present study, productivity increase during this period was not evidenced by autotrophic Gonyaulacoid species. Thus, an inference can be drawn that change in the environmental conditions (elevated SST) during the late Holocene period were not optimal to support the growth of these autotrophic species (Fig. 4A.3b). Furthermore, most of the *Spiniferites* species can grow in temperature up to 29°C (Zonneveld et al., 2013), whereas in the WAS their maximum flux was reported at the end of summer monsoon when temperature ranges from 23 to 27°C (Zonneveld and Brummer, 2000), which could be the optimum range for their proliferation in the Arabian Sea region. Thus, increased SST (28.5 to 29°C) in the EAS from ~3 to 1 ka (Govil and Naidu, 2010) could be responsible for the decline in abundance of *Spiniferites* species.

Recent modern dinoflagellate cyst distribution studies in the EAS reveals the dominance of *Protoperidinium* species in surface sediments (Godhe et al., 2000; D'Costa et al., 2008; D'Silva et al., 2011). The relative shift in dinoflagellate cyst assemblage during ~3-0.7 ka suggests that the increased trend in *Protoperidinium* abundance incited during this time and could be due to change environment conditions initiated by increased SST and SSS. Thus, it can be predicted that the increase in SST due to global warming would lead to different dinoflagellate assemblages which will be dominated by heterotrophic species in future.

4A.6 Conclusion

This study presents the first detailed investigation of dinoflagellate cyst records over the late Quaternary period in the EAS. The variation observed in dinoflagellate cyst abundance and assemblages suggests that productivity changes over the past 68 ka in the EAS were influenced by seasonal monsoon circulation. The main dinoflagellate cyst signals recorded in the EAS are as follows;

1. The productivity in the EAS was higher during the glacial than the interglacial periods and was mainly controlled by nutrient supply from subsurface water due to winter convection is driven by the NE monsoonal wind. The productivity change was highlighted by increased abundance of Gonyaulacoid species (especially *Spiniferites*). Within the glacials, productivity was higher during MIS 2 than in MIS 4 and characterised by a twofold increase in cyst abundance. During the interglacials, reduction in the primary productivity during early MIS 3 (~67.5 to 58.67 ka) and in MIS 1 was highlighted by less abundance of Gonyaulacoid cyst, which could be due to

strong summer monsoon, resulting in intense stratification and reduced light penetration.

2. Dinoflagellate cyst abundance and assemblage difference reveal that productivity was higher during the LGM than Holocene. The LGM was more dynamic with larger fluctuations in cyst abundance and assemblages. This reveals the winter mixing was not consistent throughout the LGM.

3. Variation in *Protoperidinium* species abundance over the past 68 ka represents variation in the OMZ intensity. Increased *Protoperidinium* abundance during MIS 3 and late MIS 1 (~3 ka onwards) highlighted their good preservation in sediments due to strong OMZ.

4. SST increased during the Holocene was characterised by increased abundance of *B. spongium*, *S. pachydermus*, and *O. centrocarpum*.

The present study supports the use of dinoflagellate cyst abundance and assemblages as a proxy of paleoproductivity and paleoceanographic variability in the EAS. Dinoflagellate cyst proxy demonstrates that the EAS responds to both regional and global scale climatic variations.

4B Late Quaternary productivity and climatic changes in the western Bay of Bengal

4B.1 Introduction

In the Arabian Sea, dinoflagellate cyst proxy has been used to study the paleoproductivity variability, OMZ intensity and monsoonal dynamics in sediment cores (Zonneveld, 1997c; Reichart and Brinkhuis, 2003; Chapter 4A), so far no study attempted analysis of cysts abundance in the sediment traps or the sediment cores from the Bay of Bengal. For the first time, this study reports dinoflagellate cyst assemblages changes in a sediment core that depicts the Holocene and last glacial period in the Bay of Bengal.

4B.2 Climatic and Oceanographic Setting

(Refer Chapter 2, Section 2.2.1)

4B.3 Material and Methods

4B.3.1. Sediment core

Core SK218/1 was collected at a water depth of 3307 m from the western Bay of Bengal (14°02.10'N, 82°00.2'E; Fig. 4B.1). The chronology of the core was established by using AMS carbon 14 dates (Naidu and Govil, 2010). Five samples from Holocene covering a time span from 6 to 6.89 ka and five samples from the last glacial period (18 to 23 ka) were processed for the dinoflagellate cyst study.

4B.3.2 Palynological sample preparation and analysis

(Refer Chapter 3B, Section 3B.2.3)

4B.3.3 Statistical analysis

The dinoflagellate cyst abundance data was further subjected to calculate species diversity (Shannon-Wiener diversity index i.e. H') and species richness using the software PRIMER (version 5). Further, a t-test was used to determine the variation in dinoflagellate cyst abundance during the Holocene and last glacial period.

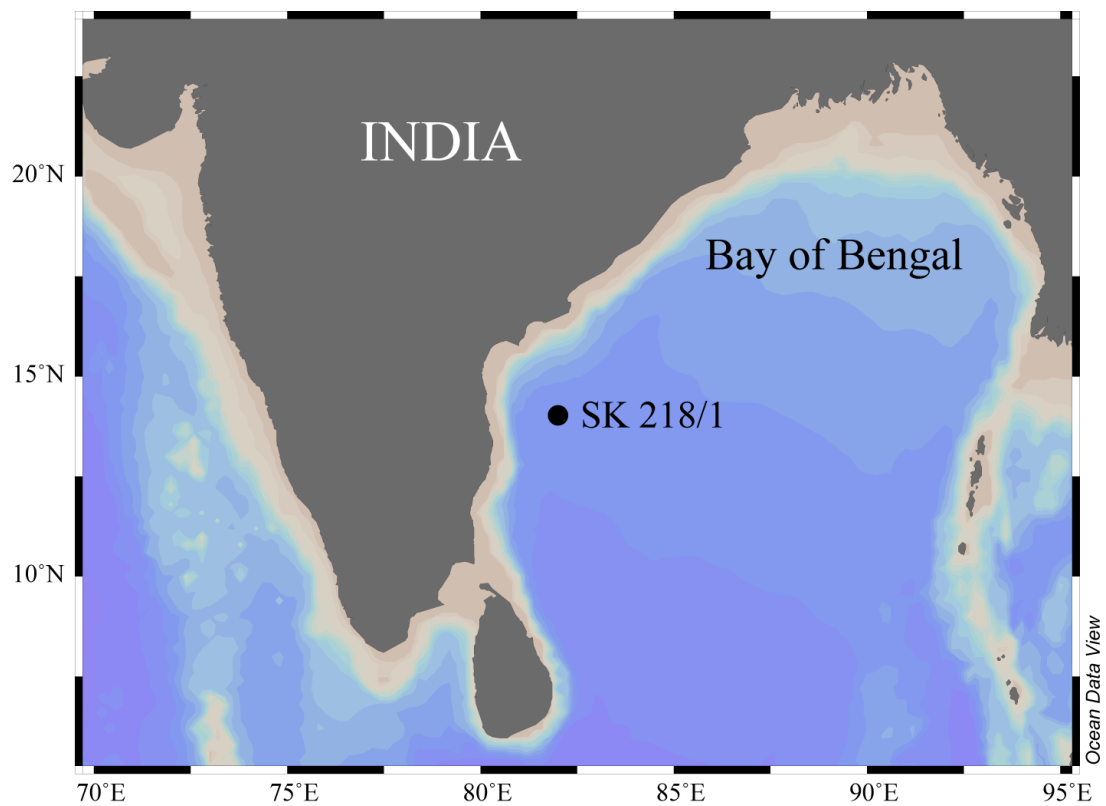


Fig. 4B.1 Location of Core SK 218/1 in the Bay of Bengal.

4B.4 Results

In Core SK218/1, a total of 21 dinoflagellate cyst species belonging to autotrophic (9 species) and heterotrophic (12 species) were identified from the sediment samples representing the Holocene and last glacial maxima (Table 4B.1). Dinoflagellate

cyst species number in each sample was varied from 2 to 12, with an average of 6. Dinoflagellate cyst assemblage during both periods was dominated by heterotrophic *Protoperidinium* species, mainly by *Protoperidinium* sp. 1, *Selenopemphix nephroides*, *Brigantedinium* spp. and *Quinquecuspsis concreta*, whereas other heterotrophic species, *Votadinium spinosum*, and *Trinovantedinium applanatum* were present in less abundance (Table 4B.1). *Selenopemphix quanta*, *Stelladinium stellatum*, *Votadinium calvum* and *Protoperidinium* type 2 were observed only during the Holocene period. *Stelladinium reidii* was present only in last glacial period. Although heterotrophic species were dominant during both the periods, their absolute abundance was more during the Holocene (~33 to 87 cyst g⁻¹) than the last glacial period (~20 to 48 cyst g⁻¹).

Autotrophic cyst assemblage was represented by mainly *Operculodinium centrocarpum*, *Spiniferites mirabilis*, *Polysphaeridium zoharyi* and *Spiniferites* spp. Another autotrophic Abundance of *S. membranaceus*, *Tuberculodinium vancampoeae*, *S. ramosus* and *S. bentorii* was less. Among the autotrophs *Spiniferites mirabilis* were dominant in the Holocene (up to 27 cysts g⁻¹), whereas *L. machaerophorum* during the last glacial period (40 cysts g⁻¹). The occurrence of autotrophic species, *S. bentorii*, *S. ramosus*, *P. zoharyi*, and *T. vancampoeae* were confined to the Holocene, whereas *L. machaerophorum* were encountered only in during the last glacial period (Table 4B.1). Absolute abundance of autotrophic species was more during the Holocene period (19 to 66 cyst g⁻¹) as compared to last glacial period (20 to 48 cyst g⁻¹).

In present study, high absolute cyst abundance was observed during the Holocene (74 to 153 cysts g⁻¹) period as compared to the last glacial period (up to 67 cysts g⁻¹; Fig. 4B.2) and this difference in the cysts distribution was significant between

the Holocene and last glacial periods (t-test: $df=20$, $p<0.003$, $n=11$). It is also evident from the t-test, which shows a significant difference in the distribution of autotrophic (t-test: $df=8$, $p\leq 0.019$, $n=5$) and heterotrophic cysts (t-test: $df=8$, $p\leq 0.01$, $n=5$) between last glacial period and Holocene (Table 4B.1). The heterotrophic (H) to autotrophic (A) dinoflagellate cyst ratio (H/A) varied in the Holocene period (0.5 to 3) as compared to the last glacial period (0.5 to 4.5; Fig. 4.2). The species diversity (Shannon-Wiener index, H') was more during the Holocene (1.6 to 2.2) than last glacial period (0.6 to 1.5), whereas species richness also showed a similar trend with increase in the Holocene (1.3 to 2.1, avg. 1.5) than last glacial period (0.3 to 0.9, avg. 0.8).

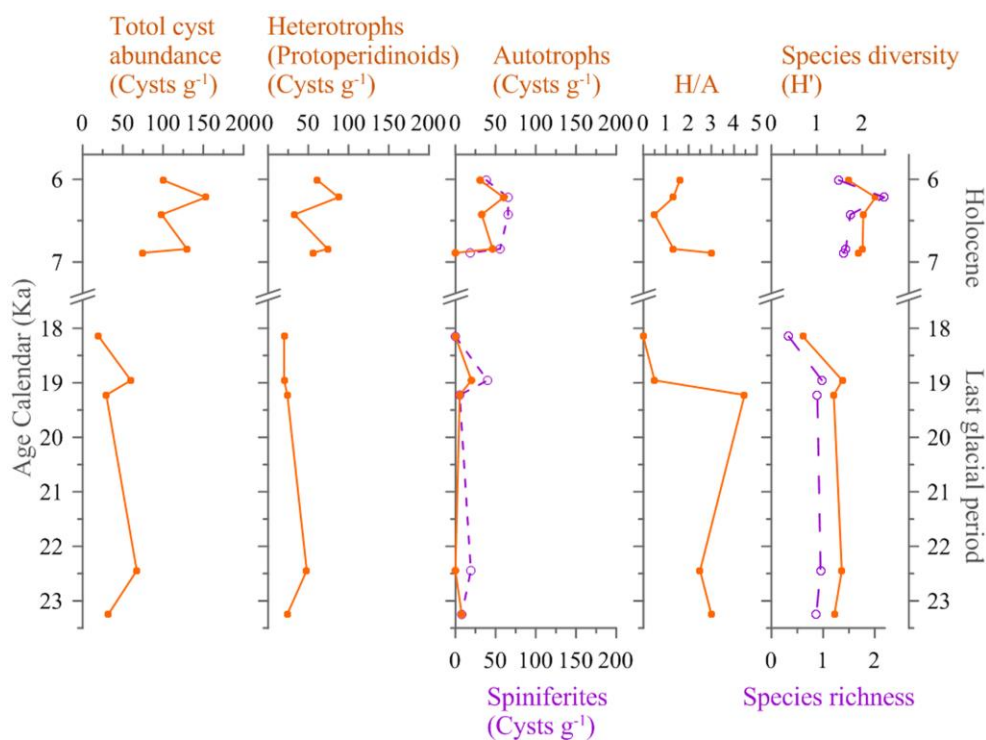


Fig. 4B.2 Fluctuations of total dinoflagellates, heterotrophs (Proto-peridinioids), autotrophs, Spiniferites, ratios of heterotrophs/autotrophs (H/A), species diversity and species richness.

Table 4B.1 Dinoflagellate cysts and their abundance (cysts g⁻¹) documented in core SK218/1 in the western Bay of Bengal

Dinoflagellate cyst (Paleontological Name)	Abbreviations	Thecate dinoflagellate affinity (Biological Name)	Holocene (ka)					Glacial (ka)				
			6.0	6.2	6.4	6.8	6.9	18.2	19.0	19.2	22.4	23.3
Autotrophic												
<i>Lingulodinium machaerophorum</i>	Lmac	<i>Lingulodinium polyedrum</i>	0	0	0	0	0	0	20	0	0	0
<i>Operculodinium centrocarpum</i>	Ocen	<i>Protoceratium reticulatum</i>	0	5	16	9	0	0	0	0	19	0
<i>Polysphaeridium zoharyi</i>	Pzoh	<i>Pyrodinium bahamense</i>	8	0	0	0	19	0	0	0	0	0
<i>Spiniferites bentorii</i>	Sben	<i>Gonyaulax digitalis</i> , <i>G. spinifera</i> complex	0	5	0	0	0	0	0	0	0	0
<i>Spiniferites mirabilis</i>	Smir	<i>Gonyaulax spinifera</i> complex	23	27	16	19	0	0	0	5	0	8
<i>Spiniferites membranaceus</i>	Smem	<i>Gonyaulax spinifera</i> complex	0	0	0	0	0	0	10	0	0	0
<i>Spiniferites ramosus</i>	Sram	<i>Gonyaulax scrippsae</i> , <i>G. spinifera</i> complex	8	16	0	9	0	0	0	0	0	0
<i>Spiniferites</i> sp.	Ssp.1	<i>Gonyaulax</i> sp.	0	11	16	19	0	0	10	0	0	0
<i>Tuberculodinium vancampoae</i>	Tvan	<i>Pyrophacus steinii</i>	0	0	16	0	0	0	0	0	0	0
Heterotrophic												
<i>Brigantedinium</i> sp.	Bsp.	<i>Protooperidinium</i> sp.	0	0	16	28	0	0	0	8	10	0
<i>Quinquecuspis concreta</i>	Qcon	<i>Protooperidinium leonis</i>	8	22	8	19	9	0	0	8	0	8
<i>Selenopemphix nephroides</i>	Snep	<i>Protooperidinium subinermis</i>	8	27	0	9	9	10	10	0	10	8
<i>Selenopemphix quanta</i>	Squa	<i>Protooperidinium conicum</i>	0	5	0	0	9	0	0	0	0	0
<i>Selenopemphix quanta</i>	Squa	<i>Protooperidinium nudum</i>	0	5	0	0	0	0	0	0	0	0
<i>Stelladinium reidii</i>	Sred	<i>Protooperidinium compressum</i>	0	0	0	0	0	0	10	0	0	0
<i>Stelladinium robustum</i>	Srob	<i>Protooperidinium</i> sp.	8	0	0	0	0	0	0	0	0	0
<i>Trinovantedinium applanatum</i>	Tapp	<i>Protooperidinium pentagonum</i>	0	0	0	0	9	0	0	0	10	0
<i>Votadinium spinosum</i>	Vspi	<i>Protooperidinium claudicans</i>	0	0	0	0	9	0	0	7	0	0
<i>Votadinium calvum</i>	Vcal	<i>Protooperidinium oblongum</i>	0	11	0	0	0	0	0	0	0	0
-	Psp.1	<i>Protooperidinium</i> sp. Type 1	38	11	8	0	9	10	0	0	19	8
-	Psp.2	<i>Protooperidinium</i> sp. Type 2	0	5	0	19	0	0	0	0	0	0

4B.5 Discussion

4B.5.1 Absolute abundance of dinoflagellate cysts

The abundance of dinoflagellate cysts varied from 20 to 158 cysts g⁻¹ (Fig. 4B.2). The abundance observed in this core SK218/1 is comparatively lower than that observed in other regions like, Santa Barbara Basin (Pospelova et al., 2006), South China Sea (Shaozhi and Harland, 1993), Balck Sea (Mudie et al., 2002) and Arabian Sea (Reichart and Brinkhuis, 2003; Zonneveld and Brummer, 2000; Chapter 4A). This raises a doubt on whether the cyst abundance represents a sound signal of export productivity or an artifact of poor cyst preservation caused due to well-oxidized conditions in the sediment-water interface at the core location. Recent redox sensitivity element proxies (U, Mo, Ce/Ce*, V, Cu, Co, and Ni) studied in the present core suggested that oxic condition prevailed during the last glacial period (25 to 15 ka) whereas during the Holocene (from 15.2 to 4.5 ka) suboxic condition was dominant in the benthic environment (Pattan et al., 2013). Overall cyst abundance recorded in the present core was less. Similarly, no visible cyst degradation was noticed in both the Holocene and last glacial period samples suggests an effect of oxidative degradation could be minimal. Moreover, the maximum cysts density observed in recent sediments along the western Bay of Bengal is also low as compared to sub-tropical and temperate regions (Chapter 3A, section 3A.4.1). Hence, it is presumed that cyst preservation changes might not have contributed to less abundance of cysts at this site. However, greater abundance of dinoflagellate cysts was reported from the sediment traps and sediment cores in the Arabian Sea from the regions of upwelling and winter convective mixing (Reichart and Brinkhuis, 2003; Zonneveld and Brummer, 2000; Chapter 4A).

Therefore, a possible reason for the less abundance of cysts at this site in the Bay of Bengal could be due to, i) low salinity and freshwater influx due to river discharge into the Bay of Bengal and the changes brought in by these events (stronger stratification, reduced light availability due to cloud cover and increased turbidity), ii) present studied core location is not influenced by upwelling and/ or strong convective mixing, and lastly, iii) the dinoflagellate population present in the water column is unable to produce sufficient quantity of cysts. Therefore, the variation in absolute abundance of dinoflagellate cysts can be attributable to the lower productivity in the presently studied location. Even though abundance was less, the variation in cysts composition and abundance between the Holocene and last glacial period indicate the similar climatic changes in the past as observed elsewhere.

4B.5.2 Link between cyst abundance to the climate change

The Bay of Bengal was 4°C warmer during the Holocene than in the last glacial period (Naidu and Govil, 2010; Govil and Naidu, 2011), the warmer SST during Holocene must have been congenial for the thriving of dinoflagellates in this region (corresponds to higher cysts abundance). Similarly, higher abundance of cysts during the Holocene than in the last glacial maxima were also noticed in the Santa Barbara Basin and Guaymas Basin (Pospelova et al., 2006; Price et al., 2013). Also, the lower ratios of heterotrophs to autotrophs (H/A) during the Holocene than in the last glacial period lends a support to the distinct SST difference between these two periods. This suggests that the H/A ratios of dinoflagellate cysts can use as a proxy for seawater temperature in the Bay of Bengal as lower ratios correspond to warm temperature and vice versa. Similarly, an abundance of cyst produced by *Spiniferites* species also

increases during the Holocene than the last glacial period, whereas cyst of *P. zoharyi* and *T. vancampoae* were found only in the Holocene. *P. zoharyi* and *T. vancampoae* are known as warm water species and can grow in higher salinity (Zonneveld et al., 2013). In modern sediments, these species appears to have subtropical to tropical distribution (Marret and Zonneveld, 2003; Zonneveld et al., 2013). Similarly, *Spiniferites* species, *S. bentorii*, and *S. miribilis* are warm-water species. Also, they can tolerate high SSS as well (Marret and Zonneveld, 2003; Zonneveld et al., 2013). Higher abundance of *Spiniferites* taxa has also been suggested to reflect the warmer water in the Southern Californian region and eastern Arabian Sea (EAS) (Prauss, 2002; Pospelova et al., 2006; Chapter 4A). Thus, the occurrence of *P. zoharyi* and *T. vancampoae* and dominance of *Spiniferites* group during the Holocene could reveal SST and SSS increase during this period. The autotrophic taxa *L. machaerophorum* was encountered only in the samples representing the last glacial period. In recent sediments, *L. machaerophorum* can be found in temperate to equatorial regions, and are abundant in regions with broad salinity variation (Zonneveld et al., 2013). The occurrence of *L. machaerophorum* in samples representing the last glacial period reveals general preference and/or sensitivity to temperature and salinity changes, which were more abrupt during last glacial period at the core location (Govil and Naidu, 2011).

4B.5.3 Productivity variability during the Holocene and last glacial period

Sediment trap experiments have demonstrated that the biological productivity and foraminiferal flux and terrigenous supply in the Arabian Sea are strongly linked to the intensity of SW monsoon (Nair et al., 1989; Curry et al., 1992). It is generally understood that the SW monsoon was stronger during interglacials than in glacials

(Prell et al., 1992 and references therein). Detailed studies have been carried out in the Arabian Sea to understand the monsoon influence on the biological productivity and terrigenous supply during the Late Quaternary (Sirocko and Sarin, 1989; Shimmiel et al., 1990; Clemens et al., 1991; Naidu 1991; Murray and Prell 1992; Naidu et al., 1993; Bhusan et al., 2001). Earlier findings from the EAS (Ganeshram et al., 2000; Pattan et al., 2003) and from the western Arabian Sea (Murray and Prell 1993; Naidu and Malmgren 1996) also revealed high productivity during interglacials as a result of strong SW monsoon and low productivity during glacials due to weak SW monsoon. On the contrary, recent studies based on foraminiferal proxies, coccolithophore, carbon and nitrogen isotopic records the accumulation rates of organic carbon and alkenones and dinoflagellate cyst record were suggested high productivity during the last glacial maximum than in the Holocene driven by the strong NE monsoons (Rostek et al., 1997; Banakar et al., 2005; Ivanochko, 2004; Singh et al., 2006, 2011; Cabarcos et al., 2014; Naidu et al., 2014; Chapter 4A). It is argued here that if the strong NE monsoon had influenced the productivity changes along the EAS, one would expect high productivity in the Bay of Bengal because the NE monsoon activity is much stronger in the Bay of Bengal than in the EAS. However, the absence of winter convective mixing and/or upwelling due to strong thermohaline stratification could hinder the productivity during the NE monsoon in the Bay of Bengal.

The influence of the SW monsoon on the community structure of dinoflagellates has been highlighted based on the recent sediment studies from the west coast of India (D'Costa et al., 2008) and north-western Bay of Bengal (Chapter 3B). The abundance of *Protoperidinoid* species has been used a proxy in the northern Arabian Sea (Reichart

and Brinkhuis, 2003) and *Spiniferites* species in the EAS (Chapter 4A). Here the absolute cyst abundance is used to discuss the productivity changes in the Bay of Bengal. In this study absolute cyst abundance was higher in the Holocene than in last glacial period (Fig. 4B.2), reflecting higher productivity during the Holocene. Increased strength of the SW monsoon during the Holocene (Rashid et al., 2007, 2010) fueled productivity in the Bay of Bengal and vice versa during the last glacial period. This further supported by the lower $\delta^{18}\text{O}_{\text{sw}}$ and SSS values reported in the present core during the Holocene (Govil and Naidu, 2011) suggests that the freshening of the Bay of Bengal due to heavy precipitation and riverine runoff caused by the strong SW monsoon. Consequently decreased absolute cyst abundance during the last glacial period suggests the weak SW monsoon resulted in less productivity in the region. Though the NE monsoon was stronger during the last glacial period in the northern Indian Ocean (Duplessy, 1982, Prell and Kutzbach, 1987) including the Bay of Bengal, productivity was relatively lower than the Holocene in this region. This tempts to suggest that overall the SW monsoon has a strong bearing on the productivity of the Bay of Bengal.

4B.6 Conclusions

The present study on dinoflagellate cysts record in the core SK 218/1 from the western Bay of Bengal reveals lowest cyst abundance (20 to 153 cysts g^{-1}) as compared to other regions. The changes in the composition of both autotrophs and heterotrophs cyst assemblages exhibited clear distinction between the Holocene and last glacial period in the present core. Higher absolute cyst abundance, an abundance of both Protoperidinoidean and Spiniferites cysts and species diversity during the Holocene than

the last glacial maxima indicate that productivity was higher during the Holocene in the Bay of Bengal. However, cyst abundance in the Bay of Bengal is less during both the Holocene and last glacial period than the Arabian Sea. This highlights the productivity differences between both the regions were consistent throughout the Late Quaternary period.

Chapter 5
Influence of benthic and pelagic linkages on
the distribution of dinoflagellates
along the South Andaman region

Chapter 5 Influence of benthic and pelagic linkages on the distribution of dinoflagellates along the South Andaman region

5.1 Introduction

Impulsive (proliferation factors) and cautious (dormancy factors) responses of dinoflagellates to the changing biotic and abiotic environmental conditions direct their faith in the ecosystem. Proliferation factors like stress tolerance and competitive dominance are responsible for the species success in the ecosystem. However, some dinoflagellate species chose dormancy factors like temporary, resting benthic or pelagic stages formation as ‘survival strategy’ to avoid the stressful conditions. These pelagic and benthic life-cycle transitions enable them to escape unfavourable environmental conditions. The benthic and pelagic transformations, (exchange between sediment and water column) are also essential for population dynamics and survival in the coastal ecosystem. Especially in seasonally variable systems, where fluctuations in environmental may restrict the favorable “window” for planktonic growth, the recurrence and timing of species in the plankton may depend on the encystment and excystment (Raffaelli et al. 2003; Kremp et al., 2009). Also, benthic-pelagic trading controls nutrient exchange into the aquatic ecosystem.

In the Indian region, the monsoonal system has a strong bearing on seasonal variation in environmental and oceanographic conditions (discussed in Chapter 2, Section 2.2.1). The monsoonal precipitation and run-off from terrigenous sources increase nutrient supply into the coastal regions. In addition to precipitation, accompanying stormy weather, wind turbulence and suspended terrigenous load in the water column influence phytoplankton community structure.

The Andaman Islands are part of the Andaman and Nicobar archipelago in the Bay of Bengal. This island habitat comprises pristine and diverse terrestrial as well as marine ecosystems, which include deciduous forests, mangroves, sea-grass beds, marshy-wet lands, sandy beaches and coral reefs. Diverse mangrove ecosystem, covering an area of 671 km² (State of Forest Report, 2003) supports unique marine flora and fauna. Andaman coral-reef ecosystems included in the WWF Global 200 (list of global priority biodiversity hotspots) (UNEP, 2004). The climate conditions in the Andaman Islands are typically tropical, with the hot and humid environment, influenced by the seasonal monsoonal cycling. The south-west monsoon (SWM) prevails from June to September as wet season and the north-east monsoon (NEM) during January-February as dry season. Both monsoon seasons are separated by the two inter-monsoonal periods i.e. pre-monsoon (March-May) and post-monsoon (October-December) (Indian Meteorological Department, IMD; Kumar, 2012). The rainfall pattern (mainly the rainfall and rainy days) significantly decreased from their mean during 1961-2000, this trend is more prominent in post-monsoons due to decline in cyclonic eddies (Kumar et al., 2012). In the recent years, increased anthropogenic activities have altered the water characteristics of this pristine eco-sensitive region (Jayaraju et al., 2011; Sahu et al., 2013; Jha et al., 2015; VishnuRadhan et al., 2015). Blooming incidences of *Noctiluca scintillans*, *Trichodesmium* species, and *Chaetoceros curvisetus* were observed in the Andaman region (Eashwar et al., 2001; Dharani et al., 2004; Sachithanandam et al., 2013; Sahu et al., 2014, Begum et al., 2015). Recent phytoplankton studies revealed the presence of a diverse population of harmful dinoflagellates in the coastal region (Sahu et al., 2014; Begum et al., 2015). However, the effect of such 'irregular' environmental and

anthropogenic events on impulsive and cautious responses on dinoflagellate population dynamics, are not known.

To understand dinoflagellate life cycle functions, knowledge of planktonic, resting stages, and factors influencing their ecology, geographic distribution, planktonic-benthic transitions is essential (discussed in Chapter 1). In this regard, the present chapter addresses following questions, 1) How dinoflagellate population responds to seasonally varying planktonic and benthic environmental cues? 2) Is there any benthic-pelagic trade support cyst forming dinoflagellate population?

5.2 Materials and methods

5.2.1 Study area

Sampling was carried out at three different sites located at the Port Blair Bay and North Bay, along the South Andaman region (Fig. 5.1). Port Blair Bay, situated near the Port Blair town, extends as a narrow stretch in a northeast-southwest direction and opens into the Andaman Sea on the eastern side (Eashwar et al., 2001; Figure 5.1). The Bay entrance is wide and deep because of a shipping channel and extends up to the centre region. The southern and western margins of the Bay comprise of shallow mud flats and are dominated by mangrove and seagrass vegetation. The Port Blair harbour (Haddo Jetty) located along the mid-eastern margin of the Bay. Port Blair Bay is a hub of anthropogenic activity of the Port Blair town and harbour (Sahu et al., 2013). Sampling in this region comprised of water and sediment collected at two stations (located in between 11.64°N to 11.67°N and 92.70°E to 92.74°E), namely Phoenix Bay (PB) and Marine Hill (MH) (Fig. 5.1). These stations experience varied natural settings and usages. PB has a commercial fishing, inland passenger port, shipyards and a yachting marina.

Severe anthropogenic sewage disposal and oil spill from shipwrecks contaminate water quality (VishnuRadhan et al., 2015; Sahu et al., 2013). MH situated at the (outer) Bay mouth with a municipal sewage channel in its vicinity.

North Bay is a smaller semi-enclosed area, located along the northern side of the Port Blair Bay entrance (Fig. 1). The mouth of the North Bay faces to the southeast, towards the open ocean, hence receives high saline open ocean water. North Bay is one of the reef-dominated areas of the Andaman islets, supporting diverse coral population and associated marine biota. Sampling was carried out at a single station in the North Bay (11.70°N and 92.74°E).

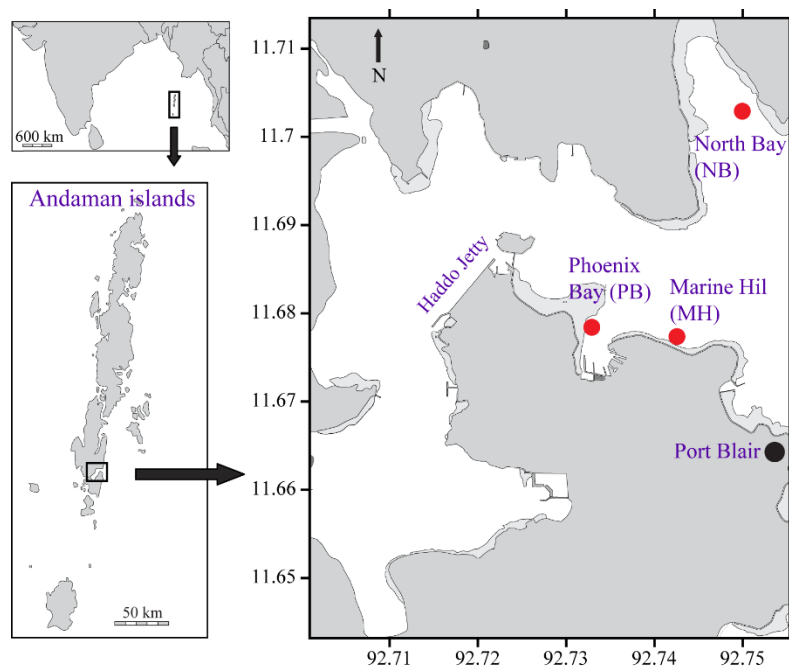


Fig. 5.1 Location of sampling stations at the Port Blair Bay and North Bay, South Andaman, India.

5.2.2 Sampling strategy

Water and sediment sampling was carried out during July 2008 to December 2011 from three fixed locations (Fig. 5.1). Based on monsoonal division sampling months are

classified as follows. For the year 2008, July-September (SWM I), November (PstM I) and for the year 2009, January-February (NEM I), March (PrM I), June-September (SWM II), October (PstM II), May (PrM II), December (PstM III).

For phytoplankton enumeration, water samples were collected from surface and near the bottom (~1m above the seabed) using a plastic bucket and Niskin sampler, respectively. Sediment sampling was carried out at two different places (~5 m apart) within each station using van Veen grab.

5.2.3 Water and sediment sample processing

For in details on phytoplankton and sediment sample processing protocols refer Chapter 2, Section 2.3.2 and Chapter 3B, Section 3B.2.2 respectively.

5.2.4 Water and sedimentary parameter

Water temperature, depth, and transparency were measured at the sampling site. Water transparency determined by measuring Secchi disc depth (SD). Surface and bottom water samples collected for salinity, dissolve oxygen, suspended particulate matter (SPM), nutrient, and chlorophyll a (Chl a) analysis. Nutrients [nitrate (NO $_3$ -N), nitrite (NO $_2$ -N), silicate (SiO $_4$ -Si) and phosphate (PO $_4$ -P)] were analysed using SKALAR SAN^{plus} analyser. Dissolved oxygen and Chl a were estimated using standard Winkler's titration and fluorometry methods (Persons et al., 1984) respectively. Salinity was measured in the laboratory using a Guideline Autosal 8400B Salinometer.

For the estimation of sedimentary texture, samples were analysed using standard wet sieving and pipette analysis methods (Buchanan, 1984).

5.2.5 Environmental data

The regional environmental parameters like monthly rainfall, air temperature, humidity and wind speed data collected by IMD, was obtained from the website of Directorate of Economics and Statistics Andaman and Nicobar Administration, Port Blair, India (<http://www.and.nic.in/stats/index.htm>). The monthly mean global solar radiant exposure data and sunshine hour data were obtained from the Solar radiant energy over India report (IMD, 2009) and the Solar Radiation handbook (MNRE and IMD, 2008) respectively.

5.2.6 Statistical analysis

Cluster analyses were carried for the surface, near bottom water planktonic dinoflagellates and cyst population using the hierarchical agglomerative (bottom-up) Unweighted Pair Group Method with Arithmetic Mean (UPGMA) using STATISTICA 8. Univariate measures [Species count (S), richness (d), evenness (J') and Shannon-Wiener diversity index (H')] were analysed for both planktonic dinoflagellates and their counterparts using PRIMER 6. Two-way ANOVA was also performed on univariate measures to evaluate significant level in their spatial-temporal variations using STATISTICA 8.

Multivariate statistical analysis performed to elucidate the role of environmental variables on dinoflagellate community in the planktonic and benthic domain using CANOCO 4.5 software for Windows (ter Braak and Smilauer, 2002). For planktonic dinoflagellates and cyst assemblage non-logarithmically transformed absolute and relative abundance data were used for statistical analysis respectively. Detrended Correspondence Analysis (DCA) was performed to determine the nature of planktonic

dinoflagellate and cyst species relationship with environmental factors. In DCA, the length of the first gradient axis was 2.5 standard deviations (sd) unit, indicating a unimodal variation (ter Braak and Smilauer, 2002) in the dinoflagellate and cyst assemblage distribution. Due to the unimodal character of data set a multivariate direct gradient analysis, Canonical Correspondence Analysis (CCA) was performed to correlate the dinoflagellate and cyst distribution with environmental parameters. The conditional effect, the amount of variability explained by only one particular variable (eliminating covariance), was calculated through forward selection. The Monte Carlo testing was used to determine the significance of each environmental parameter, based on 499 unrestrained permutations.

5.3. Results

5.3.1 Climatic variability

Air temperature in the region varied from 25.9 to 30.1°C (avg. 27.5°C) during the sampling period (Fig. 5.2a). On an annual scale, temperatures were cooler during the SWM and gradually warmed up over the post- to pre-monsoon months. Relative humidity decreased with increase in air temperature and vice versa (Fig. 5.2b). Wind speed was maximum during the SWM period (Fig. 5.2c). The rainfall pattern in the region is irregular (annual average ~3500 mm/yr) and prolonged from May to October, with maximum rainfall during June to September (IMD, Fig.5.2d). December to April are the dry months of the year (IMD, Kumar, 2012). In the region, annual solar radiant exposer and sunshine hour pattern revealed that the sunlight availability was reduced during the SWM period (Fig. 5.2e).

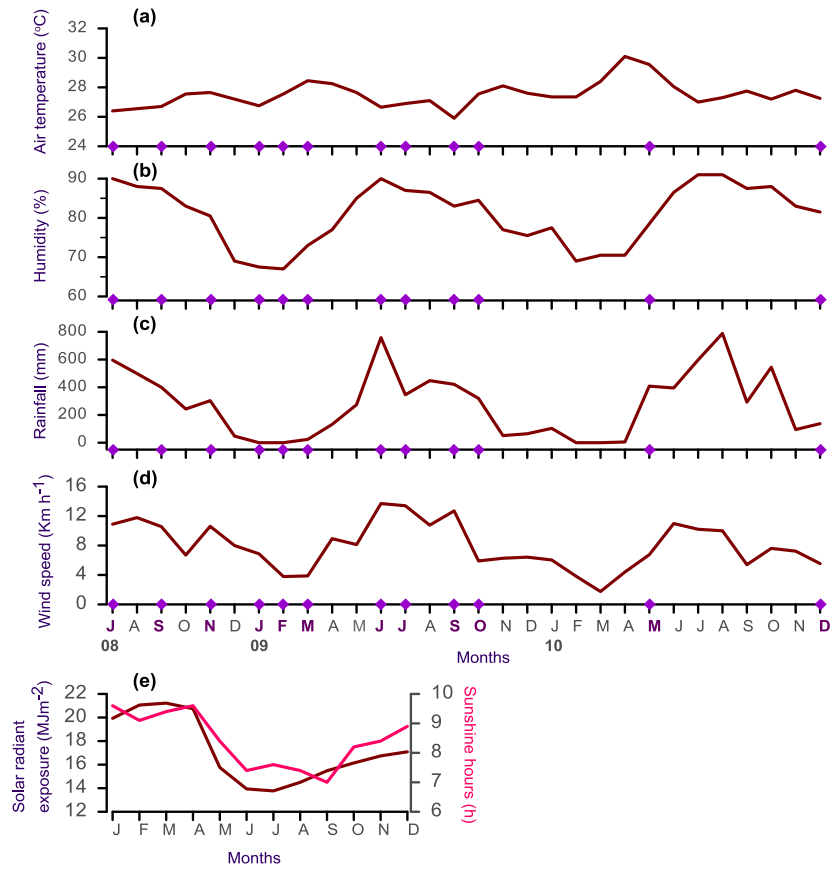


Fig. 5.2 Spatio-temporal variation in environmental parameters. a) Air temperature, b) humidity, c) rainfall, d) wind speed, e) solar radiant exposure (brown line) and e) sunshine hours (pink line). Colour symbols along x-axis represents the sampling months.

5.3.2 Hydrological characteristics

Monsoonal intervention has an important role in controlling the environmental characteristics in the region. The annual water temperature during sampling period varied from 25°C to 31°C. On a spatial scale, the North Bay was warmer than the Port Blair Bay (Fig. 5.3a). However, the annual water temperature variation in both the regions follow a similar trend, with maximum temperature during the SWMs (Fig. 5.3a). Salinity variation in the region was ~3psu (30 to 33psu), with the exception during December 2010 (at the PB), when it decreased up to 29 psu.

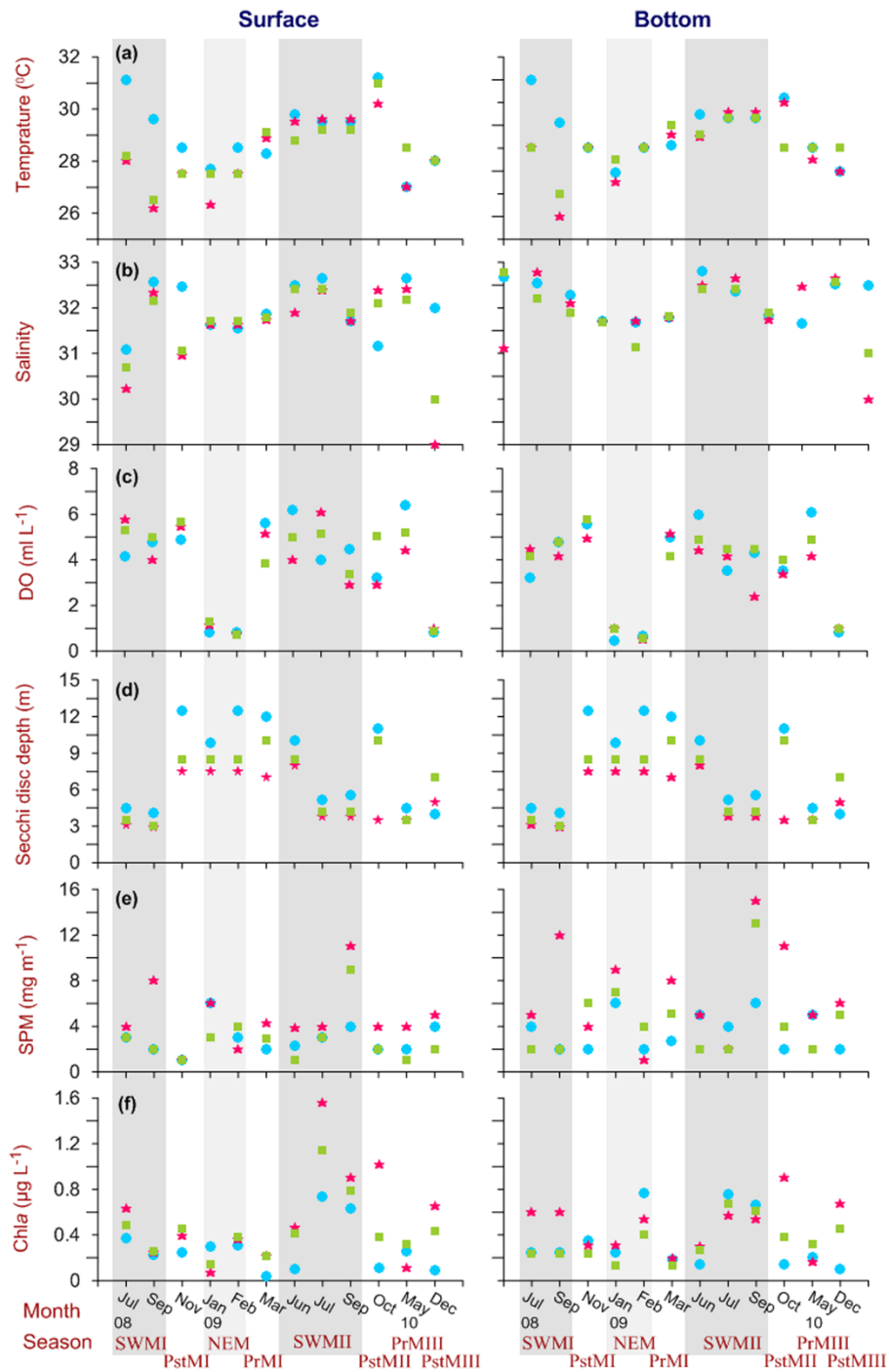


Fig. 5.3 Spatio-temporal variation in water parameters. a) temperature, b) salinity, c) DO, d) Secchi disc depth (SD), e) suspended particle matter (SPM) and e) Chlorophyll (Chla). SWM and NEM months are highlighted in dark and light shaded vertical bars. Intermediate non-shaded bars represents PrM and PstM months. Station codes: ★ Phoenix Bay (PB) ■ Marine Hill (MH) ● North Bay (NB)

Temperature and salinity variations in surface and near-bottom water were not conspicuous (no thermohaline stratification) and followed the similar temporal trend in both the regions (Fig. 5.3a and b). Dissolved oxygen concentration in surface and near-bottom water varied temporally, with hypoxic conditions ($<1.28 \text{ ml L}^{-1}$) during the NE monsoons (Fig. 5.3c). Water transparency was reduced during the SWMs due to more suspended particulate load in the water column (Fig. 5.3d). The near-bottom water was turbid. On a spatial scale, light penetration was deeper at the North Bay throughout study period than the Port Blair Bay (Fig. 5.3d).

Nutrient concentration in the water column varied seasonally as well as spatially. Nitrate and nitrite concentrations were higher in surface water, especially during July 2008 and June 2009 (Fig. 5.4a and b). Spatially it varied, with a higher concentration of the PB>MH>NB (Fig. 5.4a). Silicate concentration was higher in near-bottom water during the March-June 2009 and May 2010 than the surface water. Spatially less variation was observed in silicate concentration (Fig. 5.4c). Phosphate concentration was elevated in near-bottom water, especially at PB during SWM II and October 2009 (Fig. 5.4d). In surface water, it was elevated during SWM II, particularly at the PB (0.27 to $0.46 \mu\text{M L}^{-1}$). At the North Bay, seasonality was not observed in phosphate concentration, the highest concentration was observed during September 2008 ($0.82 \mu\text{M L}^{-1}$) and October 2009 ($0.84 \mu\text{M L}^{-1}$) (Fig. 5.4d). Chl a concentration in the region varied seasonally at all stations (0.04 to $1.55 \mu\text{M L}^{-1}$), with elevated values during SWM II in the water column (Fig. 5.3f). At PB, second SWM II peak in Chl a was observed during PstM II (October 2009) in the surface ($1.01 \mu\text{M L}^{-1}$) and near bottom water ($0.9 \mu\text{M L}^{-1}$).

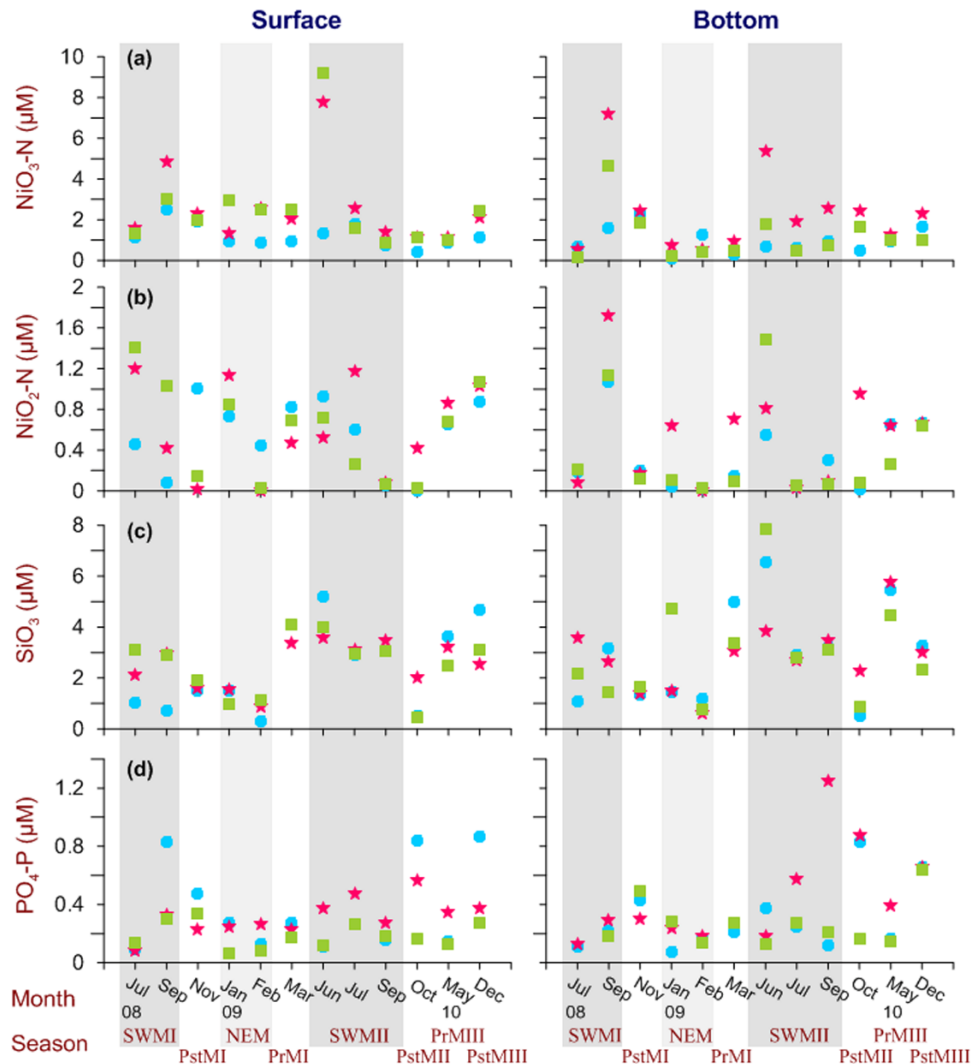


Fig. 5.4 Spatio-temporal variation in nutrient concentrations, a) nitrate, b) nitrite, c) silicate and phosphate. SWM and NEM periods are shown by dark and light shaded vertical bars. Intermediate non-shaded bars represents PrM and PstM months. Station codes: ★ Phoenix Bay (PB) ■ Marine Hill (MH) ● North Bay (NB)

5.3.3 Planktonic dinoflagellate population

The planktonic dinoflagellate population observed in the South Andaman region was diverse (Table 5.1). Dinoflagellate constituted up to 96% and 61% of total phytoplankton community at the Port Blair Bay and North Bay respectively. Total of 93 dinoflagellate morphotypes were recorded in the surface (78 species) and bottom water (72 species) from the study region (Table 5.1).

Table 5.1 List of planktonic dinoflagellate species and their percentage contribution (throughout sampling period) recorded in the surface and near-bottom water at the Phoenix Bay (PB), Marine Hill (MH) and North Bay (NB) along the South Andaman region. Abbri: species abbreviations used for statistical analysis. † Harmful Algal bloom species; †† Bloom-forming species; ††† Red-tide-forming species; € Cyst forming species

	Abbri	Surface water			Near bottom water		
		PB	MH	NB	PB	MH	NB
Phototrophic							
<i>Akashiwo sanguinea</i> ††	Asan	0.8	1.2		1.2	3.3	
<i>Alexandrium tamarense</i> † € complex	Atam	4.5	2.7	1.5	1.2	1.0	1.2
<i>Alexandrium minutum</i> †€					1.0		
<i>Alexandrium</i> spp.	Aspp	1.1	1.3	1.5			
<i>Amphidinium</i> spp.	Asp	0.1	0.3	3.7		0.5	3.1
<i>Amphidinium sphenoides</i>	Asph	12.3	2.7	0.7	6.6	4.3	2.5
<i>Azadinium caudatum</i>		0.3					3.7
<i>Corythodinium tessellatum</i>		1.3					
<i>Dinophysis caudata</i> †	Dcau	3.6	1.3	6.6	2.6	2.9	1.9
<i>Dinophysis infundibulus</i> †							0.6
<i>Dinophysis</i> spp.	Dsp					0.2	0.6
<i>Gambierdiscus</i> spp.					0.5		
<i>Goniodoma polyedricum</i>				2.2		1.0	
<i>Gonyaulax digitalis</i> €	Gdig		3.0	4.4		1.9	
<i>Gonyaulax polygramma</i> ††	Gpol		0.7	3.7	1.2	1.4	0.6
<i>Gonyaulax scrippsae</i> €			0.3	1.5			1.2
<i>Gonyaulax</i> spp.	Gsp	2.6	0.3		3.3	0.5	4.9
<i>Gonyaulax spinifera</i> ††€	Gspi	1.9	1.0	2.9	0.9	0.5	1.2
<i>Gymnodium</i> spp.	Gysp	2.5	1.0	2.9	0.9	1.4	3.7
<i>Gyrodinium fusiforme</i>		1.3	0.3				
<i>Gyrodinium spirale</i>				1.5			
<i>Heterocapsa triquetra</i>					0.2		
<i>Lingulodinium polyedrum</i> †€		0.4					
<i>Ornithocercus heteroporus</i>							1.2
<i>Ornithocercus steinii</i>							0.6
<i>Oxytoxum crassum</i>		0.3			0.5		
<i>Oxytoxum laticeps</i>		0.3	1.7	1.5	0.2		
<i>Oxytoxum parvum</i>			0.3	2.9			0.6
<i>Oxytoxum scolopax</i>		0.3		0.7	0.2	0.5	
<i>Oxytoxum</i> spp.		0.1					
<i>Prorocentrum compressum</i>			0.2			0.2	0.6
<i>Prorocentrum gracile</i>		0.8	0.3			2.9	
<i>Prorocentrum micans</i> †††	Pmic	6.5	8.1	10.3	5.2	7.2	11.1
<i>Prorocentrum minimum</i> ††		0.2				1.0	
<i>Prorocentrum</i> spp.		0.1				0.5	
<i>Phalacroma favus</i>					0.2		
<i>Phalacroma rotundatum</i> †	Prot	0.3	0.5		0.5	1.2	2.5
<i>Phalacroma</i> spp.			0.2				
<i>Podolampas bipes</i>			0.3				
<i>Podolampas elegans</i>				0.7			
<i>Podolampas spinifera</i>				0.7			
<i>Pronoctiluca pelagica</i>		2.9		1.5			

Continued...

Table 5.1...Continued...

	Abbri	Surface water			Near bottom water		
		PB	MH	NB	PB	MH	NB
<i>Pyrocystis lunula</i>		0.1					
<i>Pyrophacus horologium</i>				0.7		1.0	
<i>Pyrophacus steinii</i> ^ε		0.1					
<i>Scrippsiella</i> spp.			0.7	1.5		1.0	1.2
<i>Scrippsiella trochoidea</i> ^{††ε}	Stro	11.4	12.6	2.2	24.8	12.0	9.3
<i>Tripos belone</i>		0.1	0.3				
<i>Tripos brevis</i>				2.2			
<i>Tripos candelabrum</i>						0.5	
<i>Tripos dens</i>					0.2		
<i>Tripos extensus</i>			0.2		0.2	2.2	
<i>Tripos furca</i> ^{††}	Tfur	13.7	21.6	6.6	15.3	12.4	8.6
<i>Tripos fusus</i> ^{††}	Tfus	5.0	1.3	1.5	3.8	3.3	
<i>Tripos horridus</i> f. <i>denticulatus</i>	Thor	1.6	0.3	0.7		1.0	2.5
<i>Tripos lineatus</i>			0.3		0.9		
<i>Tripos inflatus</i>			0.2				
<i>Tripos longirostrus</i>							1.2
<i>Tripos trichoceros</i>					0.2		0.6
<i>Tripos macroceros</i>		0.1			0.5	0.5	1.2
<i>Tripos muelleri</i>				0.7		1.4	1.2
<i>Tripos pentagonus</i>	Tpen	1.3	0.3	0.7	0.2		
<i>Tripos teres</i>		0.1	0.3			0.5	
<i>Tripos</i> spp.		0.1	0.3				
<i>Peridinium quinquecorne</i> ^{††ε}	Pqui	4.4	0.0		5.9		
Heterotrophic							
<i>Archaeoperidinium minutum</i> ^ε		0.1	0.3				0.6
<i>Blepharocysta</i> spp.	Bsp	0.3	2.0	3.7	0.2	1.0	
<i>Diplopsalis</i> spp.	Dsp	1.4	0.0	0.7	0.1	1.0	2.5
<i>Protoperidinium claudicans</i> ^ε	Pcla		0.3	5.1		5.3	
<i>Protoperidinium conicum</i> ^ε			0.3		0.2		
<i>Protoperidinium crassipes</i> ^ε			0.7				1.2
<i>Protoperidinium depressum</i>				0.2			
<i>Protoperidinium divergens</i>	Pdiv	1.4	1.7	0.7		0.5	1.2
<i>Protoperidinium elegans</i>		0.1				2.9	
<i>Protoperidinium fatulipes</i>	Pfat	0.3	8.3		0.9		
<i>Protoperidinium mediterraneum</i>		0.1	1.0	1.5		0.2	1.2
<i>Protoperidinium ovatum</i>			0.3				
<i>Protoperidinium oblongum</i> ^ε					0.9	0.5	
<i>Protoperidinium pacificum</i>			0.3				
<i>Protoperidinium pallidum</i>	Ppal	1.0	1.0		1.7	1.4	1.9
<i>Protoperidinium pellucidum</i>	Ppel	0.5	1.3	1.5	1.9		
<i>Protoperidinium pentagonum</i> ^ε		0.1	2.7			0.5	
<i>Protoperidinium punctulatum</i>			0.2				
<i>Protoperidinium</i> spp.	Psp	0.9	6.0	2.9	5.9	5.7	5.6
<i>Protoperidinium steinii</i>	Pste	1.3	1.0	0.7	0.2		2.5
<i>Protoperidinium subinermis</i> ^ε		0.9	1.0		0.7		
<i>Protoperidinium thorianum</i> ^ε			0.3				

Continued...

Table 5.1...Continued...

	Abbri	Surface water			Near bottom water		
		PB	MH	NB	PB	MH	NB
<i>Protoperidinium leonis</i> ^ε			1.3		1.0	2.5	
<i>Preperidinium meunieri</i> ^ε	Pmeu	1.4	0.2		1.7	2.4	0.6
<i>Noctiluca scintillans</i> ^{†††}	Nsci	6.0	2.7	8.8	7.8	7.7	8.6
Minute thecate dinoflagellate	MTD	1.7		1.5	0.2		2.5
Unidentified globular dinoflagellate		0.1	0.5	4.4	0.7	1.2	

Amongst 93 dinoflagellates, 77 were identified up to species level and 14 up to genus level. Because of small size (<20μ) and lack of identification features, two forms of the thecate and nonthecate dinoflagellates are represented as minute thecate dinoflagellate (MTD) and unidentified globular dinoflagellate (UGD) respectively. Of the 77 identified dinoflagellates species, 18 species are known to form resting stages or cysts (Table 5.1). In this study, genus *Ceratium* is expressed as *Tripes* and accordingly species names also revised as reinstated by Gomez (2013). The light microscopic photomicrographs of planktonic dinoflagellates are provided in the Fig. 5.5.1

In the Port Blair Bay, *Tripes furca* (13.7%), *Scrippsiella trochoidea* (11.4%), *Amphidinium sphenoides* (12.3%), *Prorocentrum micans* (6.5%) and *Noctiluca scintillans* (6%) dominated dinoflagellate assemblage in surface water at PB (Table 5.1). In near bottom water, *S. trochoidea* (24.8%), *T. furca* (15.3%), *N. scintillans* (7.8%), *Peridinium quinquecorne* (5.9%) and *Protoperidinium spp.* (5.9%) were dominant (Table 5.1). At the MH, *T. furca* (21.6%), *S. trochoidea* (12.6%), *P. micans* (8.1%) and *Protoperidinium spp.* (6.0%) were dominant in the water column, whereas *P. fatulipes* was observed in only surface water (Table 5.1). *P. micans*, *T. furca*, and *N. scintillans* were dominated dinoflagellate assemblage at the North Bay. The dominance of *S. trochoidea* was observed only in near-bottom water (Table 5.1).

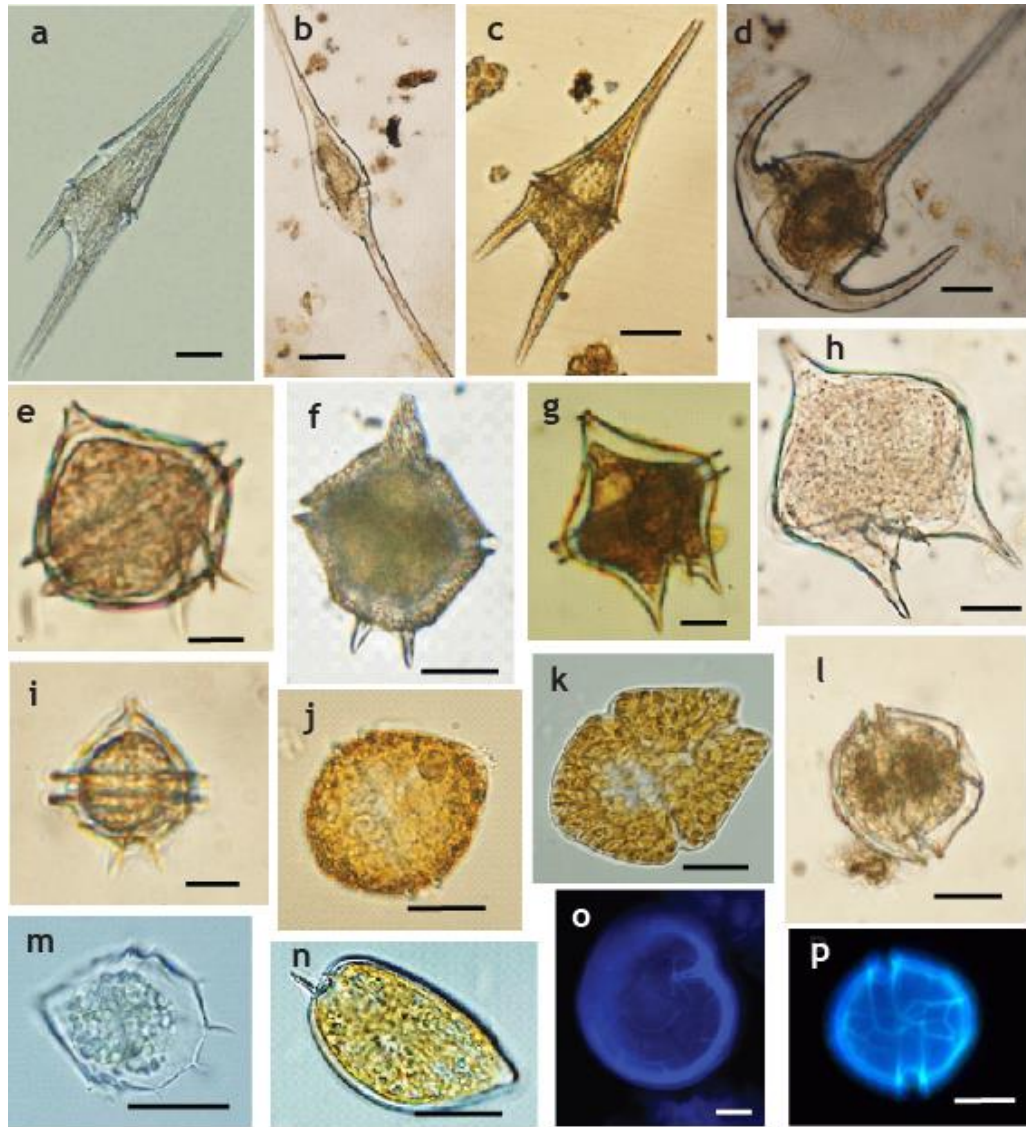


Fig. 5.5.1 Photomicrographs of planktonic dinoflagellates: a) *Tripos furca*; b) *Tripos fusus*; c) *Tripos lineatus*; d) *Tripos muelleri*; e) *Protoperidinium pallidum*; f) *Gonyaulax digitalis*; g) *Protoperidinium crassipes*; h) *Protoperidinium oblongum*; i) *Protoperidinium pellucidum*; j) *Scripsiella trochoidea*; k) *Akashiwo sanguinea*; l) *Alexandrium tamarense* complex; m) *Peridinium quinquecorne*; n) *Prorocentrum micans*; o) *Pyrophacus horologium*; p) *Alexandrium minutum*. All scale bars 20 μ m.

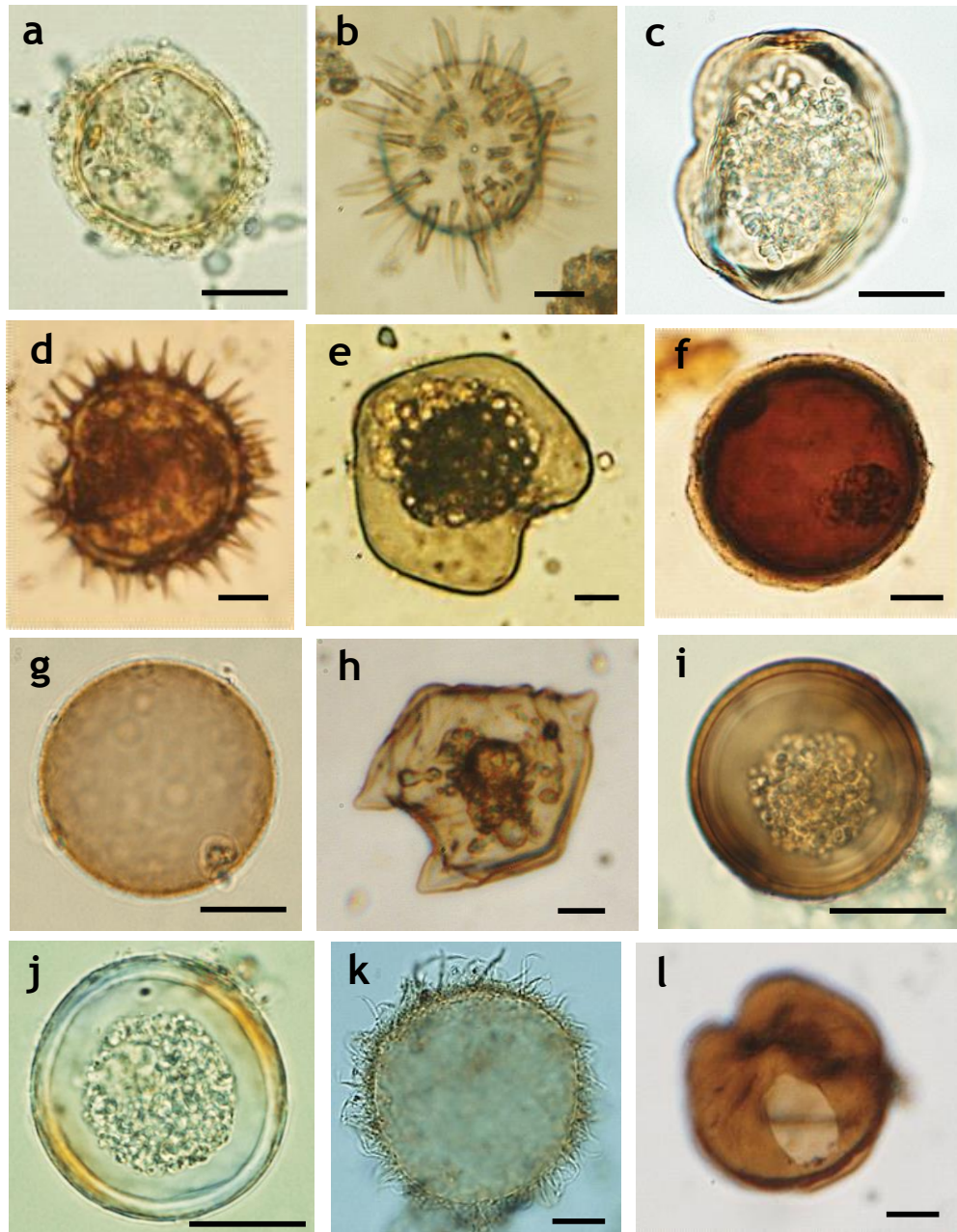


Fig. 5.5.2. Photomicrographs of some dominant and unidentified dinoflagellates cysts of: a) *Alexandrium* sp.; b) *Lingulodinium polyedrum*; c) *Protoperidinium subinerme*; d) *Protoperidinium conicum*; e) *Protoperidinium oblongum*; f) Round Brown cyst 1; g) Round Brown cyst 2; h) *Protoperidinium steidingerae*; i) Dinoflagellate cyst 1; j) Dinoflagellate cyst 2; k) *Bitectatodinium spongium*; l) *Protoperidinium subinerme*. All scale bars 20 μ m.

5.3.4 Dinoflagellate cyst population

A total of 48 dinoflagellate cyst morphotypes were observed in surface sediments analysed from the Port Blair and North Bay, South Andaman region (Table 5.2). Out of 49 morphotypes, 38 were identified up to species level and 6 up to genus level. Round brown cyst with outer walled layer was represented as RBC1 and RBC2. Round brown cysts with outer spiny orientation, which could not be identified, were grouped as spiny round brown cyst (SBC) (Table 5.2). Cyst based genera *Echinidinium* and *Islandinium* are likely to produce this type of cysts. The two unidentified cyst morphotypes are represented as dinoflagellate cyst type 1-2 (Fig. 5.5.2).

Dinoflagellate cyst assemblage in the Port Blair Bay was dominated by cyst of, *S. trochoidea* (up to 15%) and heterotrophic *Protoperidinium* spp. (*Brigantedinium* spp., up to 18%). Subsequently, cysts of heterotrophic species, *P. pentagonum* (*Trinovantedinium applanatum*, 5.9%), RBC (5.9%), *G. scrippsae* (*S. ramosus*, 4.8%) and *L. polyedricum* (*L. machaerophorum*, 5.1%), *P. subinermis* (*Selenopemphix nephroides*, 6.2%) were dominant at PB and MH respectively (Table 5.2). At the North Bay, *Brigantedinium* spp. (14.9%), *P. subinermis* (6.8%), *S. trochoidea* (11.6%) and *Gonyaulax spinifera* spp. (*Spiniferites mirabilis*, 4.7%) were abundant (Table 5.2).

5.3.5 Spatio-temporal variation in dinoflagellate population

Planktonic dinoflagellates were abundant in surface water (40 to 3700 cells L⁻¹) than in near-bottom water (5 to 1780 cells L⁻¹). Dinoflagellate abundance was higher in the Port Blair Bay, especially at PB in the surface (60 to 3700 cells L⁻¹) as well as in near-bottom waters (5 to 1980 cells L⁻¹).

Table 5.2 List of dinoflagellate cyst species and their percentage contribution (throughout sampling period) recorded in surface sediments at the Phoenix Bay (PB), Marine Hill (MH) and North Bay (NB) along the South Andaman region.

Thecate dinoflagellate affinity (Biological Name)	Dinoflagellate cyst (Paleontological Name)	Abbreviations	PB	MH	NB
Phototrophic					
<i>Alexandrium pseudogonyaulax</i>	-			0.3	
<i>Alexandrium</i> sp.	-	Asp	1.0	1.1	3.4
<i>Gonyaulax</i> sp.	<i>Bitectatodinium spongium</i>		0.4		0.2
<i>Cochlodinium polykrikoides</i>	-			0.4	
<i>Scrippsiella lachrymosa</i>	-			1.1	
<i>Scrippsiella trochoidea</i> 1	-	Stro1	15.1	13.0	11.6
<i>Scrippsiella trochoidea</i> 2	-	Stro2	1.1	7.9	0.8
<i>Scrippsiella spinifera</i>	-		0.2	1.7	0.8
<i>Gonyaulax digitalis</i>	<i>Spiniferites bentorii</i>	Sben	3.3	2.3	5.4
<i>Gonyaulax scrippsae</i>	<i>Spiniferites ramosus</i>	Sram	4.8	2.2	4.6
<i>Gonyaulax membranacea</i>	<i>Spiniferites membranaceus</i>	Smem	2.4	1.3	2.2
<i>Gonyaulax mirabilis</i>	<i>Spiniferites mirabilis</i>	Smir	3.1	1.6	4.7
<i>Gonyaulax spinifera</i> spp.	<i>Spiniferites pachydermus</i>	Spac	0.9		2.3
<i>Gonyaulax</i> sp.	<i>Spiniferites</i> sp.				0.5
-	<i>Impagidinium</i> sp.		0.6	0.3	
-	<i>Nematosphaeropsis labyrinthus</i>		0.4		
<i>Gymnodinium impudicum</i>	-	Gimp	1.8	2.9	2.3
<i>Lingulodinium polyedrum</i>	<i>Lingulodinium machaerophorum</i>	Lmac	4.6	5.1	3.2
<i>Protoceratium reticulatum</i>	<i>Operculodinium centrocarpum</i>	Ocen	4.1	4.8	2.2
<i>Pentapharsodinium dalei</i>	-	Pdal	2.1	2.3	4.6
<i>Pyrodinium bahamense</i>	<i>Polysphaeridium zoharyi</i>	Pzoh	1.7	0.8	0.8
<i>Pyrophacus steinii</i>	<i>Tuberculodinium vancampoae</i>	Tvan	0.6		2.2
Heterotrophic					
<i>Archaeoperidinium minutum</i>	<i>Archaeoperidinium minutum</i>	Amin	2.0	0.7	
<i>Protoperidinium avellana</i>	<i>Brigantedinium cariacoense</i>				
<i>Protoperidinium conicoides</i>	<i>Brigantedinium simplex</i>				
<i>Protoperidinium denticulatum</i>	<i>Brigantedinium irregulare</i>				
<i>Protoperidinium thorianum</i>	<i>Brigantedinium</i> sp.				
<i>Brigantedinium</i> sp.	<i>Brigantedinium</i> sp.	Bspp	18.3	15.6	14.9
<i>Diplopsalis lebourae</i>	-		1.1		
<i>Diplopsalis</i> sp.	-				0.5
-	<i>Echinidinium</i> spp	Espp	1.3	2.1	0.1
<i>Protoperidinium oblongum</i>	<i>Votadinium calvum</i>	Vcal	1.5	0.7	1.8
<i>Protoperidinium claudicans</i>	<i>Votadinium spinosum</i>		0.2	1.4	0.2
<i>Protoperidinium latissimum</i>	-		0.4		0.3
<i>Protoperidinium leonis</i>	<i>Quinquecuspis concreta</i>	Qcon	3.8	3.1	4.4
<i>Protoperidinium pentagonum</i>	<i>Trinovantedinium applanatum</i>	Tapp	5.1	3.9	2.5
<i>Protoperidinium americanum</i>	-				1.3
<i>Peridinium quinquecorne</i> -	-			0.4	
<i>Protoperidinium robustum</i>	<i>Stelladinium robustum</i>	Srob	1.5	1.4	1.1
<i>Protoperidinium stellatum</i>	<i>Stelladinium stellatum</i>		0.9	0.3	1.1
<i>Protoperidinium compressum</i>	<i>Stelladinium redii</i>	Sred	0.3	1.3	2.0
<i>Protoperidinium subinerme</i>	<i>Selenopemphix nephroides</i>	Snep	3.0	6.2	6.8

Continued...

Table 5.2...Continued...

Thecate dinoflagellate affinity NB (Biological Name)	Dinoflagellate cyst (Paleontological Name)	Abbreviations	PB	MH	
<i>Protoperidinium conicum</i>	<i>Selenopemphix quanta</i>	Squa	2.5	1.6	0.8
<i>Protoperidinium steidingerae</i>	-		0.8	0.9	
Round brown cyst type 1	-	RBC1	4.9	4.5	2.1
Round brown cyst type 2	-	RBC1	1.0		3.0
Spiny brown cyst	-	SBC	1.0		3.1
Dinoflagellate cyst 1	-	DC1	1.1	3.7	1.0
Dinoflagellate cyst 2	-	DC2	0.9	3.3	0.8

In the North Bay, dinoflagellate abundance was comparatively less in both surface (40 to 300 cells L⁻¹) and near bottom water (20 to 420 cells L⁻¹). Two-way ANOVA exhibits spatiotemporal variation in dinoflagellate abundance in the water column was non-significant ($p > 0.05$) (Table 5.3). However, other univariate variables i.e. species count, Shannon-Wiener diversity, Margalef's species richness and evenness showed significant temporal variation only in near-bottom water (Table 5.3). In sediment, cyst abundance and other univariate variables exhibited significant variation both spatially and temporally (Table 5.3).

The complexity in planktonic and cyst morphotypes of dinoflagellate population within the region further highlighted in the cluster analysis. UPGMA cluster analysis of dinoflagellate abundance using 0.4 (50%) as an arbitrary cut-off form six and seven groups of stations in surface and near-bottom waters respectively (Fig. 5.6 and 5.7). In surface water, the dominance of *P. micans* was observed at Group I stations, whereas *T. furca* and *D. caudata* were abundant at group II and III stations respectively (Fig. 5.6). At group IV stations, *N. scintillans* dominated dinoflagellate assemblage. Group V comprised of stations from the Port Blair Bay, where *S. trochoidea* dominated dinoflagellate assemblage. In near bottom water, at group I stations *N. scintillans*

dominated dinoflagellate assemblage (Fig. 5.7). Group II comprised of the Port Blair Bay stations and was characterised by the occurrence of *Phalacroma rotundatum*. *P. micans* was dominant at group III stations. Group IV was characterised by the dominance *S. trochoidea* and *T. furca*. Group V and VI stations clustered together due to the presence of *A. sphenoides* and *Protoperidinium* sp. respectively. *Gymnodinium* sp. and *Protoperidinium* sp. dominated dinoflagellate community at group VII stations.

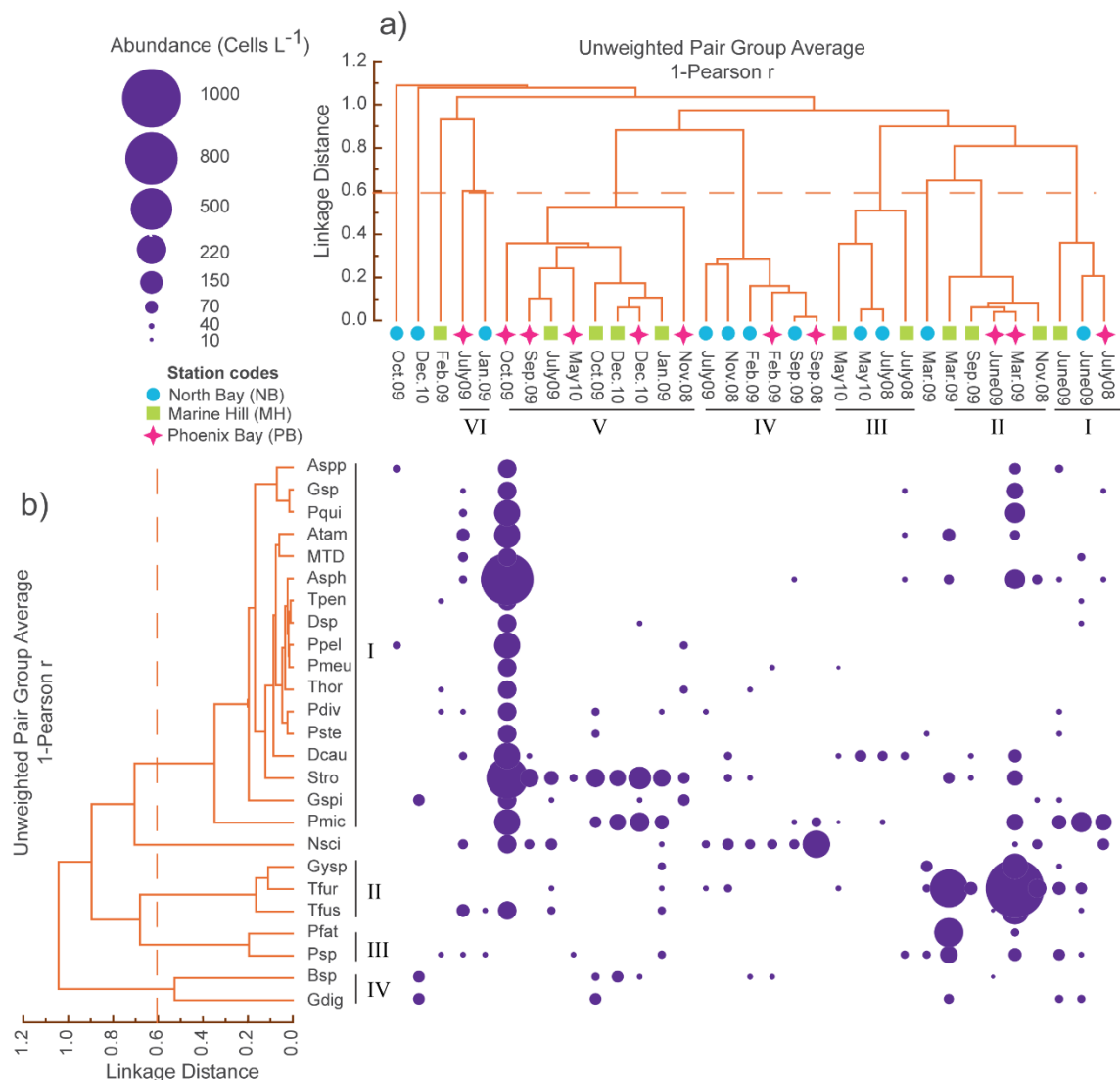


Fig. 5.6 Cluster dendrogram of (a) sampling stations-months, and (b) dominant species based on similarities in planktonic dinoflagellates assemblage in the surface water. Circles representing the abundance of planktonic dinoflagellates.

Cluster analysis classifies complex species assemblage in accordance with their proliferation during PrM I and PstM II in the Port Blair Bay waters (Fig. 5.6 and 5.7). In surface water, Group I and II species formed mixed dinoflagellate bloom at PB during PstM II (October 2009) and PrM I (March 2009) respectively (Fig. 5.6). Group III species, *P. fatulipes* and *Protoperdinium* sp. dominated dinoflagellate assemblage at MH during PrM I (March 2009).

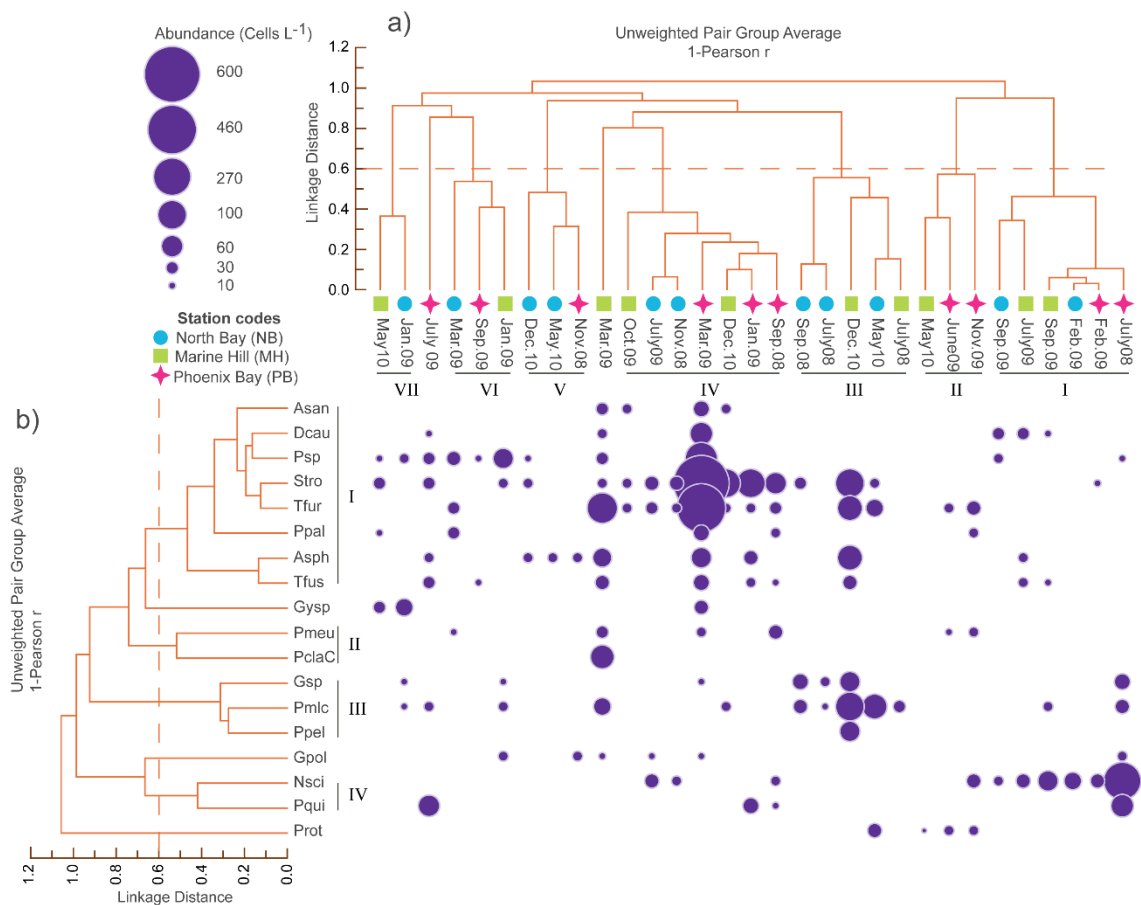


Fig. 5.7 Cluster dendrogram of (a) sampling stations-months, and (b) dominant species based on similarities in planktonic dinoflagellates in near-bottom water. Circles representing abundance data of planktonic dinoflagellates.

In near bottom water, a group I and II species bloomed at PB and MH respectively during PrM I (March 2009) (Fig. 5.8). Group III consists of *Gymnodinium* sp., *P. micans*

and *P. pellucidum* which were abundant at PB during PstM III (December 2010). Group IV species, *N. scintillans*, and *P. quinquecorne* dominated dinoflagellate assemblage at PB during SWM I (July and September 2008).

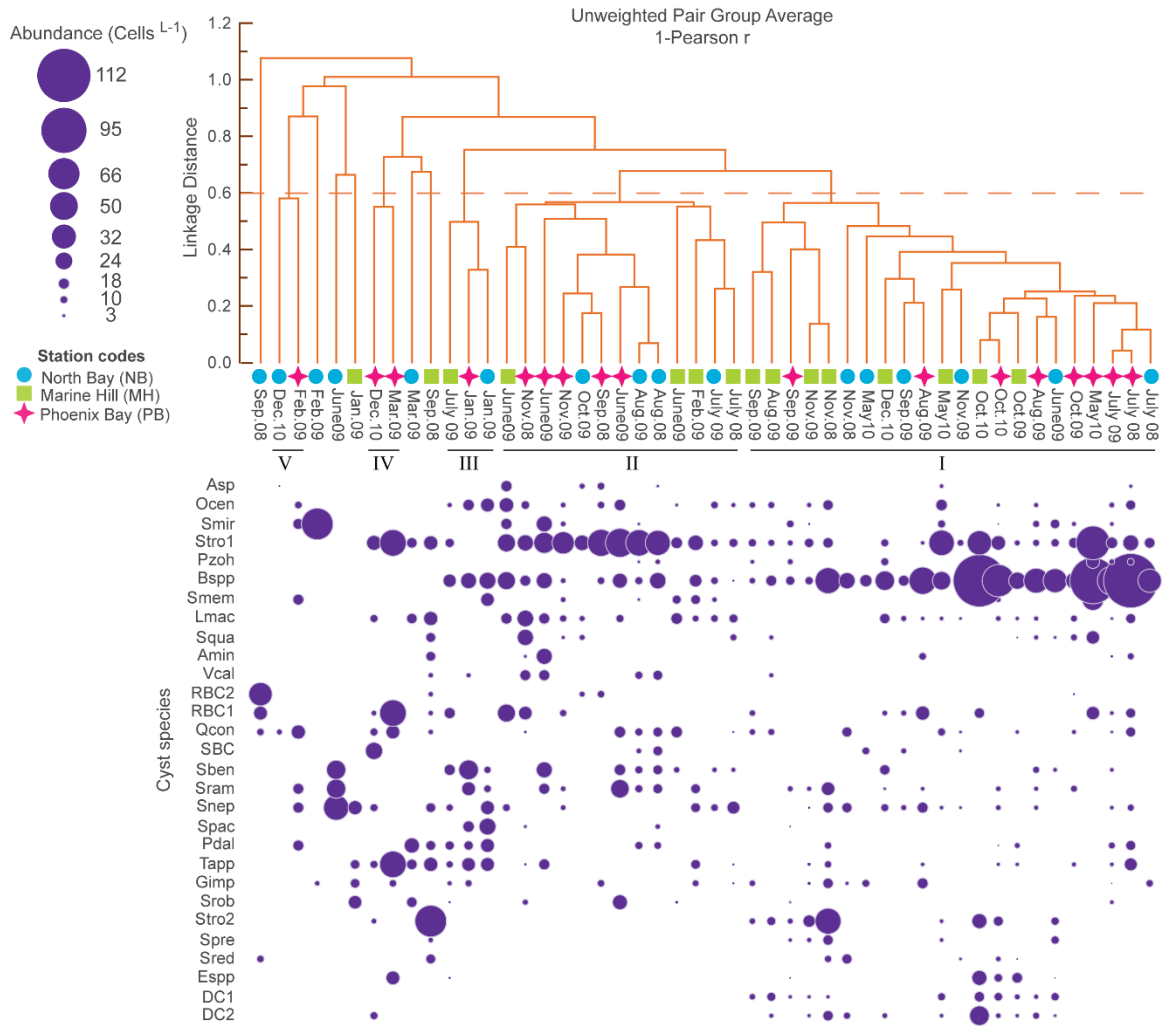


Fig. 5.8 Cluster dendrogram of sampling stations-months based on similarities in cyst assemblage in surface sediments. Circles representing dinoflagellate cyst abundance.

Cluster analysis based on dinoflagellate cyst abundance grouped sampling stations into five groups (Fig. 5.8). *Protoperidinium* spp. (*Brigantedinium* spp.) and *S. trochoidea* mostly dominated dinoflagellate cyst assemblage at the group I and II cluster,

which mainly represents samples from SWM and PstM seasons. Cyst of *G. digitalis* (*S. bentorii*), *P. reticulatum* (*O. centrocarpum*), *Protoperidinium* spp., *Pentapharsodinium dalei* and *P. pentagonum* (*Trinovantedinium applanatum*) dominated cyst assemblage at group III stations. *S. trochoidea* 1 was abundant at group IV stations. At group V stations, along with *S. trochoidea* 1, *P. leonis*, *S. trochoidea* 2, RBC1 and *P. pentagonum* dominated dinoflagellate cyst assemblage.

5.3.6 Seasonal cycling and benthic-pelagic linkages

The assemblage distribution of dinoflagellates exhibited seasonal trading within the water column and/or sediment (Fig. 5.9). At PB, SWM I was characterised by the dominance of *N. scintillans*, *Prorocentrum* spp. (*P. micans*) in surface and *Protoperidinium* spp. (including *P. quinquecorne*) in near-bottom water (Fig. 5.9a). In sediment, *Protoperidinium* spp. (*Brigantedinium* spp.) and *Scrippsiella trochoidea* cysts were abundant. During the subsequent NEM, *S. trochoidea* was dominant in near bottom. During March 2009 mixed bloom of *Triplos* spp. (*T. furca*, 1000 cells L⁻¹ and *T. fusus*, 230 cells L⁻¹) and *Protoperidinium* spp., *P. quinquecorne* (160 cells L⁻¹) was observed in surface water. Additionally, *Amphidinium* spp. (*A. sphenoides*, 800 cells L⁻¹) and *S. trochoidea* (600 cells L⁻¹) were also abundant in near-bottom water. Prior to this bloom, *S. trochoidea* and *G. Spinifera* complex cyst concentration was moderate in sediment, subsequently, it increased considerably (50% and 68% respectively) during SWM II. Planktonic dinoflagellate community during SWM II was different than SWM I, dominated by *Protoperidinium* spp. and *Triplos* spp. (*T. fusus*) in surface and bottom water respectively. During October 2009, mixed dinoflagellate bloom was observed in surface water, dominated by *A. sphenoides*, *S. trochoidea*, *Protoperidinium* spp., *P.*

quinquecorne, *Tripos* spp. (*T. furca*, *T. fusus*, and *T. pentagonus*) and *Alexandrium* spp. (*A. fundyense*). However, dinoflagellate population was not recorded in near-bottom water during this period. Subsequent elevation in *S. trochoidea* cyst abundance during November can be linked to PstM II bloom. An abrupt increase in dinoflagellate species, *Tripos* spp. (*T. furca*), *A. sphenoides*, *P. micans*, *Protoperidinium* spp., *S. trochoidea* and *G. spinifera* spp. was observed during PstM III in near-bottom water. Dominant *S. trochoidea* and *G. spinifera* spp. cysts during previous months could inoculate their population in near-bottom water.

At MH, PstM I was characterised by the presence of *Tripos* spp. (*T. furca*) in the water column (Fig. 5.9b). During NEM (especially January) *S. trochoidea* and *Prorocentrum* spp. (*P. micans*) were dominant in the surface, whereas *Protoperidinium* sp. and *Gonyaulax spinifera* spp. were dominant in near-bottom waters. Subsequently during February, dominance of *Protoperidinium* spp. (*P. claudicans*), *S. trochoidea* and *Gonyaulax spinifera* spp. the cyst was observed in sediment. During PrM, I (March) moderate bloom of *Protoperidinium* spp. (*P. fatulipes*) and *Tripos* spp. (*T. furca*) was observed in surface water (Fig. 8b, 5.6), whereas in near bottom along with *T. furca*, *P. claudicans* was dominant (Fig. 8b, 5.7). During SWM II, *S. trochoidea*, *Tripos* spp. (*T. furca*) and *Gonyaulax* spp. (*G. spinifera* and *G. digitalis*) were present in a moderate concentration in surface water, whereas cyst of *S. trochoidea* was abundant in sediment. Subsequently during PstM II, the dominance of *S. trochoidea* was encountered in surface water. The dominance of *Protoperidinium* spp. (*P. pentagonum*, *P. leonis*) and *S. trochoidea* during PstM III could be fuelled by their counterparts which were abundant in sediments during previous months.

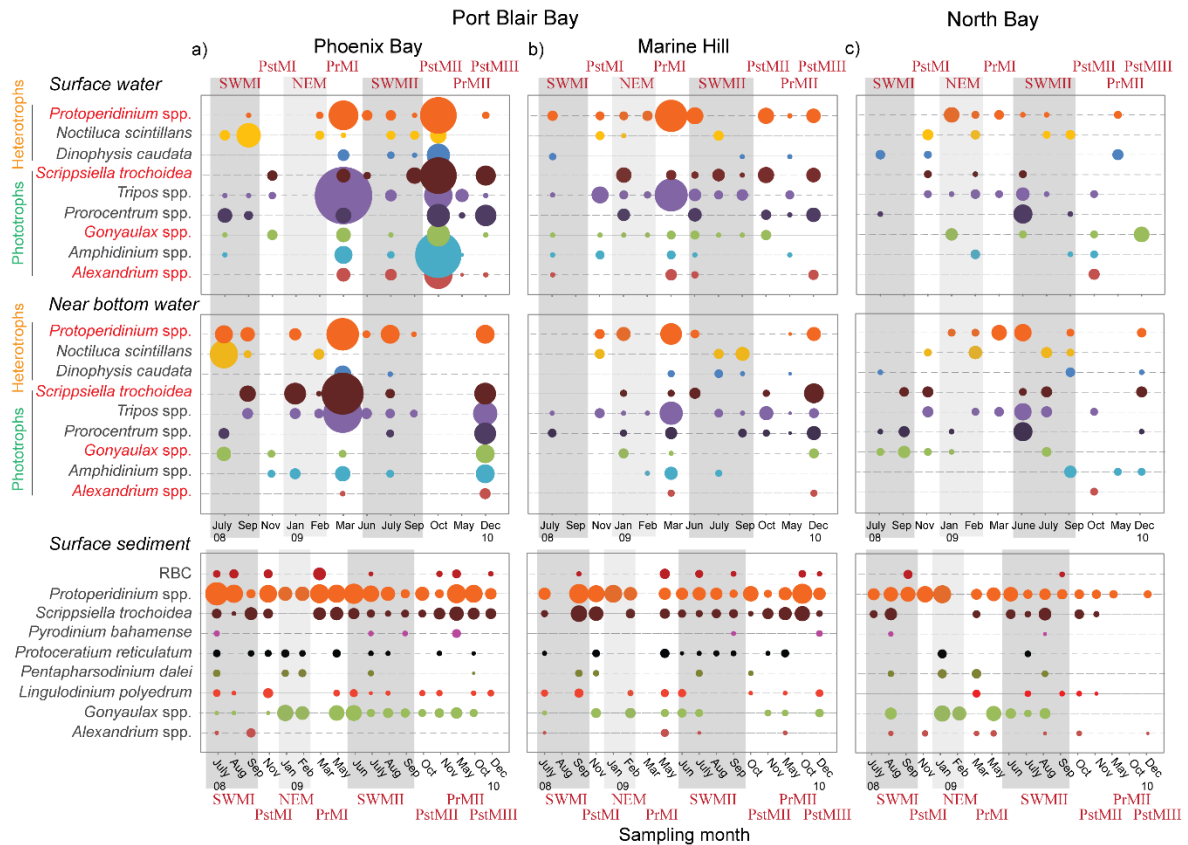


Fig. 5.9 Scenario of dominant planktonic dinoflagellates and cyst morphotypes occurrence during the different seasons in the a) Phoenix Bay, b) Marine Hill and c) North Bay. Coloured circles represent the abundance of respective species both in the planktonic and benthic domain. SWM and NEM periods are shown by dark and light shaded vertical bars respectively. Intermediate non-shaded bars represents PrM and PstM months. Cyst-forming planktonic dinoflagellates highlighted in red colour.

At the North Bay, inter-annual differences in dinoflagellate population were complex (Fig. 5.8c). Dinoflagellate population during SWM I in the water column was different than SWM II, dominated by *Gonyaulax polygramma* and *P. micans*. Onset of SWM II (June 2009) increase in dinoflagellate was observed in surface and near-bottom water, where *Tripos* spp. (*T. furca*), *P. micans* and *N. scintillans* dominated assemblage respectively. In a benthic domain, *Protoperidinium* spp. and *Gonyaulax* spp. dominated cyst assemblage.

5.3.7 Effect of environmental variables on dinoflagellate community structure

The CCA was used to elucidate responses of dinoflagellate population to different environmental variables in both pelagic and benthic domain. The CCA analysis performed on dinoflagellate assemblage data in surface water, reveals the first two CCA axis are dominant and represent 42.3% total cumulative variance (Fig. 5.10a). The CCA reveals that phosphate, Chl a , dissolved oxygen, silicate, temperature, and salinity explain a large part of data variance (marginal effect). After correcting for covariance between variables, phosphate and dissolved oxygen were significantly in relation to the CCA axis ($p < 0.05$), explaining the main part of the data variation (conditional effect) (supplementary data, Table 5.1a). The CCA1 separate sampling stations and dinoflagellate assemblage on the basis of Chl a , oxygen concentration, and nutrient (except phosphate) availability. The orientation of most dominant dinoflagellates, *A. sphenoides*, *P. micans*, *Protoperidinium* spp. and *P. fatulipes* towards the positive side of the CCA1 reveals nutrient and dissolved oxygen concentration control their distribution in this region. Dinoflagellate assemblage oriented at the negative side of the CCA1 influenced by Chl a and phosphate concentration. Dinoflagellate species oriented towards phosphate vector were associated with mostly PstM II bloom. The most frequently occurring *T. furca*, *D. caudate*, *P. quinquecorne* and *N. scintillans* was positioned in the positive direction of Chl a . In station biplot, samples from SWM and PrM months are associated with the elevated concentration of dissolved oxygen and nutrients. However, phosphate and Chl a does not reveal any seasonal clustering in stations biplot.

The CCA analysis for dinoflagellate assemblage in near-bottom water reveals that Chl a , dissolved oxygen, nitrate, nitrate, and phosphate play an important role when

analysed separately (Marginal effects) (Fig. 5.10b). Whereas together with other variables, Chla explains ($p < 0.05$) the major part of the data variation (conditional variable) (supplementary data, Table 5.1b). In CCA biplot, most dominant species, *S. trochoidea*, *P. micans*, *T. fusus* and *Gymnodinium* sp. oriented towards the positive side of CCA1. Elevated Chla, phosphate and nitrite concentrations control the distribution of these species in the study region. In station biplot, samples from the Port Blair region clustered towards the negative side of the CCA1. Elevated dissolved oxygen, silicate and nitrite concentrations during SWM and PstM were observed at these stations. *T. furca* and heterotrophic *P. rotundatum*, *P. maumieri*, *P. pallidum*, *P. pellucidum*, *P. claudicans* strongly associated with elevated nitrate and silicate concentration. *T. furca*, *N. scintillans*, *P. quinquecorne* and *D. caudate* reveals affinity towards Chla concentration and salinity.

In surface sediment, CCA biplot reflects CCA1 and 2 are dominant axis and represent total cumulative variance 66.58% (Fig. 5.10c). The CCA reveals that silt, phosphate, SPM, clay and sand explain a large part of data variance (marginal effect). Silt content explains ($p < 0.05$) the main part of the data variation (conditional effect) after correcting the covariance (supplementary data, Table 5.1c). In stations biplot, most of the samples from the North Bay are oriented towards the positive side of the CCA1. Sediment characteristic during this period was sandy, whereas dissolved oxygen and phosphate concentration was more in the overlying water column. In contrast, samples clustered towards the negative side of CCA1 are mainly from the Port Blair Bay. At these stations, sediment structure was mostly silt and clay dominated, whereas Chla and silicate concentration was higher in the overlying water column.

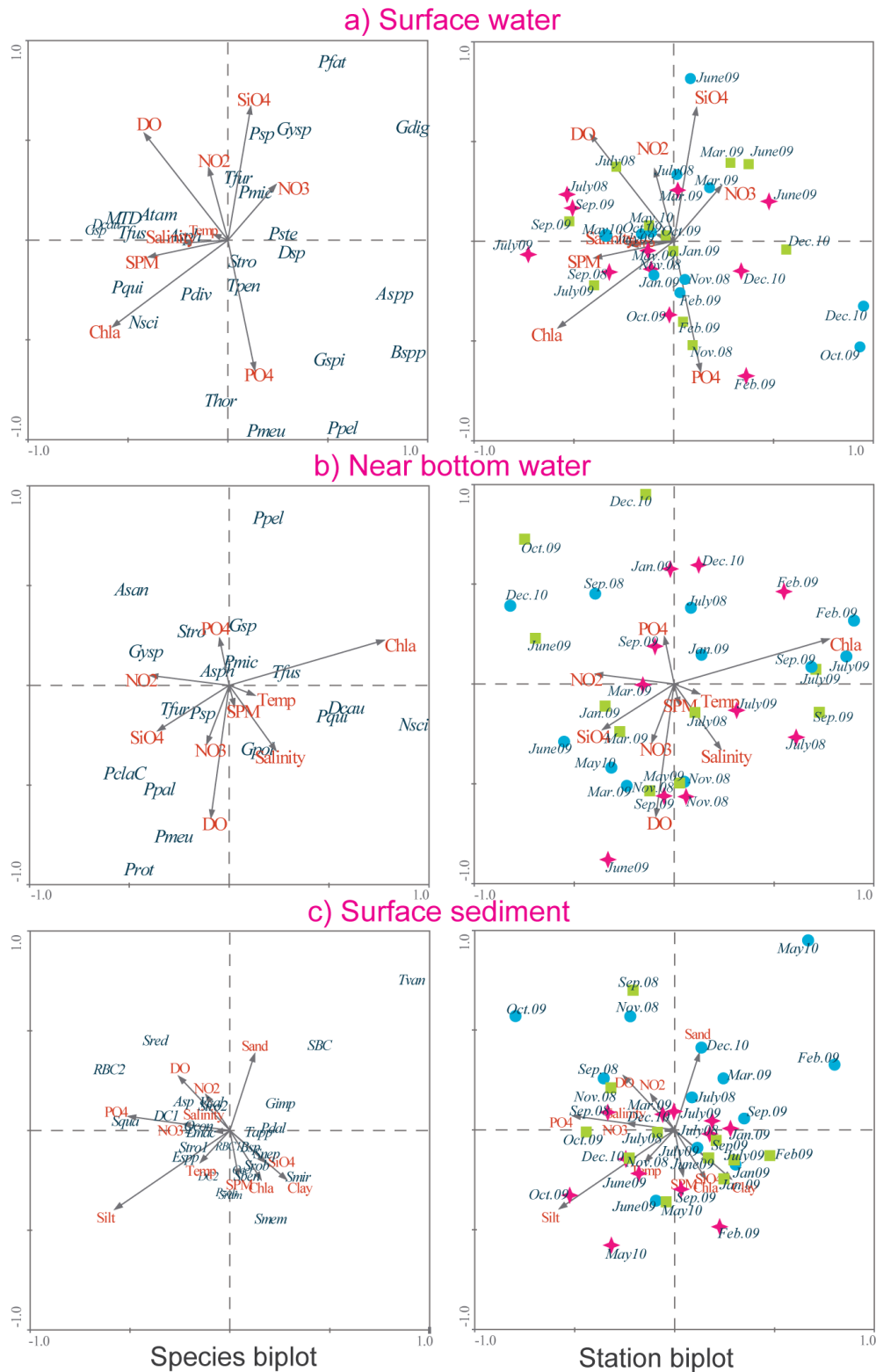


Fig. 5.10 Canonical Corresponding analysis (CCA) biplot illustrates planktonic dinoflagellate, a) surface, b) near bottom water and c) cyst species relation to environmental parameters (Grey arrows). Station codes: ● North Bay (NB) ■ Marine Hill (MH) ◆ Phoenix Bay (PB)

In species biplot, most of the heterotrophic Protoperidinoïd species, *P. pentagonum*, *P. compressum*, SBC, RBC2, *P. conicum* and *P. oblongum* are affiliated to increase phosphate and dissolved oxygen concentration (Fig. 9c). Majority species dominating cyst assemblage in the Port Blair Bay positioned towards the negative side of the CCA1. Along with the sedimentary characteristics (silt and clay), Chla and silicate concentration positively influence their occurrence. Dominant heterotrophs *Protoperidinium* spp. (*Brigantedinium* spp.), *P. subinerme* (*S. nephroides*) and phototrophic *Gonyaulax* species (*S. membranaceus*, *S. mirabilis*, *S. ramosus*, *S. bentori* and *O. centrocarpum*) oriented towards the clay, Chla and silicate vector. Dominant *S. trochoidea* cyst shows a weak affinity towards phosphate concentration.

5.4 Discussion

The dinoflagellates are well-known indicators of the environmental conditions due to their ecological responses to the changing biotic and abiotic environmental factors in the water column. However, most of them use multiple adaptive strategies (chemical, nutrient and physical stress tolerance) as well as life-cycle-functions (planozygote formation, pellicle and resting cyst) as ‘ultimate survival strategy’ to cope up with the surrounding environmental conditions (Smayda and Reynolds, 2003; Bravo and Figueroa, 2014). In this chapter, the ecological responses of dinoflagellates to changing environmental cues in the planktonic and benthic domain are discussed.

5.4.1 Dinoflagellate community structure (Importance of mixo- and heterotrophic strategies in dinoflagellate community)

Planktonic and benthic dinoflagellate population in the study region was diverse and varied over the sampling period (Table 5.1 and 5.2). Clustering pattern of sampling month-stations emphasises dominance of *P. micans*, *T. furca*, *N. scintillans*, *S. trochoidea* and *D. caudata*, which are capable of mixotrophy (Fig. 5.6 and 5.7). Mixotrophy is an important adaptive survival strategy of dinoflagellates, increases access to growth limiting nutrients, carbon, and other growth factors through phagotrophy and autotrophy (Stoecker, 1999; Bockstahler and Coats, 1993; Jeong et al., 2010). Mixotrophic “K-selection” protists dominate in more mature systems regaining from eutrophic to oligotrophic conditions (Mitra et al., 2014, Jones, 2000, Burkholder et al., 2008). These organisms are ‘generalists’ with less efficiency of converting food to energy compared to ‘specialists’ i.e. heterotrophs and autotrophs (Raven, 1997; Flynn and Mitra, 2009). Mixotrophy in dinoflagellate is much more evolved (review by Hansen, 2011). Most of the mixotrophic dinoflagellate species have permanent “peridinin-containing” chloroplasts (Hansen, 2011). Additionally, species like *D. caudata* have kleptoplastids, sequestered from cryptophytes (Park et al., 2008; Nagai et al., 2008; Minnhagen et al., 2006; Kim et al., 2012a) through feeding on ciliate *Myrionecta rubra*, which itself consumes cryptophytes (Nishitani et al., 2008). *P. quinquecorne* photosynthesizes using chloroplasts originating from the serial replacement of endosymbionts from original a pennate diatom (like *Nitzschia*) to centric diatoms like *Thalassiosira/Skeletonema* (Takano et al. 2008) or *Chaetoceros* (Horiguchi and Takano, 2006). Thus, mixotrophs have a competitive advantage over strict heterotrophs and autotrophs (Bockstahler and

Coats, 1993). The dual capacity of mixotrophic dinoflagellates to phototrophy and/or phagotrophy could enable them to flourish and proliferate in the water column.

In the benthic domain, along with mixotrophic *S. trochoidea*, the dominance of *Protoperidinium* species cyst were also responsible for the major clustering of sampling months (Fig. 5.8). Heterotrophic species (considered ‘generalists’) are well known for diversified feeding habits ranging from diatom to autotrophic dinoflagellate (Jacobson and Anderson, 1989; Naustvoll, 2000; Jeong et al., 2010). Their dominance in coastal cyst assemblage indicates ample prey (mainly diatoms) availability due to nutrient enrichment and eutrophication (Matsuoka, 2003; Godhe and McQuoid, 2003; Kim et al., 2009). Similarly, the dominance of the round, brown coloured cyst of *Protoperidinium* species (*Brigantedinium* spp.) highlights the production of diatoms due to nutrient availability in the water column (Montresor et al., 1998; Fuji and Matsuoka, 2006; Pospelova et al., 2010; Zonneveld et al., 2009). The dominance of Protoperidinoids in the Port Blair Bay can be attributed to the anthropogenic nutrient supply and subsequently availability of diatoms in abundance (Narale et al., unpublished data). The dominance of mixotrophs and heterotrophs in planktonic and benthic domain emphasises the predictive trophic state of the water column in this tropical monsoon-influenced region. Observations of present study are in accordance with the previous studies from the tropical monsoonal and anthropogenically influenced port (Mumbai and Mormugao) environments (D’Costa et al., 2008; D’Silva et al., 2013; Naik, 2010; D’Silva et al., 2011), where mixotrophs and heterotrophs were abundant in water column and sediments respectively.

5.4.2 Role of monsoonal interventions on dinoflagellate community structure

The species-environmental relationship evinced in the CCA biplot for both planktonic and resting stages of dinoflagellates. *Chla*, phosphate, and dissolved oxygen along with nitrate, silicate emerged as two groups of environmental variables controlling dinoflagellate distribution in the water column (Fig. 5.10a and b). Dissolved oxygen and nutrient (mainly nitrate and silicate) variation in the region is mainly influenced by the strength of monsoonal rainfall. Additionally, anthropogenic interventions from the surrounding inhabited area also support nutrient enrichment in the Port Blair Bay (Sahu et al., 2013; VishnuRadhan et al., 2015). However, monsoonal control was not observed in the case of phosphate concentration (Fig. 5.4d, 5.10a and b). Increased phosphate concentration during PstM months indicates addition from external sources (domestic discharge) especially at PB region (VishnuRadhan et al., 2015). Generally, detergents are the potential source of phosphate, outflow from the laundry vents operated along the embayment could be a possible source of phosphate into PB water. During the SWM high wind speed pattern (Fig. 5.2d) results in wind-driven turbulence and water mixing in the water column. This influences diffusion and mixing of oxygen, which eventually increases the dissolved oxygen concentration in the water column (Fig. 5.3c). In contrast, during the PstM and NEM seasons, reduced water mixing and increased biological oxygen consumption (respiration) affect dissolved oxygen concentration.

Chla concentration does not show a direct relationship with the nutrient availability in the water column (Fig. 5.3f). Picophytoplankton contributes substantially to eukaryotic biomass and chlorophyll concentration in the oceanic as well as coastal regions (Agawin et al., 2000; Mitbavkar et al., 2011; Mitbavkar et al., 2012; Rajaneesh

et al., 2015). Picophytoplankton has advantages relative to micro-phytoplankton in terms of resource (nutrients) acquisition and utilisation for growth and reproduction (due to reduced surface area to volume ratio) (Raven, 1997). Faster consumption of nutrients by dominant picoplanktonic population (Mitbavkar et al., unpublished data) in the region may lead to a nutrient-Chl a mismatch.

The influence of monsoonal transformations on dinoflagellate assemblages are evinced in CCA biplot, both in the water column and sediments (Fig. 5.10a and b). Mixotrophic *Triplos* species, mainly *T. furca* and *T. fusus* dominated dinoflagellate assemblage especially during PrM, PstM blooms and SWM II (Fig. 6, 7, 9), whereas other rare *Triplos* forms appeared during the NEM. *T. furca* and *T. fusus* are cosmopolitan and common bloom-forming species in coastal (eutrophic) to oceanic (oligotrophic) environments (Baek et al., 2008 and references therein). They have competitive advantage over the other phytoplankton species due to 'luxury consumption' (excessive storage of inorganic nutrients), low K_s value, ability to survive in high N:P (P limitation) conditions (Baek et al., 2008) as well as phagotrophic ability (Smalley et al., 2002, 2003). However, *T. furca* has a competitive ecological advantage over *T. fusus* due to efficient diel vertical migration ability for nutrient acquisition, light requirements and avoid turbulence (Baek et al., 2009; 2011). The abundance of *T. furca* during PrM and SWM II is markedly evinced in the CCA biplot towards nutrient (nitrate, nitrite, and silicate) vectors (productive preference). However, *T. fusus* dominance mainly during PrM and PstM blooms is oriented towards Chl a vector (predictive preference). This difference in affiliation between these two species could be due to their biological preferences and performances.

Heterotrophic dinoflagellate, *N. scintillans* dominated dinoflagellate assemblage during the SWM (both the years) and NEM (in February) (Fig. 5.10a and b). *N. scintillans* is phagotrophic dinoflagellate feeds on diversified organisms like bacteria (Kirchner et al., 1996), protozoans, zooplanktons, fish eggs (Kiorboe and Titelman, 1998) and phytoplankton (Elbrachter and Qi, 1998) as well. Abundance and bloom incidences of *N. scintillans* were supported by the increased availability of nutrients and prey (mainly phytoplankton and micro-zooplanktons) along the Indian region (D'Silva et al., 2013 and references therein), including the Andaman region. In the Port Blair Bay, *N. scintillans* bloom was previously reported during July 2000 (Eashwar et al., 2001) and December 2002 (Dharani et al., 2004). The CCA biplot (Fig. 5.10a and b) evidence *N. scintillans* distribution in the study region is closely associated with Chla concentration, which can link with the rich availability phytoplankton prey (picoplankton, diatom, and dinoflagellates) during the SWM and NEM seasons.

Dinoflagellate species, *D. caudata*, and *P. quinquecorne* were abundant in PB during PrM, PstM blooms and SWM (Fig. 5.8a). The association of *D. caudata* and *P. quinquecorne* with the Chla could be an example of utilisation of symbiont chloroplasts to enhance nutrient assimilation through photosynthesis, and may prove to be an efficient adaptation strategy in dinoflagellates in the study area.

P. micans a cosmopolitan species, responsible for red tide events as well as commonly associated with the mixed dinoflagellate bloom. This species was observed in moderate concentration in the study region. *P. micans* is a mixotrophic species, and its planktonic abundance can be related to the inorganic nutrient availability and eutrophication in coastal waters (Hodgkiss and Ho, 1997; Sahraoui et al., 2013).

However, Shipe et al. (2008) have observed that *P. micans* bloom in Santa Monica Bay, California were associated with stratified, low nutrient water. In the study region, this species does not show any seasonal pattern (Fig. 5.6, 5.7, 5.10a and b). However, its dominance is associated with another dominant species during PrM I, PstM II blooms and PstM III emphasises the role of nitrate and phosphate in their growth (Fig. 5.10a and b).

The seasonal dominance of *S. trochoidea* in plankton and subsequently in the benthic domain was observed mainly in the Port Blair Bay (Fig. 5.6 and 5.7), especially during the SWM II, PstM in surface and NEM, PrM I in near-bottom waters (Fig. 5.9). The ability of mixotrophic *S. trochoidea* to adjust with diverse environmental settings (Kim and Han, 2000) could be the reason for its successes and proliferation in the Port Blair Bay region. Additionally, the increase in cyst concentration together with the dominance of *Scrippsiella* in plankton reveals the impacts of enhanced human activities on the Bay ecosystem, as observed in the Daya Bay, South China Sea (Wang et al., 2011). This discussion further supported in the CCA orientation, which explains that *S. trochoidea* abundance is not controlled by particular environmental cue (Fig. 9a,b). However, elevated phosphate concentration could support its growth in association with other environmental factors as reported elsewhere (Garate-Lizarraga et al., 2009, southwestern Gulf of California).

Dinoflagellate cyst concentration in surface sediments is controlled by cyst formation potential of planktonic dinoflagellate in the water column as well as cyst deposition in sediments (Dale, 1983; Dale, 2001a). It is well known that dinoflagellate cyst has a specific gravity similar to silt particle (Dale, 1983). Additionally, cyst morphotypes possess cell-wall processes (ornamentations) which increase surface-to-

volume ratio and eventually residence time in the water column (Anderson et al., 1985; Sarjeant et al., 1987). Thus, cysts can be transported by the winnowing action of water currents (Anderson et al., 1985; Kawamura, 2004). The fine sediment also indirectly indicates a stable and favourable sedimentation process (Liu et al, 2012). Semi-enclosed areas, where sedimentation prevails over particle transport, can act as “sediment traps” and potential reservoirs of benthic stages (Joyce et al, 2005). In the study region, dinoflagellate cyst abundance was higher in the Port Blair Bay, than in the North Bay. Cyst assemblage distribution within the region corresponds well with the sediment texture (Fig. 5.10c). Most of the sampling months in the North Bay corresponds to sediment comprising mainly of coarse-grained sand particles, whereas the Port Blair samples and dominant dinoflagellate species oriented towards the silty clay sediments. In addition to cyst deposition, comparatively higher abundance of cyst-forming dinoflagellate taxa in the water column (Table 5.1 and 5.2) could also influence higher cyst abundance in surface sediments in the Port Blair Bay.

Cyst formation strategy is important for survival and proliferation of dinoflagellate population in the water column (as discussed in Chapter 1, Section 1.4). In the study region, benthic-pelagic linkages enable survival and maintenance of stock population in cyst forming dinoflagellates (Fig. 5.9). These transpositions were prominent in the case of dominant species, *S. trochoidea*, *Protoperidinium* species and *Gonyaulax spinifera* member species. However, modern molecular genetic studies revealed that dinoflagellate has high-level intraspecific genetic diversity (Lin et al., 2009). These changes further highlighted in recent cyst-theca relationship and genetic studies in cyst forming dinoflagellate species like *S. trochoidea*, *Protoperidinium* species and

Gonyaulax spinifera member species (Montresor et al., 2003; Gottschling et al., 2005a,b; Gribble and Anderson, 2007; Morquecho et al., 2009). These species possess ‘heterospory’, single planktonic species from different cyst morphotypes (Head, 1996). Also, a large group of cyst morphotypes from *Protoperidinium* and *Gonyaulax* species planktonic affinities are not verified/confirmed. Most of the Gonyaulacoid and Protoperidinoid species with similar in planktonic and cyst morphotypes have different molecular orientations. Due to this heterogeneity, comparison of planktonic dinoflagellates with cyst counterparts becomes a difficult task. To overcome the practical difficulties, in the present study we have combined planktonic and related cyst morphotypes from *S. trochoidea* species complex as *S. trochoidea*; *Gonyaulax spinifera* complex and associated Gonyaulacoid species as *Gonyaulax* spp.; Protoperidinoid species as *Protoperidinium* spp. Other rare dinoflagellate forms like, *Protoceratium reticulatum*, *Pentapharsodinium dalei*, *Lingulodinium polyedrum* and *Pyrophacus stenii* are kept separate.

Life cycle functions and strategies in dinoflagellates are very complex due to species-specific survival strategies (Kremp, 2013; Bravo and Figueroa, 2014). In some species, ‘planozygote’ (diploid cell with planktonic affinity) and ‘pellicle cyst’ (thin walled cyst) can be used as an alternate survival strategy to resting cyst formation (Kremp, 2013; Bravo and Figueroa, 2014). In the case of *P. minimum* and *Akashiwo sanguinea* temporary cyst formation was observed under experimental conditions (Grzebyk and Berland, 1996; Tang and Gobler, 2015). *Dinophysis* species adopt polymorphism (intermediate small size cell formation as part of the sexual life cycle) to sustain unfavorable environmental conditions (Roguera and Gonzalez-Gil, 2001). These

ultimate survival strategies support to maintain the static population in the planktonic and benthic domain.

Influence of monsoonal and anthropogenic interventions are prominent in the Port Blair Bay than the North Bay. During the SWM, increased turbulence and turbidity (suspended load) exerts shear stress on dinoflagellate population in surface layers. During such physical disturbances dinoflagellate species prefers to migrate in water column towards less disturbed environmental (Smayda, 2002). The concentration of *Protoperdinium* species towards the near bottom water and sediments (cysts) could be in response to the changed environmental condition in the surface layers. During this period, *S. trochoidea* was rarely present in the water column but dominant in cyst assemblage (Fig. 5.9a), which could be its survival strategy to avoid the shear stress during the SWM period. Although the nutrient concentration in the water column increases due to discharge from embayment region through sewage channels, increase in opportunistic phytoplankton species abundance (competition) along with ‘dilution and flushing effects’ control nutrient availability. The dinoflagellate population during the both SW monsoon seasons (SWM I and SWM II) was different. This heterogeneity in dinoflagellate assemblage was mainly affected by the monsoonal strength and duration (D’Costa et al., 2008). In 2008, the SW monsoon (SWM I) was strong and prolonged from May to September than 2009 (SWM II) (observed from rainfall and wind speed data, Fig. 2c and d). Furthermore, diverse dinoflagellate population, higher species richness, and species evenness during SWM II indicate reduced environmental stress. During the subsequent PstM and NEM season, *S. trochoidea* population was well distributed in the water column. Increased nutrient concentration, especially phosphate in

near-bottom water may trigger the excystment of *S. trochoidea* and its subsequent distribution in the water column. The planktonic dominance of *T. furca* characterized dinoflagellate community structure during the both SWM seasons. *Tripos* species classified as ‘R-strategist’ (tolerant of shear/stress forces) dinoflagellates (Smayda and Reynolds, 2003) with the ability to tolerate water mixing and turbulence stress (Smayda, 2002). Shear stress tolerance capacity of *T. furca* enable their dominance during SWM season.

During PrM I (March 2009) and PstM II (October 2009), increased nutrient supply from the harbour, domestic drainage and reduced ‘flushing effect’ due to weak water currents, mixing increases ‘nutrient retention time’ in the water column. Reduced effect of water turbulence and an increase in nutrient concentration during PrM and PstM, establish an intermediate state between SWM (strong disturbance) and NEM (weak disturbance). Intermediate frequencies of disturbances establish the unimodal diversity-disturbance relationship in marine phytoplankton, with maximum species richness and diversity (Sommer, 1995), as stated by ‘intermediate distribution hypothesis’ (IDH; Connell, 1978). Mixed-species diatom-dinoflagellate bloom during this period emphasize coexistence of competitively dominant and rapidly colonizing forms. Further, increased dinoflagellate abundance, species number, evenness, and richness highlight the intermediate level of disturbances supports the multi-species proliferation in the water column (Table. 5.3; Fig. 5.5, 5.6 and 5.8). Abundant Protoperidinoid and Gonyaulacoid cyst could fuel their planktonic population during this period. Blooming phytoplankton population consumes organic and inorganic nutrients at faster rates due to competition and survival for existence. Hence, nutrients get depleted at a faster rate towards the end

of the bloom. Eventually, nitrate and phosphate depletion conditions triggers cyst formation strategy in dinoflagellates (Ishikawa and Taniguchi, 1996; Wang et al., 2007). Increased cyst abundance of *S. trochoidea*, Protoperidinoid and Gonyaulacoid species during the subsequent month in sediments could be triggered by ‘nutrient stress’ conditions towards the bloom cessation.

According to ‘Stress-gradient hypothesis’ the frequency and/or strength of competition declines and facilitation increases with increasing environmental stress (Maestre et al., 2009). In the stressed environment, the competitive ability of certain species facilitates their growth as compared to stress-tolerance species. Thus, competitive interaction acts as a dominative structuring force in the ecosystem. Contrary, under the low-stress conditions, the less competitive ability of the stress-tolerant species makes its effects on the competitor to be null or slightly positive (Hart and Marshall, 2013). Cyst formation in certain species can act as stress-tolerance or stress-evasion strategy under the chemically and/or physically stressful environment.

Dinoflagellate species like *P. quinquecorne* commonly observed as part of benthic and epiphytic dinoflagellate assemblage (Saburova et al., 2008; Okolodkov et al., 2007), however, it is well-adapted to benthic-pelagic shallow-subtropical embayment (Garate-Lizarraga and Muneton-Gomez, 2008). They possess an endogenous tidal rhythm (vertical migration) with photic response to remain dense population in estuarine water (Trigueros and Orive, 2000). Thus, cells aggregates in subsurface water during preceding tides and remain low or negligible at the bottom during receding tides (Trigueros and Orive, 2000). Its ‘epiphytic strategy’ ensures survival and prevents leaching during receding tides (Horstmann, 1980). In the study region, the dominance of *P. quinquecorne*

during the SWM season in near-bottom water may emphasise their epiphytic strategy to avoid environmental stress. Favourable conditions during PrM and PstM blooms supports their proliferation in surface waters.

The nature of monsoon oscillations, whether persistent or abrupt is very essential, as both have different effects on community structure (D'Costa et al., 2008; Patil and Anil, 2008, 2011; Naik, 2010). In response to the environmental pulses, associated communities try to adapt gradually both structurally and functionally. Such counterintuitive events can flip the system into a contrasting state. This state represents either an alternative attractor or a transient that is slow enough to persist even if the frequency of events that push the system to this state is low (Scheffer et al. 2008). However, there is also the potential that they might initially respond gradually to a press disturbance, but at some critical point collapse and form a completely new system (Shea et al. 2004). Thus, rates of environmental change can sometimes be more important than their magnitude (Critical-rate hypothesis) (Scheffer et al. 2008).

During the December 2010, sudden rainfall was occurred in the study region due to depression over the Bay of Bengal (IMD daily weather report, 6th-8th December 2010). This counterintuitive event increased nutrient flux into the Port Blair Bay. In response to this unforeseen nutrient enrichment, mixed diatom bloom (*Guillardia* spp., *Cocconeis* spp., *Nitzschia* spp. and *Pseudonitzschia* spp.) observed in the water column (Narale et al., unpublished data). Increased nutrient concentration during this period may support dinoflagellates growth in the water column and cyst germination of *S. trochoidea* and *G. spinifera* species in the benthic domain.

The dinoflagellate abundance (in both water column and sediments) in the coral reef inhabited North Bay was less than the Port Blair Bay. The community was dominated by the phototrophic *Gonyaulax* species in surface water and sediments (Table 5.1, Fig. 5.9c). Generally, coral reefs are broadly recognized as being limited to warm, clear, shallow, saline, nutrient depleted waters (Kleypas et al., 1999). Generally, *Gonyaulax* species have a less nutrient requirement but can thrive in diverse nutrient conditions (discussed in Chapter 2 and 3B). The dominance of *Gonyaulax* species, as observed in the North Bay, signifies the less nutrient availability, high salinity and temperature (Kim et al, 2012b). Furthermore, the exclusive occurrence of oceanic heterotrophic dinoflagellates *Ornithocercus steinii* and *O. heterosporous* at this station (Table 5.1), could evince the intrusion of oceanic water into the Bay.

5.4.3 Harmful Algal Blooms (HABs) perspective in the South Andaman region!

Evaluation of dinoflagellates from benthic as well as pelagic domain provide better information on dinoflagellate species population in a given area (discussed in Chapter 3A, Section 3A.4.3). Sixteen potentially harmful and red-tide-forming species were encountered from both water and sediment samples analysed from the South Andaman coast (Table 5.1). *Alexandrium* species, *A. tamarense* complex, *A. minutum* and *A. pseudogonyaulax* are responsible harmful, red tides and toxic events worldwide (Anderson et al., 2012; Fraga et al., 2015 and references therein). Generally, *A. tamarense* complex species are associated with paralytic shellfish poisoning (PSP) outbreaks (Hallegraeff, 1993; Lilly et al., 2007; Anderson et al., 2012). However, not all *A. minutum* and *A. tamarense* complex cryptic species are toxic and responsible for PSPs or toxic events (Higman et al., 2001; John et al., 2004; Lilly et al., 2007; McCauley et al., 2009;

Yang et al., 2010; Anderson et al., 2012). In this study, *A. tamarense species* complex, *A. minutum* and *A. pseudogonyaulax*, *Alexandrium* spp. have been observed in planktonic and cyst forms respectively (Table 5.1 and 5.2). Since from this region HABs or PSPs have not reported and the potential of these *Alexandrium* species to produce toxicity event is unknown. However, their spontaneous response to elevated nutrient concentration during March and October blooms proves their potential candidature for the future blooms. Cyst of other PSPs causing *P. bahamense* were recorded for the first time in the region. Considering spread of *P. bahamense* blooms along the adjacent Southeast Asian region through natural and anthropogenic vectors (Azanza and Taylor, 2001), their cyst occurrence in the South Andaman region can be a matter of great concern.

Potential yessotoxin (YTX) producing *P. reticulatum* were recorded in sediments, whereas *G. spinifera* and *L. polyedrum* were reported in both cyst and planktonic forms. Although not all *Gonyaulax spinifera* complex members produce YTXs, their population was diverse in the region (Table 5.1). Bloom and red-tide-forming *S. trochoidea* were dominant in planktonic as well as in cyst forms (Table 5.1 and 5.2). The benthic-pelagic linkages play an important role in their survival and proliferation in the region (as discussed previously). Anoxic red-tide incidences of *T. furca*, *T. fusus*, *P. micans*, *N. scintillans*, and *P. quinquecorne* increased worldwide due to eutrophication (Hodgkiss and Ho, 1997; Hansen et al., 2004; Yu et al., 2007; Garate-Lizarraga and Muneton-Gomez, 2008; Morton et al., 2011). Mixed-phytoplankton bloom incidence during the March and October 2009 proves that the increased nutrient loading from the anthropogenic sources triggers the growth of existing resilient dinoflagellate population.

Increased concentration of *T. furca*, *T. fusus*, *P. micans* and *A. sphenoides* due to nutrient enrichment highlight their bloom-forming potential in the region.

In the regional context, PSP outbreak and HABs of *A. minutum*, *A. tamiyavanichii* and *P. bahamense* var. *compressum* is spreading widely in the Southeast Asian region (Fukuyo et al., 2011; Azanza and Taylor, 2001; Baula et al., 2011; Su-Myat et al., 2012), and caused adverse socio-economic problems in recent years (Fukuyo et al., 2011). Together with the physical vectors, increased anthropogenic interventions (marine traffic, aquaculture transfers) are potentially responsible for the regional spread of the HABs (Anderson et al., 2012; Fukuyo et al., 2011). Along the Mangalore coast, India, a toxin profile of the clams from the PSP affected region corresponded to a strain of *A. tamiyavanichii* isolated from Thailand (Karunasagar et al., 1990), which may suggest the potential of regional HAB species transport. Subsequently, cyst of *A. cf tamiyavanichii* has also been reported along the Mangalore coast (Godhe et al., 2000). Considering the increasing incidences of HABs spread along the adjacent Southeast Asian regions, the Andaman region is potentially at risk. The increasing coastal anthropogenic activities make this previously known 'pristine region' susceptible towards the HABs initiation and development.

5.5 Conclusion

This study presents detailed investigation on impulsive and causative responses of dinoflagellates to the monsoon-driven planktonic and benthic environmental cues in the South Andaman region. Dinoflagellate assemblage differences between two SWM highlight the control of monsoonal strength and associated factors on the faith of dinoflagellate population. Strong SWM I hampered phototrophic dinoflagellate growth,

a facilitated heterotrophic (*Protoperidinium* spp., *N. scintillans*), and sheer stress tolerant (*T. furca*, *P. micans*) dinoflagellate population in the region. Heterotrophic dinoflagellate abundance was governed by the preferences of their prey, i.e. conditions favouring diatoms. Cautious responses like vertical migration, epiphytic strategy maintain a subsurface population of dinoflagellates like *S. trochoidea* and *P. quinquecorne*. In contrast, weak SWM II and NEM seasons supported the growth of diverse dinoflagellate population. Intermediate static environmental conditions together with anthropogenic nutrient input supported diverse and abundant dinoflagellate population during the PrM and PstM seasons, especially at the Port Blair region.

In the region, benthic-pelagic exchange supported the cyst forming species population. During the SWM and post (PrM and PstM) bloom period cyst formation recharge benthic population of *S. trochoidea*, *Gonyaulax* and *Protoperidinium* species as part of stress evasion (either sheer or nutrient) strategy. This trade further supported their planktonic population during the NEM and inter-monsoon periods. Thus, benthic-pelagic exchanges influenced by the monsoonal environmental cues helps dinoflagellates to maintain the static population in the South Andaman region.

Appendix

Supplementary data associated with Chapter 5 can be found in Appendix III

Chapter 6
Summary

Chapter 6 Summary

Dinoflagellates (Dinophyceae) are among the dominant microphytoplankton groups, contributing substantially to eukaryotic production in the marine environment. In dinoflagellates, along with life cycle functionality, varied physiological and ecological response mechanisms enable them to survive and maintain their population in the pelagic environment. In this context, this study evaluated how does cyst forming dinoflagellate population respond to the conditions influenced by monsoonal intervention in the Bay of Bengal? This question was assessed through studying inter- and intra-annual variability in the cyst-forming dinoflagellates in the Bay of Bengal. Time series observations (48-month sampling) were carried out using a Ships-of-Opportunity network along the Chennai-Port Blair (CP) and Port Blair-Kolkata (PK) sectors (22 stations). This sampling approach was suitable as it offered a spatial and fine temporal scale resolution of the phytoplankton community (Hegde et al., 2008, Hegde, 2010; Naik, 2010; Naik et al., 2011). It was observed that small portion of planktonic dinoflagellates (~10%) have cyst-formation capability and contribute to the dinoflagellate flora in surface waters. In the region, stratified and nitrate-deficient waters, promote stasis of the resident cyst-forming dinoflagellate population. The predominance of *S. trochoidea* emphasizes mixotrophy is an essential survival strategy in the Bay of Bengal waters.

Seasonal monsoonal interventions play an important role in the distribution of cyst-forming dinoflagellates assemblage. Prevalence of mixotrophic, *S. trochoidea* during the spring-inter monsoon (SIM) and late (September) south-west monsoon (SWM) highlight light availability with a clear sky, and no rainfall facilitate their proliferation. Phototrophic dinoflagellates prevalence illustrate the effect of possible niche

differentiation on their distributions. Increased light, temperature, reduced rainfall and suspended load with low to moderate nutrient concentrations during the northeast monsoon (NEM), fall-inter monsoon (FIM) and SIM facilitate the growth of Gonyaulacoid species in the region. In the regional context, oceanic conditions in the CP region support diverse population Gonyaulacoid species and other phototrophic species, *Alexandrium* spp., *Gymnodinium catenatum*, *Scrippsiella spinifera* throughout the year.

Diverse heterotopic feeding mechanisms support *Protoperidinium* species to maintain the static population in diverse environmental and regional conditions. *Protoperidinium* abundance in the region, especially at the river mouth (RM) in the northern Bay of Bengal suggests food availability (mainly diatoms) sustain its population. Continuous enrichment of coastal waters through the Ganges-Brahmaputra riverine systems supports a comparative abundance of diatoms and in turn *Protoperidinium* population through the year. In the PK region, *Protoperidinium* abundance at the northern and southern part, especially during the SWM, suggest an effect of nutrient enrichment. However, in the CP region, increased production due to moderate wind driven advection support *Protoperidinium* population during the NEM.

Assessment of the links between cyst distribution in surface sediment and regional environmental conditions along the western Bay of Bengal was carried out. Spatial variation in cyst population reflects coastal to neritic-oceanic assemblage variation driven by monsoonal seasonality and riverine influx. The relative dominance of Protoperidinoid species along the coastal ambience can be related to prey availability, influenced by the riverine nutrient influx. The presence of the coastal-neritic species, *Brigantedinium* (*Protoperidinium*) spp. and *Selenopemphix nephroides* (*P. subinerme*),

Operculodinium centrocarpum (*P. reticulatum*), *Spiniferites mirabilis* (*G. mirabilis*) together with oceanic *Impagidinium sphaericum* (*Gonyaulax* species) at the deeper stations, emphasize the influence of (seasonal) monsoonal transformations on cyst assemblage. The dominance of oceanic *Impagidinium* (*Gonyaulax*) species towards the offshore region suggests the prevalence of low nutrient oceanic conditions driven by the stratification during the spring intermonsoon. The potentially toxic dinoflagellate, *Pyrodinium bahamense* cyst (*Polysphaeridium zoharyi*), along with other harmful species was also observed in the study region. The dominance of *Operculodinium centrocarpum* (cyst of *Protoceratium reticulatum*) in the Visakhapatnam region reflects the possible effect of anthropogenic nutrient input on cyst population. Cyst abundance was comparatively high at northern stations and was well correlated with the fine-grained (silt-clay dominated) sediments. In contrast, low cyst abundance was recorded in sandy sediments at southern stations. Further comparison of the cyst abundance with subtropical and temperate regions revealed that the cyst abundance recorded here is low (29–331 cysts g⁻¹), but it is on par with other tropical regions, including the West coast of India and South Andaman region.

To present a scenario of the dinoflagellate cyst assemblages in the Indian subcontinent the dinoflagellate cyst assemblages from the western Bay of Bengal and South Andaman region is compared with published cyst mapping data from the eastern Arabian Sea (Godhe et al., 2000; D'Costa et al., 2009; D'Silva et al., 2011; D'Silva et al., 2012a). This comparison brought out regional differences in the species composition. The total number of phototrophic, heterotrophic, as well as potentially harmful species, is higher along the eastern Arabian Sea (West coast of India). Regional differences in an

oceanographic feature like, i) less nutrient availability due to lack of upwelling and convective mixing, nutrient scavenging to deeper water, ii) competitive stress for light and nutrient scarcity, and iii) reduced biological production could be the reasons for low species diversity in the Bay of Bengal. However, the increasing coastal anthropogenic activities make this region susceptible to the HABs initiation and development. Considering the history of initiation and spread of HAB species along previously known pristine habitats, these resilient dinoflagellate forms have potential candidature for the future blooms.

Conventionally, the Bay of Bengal is supposed to be a less productive region than its counterpart i.e. the Arabian Sea (Qasim, 1977; Radhakrishna et al., 1978; Prasanna Kumar et al., 2002). Although seasonal reversal in the Asian monsoons influences both, the Arabian Sea and the Bay of Bengal, the oceanography and biology differ considerably. Biological features such as chlorophyll, primary productivity, phytoplankton abundance and mesozooplankton are lower in the Bay of Bengal as compared to Arabian Sea (Qasim, 1977; Madhupratap et al., 2003; Gauns et al., 2005). In the present study, for the first time, dinoflagellate records used as an archive to evaluate the paleoproductivity variability and the monsoonal dynamics in the eastern Arabian Sea and the western Bay of Bengal.

The dinoflagellate cyst assemblage response to the monsoon variability over the last 68 ka from the eastern Arabian Sea (EAS) was evaluated using a 4.2 m gravity sediment core AAS 9/21. Cyst records revealed that the productivity in the EAS was higher during the glacial than interglacial periods, mainly controlled by nutrient supply from subsurface water due to winter convection is driven by the NE monsoonal wind.

The productivity change was mainly highlighted by increased abundance of Gonyaulacoid species (especially *Spiniferites*). Within the glacials, productivity was higher during MIS 2 than in MIS 4 and characterised by a two-fold increase in cyst abundance. During the interglacials, reduction in the primary productivity during early MIS 3 (~67.5 to 58.67 ka) and in MIS 1 was highlighted by a lesser abundance of Gonyaulacoid cyst, which could be due to strong summer monsoon, resulting in intense stratification and reduced light penetration. Dinoflagellate cyst abundance and assemblage difference revealed that productivity was higher during the LGM than Holocene. The LGM was more dynamic with larger fluctuations in cyst abundance and assemblages. This reveals the winter mixing was not consistent throughout the LGM.

Sudden decrease in total cyst abundance, *Spiniferites* species abundance and relative abundance of all dominant species during stadial periods (Northern hemisphere cold periods), the Heinrich events (HE2 and HE1) and Younger Dryas (YD) was observed. Decreased strength of NEM and rapid SST fluctuations during this period adversely affect *Spiniferites* species abundance during the deglaciation. Variation in *Protoperidinium* species, abundance over the past 68 ka, represents variation in the OMZ intensity. Increased *Protoperidinium* abundance during MIS 3 and late MIS 1 (~3 ka onwards) highlighted their good preservation in sediments due to strong OMZ. SST increased during the Holocene was characterised by increased abundance of *B. spongium*, *S. pachydermus*, and *O. centrocarpum*. The dinoflagellate cyst proxy demonstrates that the EAS responds to both regional and global scale climatic variations.

Dinoflagellate cysts abundance and composition in a sediment core (SK218/1) from the western Bay of Bengal was examined for the last 23 ka to evaluate the

productivity variability during the Holocene and last glacial periods. Cyst abundance at this site varied from 20 to 153 cysts g^{-1} that is far less than that reported from other oceans. Holocene period harboured a higher number of cysts (74 to 153 cysts $gram^{-1}$) than the last glacial period (up to 67 cysts $gram^{-1}$). Although cyst abundance is low at this site the cyst composition and their abundance between the Holocene and last glacial period reflects the affinity to climate change between these two periods like other regions. The changes in the composition of both autotrophs and heterotrophs cyst assemblages exhibited clear distinction between the Holocene and last glacial period in the present core. Higher absolute cyst abundance, an abundance of both Protoperidinoid and Gonyaulacoid cysts and species diversity was observed during the Holocene than last glacial period. Thus, cyst assemblage variability indicates higher productivity during the Holocene than in last glacial period in the southwest monsoon-influenced Bay of Bengal region.

An evolution of dinoflagellate cyst as a proxy for paleoproductivity and paleoclimatic variability highlighted that the abundance and assemblage differences between the eastern Arabian Sea and the western Bay of Bengal seen in the recent sediments hold true in the paleo context. Dinoflagellate cyst abundance and diversity in the Bay of Bengal is less than the Arabian Sea. This variance in cyst population emphasizes the difference in the modern physical and biological characteristics between the two regions prevailed through the Late Quaternary period.

To investigate how the benthic-pelagic trade and environmental cues influence cyst-forming dinoflagellate population, monthly time-series observations were carried out along the South Andaman region. This study highlighted that cyst functions are as important as other survival strategies to maintain and thrive cyst-forming dinoflagellate

population in the South Andaman region. In the region, benthic-pelagic exchange supports the cyst forming species population. During the SWM, increased turbulence and turbidity (suspended load) exerts ‘shear stress’ on the planktonic population of *S. trochoidea*, *Gonyaulax* and *Protoperidinium* species in surface layers. Increased cyst abundance of these species in the benthic domain during subsequent month emphasises cyst formation can be used as stress tolerance strategy. During the subsequent SIM and NEM season, *S. trochoidea* population was well distributed in the water column. Increased nutrient concentration, especially phosphate in near-bottom water could be the trigger for excystment of *S. trochoidea* and its subsequent distribution in the overlying water column.

During the intermediate monsoons (Pre- and Post-monsoons) blooming phytoplankton population consumes organic and inorganic nutrients at faster rates due to competition and survival for existence. Hence, nutrients get depleted at a faster rate towards the end of the bloom. Eventually, nitrate and phosphate depleted conditions trigger cyst formation strategy in dinoflagellates (Ishikawa and Taniguchi, 1996; Wang et al., 2007). Increased cyst abundance of *S. trochoidea*, Protoperidinoid and Gonyaulacoid species during the subsequent month in sediments could be triggered by ‘nutrient stress’ conditions towards bloom cessation. Thus, benthic-pelagic exchanges as part of impulsive or cautious responses of cyst-forming species to the monsoonal environmental cues help to maintain their static population in the South Andaman region.

Overall, the results obtained during this study reveal the utility of dinoflagellates as an important biomarker to study the recent as well as past monsoonal dynamics and associated environmental, oceanographic variability in the tropical region. Further, this

study emphasises the importance of an ecological understanding of cyst functions in dinoflagellate population dynamics and harmful algal bloom studies.

Bibliography

- Agawin, N.S., Duarte, C.M., Agusti, S., 2000. Nutrient and temperature control of the contribution of picoplankton to phytoplankton biomass and production. *Limnol. Oceanogr.* 45, 591-600.
- Anand, P., Kroon, D., Singh, A.D., Ganeshram, R., Ganssen, G., Elderfield, H., 2008. Coupled sea surface temperature-seawater $\delta^{18}\text{O}$ reconstructions in the Arabian Sea at the millennial scale for the last 35 ka. *Paleoceanography* 23.
- Anderson, D.M., Wall, D., 1978. Potential importance of benthic cysts of *Gonyaulax tamarensis* and *G. excavata* in initiating toxic dinoflagellate blooms. *J. Phycol.* 14, 224-234.
- Anderson, D.M., Lively, J.J., Reardon, E.M., Price, C.A., 1985. Sinking characteristics of dinoflagellate cysts. *Limnol. Oceanogr.* 30, 1000-1009.
- Anderson, D.M., Taylor, C.D., Armbrust, E., 1987. The effects of darkness and anaerobiosis on dinoflagellate cyst germination. *Limnol. Oceanogr.* 32, 340-351.
- Anderson, D.M., Fukuyo, Y., Matsuoka K., 1995. Cyst methodologies. In: G.M. Hallegraeff, M., Cembella, A.D. (eds.), *Manual on harmful marine microalgae*, IOC Manuals and Guides, no. 33. UNESCO, Paris, 229-245.
- Anderson, D.M., 1998. Physiology and bloom dynamics of toxic *Alexandrium* species, with emphasis on life cycle transitions. In: Anderson, D.M., Cembella, A.D., Hallegraeff, G.M. (eds.), *Physiological ecology of harmful algal blooms*. Springer, NATO ASI series 41, Germany, Berlin, Verlag, 29-48.
- Anderson, D.M., Stock, C.A., Keafer, B.A., Nelson, A.B., Thompson, B., McGillicuddy, D.J., Keller, M., Matrai, P.A., Martin, J., 2005. *Alexandrium fundyense* cyst dynamics in the Gulf of Maine. *Deep-Sea. Res. II* 52, 2522-2542.
- Anderson, D.M., Cembella, A.D., Hallegraeff, G.M., 2012. Progress in understanding harmful algal blooms: paradigm shifts and new technologies for research, monitoring, and management. *Ann. Rev. Mar. Sci.* 4, 143-176.
- Aydin, H., Matsuoka, K., Minareci, E., 2011. Distribution of dinoflagellate cysts in recent sediments from Izmir Bay (Aegean Sea, Eastern Mediterranean). *Mar. Micropaleontol.* 80, 44-52.

- Azanza, R.V., Taylor, F.M., 2001. Are *Pyrodinium* blooms in the Southeast Asian region recurring and spreading? A view at the end of the millennium. *AMBIO: A Journal of the Human Environment* 30, 356-364.
- Baek, S.H., Shimode, S., Han, M.-S., Kikuchi, T., 2008. Growth of dinoflagellates, *Ceratium furca* and *Ceratium fusus* in Sagami Bay, Japan: the role of nutrients. *Harmful Algae* 7, 729-739.
- Baek, S.H., Shin, H.H., Choi, H.-W., Shimode, S., Hwang, O.M., Shin, K., Kim, Y.-O., 2011. Ecological behavior of the dinoflagellate *Ceratium furca* in Jangmok harbor of Jinhae Bay, Korea. *J. Plankton Res.* 33, 1842-1846.
- Banakar, V.K., Oba, T., Volvaiker, A.V., Kuramoto, T., Minagawa, M., 2005. A 100,000 years climate history of the Eastern Arabian Sea: Monsoon precipitation and productivity trends. *Mar. Geol.* 219, 99-108.
- Banakar, V., Oba, T., Chodankar, A.R., Kuramoto, T., Yamamoto, M., Minagawa, M., 2010. Monsoon related changes in sea surface productivity and water column denitrification in the Eastern Arabian Sea during the last glacial cycle. *Mar. Geol.* 219, 99-108.
- Banse, K., 1987. Seasonality of phytoplankton chlorophyll in the central and northern Arabian Sea. *Deep-Sea Res.* I 34, 713-723.
- Barton, A.D., Dutkiewicz, S., Flierl, G., Bragg, J., Follows, M.J., 2010. Patterns of diversity in marine phytoplankton. *Science* 327, 1509-1511.
- Baula, I.U., Azanza, R.V., Fukuyo, Y., Siringan, F.P., 2011. Dinoflagellate cyst composition, abundance and horizontal distribution in Bolinao, Pangasinan, Northern Philippines. *Harmful Algae* 11, 33-44.
- Begum, M., Sahu, B.K., Das, A.K., Vinithkumar, N.V., Kirubakaran, R., 2015. Extensive *Chaetoceros curvisetus* bloom in relation to water quality in Port Blair Bay, Andaman Islands. *Environ. Monit. Assess.* 187, 1-14.
- Bhattathiri, P., Pant, A., Sawant, S., Gauns, M., Matondkar, S., Mahanraju, R., 1996. Phytoplankton production and chlorophyll distribution in the eastern and central Arabian. *Curr. Sci.* 71, 857-862.

- Bhusan, R., Dutta, K., Somayajulu., 2001. Concentrations and burial fluxes of organic and inorganic carbon on the eastern margins of the Arabian Sea. *Mar. Geol.* 178, 95-113.
- Binder, B.J., Anderson, D.M., 1990. Biochemical composition and metabolic activity of *Scrippsiella trochoidea* (Dinophyceae) resting cysts. *J. Phycol.* 26, 289-298.
- Bockelmann, F.-D., Zonneveld, K.A., Schmidt, M., 2007. Assessing environmental control on dinoflagellate cyst distribution in surface sediments of the Benguela upwelling region (eastern South Atlantic). *Limnol. Oceanogr.* 52, 2582-2594.
- Bockstahler, K.R., Coats, D.W., 1993. Spatial and temporal aspects of mixotrophy in Chesapeake Bay dinoflagellates. *J. Euk. Microbiol.* 40, 49-60.
- Boessenkool, K.P., Gelder, M.V., Brinkhuis, H., Troelstra, S.R., 2001. Distribution of organic-walled dinoflagellate cysts in surface sediments from transects across the Polar Front offshore southeast Greenland. *J. Quat. Sci.* 16, 661-666.
- Bogus, K., Mertens, K.N., Lauwaert, J., Harding, I.C., Vrielinck, H., Zonneveld, K.A., Versteegh, G.J., 2014. Differences in the chemical composition of organic-walled dinoflagellate resting cysts from phototrophic and heterotrophic dinoflagellates. *J. Phycol.* 50, 254-266.
- Bolch, C., Blackburn, S., Cannon, J., Hallegraeff, G., 1991. The resting cyst of the red-tide dinoflagellate *Alexandrium minutum* (Dinophyceae). *Phycologia* 30, 215-219.
- Bravo, I., Anderson, D.M., 1994. The effects of temperature, growth medium and darkness on excystment and growth of the toxic dinoflagellate *Gymnodinium catenatum* from northwest Spain. *J. Plankton Res.* 16, 513-525.
- Bravo, I., Garcés, E., Diogène, J., Fraga, S., Sampedro, N., Figueroa, R.I., 2006. Resting cysts of the toxigenic dinoflagellate genus *Alexandrium* in recent sediments from the Western Mediterranean coast, including the first description of cysts of *A. kutnerae* and *A. peruvianum*. *Eur. J Phycol.* 41, 293-302.
- Bravo, I., Figueroa, R.I., 2014. Towards an ecological understanding of dinoflagellate cyst functions. *Microorganisms* 2, 11-32.
- Buchanan, J.B., 1984. Sediment analysis, In: *Methods for the study of marine benthos*, N.A. Holme & A.D. McIntyre (eds.), Oxford: Blackwell Scientific Publications,

45-65.

- Burkholder, J.M., Glibert, P.M., Skelton, H.M., 2008. Mixotrophy, a major mode of nutrition for harmful algal species in eutrophic waters. *Harmful Algae* 8, 77-93.
- Cabarcos, E., Flores, J., Singh, A., Sierro, F., 2014. Monsoonal dynamics and evolution of the primary productivity in the eastern Arabian Sea over the past 30ka. *Palaeogeogr. Palaeoclimatol. Palaeoecol.* 411, 249-256.
- Cao, Y., Zhang, Y.-J., Wang Z.-H., 2006. Effects of nitrogen and phosphorus limitation on cyst formation of *Scrippsiella trochoidea*. *Ecologic Science* 1, 004.
- Chambouvet, A., Alves-de-Souza, C., Cuff, V., Marie, D., Karpov, S., Guillou, L., 2011. Interplay between the parasite *Amoebophrya* sp. (Alveolata) and the cyst formation of the red tide dinoflagellate *Scrippsiella trochoidea*. *Protist* 162, 637-649.
- Chen, C-T.A, Tsunogai, S., 1998. Carbon and nutrients in the ocean, In: Galloway, J., Melillo, J. (eds.), *Asian change in the context of global climate change: Impact of natural and anthropogenic changes in Asia on global biogeochemical cycles*. Cambridge University Press.
- Clemens, S.C., Prell, W.L., Murray, D.W., Shimmield, G.B., Weedon. G.P., 1991. Forcing mechanisms of the Indian monsoon. *Nature* 353, 720-725.
- Colin, C., Kissel, C., Blamart, D., Turpin, L., 1998. Magnetic properties of sediments in the Bay of Bengal and the Andaman Sea: impact of rapid North Atlantic Ocean climatic events on the strength of the Indian monsoon. *Earth Planet. Sci. Lett.* 160, 623-635.
- Connell, J.H., 1978. Diversity in tropical rain forests and coral reefs. *Science* 199, 1302-1310.
- Cullen, J.L., 1981. Microfossil evidence for changing salinity patterns in the Bay of Bengal over the last 20 000 years. *Palaeogeogr. Palaeoclimatol. Palaeoecol.* 35, 315-356.
- Curry, W.B., Ostermann, D.R., Guptha, M.V.S., Ittekkot, V., 1992. Foraminiferal production and monsoonal upwelling in the Arabian Sea: evidence from sediment traps. In: Summerhayes, C.P., rell, W.L., Emies, K.C. (eds.), *Upwelling Systems:*

- Evolution Since the Early Miocene. Geological Society Special Publication, pp. 93-106.
- D'Costa, P.M., Anil, A.C., Patil, J.S., Hegde, S., D'Silva, M.S., Chourasia, M., 2008. Dinoflagellates in a mesotrophic, tropical environment influenced by monsoon. *Estuar. Coast. Shelf Sci.* 77, 77-90.
- D'Silva M.S., Anil A.C., D'Costa P. M., 2011. An overview of dinoflagellate cysts in recent sediments along the west coast of India. *Indian J. Geo-Mar. Sci.* 40, 697-709.
- D'Silva, M.S., Anil, A.C., Borole, D.V., Nath, B.N., Singhal, R.K., 2012a. Tracking the history of dinoflagellate cyst assemblages in sediments from the west coast of India. *J. Sea Res.* 73, 86-100.
- D'Silva, M.S., Anil, A.C., Naik, R.K., D'Costa, P.M., 2012b. Algal blooms: a perspective from the coasts of India. *Natural hazards* 63, 1225-1253.
- D'Silva, S.M., Anil, A.C., Savant, S.S., 2013. Dinoflagellate cyst assemblages in recent sediments of Visakhapatnam harbour, east coast of India: Influence of environmental characteristics. *Mar. Pollut. Bull.* 66, 59-72.
- Dale, B., 1983. Dinoflagellate resting cysts: 'benthic plankton', In: *Survival Strategies of the Algae*, G.A. Fryxell, (eds.) Cambridge University Press, Cambridge, 69-136.
- Dale, B., 2000. Dinoflagellate cysts as indicators of cultural eutrophication and industrial pollution in coastal sediments, In: *The Application of Microfossils to Environmental Geology*, Martin, R.E. (eds.), Kluwer Academic/Plenum Publishers, New York, 305-321.
- Dale, B., 2001a. The sedimentary records of dinoflagellate cysts: looking back into the future of phytoplankton blooms. *Sci. Mar.* 65, 257-272.
- Dale, B., 2001b. Marine dinoflagellate cysts as indicators of eutrophication and industrial pollution: A discussion. *Sci. Total Environ.* 264, 235-240.
- Dale, B., Dale, A.L., Jansen. J.F., 2002. Dinoflagellate cysts as environmental indicators in surface sediments from the Congo deep-sea fan and adjacent regions. *Palaeogeogr. Palaeoclimatol. Palaeoecol.* 185, 309-338.
- D'Costa, P.M., Anil, A.C., Patil, J.S., Hegde, S., D'Silva, M.S., Chourasia, M., 2008. Dinoflagellates in a mesotrophic, tropical environment influenced by monsoon.

- Estuar. Coast. Shelf Sci. 77, 77-90.
- De Sousa, S., Naqvi, S., Reddy, C., 1981. Distribution of nutrients in the Western Bay of Bengal. Indian J Mar Sci. 10, 327-331.
- de Vernal, A., Pedersen, T.F., 1997. Micropaleontology and palynology of core PAR87A-10: A 23,000 year record of paleoenvironmental changes in the Gulf of Alaska, northeast North Pacific. Paleocyanography 12, 821-830.
- de Vernal, A., Henry, M., Matthiessen, J., Mudie, P.J., Rochon, A., Boessenkool, K.P., Eynaud, F., Grosfjeld, K., Guiot, J., Hamel, D., 2001. Dinoflagellate cyst assemblages as tracers of sea-surface conditions in the northern North Atlantic, Arctic and sub-Arctic seas: The new 'n=677' data base and its application for quantitative paleocyanographic reconstruction. J. Quat. Sci. 16, 681-698.
- Dharani, G., Abdul Nazar, A., Kanagu, L., Venkateshwaran, P., Kumar, T., Ratnam, K., Venkatesan, R., Ravindran, M., 2004. On the recurrence of *Noctiluca scintillans* bloom in Minnie Bay, Port Blair: Impact on water quality and bioactivity of extracts. Curr. Sci. 87, 990-994.
- Dodge, J.D., 1994. Biogeography of marine armoured dinoflagellates and dinocysts in the NE Atlantic and North Sea. Rev. Palaeobot. Palynol. 84, 169-180.
- Drake, L.A., Meyer, A.E., Forsberg, R.L., Baier, R.E., Doblin, M.A., Heinemann, S., Johnson, W.P., Koch, M., Rublee, P.A., Dobbs, F.C., 2005. Potential invasion of microorganisms and pathogens via 'interior hull fouling': biofilms inside ballast-water tanks. Biol. Invasions 7, 969-982.
- Duplessy, J.C., 1982. Glacial to interglacial contrast in the northern Indian Ocean. Nature 295, 494-498.
- Eashwar, M., Nallathambi, T., Kuberaraj, K., Govindarajan, G., 2001. *Noctiluca* blooms in Port Blair Bay, Andamans. Arya 1105, 1-10.
- Elbrächter, M., Qi, Z., 1998. Aspects of *Noctiluca* (Dinophyceae) population dynamics. Physiological ecology of harmful algal blooms In: DM Anderson, AD Cembella, GM Hallegraeff (eds) Springer, Berlin, Heidelberg, 315-335.
- Elshanawanya, R., Zonneveld, K., Ibrahim, M.I., Kholeif, S.E.A., 2010. Distribution patterns of recent organic-walled dinoflagellate cysts in relation to environmental parameters in the Mediterranean Sea. Palynology 34, 233-260.

- Esper, O., Zonneveld, K.A.F., 2002. Distribution of organic-walled dinoflagellate cysts in surface sediments of the Southern Ocean (eastern Atlantic sector) between the Subtropical Front and the Weddell Gyre. *Mar. Micropaleontol.* 46, 177-208.
- Fensome, R.A., Williams, G.L., 2004. The Lentin and Williams index of fossil dinoflagellates. *AASP Foundation Contribution Series* 42, pp. 909.
- Fensome, R.A., Norris, G., Sarjeant, W., Taylor, F., Wharton, D., Williams, G., 1993. A classification of living and fossil dinoflagellates. *Micropaleontology* 7, 351
- Figueroa, R.I., Bravo, I., Garcés, E., Ramilo, I., 2006. Nuclear features and effect of nutrients on *Gymnodium catenatum* (Dinophyceae) sexual stages. *J. Phycol.* 42, 67-77.
- Figueroa, R.I., Bravo, I., Garces, E., 2008. The significance of sexual versus asexual cyst formation in the life cycle of the noxious dinoflagellate *Alexandrium peruvianum*. *Harmful Algae.* 7,653-663.
- Flynn, K.J., Mitra, A., 2009. Building the “perfect beast”: modelling mixotrophic plankton. *J. Plankton Res.* 31, 965-992.
- Fontugne, M.R., Duplessy, J.C., 1986. Variations of the monsoon regime during the upper Quaternary: evidence from carbon isotopic record of organic matter in North Indian Ocean sediment cores. *Palaeogeography, Palaeoclimatology, Palaeoecology*, 56, 69-88.
- Fraga, S., (ed) 2015. *Alexandrium* and *Pyrodinium*, in IOC-UNESCO Taxonomic Reference List of Harmful Micro Algae. Available online at <http://www.marinespecies.org/HAB>. Accessed on 2015-04-29.
- Fujii, R., Matsuoka, K., 2006. Seasonal change of dinoflagellates cyst flux collected in a sediment trap in Omura Bay, West Japan. *J. Plankton Res.* 28, 131-147.
- Fukuyo, Y., Kodama, M., Omura, T., Furuya, K., Furio, E., Cayme, M., Lim, P., Dao, V., Kotaki, Y., Matsuoka, K., 2011. Ecology and oceanography of harmful marine microalgae. In *Coastal marine science in Southeast Asia*, ed. Nishida, S., M.D. Fortes, and N. Miyazaki. Terrapub, Tokyo, 23-48. Society for the Promotion of Science: Coastal Marine Science.

- Furio, E.F., Azanza, R.V., Fukuyo, Y., Matsuoka, K., 2012. Review of geographical distribution of dinoflagellate cysts in Southeast Asian coasts. *Coast. Mar. Sci.* 35, 20-33.
- Gaines, G., Elbrächter, M., 1987. Heterotrophic nutrition. *The biology of dinoflagellates* 21, 224-268.
- Ganeshram, R.S., Pederseon, T.F., Calvert, S.E., McNeill, G.W., Fontugne, M. R., 2000. Glacial-interglacial variability in denitrification in the world's oceans: causes and consequences. *Paleoceanography* 15, 361-376.
- Gárate-Lizarraga, I., Hernandez-Orozco, M.L., Band-Schmidt, C.J., Serrano-Casillas, G., 2001. Red tides along the coasts of the Baja California Sur, México (1984 to 1999). *Oceanides* 16, 127-134.
- Gárate-Lizarraga, I., Muñetón-Gómez, M.D.S., 2008. Florecimiento de *Peridinium quinquecorne* Abé in La Ensenada de La Paz, Golfo de California (Julio 2003). *Acta Bot. Mex.* 33-47.
- Gárate-Lizarraga, I., Band-Schmidt, C.J., López-Cortés, D.J., del Socorro Muñetón-Gómez, M., 2009. Bloom of *Scrippsiella trochoidea* (Gonyaulacaceae) in a shrimp pond in the southwestern Gulf of California, Mexico. *Mar. Pollut. Bull.* 58, 145-149.
- Garcés, E., Masó, M., Camp, J., 2002. Role of temporary cysts in the population dynamics of *Alexandrium taylori* (Dinophyceae). *J. Plankton Res.* 24, 681-686.
- Garg, R., Jain, K., 1993. Occurrence of the marker dinoflagellate cyst *Apectodinium* in Narsapur Well-I, Krishna-Godavari Basin, India.
- Gauns, M., Madhupratapa, M., Ramaiaha, N., Jyothibabu, R., Fernandes, V., Paul, J.T., Prasanna Kumar, S., 2005. Comparative accounts of biological productivity characteristics and estimates of carbon fluxes in the Arabian Sea and the Bay of Bengal. *Deep-Sea Res II* 52, 2003-2017.
- GEOHAB, 2001. Global ecology and oceanography of harmful algal blooms. In: Glibert P. and G. Pitcher (eds), *Science plan*. Baltimore and Paris: SCOR and IOC. pp. 1-86.

- Gerson, V.J., Madhu, N., Jyothibabu, R., Balachandran, K., Nair, M., Revichandran, C., 2014. Oscillating environmental responses of the eastern Arabian Sea. *Indian J. Geo-Mar. Sci.* 43, 67-75.
- Giannakourou, A., Orlova, T., Assimakopoulou, G., Pagou, K., 2005. Dinoflagellate cysts in recent marine sediments from Thermaikos Gulf, Greece: Effects of resuspension events on vertical cyst distribution. *Cont. Shelf Res.* 25, 2585-2596.
- Godad, S.P., 2014. Variability of SST, Monsoon productivity and OMZ over last 40 ka in the Arabian Sea. PhD thesis, Goa University, pp. 1-110.
- Godhe, A., McQuoid, M.R., 2003. Influence of benthic and pelagic environmental factors on the distribution of dinoflagellate cysts in surface sediments along the Swedish west coast. *Aquat. Microb. Ecol.* 32, 185-201.
- Godhe, A., Karunasagar I., Karlson, B., 2000. Dinoflagellate cysts in recent marine sediments from SW India. *Bot. Mar.* 43, 39-48.
- Godhe, A., Noren, F., Kuylenstierna, M., Ekberg, C., Karlson, B., 2001. Relationship between planktonic dinoflagellate abundance, cysts recovered in sediment traps and environmental factors in the Gullmar Fjord, Sweden. *J. Plankton Res.* 23, 923-938.
- Gomes, H.R., Goes, J.I., Saino, T., 2000. Influence of physical processes and freshwater discharge on the seasonality of phytoplankton regime in the Bay of Bengal. *Cont. Shelf Res.* 20, 313-330.
- Gomez, F., 2013. Reinstatement of the dinoflagellate genus *Tripos* to replace *Neoceratium*, marine species of *Ceratium* (Dinophyceae, Alveolata). *CICIMAR Océánides* 28, 1-22.
- González, C., Dupont, L.M., Mertens, K., Wefer, G., 2008. Reconstructing marine productivity of the Cariaco Basin during marine isotope stages 3 and 4 using organic-walled dinoflagellate cysts. *Paleoceanography*, 23, 1-19
- Gottschling, M., Keupp, H., Plötner, J., Knop, R., Willems, H., Kirsch, M., 2005a. Phylogeny of calcareous dinoflagellates as inferred from ITS and ribosomal sequence data. *Mol. Phylogenet. Evol.* 36, 444-455.

- Gottschling, M., Knop, R., Plötner, J., Kirsch, M., Willems, H., Keupp, H., 2005b. A molecular phylogeny of *Scrippsiella sensu lato* (Calciadinellaceae, Dinophyta) with interpretations on morphology and distribution. *Eur. J. Phycol.* 40, 207-220.
- Govil, P., Naidu, P.D., 2011. Variations of Indian monsoon precipitation during the last 32 kyr reflected in the surface hydrography of the Western Bay of Bengal. *Quat. Sci. Rev.* 30, 3871-3879.
- Grasshoff, K., Ehrhardt, M. and Kremling, K. (1983) *Methods of seawater analysis*, Second revised and extended edition, Verlag Chemie, Weinheim.
- Gribble, K.E., Anderson, D.M., 2007. High intraindividual, intraspecific, and interspecific variability in large-subunit ribosomal DNA in the heterotrophic dinoflagellates *Protoperidinium*, *Diplopsalis*, and *Preperidinium* (Dinophyceae). *Phycologia* 46, 315-324.
- Gribble, K.E., Nolan, G., Anderson, D.M., 2007. Biodiversity, biogeography and potential trophic impact of *Protoperidinium* spp. (Dinophyceae) off the southwestern coast of Ireland. *J. Plankton Res.* 29, 931-947.
- Grzebyk, D., Berland, B., 1996. Influences of temperature, salinity and irradiance on growth of *Prorocentrum minimum* (Dinophyceae) from the Mediterranean Sea. *J. Plankton Res.* 18, 1837-1849.
- Haake, B., Ittekkot, V., Rixen, T., Ramaswamy, V., Nair, R., Curry, W., 1993. Seasonality and interannual variability of particle fluxes to the deep Arabian Sea. *Deep-Sea Res. I* 40, 1323-1344.
- Hackett, J.D., Anderson, D.M., Erdner, D.L., Bhattacharya, D., 2004. Dinoflagellates: a remarkable evolutionary experiment. *Am. J. Bot.* 91, 1523-1534.
- Hair, J.F., Anderson, R.E., Tatham, R.L., Black, W.C., 1992. *Multivariate data analysis with Readings*, MacMillan Publishing Company, New York.
- Hallegraeff, G.M., 1993. A review of harmful algal blooms and their apparent global increase. *Phycologia* 32, 79-99.
- Hansen, P.J., Miranda, L., Azanza, R., 2004. Green *Noctiluca scintillans*: a dinoflagellate with its own greenhouse. *Mar. Ecol. Prog. Ser.* 275, 79-87.
- Hansen, P.J., 2011. The role of photosynthesis and food uptake for the growth of marine mixotrophic dinoflagellates I. *J. Eukaryot. Microbiol.* 58, 203-214.

- Harland, R., Nordberg, K., Filipsson, H.L., 2006. Dinoflagellate cysts and hydrographical change in Gullmar Fjord, west coast of Sweden. *Sci. Total Environ.* 355, 204-231.
- Hart, S.P., Marshall, D.J., 2013. Environmental stress, facilitation, competition, and coexistence. *Ecology* 94, 2719-2731.
- Hasle, G., 1978. The inverted microscope method. *Phytoplankton Manual*. UNESCO, Paris 8896.
- Head, M., 1996. Modern dinoflagellate cysts and their biological affinities. In *Palynology: principles and applications 3*, In: Jansonius, J., McGregor, D.C. (eds.), 1197-1248. Dallas, TX, Association of Stratigraphic Palynologist Foundation.
- Hegde, S., 2010. Studies on phytoplankton community with reference to diatoms. PhD thesis. Goa University.
- Hegde, S., Anil, A.C., Patil, J.S., Mitbavkar, S., Krishnamurthy, V., Gopalakrishna V. V., 2008. Influence of environmental settings on the prevalence of *Trichodesmium* spp. in the Bay of Bengal. *Mar. Ecol. Prog. Ser.* 356, 93-101.
- Hesse, K.J., Tillmann, U., Nehring, S., Brockmann, U., 1996. Factors controlling phytoplankton distribution in coastal waters of the German Bight North Sea. *Biology and ecology of shallow coastal waters*. In: A. Eleftheriou, A.D. Ansell, Smith C.J. (eds.), Olsen and Olsen, Fredensborg, 11-22.
- Hessler, I., Young, M., Holzwarth, U., Mohtadi, M., Luckge, A., Behling, H., 2013. Imprint of eastern Indian Ocean surface oceanography on modern organic-walled dinoflagellate cyst assemblages. *Mar. Micropaleontol.* 101, 89-105.
- Higman, W.A., Stone, D.M., Lewis, J.M., 2001. Sequence comparisons of toxic and non-toxic *Alexandrium tamarense* (Dinophyceae) isolates from UK waters. *Phycologia* 40, 256-262.
- Hodgkiss, I., Ho, K., 1997. Are changes in N: P ratios in coastal waters the key to increased red tide blooms?, *Asia-Pacific Conference on Science and Management of Coastal Environment*. Springer, pp. 141-147.
- Holzwarth, U., Esper, O., Zonneveld, K., 2007. Distribution of organic-walled dinoflagellate cysts in shelf surface sediments of the Benguela upwelling system in relationship to environmental conditions. *Mar. Micropaleontol.* 64, 91-119.

- Hoppenrath M, M. Elbrachter, and G. Drebes. 2009. Marine phytoplankton. Selected microphytoplankton species from the North Sea around Helgoland and Sylt. E. Schweizerbart'sche Verlagsbuchhandlung, (Nagele u. Obermiller) Stuttgart.
- Horiguchi, T., Takano, Y., 2006. Serial replacement of a diatom endosymbiont in the marine dinoflagellate *Peridinium quinquecorne* (Peridiniales, Dinophyceae). *Phycol. Res.* 54, 193-200.
- Horstmann, U., 1980. Observations on the peculiar diurnal migration of a red tide dinophyceae in tropical shallow waters. *J. Phycol.* 16, 481-485.
- Hwang, C.-H, Kim, K.-Y., Lee, Y., Kim, C.-H., 2011. Spatial distribution of dinoflagellate resting cysts in Yellow Sea surface sediments. *Algae* 26, 41-50.
- IPCC, 2013: Climate Change 2013: The Physical Science Basis. Contribution of Working Group I to the Fifth Assessment Report of the Intergovernmental Panel on Climate Change. Stocker, T.F., Qin, D., Plattner, G.-K., Tignor, M., Allen, S.K., Boschung, J., Nauels, A., Xia, Y., Bex, V., Midgley, P.M. (eds.). Cambridge University Press, Cambridge, United Kingdom and New York, NY, USA, pp. 1535.
- Ishikawa, A., Taniguchi, A., 1996. Contribution of benthic cysts to the population dynamics of *Scrippsiella* spp. (Dinophyceae) in Onagawa Bay, northeast Japan. *Mar. Ecol. Prog. Ser. Oldendorf* 140, 169-178.
- Ittekkot, V., Kudrass, H.-R., Quadfasel, D., Unger, D., 2003. The Bay of Bengal-an introduction. *Deep- Sea Res. II* 50, 853-854.
- Ivanochko, T.S., 2004. Sub-orbital scale variations in the intensity of the Arabian Sea monsoon, PhD thesis, University of Edinburgh, pp. 1-229.
- Ivanochko, T.S., Ganeshram, R.S., Brummer, G. -J.A., Ganssen, G., Jung, S.J., Moreton, S.G., Kroon, D., 2005. Variations in tropical convection as an amplifier of global climate change at the millennial scale. *Earth Planet Sci. Lett.* 235, 302-314.
- Ivanova, E., Schiebel, R., Singh, A.D., Schmiedl, G., Niebler, H. S., Hemleben, C., 2003. Primary production in the Arabian Sea during the last 135000 years. *Palaeogeogr. Palaeoclimatol. Palaeoecol.* 197, 61-82.
- Jacobson, D.M., Anderson, D.M., 1989. Thecate heterotrophic dinoflagellates: feeding behavior and mechanisms. *J. Phycol.* 22, 249-258.

- Jacobson, D.M., Anderson, D.M., 1992. Ultrastructure of the feeding apparatus and myonemal system of the heterotrophic dinoflagellate *Proto-peridinium spinulosum*. J Phycol. 28, 69-82.
- Jain, K., Taugourdeau-Lantz, J., 1973. Palynology of Dalmiapuram Grey Shale, Dalmiapuram Formation, District Trichinopoly, South India-. 1. Taxonomy. Geophytology 3, 52-68.
- Jain, K., 1978. An Upper Cretaceous dinoflagellate assemblage from Vriddhachalam area, Cauvery Basin, South India. The Palaeobotanist 25, 146-160.
- Jayaraju, N., Reddy, B.S.R., Reddy, K., 2011. Anthropogenic impact on Andaman coast monitoring with benthic foraminifera, Andaman Sea, India. Environ. Earth Sci. 62, 821-829.
- Jeong, H., Latz, M.I., 1994. Growth and grazing rates of the heterotrophic dinoflagellates *Proto-peridinium* spp. on red tide dinoflagellates. Mar. Ecol. Prog.Ser.106, 173-173.
- Jeong, H.J., Yoo, Y., Park, J.Y., Song, J.Y., Kim, S.T., Lee, S.H., Kim, K.Y., Yih, W.H., 2005. Feeding by phototrophic red-tide dinoflagellates: five species newly revealed and six species previously known to be mixotrophic. Aquat. Microb. Ecol. 40, 133-150.
- Jeong, H.J., Du Yoo, Y., Kim, J.S., Seong, K.A., Kang, N.S., Kim, T.H., 2010. Growth, feeding and ecological roles of the mixotrophic and heterotrophic dinoflagellates in marine planktonic food webs. Ocean science journal 45, 65-91.
- Jha, D.K., Devi, M.P., Vidyalakshmi, R., Brindha, B., Vinithkumar, N.V., Kirubakaran, R., 2015. Water quality assessment using water quality index and geographical information system methods in the coastal waters of Andaman Sea, India. Mar. Pollut. Bull. 100, 555-561.
- John, U., Groben, R., Beszteri, B., Medlin, L., 2004. Utility of amplified fragment length polymorphisms (AFLP) to analyse genetic structures within the *Alexandrium tamarense* species complex. Protist 155, 169-179.
- Jones, R.I., 2000. Mixotrophy in planktonic protists: an overview. Freshwater Biol. 45, 219-226.
- Joyce, L.B., Pitcher, G.C., du Randt, A., Monteiro, P.M.S., 2005. Dinoflagellate cysts

- from surface sediments of Saldanha Bay, South Africa: an indication of the potential risk of harmful algal blooms. *Harmful Algae* 4, 309-318.
- Karunasagar, I., Karunasagar, I., Oshima, Y., Yasumoto, T., 1990. A toxin profile for shellfish involved in an outbreak of paralytic shellfish poisoning in India. *Toxicon* 28, 868-870.
- Kawamura, H., 2004. Dinoflagellate cyst distribution along a shelf to slope transect of an oligotrophic tropical sea (Sunda Shelf, South China Sea). *Phycol. Res.* 52, 355-375.
- Kessarkar, P.M., Rao, V.P., Naqvi, S.W.A, Chivas, A.R., Saino, T., 2010. Fluctuations in productivity and denitrification in the southeastern Arabian Sea during the Late Quaternary. *Curr. Sci.* 99, 485-491.
- Khowaja-Ateequzzaman, Garg, R., Mehrotra, N. C., 2006. A Catalogue of Dinoflagellate Cysts from India. Birbal Sahani Institute of Palaeobotany.
- Kim, Y.-O., Han, M.-S., 2000. Seasonal relationships between cyst germination and vegetative population of *Scrippsiella trochoidea* (Dinophyceae). *Mar. Ecol. Prog. Ser.* 204, 111-118.
- Kim, S.Y., Moon, C.H., Cho, H.J., Lim, D.I., 2009. Dinoflagellate Cysts in Coastal Sediments as Indicators of Eutrophication: A Case of Gwangyang Bay, South Sea of Korea. *Estuaries and Coasts* 32, 1225-1233.
- Kim, M., Nam, S.W., Shin, W., Coats, D.W., Park, M.G., 2012a. *Dinophysis caudata* (dinophyceae) sequesters and retains plastids from the mixotrophic ciliate prey mesodinium rubrum1. *J. Phycol.* 48, 569-579.
- Kim, S.-Y., Lim, D.-I., Cho, H.-J., 2012b. Dinoflagellate cyst assemblages from the northern shelf sediments of the East China Sea: An indicator of marine productivity. *Mar. Micropaleontol.* 96, 75-83.
- Kiorboe, T., Titelman, J., 1998. Feeding, prey selection and prey encounter mechanisms in the heterotrophic dinoflagellate *Noctiluca scintillans*. *J. Plankton Res.* 20, 1615-1636.
- Kirchner, M., Sahling, G., Uhlig, G., Gunkel, W., Klings, K.-W., 1996. Does the red tide-forming dinoflagellate *Noctiluca scintillans* feed on bacteria? *Sarsia* 81, 45-55.

- Kjaeret, A.H., Naustvoll, L. J., Paasche, E., 2000. Ecology of the heterotrophic dinoflagellate genus *Protoberidinium* in the inner Oslofjord (Norway). *Sarsia* 85, 453-460.
- Kleypas, J.A., McManus, J.W., Meñez, L.A., 1999. Environmental limits to coral reef development: where do we draw the line? *American Zoologist* 39, 146-159.
- Kokinos, J.P., Anderson, D.M., 1995. Morphological development of resting cysts in cultures of the marine dinoflagellate *Lingulodinium polyedrum* (= *L. machaerophorum*). *Palynology* 19, 143-166.
- Kremp, A., Anderson, D.M., 2000. Factors regulating germination of resting cysts of the spring bloom dinoflagellate *Scrippsiella hangoei* from the northern Baltic Sea. *J. Plankton Res.* 22, 1311-1327.
- Kremp, A., Parrow, M.W., 2006. Evidence for asexual resting cysts in the life cycle of the marine Peridinioid dinoflagellate, *Scrippsiella hangoei*. *J. Phycol.* 42, 400-409.
- Kremp, A., Lindholm, T., Dreßler, N., Erler, K., Gerdts, G., Eirtovaara, S., Leskinen, E., 2009. Bloom forming *Alexandrium ostenfeldii* (Dinophyceae) in shallow waters of the Åland archipelago, northern Baltic Sea. *Harmful Algae* 8, 318-328.
- Kremp, A., 2013. Diversity of dinoflagellate life cycles: facets and implications of complex strategies. *Biological and geological perspectives of dinoflagellates* 5, 197.
- Kumar, A., 1980. Fossil dinophyceae and its uses in petroleum exploration with special reference to India. *Palaeontol. Soc. India* 23, 4-15.
- Kumar, N., Yadav, B., Tyagi, A., Jaswal, A., 2012. Trend and spatial distribution of rainfall and rainy days over Andaman & Nicobar Islands. *Nat. Hazards* 63, 575-587.
- Lentin, J., Williams, G.L., 1975. Fossil dinoflagellates: index to genera and species. Supplement. *Can. J. Bot.* 53, 2147-2157.
- Lentin, J.K., Williams, G.L., 1993. Fossil dinoflagellates: index to genera and species, *Am. Assoc. of Strat. Palynol. Found. Cont. Ser.*, 28, 864.
- Lewis, J., Rochon, A., Harding, I., 1999. Preliminary observations of cyst-theca relationships in *Spiniferites ramosus* and *Spiniferites membranaceus* (Dinophyceae). *Grana* 38, 113-124.

- Lilly, E.L., Halanych, K.M., Anderson, D.M., 2007. Species boundaries and global biogeography of the *Alexandrium tamarens* complex (Dinophyceae) 1. J. Phycol. 43, 1329-1338.
- Lim, P.T., Leaw, C.P., Usup, G., Kobiyama, A., Koike, K., Ogata, T., 2006. Effects of light and temperature on growth, nitrate uptake, and toxin production of two tropical Dinoflagellates: *Alexandrium tamiyavanichii* and *Alexandrium* (Dinophyceae) 1. J. Phycol. 42, 786-799.
- Limaye, R.B., Kumaran, K., Nair, K., Padmalal, D., 2007. Non-pollen palynomorphs as potential palaeoenvironmental indicators in the Late Quaternary sediments of the west coast of India. Curr. Sci. 92, 1370.
- Limoges, A., Kieft, J.-F., Radi, T., Ruíz-Fernandez, A.C., de Vernal, A., 2010. Dinoflagellate cyst distribution in surface sediments along the south-western Mexican coast (14.76 N to 24.75 N). Mar. Micropaleontol. 76, 104-123.
- Lin, S., Zhang, H., Hou, Y., Zhuang, Y., Miranda, L., 2009. High-level diversity of dinoflagellates in the natural environment, revealed by assessment of mitochondrial *cox1* and *cob* genes for dinoflagellate DNA barcoding. App. Environ. Microb. 75, 1279-1290.
- Liu, D., Shi, Y., Di, B., Sun, Q., Wang, Y., Dong, Z., Shao, H., 2012. The impact of different pollution sources on modern dinoflagellate cysts in Sishili Bay, Yellow Sea, China. Mar. Micropaleontol. 84, 1-13.
- Lombard, E.H., Capon, B., 1971. Observations on the tidepool ecology and behaviour of *Peridinium gregarium* 1, 2. J. Phycol. 7, 188-194.
- Luckge, A., Dooze-Rolinski, H., Khan, A.A., Schulz, H., Von Rad, U., 2001. Monsoonal variability in the northeastern Arabian Sea during the past 5000 years: geochemical evidence from laminated sediments. Palaeogeogr. Palaeoclimatol. Palaeoecol. 167, 273-286.
- Lundgren, V., Granéli, E., 2011. Influence of altered light conditions and grazers on *Scrippsiella trochoidea* (Dinophyceae) cyst formation. Aquat. Microb. Ecol. 63, 231.
- Madhav, V.G., Kondalarao, B., 2004. Distribution of phytoplankton in the coastal waters of east coast of India. Indian J. Geo-Mar. Sci. 33, 262-268.

- Madhu, N., Jyothibabu, R., Maheswaran, P., Gerson, V.J., Gopalakrishnan, T., Nair, K., 2006. Lack of seasonality in phytoplankton standing stock (chlorophyll a) and production in the western Bay of Bengal. *Cont. Shelf Res.* 26, 1868-1883.
- Madhupratap, M., Prasanna Kumar, S., Bhattathiri, P., Kumar, M.D., Raghukumar, S., Nair, K., Ramaiah, N., 1996. Mechanism of the biological response to winter cooling in the northeastern Arabian Sea. *Nature* 384, 549-552.
- Madhupratap, M., Gauns, M., Ramaiah, N., Kumar, S.P., Muraleedharan, P., De Sousa, S., Sardesai, S., Muraleedharan, U., 2003. Biogeochemistry of the Bay of Bengal: physical, chemical and primary productivity characteristics of the central and western Bay of Bengal during summer monsoon 2001. *Deep- Sea Res. II* 50, 881-896.
- Maestre, F.T., Callaway, R.M., Valladares, F., Lortie, C.J., 2009. Refining the stress-gradient hypothesis for competition and facilitation in plant communities. *J. Ecol.* 97, 199-205.
- Marret, F., de Vernal, A., McDonald, D., Pederson, T., 2001. Middle Pleistocene to Holocene palynostratigraphy of ODP Site 887 in the Gulf of Alaska, northeast North Pacific. *Can. J Earth Sci.* 38, 373-386.
- Marret, F., Zonneveld, K.A., 2003. Atlas of modern organic-walled dinoflagellate cyst distribution. *Rev. Palaeobot. Palyno.* 125, 1-200.
- Matsuoka, K., Fukuyo, Y., 2000. Technical Guide for Modern Dinoflagellate Cyst Study. WESTPAC-HAB/WESTPAC/IOC, Japan Society for the Promotion of Science, Japan, 1-29
- Matsuoka, K., Joyce, L.B., Kotani, Y., Matsuyama, Y., 2003. Modern dinoflagellate cysts in hypertrophic coastal waters of Tokyo Bay, Japan. *J. Plankton Res.* 25, 1461-1470.
- Matthiessen, J., de Vernal, A., Head, M., Okolodkov, Y., Zonneveld, K.A.F., Harland, R., 2005. Modern organic-walled dinoflagellate cysts in arctic marine environments and their (paleo-) environmental significance. *Palaontologische Zeitschrift* 79, 3-51.
- McCauley, L.A., Erdner, D.L., Nagai, S., Richlen, M.L., Anderson, D.M., 2009. Biogeographic analysis of the globally distributed harmful algal bloom species

- Alexandrium minutum* (Dinophyceae) based on rRNA gene sequences and microsatellite markers. J. Phycol. 45, 454-463.
- McMinn, A., 1990. Recent dinoflagellate cyst distribution in eastern Australia. Rev. Palaeobot. Palyno. 65, 305-310.
- Mehrotra, N.C., Sarjeant, W.A., 1984a. *Dingodinium*, a dinoflagellate cyst genus exhibiting variation in archeopyle character. Micropaleontology 292-305.
- Mehrotra, N.C., Sarjeant, W.A., 1984b. The dinoflagellate cyst genus *Polygonifera*; emendation and taxonomic stabilization. J. Micropalaeontol. 3, 43-53.
- Mehrotra, N.C., Sarjeant, W.A., 1986. Early to Middle Cretaceous dinoflagellate cysts from the Periyavadavadi Shallow well-1, Cauvery basin, India. Geobios 19, 705-753.
- Mehrotra, N.C. and Sarjeant, W.A.S., 1987. Late Cretaceous to early Tertiary dinoflagellate cysts from Narasapur well-1, Godavari-Krishna Basin, South India. Geobios, 20, 149-191.
- Mehrotra, N., Sarjeant, W., 1990. Late Triassic palynomorphs from the Andaman Island: A reply to A. Kumar. Mod. Geol. 14, 255-264.
- Mehrotra, N.C., Sarjeant, W.A., 1998. Late Cretaceous to Early Tertiary dinoflagellate cysts from the Krishna-Godavari basin-cyst morphology and review of biostratigraphical dating. The Palaeobotanist 47, 50-59.
- Mehrotra, N., Aswal, H., 2003. Atlas of dinoflagellate cysts from Mesozoic-Tertiary sediments of Krishna-Godavari Basin. Volume-I: Late Jurassic-Cretaceous dinoflagellate cysts, Palaeontographica Indica, 1-145.
- Mehrotra, N., Singh, K., 2003. Atlas of Dinoflagellate Cysts from Mesozoic-Tertiary Sediments of Krishnagodavari Basin Volume II: Tertiary Dinoflagellate Cysts. Publication Division, KDM Institute of Petroleum Exploration Oil and Natural Gas Corporation Limited.
- Mehrotra, N.C., Venkatachala, B.S. and Kapoor, P.N., 2005. Palynology in hydrocarbon exploration. Part II: Spatial and temporal distribution of significant spores/pollen and dinoflagellate cyst taxa from the Mesozoic-Tertiary sediments. Geol. Soc. India Mem., no. 61, p. 1-128.

- Mehrotra, N., Shanmukhappa, M., Babu, R., Kumar, M., Singh A., Singh, B., Kapoor, P., 2012. Development of Palynology in Fossil Fuel Exploration in India with Emphasis on Recent Significant Contributions from Western-Offshore, Krishna-Godavari Basin and Frontier Areas, Proc Indian natn Sci Acad, pp. 457-473.
- Menden-Deuer, S., Lessard, E.J., Satterberg, J., Grünbaum, D., 2005. Growth rates and starvation survival of three species of the pallium-feeding, thecate dinoflagellate genus *Protoperidinium*. Aquat. Microb. Ecol. 41, 145-152.
- Mertens, K. N., Wolny, J., Carbonell-Moore, C., Bogus, K., Ellegaard, M., Limoges, A., de Vernal, A. Gurdebeke, P., Omura, T., Al-Muftah, A., Matsuoka, K., 2015. Taxonomic re-examination of the toxic armored dinoflagellate *Pyrodinium bahamense* Plate 1906: Can morphology or LSU sequencing separate *P. bahamense* var. *compressum* from var. *bahamense*? Harmful Algae. 41, 1-24.
- Minnhagen, S., Janson, S., 2006. Genetic analyses of *Dinophysis* spp. support kleptoplastidy. FEMS microbial. Ecol. 57, 47-54.
- Mitbavkar, S., Anil, A.C., 2011. Tiniest primary producers in the marine environment: an appraisal from the context of waters around India. Curr. Sci. 100, 986-988.
- Mitbavkar, S., Rajaneesh, K., Anil, A., Sundar, D., 2012. Picophytoplankton community in a tropical estuary: detection of *Prochlorococcus*-like populations. Estuar. Coast. Shelf S. 107, 159-164.
- Mitra, A., Flynn, K.J., Burkholder, J., Berge, T., Calbet, A., Raven, J.A., Granéli, E., Glibert, P.M., Hansen, P.J., Stoecker, D.K., 2014. The role of mixotrophic protists in the biological carbon pump. Biogeosciences 11, 995-1005.
- Moestrup O., Akselmann R., Fraga S., Hansen G., Hoppenrath M., Iwataki M., Komarek J., Larsen J., Lundholm N., Zingone A. (eds.), 2009 onwards. IOC-UNESCO Taxonomic Reference List of Harmful Micro Algae. Accessed at <http://www.marinespecies.org/hab> on 2015-04-29.
- Moestrup, Ø., Lindberg, K., Daugbjerg, N., 2009. Studies on woloszynskioid dinoflagellates IV: The genus *Biecheleria* gen. nov. Phycol. Res. 57, 203-220.
- Monterey, G.I., Levitus. S., 1997. Seasonal variability of mixed layer depth for the world ocean. NOAA atlas NESDIS 14. US Government Printing office, Washington, D.C. pp. 96.

- Montresor, M., Sgroso, S., Procaccini, G., Kooistra, W.H., 2003. Intraspecific diversity in *Scrippsiella trochoidea* (Dinophyceae): evidence for cryptic species. *Phycologia* 42, 56-70.
- Montresor, M., Zingone, A., Sarno, D., 1998. Dinoflagellate cyst production at a coastal Mediterranean site. *J. Plankton Res.* 20, 2291-2312.
- Morquecho, L., Lechuga-Deveze, C.H., 2004. Seasonal occurrence of planktonic dinoflagellates and cyst production in relationship to environmental variables in subtropical Bahia Concepcion, Gulf of California. *Bot. Mar.* 47, 313-322.
- Morquecho, L., Gongora-González, D.T., Okolodkov, Y.B., 2009. Cyst- theca relationships of *Gonyaulacales* and *Peridinales* (Dinophyceae) from Bahia concepcion, Gulf of California. *Acta Bot. Mex.* 88, 9-29.
- Morrison, J., Codispoti, L., Gaurin, S., Jones, B., Manghnani, V., Zheng, Z., 1998. Seasonal variation of hydrographic and nutrient fields during the US JGOFS Arabian Sea Process Study. *Deep-Sea Res. II* 45, 2053-2101.
- Morton, S.L., Shuler, A., Paternoster, J., Fanolua, S., Vargo, D., 2011. Coastal eutrophication, land use changes and *Ceratium furca* (Dinophyceae) blooms in Pago Pago Harbor, American Samoa 2007-2009. *Chin. J. Oceanol. Limn.* 29, 790-794.
- Moscatello, S., Rubino, F., Saracino, O.D., Fanelli, G., Belmonte, G., Boero, F., 2004. Plankton biodiversity around the Salento Peninsula (South East Italy): an integrated water/sediment approach. *Sci. Mar.* 68, 85-102.
- Mudie, P.J., Harland, R., 1996. Aquatic quaternary. *Palynology: principles and applications*, 2, 843-877.
- Mudie, P.J., Rochon, A., Aksu, A.E., Gillespie, H., 2002. Dinoflagellate cysts, freshwater algae and fungal spores as salinity indicators in Late Quaternary cores from Marmara and Black seas. *Mar. Geol.* 190, 203-231.
- Murray, D.W., Prell, W.L., 1992. Late Pliocene and Pleistocene oscillations and monsoon upwelling recorded in sediments from the Owen Ridge, northwestern Arabian Sea. In: Summerhayes, C.P., Prell, W.L., Emies, K.C. (eds.), *Upwelling Systems: Evolution Since the Early Miocene*. Geological Society Special Publication 64, pp 301-321.

- Murty, M.R., Shrivastava. P., 1979. Clay minerals in the shelf sediments of the northwestern part of the Bay of Bengal. *Mar Geol.* 33, M21-M32.
- Musale, A.S., Desai, D.V., 2010. Distribution and abundance of macrobenthic polychaetes along the South Indian coast. *Environ. Monit. Assess.* 178, 423-436.
- Nagai, S., Nitshitani, G., Tomaru, Y., Sakiyama, S., Kamiyama, T., 2008. Predation by the toxic dinoflagellate *Dinophysis fortii* on the ciliate *Myrionecta rubra* and observation of sequestration of ciliate chloroplasts. *J. Phycol.* 44, 909-922.
- Naidu, P.D., 1991. Glacial to interglacial contrasts in the calcium carbonate content and influence of Indus discharge in two eastern Arabian Sea cores. *Palaeogeogr. Palaeoclimatol. Palaeoecol.* 86, 255-263.
- Naidu, P.D., Malmgren, B.A., Bornmalm, L., 1993. Quaternary history of calcium carbonate fluctuations in the western equatorial Indian Ocean (Somali Basin). *Palaeogeogr. Palaeoclimatol. Palaeoecol.* 103, 21-30.
- Naidu, P.D., Malmgren, B.A., 1996. A high-resolution record of late Quaternary upwelling along the Oman Margin, Arabian Sea based on planktonic foraminifera. *Paleoceanography* 11, 129-140.
- Naidu, P.D., Malmgren, B.A., 1999. Quaternary carbonate record from the equatorial Indian Ocean and its relationship with productivity changes. *Mar. Geol.* 161, 49-62.
- Naidu, P.D., Govil, P., 2010. New evidence on the sequence of deglacial warming in the tropical Indian Ocean. *J Quaternary Sci.* 25, 1138-1143.
- Naidu, P.D., Singh, A.D., Ganeshram, R., Bharti, S.K., 2014. Abrupt climate-induced changes in carbonate burial in the Arabian Sea: Causes and consequences. *Geochem. Geophys. Geosy.* 15, 1398-1406.
- Naik, R.K., 2010. Studies on phytoplankton with reference to dinoflagellates. Ph.D. Thesis, University of Goa, 1-145.
- Naik, R.K., Hegde, S., Anil, A.C., 2011. Dinoflagellate community structure from the stratified environment of the Bay of Bengal, with special emphasis on harmful algal bloom species. *Environ. Monit. Assess.* 182, 15-30.

- Nair, R.R., Ittekot, V., Manganini, S.J., Ramaswamy, V., Haake, B., Degens, E.T., Desai, B.N., Honjo, S., 1989. Increased particle fluxes to the oceans related to the monsoons. *Nature* 338, 749-751.
- Narvekar, J., Prasanna Kumar, S., 2014. Mixed layer variability and chlorophyll a biomass in the Bay of Bengal. *Biogeosciences* 11, 3819-3843.
- Naustvoll, L.-J., 2000. Prey size spectra and food preferences in thecate heterotrophic dinoflagellates. *Phycologia*. 39, 187-198.
- Nehring, S., 1997. Dinoflagellate resting cysts from recent German coastal sediments. *Bot. Mar.* 40, 307-324.
- Nishitani, G., Nagai, S., Sakiyama, S., Kamiyama, T., 2008. Successful cultivation of the toxic dinoflagellate *Dinophysis caudata* (Dinophyceae). *Plankton and Benthos Research* 3, 78-85.
- Okolodkov, Y.B., 2005. *Protoperidinium* Bergh (Dinoflagellata) in the southeastern Mexican Pacific Ocean: part I. *Bot. Mar.* 48, 284-296.
- Okolodkov, Y.B., Campos-Bautista, G., Gárate-Lizárraga, I., González-González, J.A.G., Hoppenrath, M., Arenas, V., 2007. Seasonal changes of benthic and epiphytic dinoflagellates in the Veracruz reef zone, Gulf of Mexico. *Aquat. Microb. Ecol.* 47, 223.
- Onda, D.F.L., Lluisma, A.O., Azanza, R.V., 2014. Development, morphological characteristics and viability of temporary cysts of *Pyrodinium bahamense* var. *compressum* (Dinophyceae) in vitro. *Eur. J. Phycol.* 49, 265-275.
- Orlova, T.Y., Morozova, T.V., Gribble, K.E., Kulis, D.M., Anderson, D.M., 2004. Dinoflagellate cysts in recent marine sediments from the east coast of Russia. *Bot. Mar.* 47, 184-201.
- Oshima, Y., Bolch, C.J., Hallegraeff, G.M., 1992. Toxin composition of resting cysts of *Alexandrium tamarense* (Dinophyceae). *Toxicon* 30, 1539-1544.
- Park, M.G., Park, J.S., Kim, M., Yih, W., 2008. Plastid dynamics during survival of *Dinophysis caudata* without its ciliate prey. *J. Phycol.* 44, 1154-1163.
- Patil, J.S., 2003. Studies on ecology of diatoms. Ph.D. Thesis, University of Goa.
- Patil, J.S., Anil, A.C., 2008. Temporal variation of diatom benthic propagules in a monsoon-influenced tropical estuary. *Continental Shelf Research* 28, 2404-2416.

- Patil, J.S., Anil, A.C., 2011. Variations in phytoplankton community in a monsoon-influenced tropical estuary. *Environ. Monit. Assess.* 182, 291-300.
- Pattan, J.N., Masuzawa, T., Naidu, P.D., Parthiban, G., Yamamoto, M., 2003. Productivity fluctuations in the southeastern Arabian Sea during the last 140 ka. *Palaeogeogr. Palaeoclimatol. Palaeoecol.* 193, 575-590.
- Pattan, J.N., Mir, I.A., Parthiban, G., Karapurkar, S.G., Matta, V.M., Naidu, P.D., Naqvi, S.W.A., 2013. Coupling between suboxic condition in sediments of the western Bay of Bengal and southwest monsoon intensification: A geochemical study. *Chemical Geology*, 343, 55-66.
- Paul, J.T., Ramaiah, N., Sardesai, S., 2008. Nutrient regimes and their effect on distribution of phytoplankton in the Bay of Bengal. *Mar. Environ. Res.* 66, 337-344.
- Persons, T., Maita, Y., Lalli, C., 1984. A manual of chemical and biological methods for seawater analysis. Pergamon Press, Oxford, 173p.
- Persson, A., Rosenberg, R., 2003. Impact of grazing and bioturbation of marine benthic deposit feeders on dinoflagellate cysts. *Harmful Algae* 2 43-50.
- Pfiester, L. A., and D. M. Anderson. 1987. Dinoflagellate reproduction, In: Taylor, F.J.R. (ed.), *The Biology of Dinoflagellates*. Botanical Monographs, Blackwell Scientific Publications.
- Phillips, S.C., Johnson, J.E., Giosan, L., Rose, K., 2014. Monsoon-influenced variation in productivity and lithogenic sediment flux since 110 ka in the offshore Mahanadi Basin, northern Bay of Bengal. *Marine and Petroleum Geology*, 58, 502-525.
- Ponton, C., Giosan, L., Eglinton, T.I., Fuller, D.Q., Johnson, J.E., Kumar, P. and Collett, T.S., 2012. Holocene aridification of India. *Geophysical Research Letters*, 39, 3.
- Pospelova, V., Pedersen, T.F., de Vernal, A., 2006. Dinoflagellate cysts as indicators of climatic and oceanographic changes during the past 40 kyr in the Santa Barbara Basin, southern California. *Paleoceanography*. 21, 1-16.
- Pospelova, V., de Vernal, A., Pedersen, T.F., 2008. Distribution of dinoflagellate cysts in surface sediments from the northeastern Pacific Ocean (43-25 N) in relation to

- sea-surface temperature, salinity, productivity and coastal upwelling. *Mar. Micropaleontol.* 68, 21-48.
- Pospelova, V., Kim, S. J., 2010. Dinoflagellate cysts in recent estuarine sediments from aquaculture sites of southern South Korea. *Mar. Micropaleontol.*, 76, 37-51.
- Prasanna Kumar, S., Madhupratap, M., Kumar, M.D., Gauns, M., Muraleedharan, P., Sarma, V., De Souza, S., 2000. Physical control of primary productivity on a seasonal scale in central and eastern Arabian Sea. *J. Earth Syst. Sci.* 109, 433-441.
- Prasanna Kumar, S., Muraleedharan, P., Prasad, T., Gauns, M., Ramaiah, N., De Souza, S., Sardesai, S., Madhupratap, M., 2002. Why is the Bay of Bengal less productive during summer monsoon compared to the Arabian Sea? *Geophys. Res. Lett.* 29, 88.81-88.84.
- Prasanna Kumar, S., Narvekar, J., Nuncio, M., Kumar, A., Ramaiah, N., Sardesai, S., Gauns, M., Fernandes, V., Paul, J., 2010. Is the biological productivity in the Bay of Bengal light limited? *Curr. Sci.* 98, 1331-1339.
- Prauss, M., 2002. Recent global warming and its influence on marine palynology within the central Santa Barbara Basin, offshore southern California, U.S.A. *Palynology* 26, 217-238.
- Prell, W.L., Hutson, W.H., Williams, D.F., Bé, A.W., Geitzenauer, K., Molfino, B., 1980. Surface circulation of the Indian Ocean during the last glacial maximum, approximately 18,000 yr BP. *Quaternary Research*, 14, 309-336.
- Prell, W.L., Murray, D. W., Clemens, S. C., Anderson, D. M., 1992. Evolution and Variability of the Indian Ocean Summer Monsoon: Evidence from Western Arabian Sea Drilling program. *Geophysical Monograph* 70, pp.447-469.
- Prézelin, B., Samuelsson, G., Matlick, H., 1986. Photosystem II photoinhibition and altered kinetics of photosynthesis during nutrient-dependent high-light photoadaptation in *Gonyaulax polyedra*. *Mar. Biol.* 93, 1-12.
- Price, A.M., Mertens, K.N., Pospelova, V., Pedersen, T.F., Ganeshram, R.S., 2013. Late Quaternary climatic and oceanographic changes in the Northeast Pacific as recorded by dinoflagellate cysts from Guaymas Basin, Gulf of California (Mexico). *Paleoceanography* 28, 200-212.

- Qasim, S., 1977. Biological productivity of the Indian Ocean. *Indian J Mar. Sci.* 6, 122-137.
- Qi, Y., Chen, J., Wang, Z., Xu, N., Wang, Y., Shen, P., Lu, S., Hodgkiss, I., 2004. Some observations on harmful algal bloom (HAB) events along the coast of Guangdong, southern China in 1998. *Hydrobiologia* 512, 209-214.
- Radhakrishna, K., Bhattathiri, P., Devassy. V., 1978. Primary productivity of the Bay of Bengal during August-September 1976. *Indian J Mar. Sci.*7, 94-98.
- Radi, T., de Vernal. A., 2008. Dinocysts as proxy of primary productivity in mid-high latitudes of the Northern Hemisphere. *Mar. Micropaleontol.* 68, 84-114.
- Radi, T., Bonnet, S., Cormier, M.-A., de Vernal, A., Durantou, L., Faubert, E., Head, M.J., Henry, M., Pospelova, V., Rochon. A., 2013. Operational taxonomy and (paleo-) autecology of round, brown, spiny dinoflagellate cysts from the Quaternary of high northern latitudes. *Mar. Micropaleontol.* 98, 41-57.
- Raffaelli, D., Bell, E., Weithoff, G., Matsumoto, A., Cruz-Motta, J.J., Kershaw, P., Parker, R., Parry, D., Jones, M., 2003. The ups and downs of benthic ecology: Considerations of scale, heterogeneity and surveillance for benthic-pelagic coupling. *Journal of Experimental Marine Biology and Ecology* 285, 191-203.
- Rajaneesh, K., Mitbavkar, S., Anil, A., Sawant, S., 2015. *Synechococcus* as an indicator of trophic status in the Cochin backwaters, west coast of India. *Ecol. Indic.* 55, 118-130.
- Ram, S., Murthy, T., Reghunath, R., Raghavan, B., 1996. First report of fossil Dinoflagellates from the West coast of India and some observations. *Curr. Sci.* 70, 935-939.
- Rao, V.P., Reddy, N.P., Rao C. M., 1988. Clay mineral distribution in the shelf sediments off the northern part of the east coast of India. *Cont. Shelf Res.* 8, 145-151.
- Rashid, H., England, E., Thompson, L., Polyak, L., 2011. Late glacial to Holocene Indian summer monsoon variability based upon sediment. *Terr. Atmos. Ocean. Sci.* 22, 215-228.
- Raven, J., 1997. Phagotrophy in phototrophs. *Limnology and oceanography* 42, 198-205.

- Reguera, B. and González-Gil, S., 2001. Small cell and intermediate cell formation in species of *Dinophysis* (Dinophyceae, Dinophysiales). *Journal of Phycology*, 37, 318-333.
- Reichart, G.-J., Lourens, L., Zachariasse, W., 1998. Temporal variability in the northern Arabian Sea Oxygen Minimum Zone (OMZ) during the last 225,000 years. *Paleoceanography* 13, 607-621.
- Reichart, G.-J., Brinkhuis, H., 2003. Late Quaternary *Protoperidinium* cysts as indicators of paleoproductivity in the northern Arabian Sea. *Mar. Micropaleontol.* 49, 303-315.
- Ribeiro, S., Berge, T., Lundholm, N., Andersen, T.J., Abrantes, F., Ellegaard, M., 2011. Phytoplankton growth after a century of dormancy illuminates past resilience to catastrophic darkness. *Nat. Commun.* 2, 311.
- Rintala, J.-M., Spilling, K., Blomster, J., 2007. Temporary cyst enables long-term dark survival of *Scrippsiella hangoei* (Dinophyceae). *Mar. Biol.* 152, 57-62.
- Rochon, A., de Vernal, A., Turon, J.L., Matthiessen, J., Head, J., 1999. Distribution of recent dinoflagellate cysts in surface sediments from the North Atlantic Ocean and adjacent seas in relation to sea surface parameters. *American Association of Stratigraphic Palynologists Ser.* 35. 150 pp.
- Rochon, A., Lewis, J., Ellegaard, M., Harding, I.C., 2009. The *Gonyaulax spinifera* (Dinophyceae) “complex”: Perpetuating the paradox? *Review Palaeobot. Palyno.* 155, 52-60.
- Rostek, F., Bard, E., Beaufort, L., Sonzogni, C., Ganssen, G., 1997. Sea surface temperature and productivity records for the past 240 kyr in the Arabian Sea. *Deep Sea Res. II* 44, 1461-1480.
- Saburova, M., Al-Yamani, F., Polikarpov, I., 2008. Biodiversity of free-living flagellates in Kuwait’s intertidal sediments, Environment, biodiversity and conservation in the Middle East. *Proceedings of the first Middle Eastern Biodiversity Congress, Aqaba, Jordan*, pp. 20-23.
- Sachithanandam, V., Mohan, P., Karthik, R., Elangovan, S.S., Padmavathi, G., 2013. Climate changes influence the phytoplankton bloom (Prymnesiophyceae:

- Phaeocystis* spp.) in North Andaman coastal region. Indian Journal of Geo-Marine Sciences 42, 58-66.
- Sahraoui, I., Bouchouicha, D., Mabrouk, H.H., Hlaili, A.S., 2013. Driving factors of the potentially toxic and harmful species of *Prorocentrum* Ehrenberg in a semi-enclosed Mediterranean lagoon (Tunisia, SW Mediterranean). Mediterranean Marine Science 14, 353-362.
- Sahu, B.K., Begum, M., Khadanga, M., Jha, D.K., Vinithkumar, N., Kirubakaran, R., 2013. Evaluation of significant sources influencing the variation of physico-chemical parameters in Port Blair Bay, South Andaman, India by using multivariate statistics. Mar. Pollut. Bull. 66, 246-251.
- Sahu, B.K., Begum, M., Kumarasamy, P., Vinithkumar, N., Kirubakaran, R., 2014. Dominance of *Trichodesmium* and associated biological and physico-chemical parameters in coastal waters of Port Blair, South Andaman Island. Indian J. Geo-Mar. Sci. 43, 1-7.
- Sarai, C., Yamaguchi, A., Kawami, H., Matsuoka, K., 2013. Two new species formally attributed to *Protoperidinium oblongum* (Aurivillius) Park et Dodge (Peridinales, Dinophyceae): evidence from cyst incubation experiments. Rev. Palaeobot. Palyno. 192, 103-118.
- Sardessai, S., Ramaiah, N., Prasanna Kumar, S., De Sousa, S., 2007. Influence of environmental forcings on the seasonality of dissolved oxygen and nutrients in the Bay of Bengal. J Mar. Res. 65, 301-316.
- Sarjeant, W.A., Lacalli, T., Gaines, G., 1987. The cysts and skeletal elements of dinoflagellates: speculations on the ecological causes for their morphology and development. Micropaleontology, 1-36.
- Sarkar, A., Ramesh, R., Somayajulu, B., Agnihotri, R., Jull, A., Burr, G., 2000. High resolution Holocene monsoon record from the eastern Arabian Sea. Earth Planet. Sci. Lett. 177, 209-218.
- Sarma, V., Krishna, M., Viswanadham, R., Rao, G., Rao, V., Sridevi, B., Kumar, B., Prasad, V., Subbaiah, C.V., Acharyya, T., 2013. Intensified oxygen minimum zone on the western shelf of Bay of Bengal during summer monsoon: influence of river discharge. J Oceanogr. 69, 45-55.

- Satta, C.T., Angles, S., Garce, E., Lugli, A., Padedda, B.M., Sechi, N., 2010. Dinoflagellate cysts in recent sediments from two semi-enclosed areas of the Western Mediterranean Sea subject to high human impact. *Deep-Sea Res. II* 57, 256-267.
- Satta, C.T., Anglès, S., Lugliè, A., Guillén, J., Sechi, N., Camp, J., Garcés, E., 2013. Studies on dinoflagellate cyst assemblages in two estuarine Mediterranean bays: A useful tool for the discovery and mapping of harmful algal species. *Harmful Algae* 24, 65-79.
- Scheffer, M., Van Nes, E.H., Holmgren, M., Hughes, T., 2008. Pulse-driven loss of top-down control: the critical-rate hypothesis. *Ecosystems* 11, 226-237.
- Schlitzer, R., 2008. Ocean Data View. <http://odv.awi.de>.
- Schmitt, R.W., 2008. Salinity and the global water cycle. *Oceanography* 21, 12-19.
- Schnepf, E., Deichgräber, G., 1984. "Myzocytosis", a kind of endocytosis with implications to compartmentation in endosymbiosis. *Naturwissenschaften* 71, 218-219.
- Schnepf, E., and M. Elbrachter. 1992. Nutritional strategies in dinoflagellates: a review with emphasis on cell biological aspects. *Eur. J Protistol.* 28: 3-24.
- Schott, F.A., Xie, S.P., McCreary, J.P., 2009. Indian Ocean circulation and climate variability. *Rev. Geophys.* 47.
- Schwinghamer, P., Hawryluk, M., Powell, C., MacKenzie, C., 1994. Resuspended hypnozygotes of *Alexandrium fundyense* associated with winter occurrence of PSP in inshore Newfoundland waters. *Aquaculture* 122, 171-179.
- Sgrosso, S., Esposito, F., Montresor, M., 2001. Temperature and daylength regulate encystment in calcareous cyst-forming dinoflagellates. *Mar. Ecol. Prog. Ser.* 211, 77-87.
- Shankar, D., Vinayachandran, P., Unnikrishnan, A., 2002. The monsoon currents in the north Indian Ocean. *Prog. Oceanogr.* 52, 63-120.
- Shaozhi, M., Harland, R., 1993. Quaternary organic-walled dinoflagellate cysts from the south China Sea and their paleoclimatic significance. *Palynology* 17, 47-65.

- Shea, K., Roxburgh, S.H., Rauschert, E.S., 2004. Moving from pattern to process: coexistence mechanisms under intermediate disturbance regimes. *Ecol. Lett.* 7, 491-508.
- Shenoi, S., Shankar, D., Shetye, S., 2002. Differences in heat budgets of the near-surface Arabian Sea and Bay of Bengal: Implications for the summer monsoon. *J. Geophys. Res.: Oceans (1978-2012)* 107, 5-1-5-14.
- Shetye, S.R., Shenoi, S.S.C., Antony, M., Kumar, V.K., 1985. Monthly-mean wind stress along the coast of the north Indian Ocean. *Proceedings of the Indian Academy of Sciences-Earth and Planetary Sciences* 94, 129-137.
- Shetye, S., Shenoi, S., Gouveia, A., Michael, G., Sundar, D., Nampoothiri, G., 1991. Wind-driven coastal upwelling along the western boundary of the Bay of Bengal during the southwest monsoon. *Cont. Shelf Res.* 11, 1397-1408.
- Shetye, S., Gouveia, A., Shenoi, S., Sundar, D., Michael, G., Nampoothiri, G., 1993. The western boundary current of the seasonal subtropical gyre in the Bay of Bengal. *J. Geophys. Res.* 98, 945-954.
- Shetye, S.S., Sudhakar, M., Mohan, R., Jena, B., 2014. Contrasting productivity and redox potential in Arabian Sea and Bay of Bengal. *J Earth Sci.* 25, 366-370.
- Shimmiel, G.B., Mowbray, S.R., Weedon, G.P., 1990. A 350 ka history of the Indian southwest monsoon - evidence from deep sea cores, northwest Arabian Sea. *Transactions of the Royal Society of. Edinburgh: Earth Sciences* 81, 289-299.
- Shin, H.H., Yoon, Y.H., Matsuoka, K., 2007. Modern dinoflagellate cysts distribution off the eastern part of Geoje Island Korea. *Ocean Sci. J.* 42, 31-39.
- Shipe, R., Leinweber, A., Gruber, N., 2008. Abiotic controls of potentially harmful algal blooms in Santa Monica Bay, California. *Cont. Shelf Res.* 28, 2584-2593.
- Singh, A.D., Kroon, D., Ganeshram, R., 2006. Millennial scale variations in productivity and OMZ intensity in the eastern Arabian Sea. *J. Geol. Soc. India* 68, 369-377.
- Singh, A.D., Jung, S.J., Darling, K., Ganeshram, R., Ivanochko, T., Kroon, D., 2011. Productivity collapses in the Arabian Sea during glacial cold phases. *Paleoceanography* 26, PA3210.
- Sirocko, F., Sarnthein, M., 1989. Wind-borne deposits in the Northwestern Indian Ocean: record of Holocene sediments versus modern satellite data. In: Leinen, M.,

- Sarnthein, M. (eds.), Paleoclimatology and Paleometeorology: Modern and Past Patterns of Global Atmospheric Transport. NATO, ASI ser. C, 282 Kluwer, Dordrecht, pp. 401-433.
- Smalley, G.W., Coats, D.W., 2002. Ecology of the Red-Tide Dinoflagellate *Ceratium furca*: Distribution, Mixotrophy, and Grazing Impact on Ciliate Populations of Chesapeake Bay. *J. Eukaryot. Microbiol.* 49, 63-73.
- Smalley, G.W., Coats, D.W., Stoecker, D.K., 2003. Feeding in the mixotrophic dinoflagellate *Ceratium furca* is influenced by intracellular nutrient concentrations. *Mar Ecol- Prog. Ser.* 262, 137-151.
- Smayda, T.J., 1997. Harmful algal blooms: their ecophysiology and general relevance to phytoplankton blooms in the sea. *Limnol. Oceanogr.* 42, 1137-1153.
- Smayda, T.J., 2002. Turbulence, watermass stratification and harmful algal blooms: an alternative view and frontal zones as “pelagic seed banks”. *Harmful Algae* 1, 95-112.
- Smayda, T.J., Reynolds, C.S., 2003. Strategies of marine dinoflagellate survival and some rules of assembly. *J. Sea Res.* 49, 95-106.
- Solar Radiation Hand Book (2008) by Solar Energy Centre, MNRE and Indian Meteorological Department, Pune, 1-80.
- Solar radiation over India, 2009. Tyagi, A.P., Bhatia, R.C., Vashistha, R.D., Gupta, M.K., Tripathi, T.C., Bandyopadhyay, B., Sastry, O.S., Ashvini Kumar, Desikan, V. (eds.) by Indian Meteorological Department, Ministry of Earth Sciences, New Delhi, 1-4179.
- Solignac, S., Grosfeld, K., Giraudeau, J., de Vernal, A., 2009. Distribution of recent dinocyst assemblages in the western Barents Sea. *Norw. J. Geol.* 89, 109-119.
- Sommer, U., 1995. An experimental test of the intermediate disturbance hypothesis using cultures of marine phytoplankton. *Limnol. Oceanogr.* 40, 1271-1277.
- Sonneman, J.A., Hill, D.R.A., 1997. A taxonomic survey of cyst-producing dinoflagellates from recent sediments of Victorian coastal waters, Australia. *Bot. Mar.* 40, 149-177.
- Sournia, A., 1995. Red tide and toxic marine phytoplankton of the world ocean: an inquiry into biodiversity. LAVOISIER, Paris (France). 103-112.

- Sprangers, M., Dammers, N., Brinkhuis, H., van Weering, T.C.E., Lotter., A.F., 2004. Modern organic-walled dinoflagellate cyst distribution offshore NW Iberia, tracing the upwelling system. *Rev. Palaeobot. Palyno.* 128, 97-106.
- Srivastava, J., Farooqui, A., 2013. Late Holocene mangrove dynamics and coastal environmental changes in the Northeastern Cauvery River Delta, India. *Quaternary International* 298, 45-56.
- Srivastava, J., Farooqui, A., Hussain, S.M., 2013. Climate-induced Late-Holocene ecological changes in Pichavaram estuary, India. *Mar. Ecol.* 34, 474-483.
- State of Forest Report (2003), Forest Research Institute, Dehradun.
- Steidinger, K.A., 1975. Basic factors influencing red tides. Florida Department of Natural Resources Marine Research Laboratory, 153-162.
- Steidinger, K., Tester, L., Taylor, F.J.R., 1980. A redescription of *Pyrodinium bahamense* var. *compressa* (Böhm) stat. nov. from Pacific red tides. *Phycologia* 19, 329-334.
- Stoecker, D.K., 1999. Mixotrophy among dinoflagellates1. *J. Euk. Microbiol.* 46, 397-401.
- Subrahmanyam, R., 1968. The dinophyceae of the Indian Seas, part 1, genus *Ceratium* Schrank. Memoir II, Marine Biological Association of India. City Printers, Ernakulam, Cochin-II.
- Su-Myat, Maung-Saw-Htoo-Thaw, Matsuoka K., Khin-Ko-Lay, Koike K., 2012. Phytoplankton surveys off the southern Myanmar coast of the Andaman Sea: an emphasis on dinoflagellates including potentially harmful species. *Fisheries Sci.* 78, 1091-1106.
- Su-Myat, Koike, K., 2013. A red tide off the Myanmar coast: Morphological and genetic identification of the dinoflagellate composition. *Harmful Algae* 27, 149-158.
- Susek, E., 2005. Environmental factors influencing cyst formation and preservation of organic-walled dinoflagellates: an environmental and laboratory study. Diss. PhD. Thesis. Department of Geosciences at the University of Bremen. 1-123.
- Susek, E., Zonneveld, K.A., Fischer, G., Versteegh, G.J., Willems, H., 2005. Organic-walled dinoflagellate cyst production in relation to upwelling intensity and lithogenic influx in the Cape Blanc region (off north-west Africa). *Phycol. Res.* 53, 97-112.

- Takano, Y., Hansen, G., Fujita, D., Horiguchi, T., 2008. Serial replacement of diatom endosymbionts in two freshwater dinoflagellates, *Peridiniopsis* spp. (Peridinales, Dinophyceae). *Phycologia* 47, 41-53.
- Tang, Y.Z., Gobler, C.J., 2015. Sexual resting cyst production by the dinoflagellate *Akashiwo sanguinea*: a potential mechanism contributing to the ubiquitous distribution of a harmful alga. *J. Phycol.* 51, 298-309.
- Targarona, J., Warnaar, J., Boessenkool, K.P., Brinkhuis, H., Canals, M., 1999. Recent dinoflagellate cyst distribution in the North Canary Basin, NW Africa. *Grana* 38, 170-178.
- Taylor, F.J.R., 1976. Dinoflagellates from the international Indian Ocean expedition. A report on material collected by R. V. Anton Bruun 1963-1964. Plates 1-46.
- Taylor, F., Pollinger, U., 1987. The ecology of dinoflagellates. In: F.J.R. Taylor, (ed.) *The biology of dinoflagellates*, 398-329. Oxford: Blackwell Scientific Publications.
- ter Braak, C.J.F., Smilauer, P., 2002. CANOCO reference manual and CanoDraw for Windows user's guide: software for canonical community ordination (version 4.5). Section on Permutation Methods. Microcomputer Power, Ithaca, New York.
- Tomas, C.R., 1997. Identifying marine phytoplankton. Academic Press, San Diego, California, pp. 387-589.
- Tomczak, M., Godfrey, J.S., 2013. *Regional oceanography: an introduction*. Elsevier.
- Trigueros, J.M., Orive, E., 2000. Tidally driven distribution of phytoplankton blooms in a shallow, macrotidal estuary. *J. Plankton Res.* 22, 969-986.
- Tripathy, S.C., Kusumakimari, B.A.V.L., Sarma, V.V., Murty, T.V.R., 2005. Evaluation of trophic state and plankton abundance from the environmental parameters of Visakhapatnam Harbour and near-shore waters, east coast of India. *Asian J. Microbiol. Biotech. Env. Sc.* 7, 831-838.
- UNEP (2004) *Andaman and Nicobar Islands: ecologically-sustainable Island development*. Government of India, New Delhi.
- Usup, G., Ahmad, A., Matsuoka, K., Lim, P.T., Leaw, C.P., 2012. Biology, ecology and bloom dynamics of the toxic marine dinoflagellate *Pyrodinium bahamense*. *Harmful Algae.* 14, 301-312.

- Varkey, M., Murty, V., Suryanarayana, A., 1996. Physical oceanography of the Bay of Bengal and Andaman Sea. *Oceanography and marine biology: an annual review* 34, 1-70p.
- Varma, C., Dangwal, A., 1964. Tertiary hystrichosphaerids from India. *Micropaleontology* 63-71.
- Vásquez-Bedoya, L.F., Radi, T., Ruiz-Fernández, A.C., De Vernal, A., Machain-Castillo, M.L., Kieft, J.F., Hillaire-Marcel, C., 2008. Organic-walled dinoflagellate cysts and benthic foraminifera in coastal sediments of the last century from the Gulf of Tehuantepec, South Pacific Coast of Mexico. *Mar. Micropaleontol.*, 68, 49-65.
- Versteegh, G.J., Zonneveld, K.A.F., 2002. Use of selective degradation to separate preservation from productivity. *Geology* 30, 615-618.
- Vijaykumaran, K., 2005. Productivity parameters in relation to hydrography of the inshore surface waters off Visakhapatnam. *J. Mar. Biol. Ass. India* 47, 115-120.
- VishnuRadhan, R., David Thresyamma, D., Sarma, K., George, G., Shirodkar, P., Vethamony, P., 2015. Influence of natural and anthropogenic factors on the water quality of the coastal waters around the South Andaman in the Bay of Bengal. *Nat. Hazards* 78, 309-331.
- von Stosch, H.v., 1973. Observations on vegetative reproduction and sexual life cycles of two freshwater dinoflagellates, *Gymondinium pseudopalustre* Schiller and *Woloszynskia apiculata* sp. nov. *Brit. Phycol. J.* 8, 105-134.
- Wall, D., Dale, B., 1968. Modern dinoflagellate cysts and evolution of the Peridinales. *Micropaleontology* 14, 265-304.
- Wang, Z.H., Matsuoka, K., Qi, Y.Z., Chen, J.F., Lu, S.H., 2004. Dinoflagellate cyst records in recent sediments from Daya Bay, South China Sea. *Phycol. Res.* 52, 396-407.
- Wang, Z.-H., Qi, Y.-Z., Yang, Y.-F., 2007. Cyst formation: an important mechanism for the termination of *Scrippsiella trochoidea* (Dinophyceae) bloom. *J. Plankton Res.* 29, 209-218.
- Wang, Z.-H., Mu, D.-H., Li, Y.-f., Cao, Y., Zhang, Y.-J., 2011. Recent eutrophication and human disturbance in Daya Bay, the South China Sea: Dinoflagellate cyst and geochemical evidence. *Estuar. Coast. Shelf S.* 92, 403-414.

- Weninger, B., Joris, O., Danzeglocke, U., 2006. Calpal-Cologne Radiocarbon Calibration and Paleoclimate Research Package, Inst. für Ur-und Frühgeschichte Radiocarbon Lab., Univ. zu Köln, Köln, Germany.
- Wyrski, K., 1973. Physical oceanography of the Indian Ocean, The biology of the Indian Ocean. Springer, pp. 18-36.
- Xiaoping, G., Dodge, J.D., Lewis, J., 1989. An ultrastructural study of planozygotes and encystment of a marine dinoflagellate, *Scrippsiella* sp. Brit. Phycol. J. 24, 153-165.
- Yang, I., John, U., Beszteri, S., Glöckner, G., Krock, B., Goesmann, A., Cembella, A.D., 2010. Comparative gene expression in toxic versus non-toxic strains of the marine dinoflagellate *Alexandrium minutum*. BMC Genomics 11, 248.
- Yin, K., Song, X.-X., Liu, S., Kan, J., Qian, P.-Y., 2008. Is inorganic nutrient enrichment a driving force for the formation of red tides?: A case study of the dinoflagellate *Scrippsiella trochoidea* in an embayment. Harmful Algae 8, 54-59.
- Yu, J., Tang, D., Oh, I., Yao, L., 2007. Response of harmful algal blooms to environmental changes in Daya Bay, China. Terrestrial Atmospheric and Oceanic Sciences 18, 1011.
- Zhuo-Ping, C., Wei-Wei, H., Min, A., Shun-Shan, D., 2009. Coupled effects of irradiance and iron on the growth of a harmful algal bloom-causing microalga *Scrippsiella trochoidea*. Acta Ecol. Sin. 29, 297-301.
- Zonneveld, K.A.F., Brummer, G.A., 1995. Paleoclimatic and palaeo-ecological changes during the last deglaciation in the Eastern Mediterranean- implication for dinoflagellate ecology. Rev. Palaeobot. Palyno. 84, 221-253.
- Zonneveld, K.A.F., 1997a. Dinoflagellate cyst distribution in surface sediments from the Arabian Sea (northwestern Indian Ocean) in relation to temperature and salinity gradients in the upper water column. Deep-Sea Res. II 44, 1411-1443.
- Zonneveld, K.A.F., 1997b. New species of organic walled dinoflagellate cysts from modern sediments of the Arabian Sea (Indian Ocean). Review Palaeobot. Palyno. 97, 319-337.
- Zonneveld, K.A.F., Versteegh, G.J.M., de Lange, G.J., 1997d. Preservation of organic-walled dinoflagellate cysts in different oxygen regimes: A 10,000 year natural

- experiment. *Mar. Micropaleontol.* 29, 393-405.
- Zonneveld, K.A.F., Ganssen, G., Troelstra, S., Versteegh, G.J.M., Visscher, H., 1997c. Mechanisms forcing abrupt fluctuations of the Indian Ocean summer monsoon during the last deglaciation. *Quat. Sci. Rev.* 16, 187-201.
- Zonneveld, K.A.F., Brummer, G.A., 2000. (Palaeo-) ecological significance, transport and preservation of organic-walled dinoflagellate cysts in the Somali Basin, NW Arabian Sea. *Deep-Sea Res. II* 47, 2229-2256.
- Zonneveld, K.A.F., Susek, E., 2006. Effects of temperature, light and salinity on cyst production and morphology of *Tuberculodinium vancampoe* (the resting cyst of *Pyrophacus steinii*). *Rev. Palaeobot. Palyno.* 145, 77-88.
- Zonneveld, K.A.F., Bockelmann, F., Holzwarth, U., 2007. Selective preservation of organic-walled dinoflagellate cysts as a tool to quantify past net primary production and bottom water oxygen concentrations. *Mar. Geol.* 237, 109-126.
- Zonneveld, K.A.F., Chen, L., Mobius, J., Mahmoud, M.S., 2009. Environmental significance of dinoflagellate cysts from the proximal part of the Po-river discharge plume (off southern Italy, Eastern Mediterranean). *J Sea Res.* 62, 189-213.
- Zonneveld, K.A.F., Marret, F., Versteegh, G.J.M., Bogus, K., Bouimtarh, I., Crouch, E., de Vernal, A., Elshani, R., Esper, O., Forke, S., Grøsfjeld, K., Henry, M., Holzwarth, U., Bonnet, S., Edwards, L., Kieft, J.-F., Kim, S.-Y., Ladouceur, S., Ledu, D., Chen, L., Limoges, A., Lu, S.-H., Mahmoud, M.S., Marino, G., Matsouka, K., Londeix, L., Matthiessen, J., Mildenhall, D.C., Mudie, P., Neil, H.L., Pospelova, V., Qi, Y., Radi, T., Rochon, A., Sangiorgi, F., Solignac, S., Turon, J.-L., Wang, Y., Wang, Z., Young, M., Richerol, T., Verleye, T., 2013. Atlas of modern dinoflagellate cyst distribution based on 2405 datapoints. *Rev. Palaeobot. Palyno.* 191, 1-198.
- Zonneveld, K.A., Pospelova, V., 2015. A determination key for modern dinoflagellate cysts. *Palynology* 39, 387-409.

Appendix

Appendix I

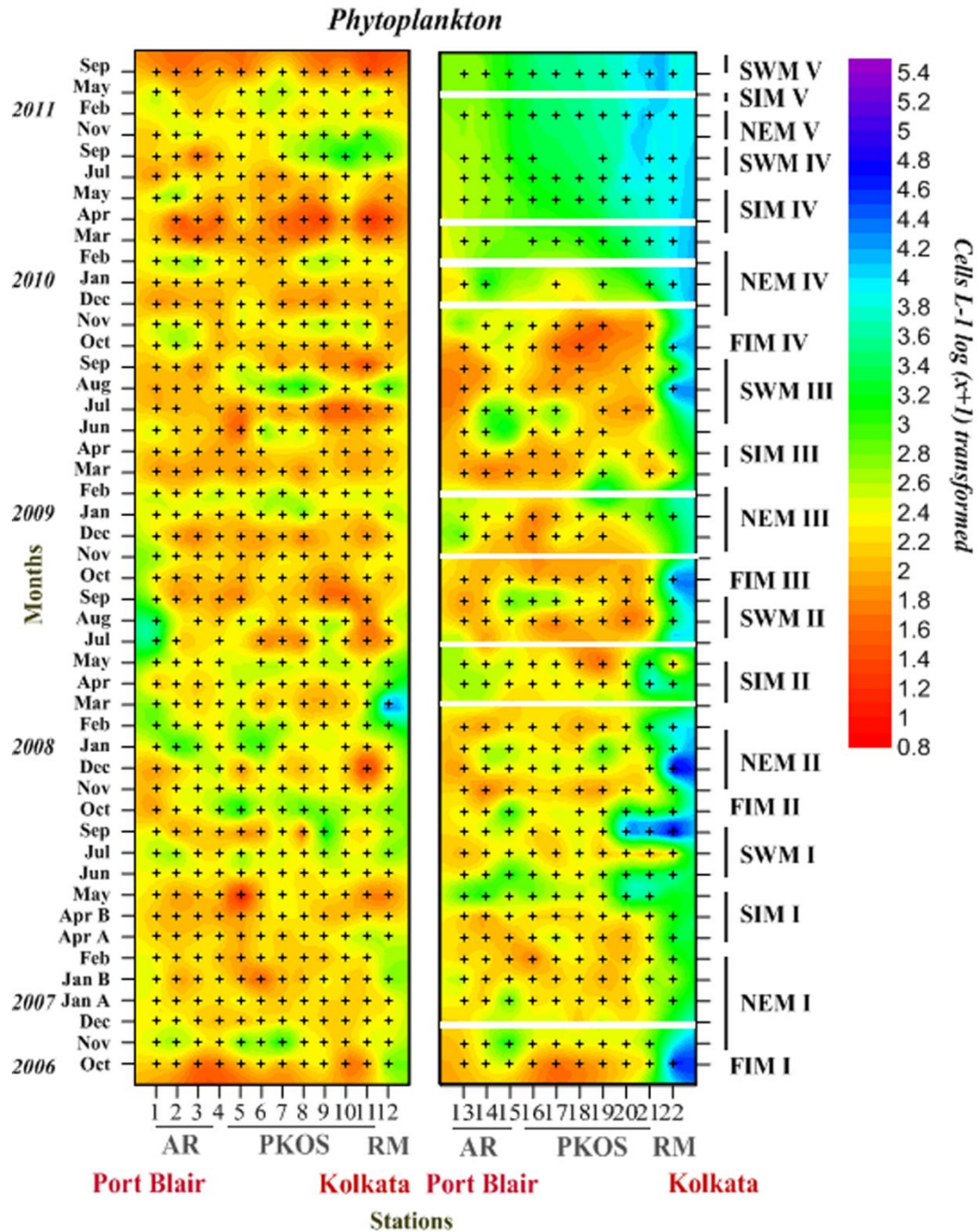


Fig. 2.1 Spatial and temporal variation in phytoplankton (a and b) abundance Cells L⁻¹ [log (x+1) transformed] along the Chennai-Port Blair and Port Blair-Kolkata transects. Superimposed post map (+) symbols on contours denote the sampling stations for which data is available. White lines superimposed (Fig. 2.1) on contours (along Port Blair-Kolkata transect) denotes the no sampling months.

Table 2.1 List of dinoflagellates with abundance (Cells L⁻¹) and their percentage composition (%) observed during the study period along the Chennai-Port Blair (CP) and Port Blair-Kolkata (PK) transects

Species Name	CPOS		PKOS		AR		RP	
	Abundance	%	Abundance	%	Abundance	%	Abundance	%
Phototrophs								
<i>Alexandrium concavum</i>	5	0.0						
<i>Alexandrium minutum</i>	10	0.0	5	0.0				
<i>Alexandrium tamarense</i>	85	0.1	45	0.3	10	0.1		
<i>Alexandrium spp.</i>	1711	2.4	245	1.6	205	2.9	170	1.6
<i>Amphidinium carterae</i>					15	0.2		
<i>Amphidinium sp.</i>	4310	6.0	1020	6.7	515	7.3	190	1.8
<i>Amphidoma caudata</i>	15	0.0	5	0.0				
<i>Amphidinium sphenoides</i>	105	0.1						
<i>Amphisolenia astragalus</i>	5	0.0						
<i>Amphisolenia globifera</i>	5	0.0						
<i>Amphisolenia thrinax</i>	5	0.0						
<i>Amphidoma spp.</i>	55	0.1	45	0.3				
<i>Acanthogonyaulax spinifera</i>	15	0.0			5	0.1		
<i>Amphisolenia bidentata</i>	360	0.5	75	0.5	10	0.1		
<i>Amphisolenia spp.</i>	180	0.3	40	0.3	5	0.1		
<i>Balechina coerulea</i>	15	0.0	5	0.0				
<i>Balechina spp.</i>	75	0.1	15	0.1	10	0.1		
<i>Blepharocysta spp.</i>	1167	1.6	290	1.9	130	1.8	35	0.3
<i>Ceratocorys armata</i>	5	0.0						
<i>Ceratocorys horrida</i>	125	0.2	50	0.3	15	0.2		
<i>Ceratocorys reticulata</i>	10	0.0						
<i>Ceratocorys gourretii</i>	10	0.0						
<i>Ceratocorys spp.</i>	20	0.0						
<i>Corythodinium diploconus</i>	5	0.0						
<i>Corythodinium globosum</i>	10	0.0						
<i>Corythodinium tessellatum</i>	245	0.3	50	0.3	15	0.2		

Species Name	CPOS		PKOS		AR		RP	
	Abundance	%	Abundance	%	Abundance	%	Abundance	%
<i>Corythodinium</i> spp.	30	0.0	5	0.0	10	0.1		
<i>Corythodinium</i> spp.					5	0.1		
<i>Dissodium bicorne</i>	20	0.0						
<i>Dissodium elegans</i>	35	0.0			10	0.1		
<i>Dissodium lunula</i>	55	0.1						
<i>Dissodium</i> spp.	40	0.1	20	0.1				
<i>Ensiculifera</i> spp.	291	0.4	70	0.5	30	0.4	35	0.3
<i>Gambierdiscus</i> spp.	20	0.0			5	0.1	5	0.0
<i>Goniodoma polyedricum</i>	555	0.8	210	1.4	40	0.6	10	0.1
<i>Goniodoma phaericum</i>	130	0.2	20	0.1	10	0.1		
<i>Goniodoma</i> spp.	30	0.0	15	0.1				
<i>Gonyaulax birostris</i>	10	0.0						
<i>Gonyaulax monospina</i>	170	0.2	45	0.3	10	0.1	50	0.5
<i>Gonyaulax digitalis</i>	20	0.0	5	0.0	5	0.1		
<i>Gonyaulax fragilis</i>	5	0.0						
<i>Gonyaulax fusiformis</i>	5	0.0						
<i>Gonyaulax hyalina</i>	20	0.0	10	0.1				
<i>Gonyaulax kofoidii</i>	80	0.1	10	0.1	15	0.2		
<i>Gonyaulax minuta</i>	50	0.1	5	0.0				
<i>Gonyaulax pacifica</i>			5	0.0				
<i>Gonyaulax polygramma</i>	765	1.1	225	1.5	75	1.1	30	0.3
<i>Gonyaulax rotundata</i>	10	0.0						
<i>Gonyaulax scrippsae</i>	160	0.2	15	0.1	40	0.6	20	0.2
<i>Gonyaulax sphaericum</i>	15	0.0						
<i>Gonyaulax spinifera</i>	175	0.2	20	0.1	30	0.4		
<i>Gonyaulax subulata</i>	15	0.0						
<i>Gonyaulax</i> spp.	2120	3.0	570	3.7	200	2.8		
<i>Gotius</i> spp.					5	0.1	75	0.7
<i>Gymnodinium catenatum</i>	30	0.0						
<i>Gymnodinium breve</i>			15	0.1				
<i>Akashiwo sanguinea</i>	40	0.1	5	0.0	10	0.1		
<i>Gymnodium</i> spp.	1506	2.1	430	2.8	175	2.5		
<i>Gyrodinium</i> spp.	150	0.2	5	0.0	5	0.1	125	1.2
<i>Heterocapsa niei</i>	35	0.0	10	0.1	5	0.1		

Species Name	CPOS Abundance	PKOS %	AR Abundance	RP %	5 Abundance	0.1 %	Abundance	%
<i>Heterodinium</i> spp..	15	0.0	5	0.0				
<i>Hetaraulacus polyedricus</i>	70	0.1	20	0.1	10	0.1		
<i>Hetaraulacus</i> spp.	5	0.0						
<i>Lingulodinium polyedrum</i>	40	0.1			5	0.1		
<i>Oxytoxum nanum</i>	15	0.0			10	0.1		
<i>Oxytoxum constrictum</i>	10	0.0						
<i>Oxytoxum subulatum</i>	5	0.0						
<i>Oxytoxum parvum</i>	165	0.2	35	0.2	25	0.4		
<i>Oxytoxum globosum</i>	25	0.0						
<i>Oxytoxum laticeps</i>	260	0.4	45	0.3	25	0.4		
<i>Oxytoxum milneri</i>	110	0.2	25	0.2	20	0.3		
<i>Oxytoxum reticulatum</i>	10	0.0						
<i>Oxytoxum scolopax</i>	815	1.1	130	0.9	65	0.9	20	0.2
<i>Oxytoxum semicollatum</i>	10	0.0						
<i>Oxytoxum sceptrum</i>			5	0.0				
<i>Oxytoxum subulatum</i>	10	0.0						
<i>Oxytoxum variabile</i>	5	0.0						
<i>Oxytoxum</i> spp.	686	1.0	155	1.0	55	0.8		
<i>Phalacroma rotundata</i>					5	0.1		
<i>Phalacroma</i> spp.	15	0.0	5	0.0				
<i>Paleophalacroma</i> spp.	35	0.0						
<i>Podolampas antarctica</i>			5	0.0	10	0.1		
<i>Podolampas bipes</i>	80	0.1	5	0.0	15	0.2		
<i>Podolampas elegans</i>	45	0.1	15	0.1	5	0.1		
<i>Podolampas palmipes</i>	400	0.6	55	0.4	45	0.6	5	0.0
<i>Podolampas spinifera</i>	185	0.3	10	0.1	10	0.1		
<i>Podolampas</i> spp.	35	0.0						
<i>Pyrophacus horologium</i>	100	0.1	15	0.1			15	0.1
<i>Pyrophacus steinii</i>	55	0.1	5	0.0	10	0.1		
<i>Pyrophacus</i> spp.	175	0.2	35	0.2	10	0.1	120	1.2
<i>Polykrikos</i> spp.					15	0.2		
<i>Tripos arietinus</i>	40	0.1	5	0.0	10	0.1		
<i>Tripos azoricus</i>	40	0.1	10	0.1	20	0.3		
<i>Tripos brevis</i>	226	0.3	10	0.1	15	0.2	5	0.0

Species Name	CPOS	PKOS	AR	RP	Abundance	%	Abundance	%
	Abundance	%	Abundance	%				
<i>Tripes belone</i>	5	0.0						
<i>Tripes euarquatus</i>	5	0.0						
<i>Tripes concilians</i>	15	0.0	5	0.0				
<i>Tripes contortus</i>	90	0.1						
<i>Tripes declinatus</i>	725	1.0	130	0.9	85	1.2		
<i>Tripes deflexus</i>	95	0.1	15	0.1			20	0.2
<i>Tripes dens</i>	55	0.1	15	0.1	5	0.1		
<i>Tripes digitatus</i>	75	0.1	10	0.1	30	0.4		
<i>Tripes extensus</i>	135	0.2	15	0.1	5	0.1	20	0.2
<i>Tripes furca</i>	1865	2.6	375	2.5	195	2.8	675	6.5
<i>Tripes fusus</i>	1025	1.4	245	1.6	105	1.5	80	0.8
<i>Tripes horridus</i>	555	0.8	80	0.5	35	0.5	150	1.5
<i>Tripes inflatus</i>	145	0.2	45	0.3	25	0.4	10	0.1
<i>Tripes incisus</i>	5	0.0						
<i>Tripes arcuatus</i>	25	0.0						
<i>Tripes kofoidii</i>	45	0.1	20	0.1				
<i>Tripes inflatus</i>	30	0.0			5	0.1	5	0.0
<i>Tripes lineatus</i>	140	0.2	15	0.1	20	0.3		
<i>Tripes inflatus</i>	80	0.1	5	0.0	10	0.1		
<i>Tripes lunula</i>	10	0.0	5	0.0				
<i>Tripes limulus</i>	5	0.0						
<i>Tripes macroceros</i>	125	0.2	25	0.2			15	0.1
<i>Tripes minutus</i>	10	0.0						
<i>Tripes pentagonus</i>	260	0.4	40	0.3	20	0.3		
<i>Tripes setaceus</i>			10	0.1				
<i>Tripes pulchellus</i>	15	0.0	10	0.1				
<i>Tripes schmidtii</i>	270	0.4	60	0.4	55	0.8	30	0.3
<i>Tripes symmetricus</i>								
<i>Tripes teres</i>	595	0.8	100	0.7	40	0.6		
<i>Tripes trichoceros</i>	450	0.6	75	0.5	20	0.3	185	1.8
<i>Tripes muelleri</i>	290	0.4	65	0.4	45	0.6	20	0.2
<i>Tripes muelleri</i> var. <i>atlanticu</i>	60	0.1	30	0.2			10	0.1
<i>Tripes vultur</i>	180	0.3	40	0.3	20	0.3	80	0.8
<i>Tripes massiliensis</i>	30	0.0	5	0.0				

Species Name	CPOS		PKOS		AR		RP	
	Abundance	%	Abundance	%	Abundance	%	Abundance	%
<i>Tripos ranipes</i>	35	0.0						
<i>Tripos</i> spp.	350	0.5	50	0.3	60	0.8	50	0.5
<i>Dinophysis acuta</i>	20	0.0	5	0.0				
<i>Dinophysis acuminata</i>	60	0.1	5	0.0			10	0.1
<i>Dinophysis caudata</i>	2065	2.9	95	0.6	60	0.8	1685	16.3
<i>Dinophysis doryphorum</i>	85	0.1	5	0.0	5	0.1		
<i>Dinophysis exigua</i>	10	0.0						
<i>Dinophysis hastata</i>	20	0.0						
<i>Dinophysis infundibulum</i>								
<i>Dinophysis miles</i>			25	0.2				
<i>Dinophysis parvula</i>	15	0.0						
<i>Dinophysis ovum</i>	15	0.0			5	0.1		
<i>Dinophysis rotundata</i>	10	0.0	5	0.0			10	0.1
<i>Dinophysis schuetii</i>					5	0.1		
<i>Dinophysis</i> spp.	230	0.3	55	0.4	25	0.4	15	0.1
<i>Prorocentrum concavum</i>	45	0.1	5	0.0	5	0.1		
<i>Prorocentrum arcuatum</i>								
<i>Prorocentrum balticum</i>	15	0.0			10	0.1		
<i>Prorocentrum belizeanum</i>	20	0.0	5	0.0				
<i>Prorocentrum dentatum</i>			10	0.1				
<i>Prorocentrum compressum</i>	620	0.9	130	0.9	80	1.1		
<i>Prorocentrum cordatum</i>								
<i>Prorocentrum emarginatum</i>	15	0.0	10	0.1				
<i>Prorocentrum gracile</i>	460	0.6	40	0.3	40	0.6	125	1.2
<i>Prorocentrum lenticulatum</i>	45	0.1			10	0.1		
<i>Prorocentrum lima</i>					5	0.1		
<i>Prorocentrum micans</i>	1475	2.1	140	0.9	125	1.8	880	8.5
<i>Prorocentrum minimum</i>	5	0.0						
<i>Prorocentrum mexicanum</i>	10	0.0						
<i>Prorocentrum oblongum</i>	20	0.0	5	0.0	5	0.1		
<i>Prorocentrum obtusum</i>	85	0.1	25	0.2				
<i>Prorocentrum scutellum</i>	130	0.2	10	0.1	10	0.1	5	0.0
<i>Prorocentrum sigmoides</i>	215	0.3	40	0.3	15	0.2	30	0.3
<i>Prorocentrum</i> spp.	2200	3.1	585	3.8	250	3.5	200	1.9

Species Name	CPOS		PKOS		AR		RP	
	Abundance	%	Abundance	%	Abundance	%	Abundance	%
<i>Pyrocystis fusiformis</i>	95	0.1			25	0.4		
<i>Pyrocystis globosa</i>	5	0.0						
<i>Pyrocystis lunula</i>	10	0.0						
<i>Pyrocystis noctiluca</i>	360	0.5	75	0.5	20	0.3	45	0.4
<i>Pyrocystis rhomboides</i>	10	0.0						
<i>Pyrocystis robusta</i>	70	0.1	10	0.1				
<i>Pyrocystis</i> spp.	196	0.3	10	0.1			40	0.4
<i>Cochlodinium</i> spp.	30	0.0						
<i>Scrippsiella spinifera</i>	30	0.0						
<i>Scrippsiella trochoidea</i>	9253	12.9	2135	14.0	855	12.1	805	7.8
<i>Scrippsiella</i> spp.	1520	2.1	490	3.2	105	1.5	110	1.1
<i>Citharistes regius</i>	10	0.0	5	0.0				
Heterotrophs								
<i>Diplopsalis lenticulata</i>	40	0.1	30	0.2				
<i>Diplopsalis</i> spp.	200	0.3	70	0.5	25	0.4	5	0.0
<i>Gyrodinium</i> spp.	450	0.6	110	0.7	40	0.6	10	0.1
<i>Histioneis carinata</i>	10	0.0						
<i>Histiones</i> spp.	35	0.0	5	0.0	5	0.1		
<i>Noctiluca scintillans</i>	110	0.2	10	0.1	15	0.2		
<i>Noctiluca</i> spp.	5	0.0						
<i>Ornithocercus formosus</i>			10	0.1				
<i>Ornithocercus</i> spp.	10	0.0						
<i>Ornithocercus magnificus</i>	200	0.3	55	0.4	45	0.6		
<i>Ornithocercus quadratus</i>	40	0.1	20	0.1				
<i>Ornithocercus steinii</i>	55	0.1	20	0.1				
<i>Ornithocercus thumii</i>	280	0.4	75	0.5	55	0.8		
<i>Ornithocercus</i> spp.	86	0.1	5	0.0	10	0.1		
<i>Oxyphysis oxytoxoides</i>	10	0.0	5	0.0				
<i>Pentapharsodinium tyrrhenicum</i>	30	0.0						
<i>Phalacroma argus</i>	25	0.0					20	0.2
<i>Phalacroma circumsutum</i>	10	0.0						
<i>Phalacroma cuneus</i>			5	0.0				

Species Name	CPOS		PKOS		AR		RP	
	Abundance	%	Abundance	%	Abundance	%	Abundance	%
<i>Phalacroma doryphorum</i>	5	0.0						
<i>Phalacroma favus</i>	5	0.0						
<i>Phalacroma rapa</i>	45	0.1	20	0.1				
<i>Phalacroma rotundatum</i>	80	0.1	20	0.1				
<i>Phalacroma</i> spp.	380	0.5	120	0.8	40	0.6	90	0.9
<i>Pronoctiluca acuta</i>	5	0.0						
<i>Pronoctiluca pelagica</i>	30	0.0	5	0.0				
<i>Pronoctiluca</i> spp.	25	0.0	5	0.0	5	0.1		
<i>Pronoctiluca spinifera</i>	10	0.0			5	0.1		
<i>Pronoctiluca rostrata</i>	5	0.0						
<i>Protopteridinium abei</i>	15	0.0						
<i>Protopteridinium acbromaticum</i>	10	0.0						
<i>Protopteridinium biconicum</i>	10	0.0						
<i>Protopteridinium brevipes</i>	5	0.0						
<i>Protopteridinium claudicans</i>	180	0.3	15	0.1	10	0.1	130	1.3
<i>Protopteridinium conicum</i>	245	0.3	20	0.1	5	0.1	175	1.7
<i>Protopteridinium crassipes</i>	40	0.1					20	0.2
<i>Protopteridinium curvipes</i>							80	0.8
<i>Protopteridinium divergens</i>	790	1.1	75	0.5	75	1.1	370	3.6
<i>Protopteridinium elegans</i>	45	0.1	10	0.1	10	0.1	10	0.1
<i>Protopteridinium heteracanthum</i>			10	0.1				
<i>Protopteridinium inflatum</i>								
<i>Protopteridinium latispinum</i>	10	0.0	10	0.1				
<i>Protopteridinium latispinum</i>	55	0.1						
<i>Protopteridinium leonis</i>	210	0.3	55	0.4	25	0.4	40	0.4
<i>Protopteridinium mediterraneum</i>	200	0.3	65	0.4	10	0.1	10	0.1
<i>Archaepteridinium minutum</i>	430	0.6	60	0.4	65	0.9	165	1.6
<i>Protopteridinium oblongum</i>	130	0.2			5	0.1	95	0.9
<i>Protopteridinium oceanicum</i>	25	0.0	10	0.1				
<i>Protopteridinium ovatum</i>	10	0.0			5	0.1		
<i>Protopteridinium ponticum</i>			25	0.2				
<i>Protopteridinium pacificum</i>	175	0.2	55	0.4	40	0.6		
<i>Protopteridinium pallidum</i>	155	0.2	55	0.4	10	0.1	25	0.2

<i>Protooperidinium pedunculatum</i>	225	0.3	5	0.0	10	0.1	140	1.4
<i>Protooperidinium pellucidum</i>	195	0.3	5	0.0	10	0.1	40	0.4
<i>Protooperidinium pentagonum</i>	95	0.1	5	0.0	35	0.5	10	0.1
<i>Protooperidinium steinii</i>	145	0.2	35	0.2	15	0.2		
<i>Protooperidinium subinerme</i>	50	0.1	5	0.0	5	0.1	5	0.0
<i>Protooperidinium sourniai</i>			10	0.1	10	0.1		
<i>Protooperidinium tristylum</i>	10	0.0						
<i>Protooperidinium tuba</i>	125	0.2			20	0.3	100	1.0
<i>Protooperidinium spp.</i>	5856	8.2	1400	9.2	590	8.3	1125	10.9
<i>Preperidinium meunieri</i>	940	1.3	160	1.0	40	0.6	505	4.9
<i>UTD</i>	12280	17.1	2855	18.7	1355	19.1	875	8.5

Table 2.2a

The coefficient of correlation between environmental variables and first two axes (RDA1 and 2) of redundancy analysis during SWM season. Environmental variables abbreviations: SSS, sea surface salinity; SST, sea surface temperature; DIN, dissolved inorganic nitrogen; DIP, dissolved inorganic phosphate; PAR, Photosynthetically active radiation; Diatoms, diatom abundance.

Environmental variable	RDA1	RDA2
SSS	0.3851	-0.2890
SST	0.3789	1.5056
PAR	-0.1883	-0.0720
Wind	0.0864	-0.3474
DIN	0.3584	-0.2962
DIP	-0.3012	0.0198
Diatom	1.4473	1.1797

Table 2.2b

Scores of cyst-forming dinoflagellates to the first two axes (RDA 1 and 2) of redundancy analysis during SWM season.

Species Name	RDA1	RDA2
<i>Alexandrium</i> spp.	-0.0348	0.0684
<i>Gonyaulax scrippsae</i>	0.1539	-0.1834
<i>Gonyaulax spinifera</i>	-0.1054	0.1541
<i>Gonyaulax</i> spp.	0.0672	-0.4399
<i>Lingulodinium polyedrum</i>	-0.1054	0.1541
<i>Pyrophacus horologium</i>	0.6132	-0.0001
<i>Pyrophacus steinii</i>	-0.0742	-0.0883
<i>Scrippsiella trochoidea</i>	0.5637	-0.3429
<i>Scrippsiella</i> spp.	0.1585	-0.0890
<i>Pentapharsodinium tyrrhenicum</i>	0.2178	-0.1273
<i>Protoperidinium claudicans</i>	-0.1020	-0.1653
<i>Protoperidinium conicum</i>	0.7358	-0.1849
<i>Protoperidinium divergens</i>	0.6868	-0.2399
<i>Protoperidinium leonis</i>	-0.1269	0.3696
<i>Archaeperidinium minutum</i>	0.3256	0.2575
<i>Protoperidinium oblongum</i>	-0.0457	0.1941
<i>Protoperidinium</i> spp.	0.8322	0.2932
<i>Preperidinium meunieri</i>	-0.2031	0.3240

Table 2.3a

The coefficient of correlation between environmental variables and first two axis (RDA1 and 2) of redundancy analysis during FIM season. For abbreviations of environmental variables please refer legends of table 2.2a

Environmental variable	RDA1	RDA2
SSS	-0.4400	0.2452
SST	-0.3946	0.4300
Wind	0.0863	-0.0061
DIN	-0.2246	0.2486
DIP	-0.9224	0.3522
Diatom	0.4845	0.5737
PAR	-0.6348	-0.2085

Table 2.3b

Scores of cyst-forming dinoflagellates to the first two axis (RDA 1 and 2) of redundancy analysis during FIM season.

Species Name	RDA1	RDA2
<i>Alexandrium tamarense</i>	-0.1815	-0.0018
<i>Alexandrium</i> spp.	-0.0481	0.0749
<i>Gonyaulax scrippsae</i>	0.1639	0.0926
<i>Gonyaulax spinifera</i>	-0.1030	0.5872
<i>Gonyaulax</i> spp.	-0.0139	-0.0062
<i>Lingulodinium polyedrum</i>	-0.1622	-0.0681
<i>Pyrophacus horologium</i>	0.2103	0.0261
<i>Pyrophacus steinii</i>	-0.1767	-0.0951
<i>Scrippsiella trochoidea</i>	0.6670	-0.1335
<i>Scrippsiella</i> spp.	-0.2955	-0.1558
<i>Protoperidinium claudicans</i>	0.1355	0.8776
<i>Protoperidinium conicum</i>	-0.0002	-0.0732
<i>Protoperidinium divergens</i>	0.0511	0.7822
<i>Protoperidinium leonis</i>	0.1960	0.0766
<i>Archaeoperidinium minutum</i>	0.1253	0.8798
<i>Protoperidinium ponticum</i>	0.2103	0.0261
<i>Protoperidinium pentagonum</i>	-0.1810	0.2875
<i>Protoperidinium subinerme</i>	-0.1622	-0.0681
<i>Protoperidinium</i> spp.	0.3710	0.7132
<i>Preperidinium meunieri</i>	-0.0449	-0.0544

Table 2.4a

The coefficient of correlation between environmental variables and first two axis (RDA1 and 2) of redundancy analysis during NEM season. For abbreviations of environmental variables please refer legends of table 2.2a

Environmental variable	RDA1	RDA2
SSS	-0.1222	0.5133
SST	0.0972	-0.4809
PAR	-0.1563	0.2266
Wind	0.0231	0.3194
DIN	0.0985	0.7835
DIP	-0.1547	-0.1947
Diatom	0.9883	0.0386

Table 2.4b

Scores of cyst-forming dinoflagellates to the first two axis (RDA 1 and 2) of redundancy analysis during NEM season.

Species Name	RDA1	RDA2
<i>Alexandrium minutum</i>	-0.0607	-0.1557
<i>Alexandrium</i> spp.	-0.0855	0.1014
<i>Gonyaulax scrippsae</i>	-0.1394	0.2143
<i>Gonyaulax spinifera</i>	-0.1155	0.1446
<i>Gonyaulax</i> spp.	0.3199	-0.3025
<i>Gymnodinium catenatum</i>	-0.0474	0.2642
<i>Pyrophacus horologium</i>	-0.0563	-0.0367
<i>Scrippsiella spinifera</i>	-0.0838	0.3948
<i>Scrippsiella trochoidea</i>	0.3838	-0.3930
<i>Scrippsiella</i> spp.	-0.1666	0.1246
<i>Diplopsalis lenticula</i>	-0.0216	-0.1696
<i>Protoperidinium claudicans</i>	-0.0412	-0.1328
<i>Protoperidinium conicum</i>	0.9865	0.0390
<i>Protoperidinium curvipes</i>	0.9865	0.0390
<i>Protoperidinium divergens</i>	0.9803	0.0277
<i>Protoperidinium leonis</i>	0.5938	0.1484
<i>Archaeperidinium minutum</i>	0.9524	-0.1095
<i>Protoperidinium oblongum</i>	0.9865	0.0390
<i>Protoperidinium pentagonum</i>	-0.1390	0.0524
<i>Protoperidinium subinerme</i>	0.6591	0.2049
<i>Protoperidinium</i> spp.	0.9810	0.0280
<i>Preperidinium meunieri</i>	0.9747	0.0019

Table 2.5a

Coefficient of correlation between environmental variables and first two axis (RDA1 and 2) of redundancy analysis during SIM season. For abbreviations of environmental variables please refer legends of table 2.2a

Environmental variable	RDA1	RDA2
SSS	-0.1222	0.5133
SST	0.0972	-0.4809
PAR	-0.1563	0.2266
Wind	0.0231	0.3194
DIN	0.0985	0.7835
DIP	-0.1547	-0.1947
Diatom	0.9883	0.0386

Table 2.5b

Scores of cyst-forming dinoflagellates to the first two axis (RDA 1 and 2) of redundancy analysis during SIM season.

Species Name	RDA1	RDA2
<i>Alexandrium tamarense</i>	-0.1815	-0.0018
<i>Alexandrium</i> spp.	-0.0481	0.0749
<i>Gonyaulax scrippsae</i>	0.1639	0.0926
<i>Gonyaulax spinifera</i>	-0.1030	0.5872
<i>Gonyaulax</i> spp.	-0.0139	-0.0062
<i>Lingulodinium polyedrum</i>	-0.1622	-0.0681
<i>Pyrophacus horologium</i>	0.2103	0.0261
<i>Pyrophacus steinii</i>	-0.1767	-0.0951
<i>Scrippsiella trochoidea</i>	0.6670	-0.1335
<i>Scrippsiella</i> spp.	-0.2955	-0.1558
<i>Protoperidinium claudicans</i>	0.1355	0.8776
<i>Protoperidinium conicum</i>	-0.0002	-0.0732
<i>Protoperidinium divergens</i>	0.0511	0.7822
<i>Protoperidinium leonis</i>	0.1960	0.0766
<i>Archaeperidinium minutum</i>	0.1253	0.8798
<i>Protoperidinium ponticum</i>	0.2103	0.0261
<i>Protoperidinium pentagonum</i>	-0.1810	0.2875
<i>Protoperidinium subinerme</i>	-0.1622	-0.0681
<i>Protoperidinium</i> spp.	0.3710	0.7132
<i>Preperidinium meunieri</i>	-0.0449	-0.0544

Appendix II

Table 3B.1 Environmental parameters used in CCA analysis

Abbreviations of environmental variables: SSS, salinity; SST, temperature; MLD, mixed layered depth; Chla, chlorophylla concentration at the surface; P, Phosphate; N, Nitrate; S, Silicate; Corg, total organic carbon; WD, Water depth. SWM, South west monsoon; FIM, fall inter monsoon; NEM, north east monsoon; SIM, summer inter monsoon.

	Abbreviations	Coastal stations				Neritic-Oceanic stations	
		SK261-01	SK261-02	SK261-03	SK261-04	SK261-05	SK261-06
Latitude[°N]		13.1	17.1	19.9	20.9	20.5	19.0
Longitude[°E]		80.3	82.9	86.5	89.3	89.5	89.9
SST[°C] annual	SSTAnnual	28.3	27.9	28.1	27.6	27.7	27.9
SSS[psu] annual	SSSAnnual	33.6	31.7	32.4	29.8	30.3	30.9
MLD[m] annual	MLDAnnual	4.8	2.9	5.5	6.4	5.0	7.7
Nitrate[μmol/l] Oct	NSIM	0.6	1.4	0.6	0.8	0.7	0.7
Nitrate [μmol/l] Jun-Sep	NSWM	0.2	1.1	0.8	1.6	1.3	0.9
Nitrate [μmol/l] Nov-Feb	NFIM	1.1	1.6	1.3	0.7	0.7	0.7
Nitrate [μmol/l] Mar-May	NNEM	0.4	1.4	1.0	0.7	0.7	0.6
Silicate [μmol/l] Oct	SSIM	3.3	3.9	5.8	2.3	2.6	2.8
Silicate [μmol/l] Jun-Sep	SSWM	2.2	8.7	4.3	10.6	10.3	10.0
Silicate [μmol/l] Nov-Feb	SFIM	4.7	2.6	6.3	2.7	2.9	3.2
Silicate [μmol/l] Mar-May	SNEM	3.6	2.3	5.3	3.1	3.1	3.1
Phosphate [μmol/l] Oct	PSIM	0.2	0.2	0.3	0.1	0.1	0.1
Phosphate [μmol/l] Jun-Sep	PSWM	0.4	0.3	0.3	0.2	0.2	0.2
Phosphate [μmol/l] Nov-Feb	PFIM	0.2	0.4	0.7	0.3	0.4	0.4
Phosphate [μmol/l] Mar-May	PNEM	0.4	0.3	0.5	0.2	0.3	0.3
chlorophyll a [mg m-3] Oct	ChlaSIM	0.4	2.1	1.3	1.2	0.3	0.3
chlorophyll a [mg m-3] Jun-Sep	ChlaSWM	1.6	1.0	0.5	2.4	1.0	0.2
chlorophyll a [mg m-3] Nov-Feb	ChlaFIM	0.8	2.4	0.8	4.7	0.2	0.2
chlorophyll a [mg m-3] Mar-May	ChlaNEM	0.8	1.4	0.6	1.1	0.3	0.3
Water depth[m]	WD	56.0	62.0	86.0	108.0	135.0	154.0
Total organic carbon[%]	C _{org}	0.3	1.1	1.5	0.8	1.8	0.8

Fig. 3B.2 Result of CCA correlating the dinoflagellate cyst distribution with environmental parameters in surface water. Conditional effects representing the amount of variance explained by the particular variable in the surface water.

For abbreviations refer legends of Table 3B.1

Marginal Effects		
Variable	Var.N	Lambda1
WD	21	0.36
ChlaNEM	20	0.32
ChlaSIM	17	0.3
MAnnual	3	0.29
ChlaFIM	19	0.23
PSWM	14	0.22
NFIM	7	0.22
NNEM	8	0.18
TOC	4	0.18
ChlaSWM	18	0.17
SSWM	10	0.16
PSIM	13	0.16
SAnnual	2	0.15
NSIM	5	0.15
NSWM	6	0.15
TAnnual	1	0.13
SSIM	9	0.1
PFIM	15	0.08
SFIM	11	0.08
SNEM	12	0.08
PNEM	16	0.07

Conditional Effects				
Variable	Var.N	LambdaA	P	F
WD	21	0.36	0.026	2.32
NSWM	6	0.22	0.218	1.56
MAnnual	3	0.17	0.286	1.47
NSIM	5	0.16	0.314	1.92
TAnnual	1	0.08	1	0

Appendix III

Table 5.1 a) Result of CCA correlating the planktonic dinoflagellate distribution with environmental parameters in surface water. Conditional effects representing the amount of variance explained by the particular variable in the surface water. Significant environmental variable highlighted in red (P<0.05 is at 5% significance level).

Marginal Effects		
Variable	Var.N	Lambda1
PO4	4	0.16
Chla	9	0.16
DO	8	0.16
SiO4	3	0.14
Temp	5	0.13
Salinity	6	0.12
NO2	2	0.08
NO3	1	0.07
SPM	7	0.07

Conditional Effects				
Variable	Var.N	LambdaA	P	F
PO4	4	0.16	0.038	1.71
DO	8	0.16	0.030	1.64
Chla	9	0.14	0.054	1.55
Temp	5	0.11	0.268	1.17
Salinity	6	0.11	0.270	1.16
SiO4	3	0.10	0.290	1.14
NO3	1	0.08	0.568	0.89
SPM	7	0.07	0.824	0.70
NO2	2	0.07	0.684	0.80

Table 5.1 b) Result of CCA correlating the planktonic dinoflagellate distribution with environmental parameters in near bottom water. Conditional effects representing the amount of variance explained by the particular variable in the surface water. Significant environmental variable highlighted in red (P<0.05 is at 5% significance level).

Marginal Effects		
Variable	Var.N	Lambda1
Chla	9	0.20
DO	8	0.13
NO2	2	0.11
NO3	1	0.11
PO4	4	0.10
Salinity	6	0.10
SiO4	3	0.09
Temp	5	0.09
SPM	7	0.05

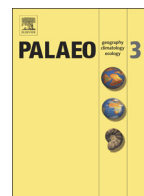
Conditional Effects				
Variable	Var.N	LambdaA	P	F
Chla	9	0.20	0.006	2.15
NO3	1	0.13	0.144	1.39
DO	8	0.11	0.280	1.18
Salinity	6	0.10	0.386	1.08
NO2	2	0.11	0.310	1.14
PO4	4	0.10	0.328	1.14
SiO4	3	0.07	0.772	0.71
Temp	5	0.06	0.800	0.67
SPM	7	0.06	0.826	0.60

Table 5.1 c) Result of CCA correlating the dinoflagellate cyst distribution with environmental parameters in surface sediments. Conditional effects representing the amount of variance explained by the particular variable in the surface water. Significant environmental variable highlighted in red ($P < 0.05$ is at 5% significance level).

Marginal Effects		
Variable	Var.N	Lambda1
Silt	11	0.17
Sand	10	0.11
Chla	9	0.10
SPM	7	0.10
Temp	5	0.10
Clay	12	0.09
DO	8	0.09
PO4	4	0.09
SiO4	3	0.08
NO2	2	0.07
Salinity	6	0.06
NO3	1	0.05

Conditional Effects				
Variable	Var.N	LambdaA	P	F
Silt	11	0.17	0.006	2.06
Sand	10	0.11	0.140	1.31
Temp	5	0.10	0.204	1.23
SPM	7	0.10	0.236	1.22
DO	8	0.09	0.292	1.11
SiO4	3	0.12	0.110	1.43
NO2	2	0.09	0.304	1.16
Chla	9	0.08	0.320	1.07
PO4	4	0.06	0.802	0.75
Salinity	6	0.07	0.670	0.83
NO3	1	0.06	0.768	0.74
Clay	12	0.04	0.930	0.41

Publications



Evolution of productivity and monsoonal dynamics in the eastern Arabian Sea during the past 68 ka using dinoflagellate cyst records



Dhiraj Dhondiram Narale, Pothuri Divakar Naidu *, Arga Chandrashekar Anil, Shital P. Godad

CSIR-National Institute of Oceanography, Dona Paula, Goa 403 004, India

ARTICLE INFO

Article history:

Received 13 February 2015
Received in revised form 27 May 2015
Accepted 3 June 2015
Available online 17 June 2015

Keywords:

Eastern Arabian Sea
Monsoons
Productivity
Marine isotopic stages
Dinoflagellate cyst

ABSTRACT

For the first time here we report the dinoflagellate cyst assemblage response to the monsoon variability over the last 68 ka from the Eastern Arabian Sea (EAS). Based on the cyst assemblage, five dinoflagellate cyst zones were established, corresponding to four Marine Isotopic Stages (MIS 1–4). An increased abundance of autotrophic Gonyaulacoid species (especially *Spiniferites*) during glacials (MIS 2 and 4) and late MIS 3 (~41.67 to 25.3 ka) reflects high productivity driven by strong winter convection during the Northeast monsoon. In contrast, their decreased abundance during MIS 1 and early MIS 3 (~58.6 to 42.87 ka) reveals decrease in productivity due to strong stratification caused by intense monsoon precipitation induced runoff from the Western Ghats and reduced light penetration driven by cloud cover. The variation in heterotrophic *Protoperidinium* species abundance could be related to variation in the Oxygen Minimum Zone (OMZ) intensity, with better preservation during intense OMZ in MIS 3 and the late Holocene (~3 ka onwards). Therefore, it is proposed here that the abundance of *Protoperidinium* can be used as an index of OMZ in the EAS.

© 2015 Elsevier B.V. All rights reserved.

1. Introduction

The Asian Monsoon system has a strong bearing on the biological productivity of the Arabian Sea. The present-day climatic and oceanographic conditions predominating in the Eastern Arabian Sea (EAS) are influenced by both the South West (SW or summer) and North East (NE or winter) monsoon systems. The EAS experiences moderate upwelling and high precipitation along the entire margin during summer and winter vertical mixing in the northern part, and fresh water inflow during winter from the Bay of Bengal in the south (Banse et al., 1987; Bhattathiri et al., 1996; Prasanna Kumar et al., 2000; Gerson et al., 2014). These regional climatic and oceanographic features could also play a significant role in the evolution of productivity variation in the EAS during the Late Quaternary Period. The paleoclimatological and paleoceanographic records have provided detailed information on the late Quaternary climate variability and paleoproductivity variations in the region. Studies from the Western Arabian Sea (WAS) revealed that productivity was lower during the last glacial period due to a weaker SW monsoon and reduced upwelling (Naidu and Malmgren, 1996; Ivanochko et al., 2005). On the contrary, high productivity during the last glacial period was reported in the Northern Arabian Sea (NAS), with an intensified NE monsoon resulting in intense deeper water mixing and increased advection of nutrient-rich subsurface water (Reichert et al., 1998; Luckge et al., 2001; Ivanova et al., 2003).

In the EAS recent studies using paleoproductivity proxies, such as abundance of planktonic foraminifera, coccolithophore, organic carbon, carbon and nitrogen isotopic records infer that productivity was higher during the Last Glacial Maximum (LGM) than in the Holocene (Ivanochko, 2004; Singh et al., 2006, 2011; Cabarcos et al., 2014; Naidu et al., 2014). In this context, the present study used dinoflagellate cyst records over the last 68 ka to contribute further to the existing paleoclimatic and paleoceanographic information in the EAS.

Dinoflagellate is one of the dominant group of the primary producers in the marine ecosystem, and have a complex life cycle which includes cyst (resting stage) formation. The rigid cell wall of dinoflagellate cyst comprises a bio-macromolecule, dinosporin (Fensome et al., 1993; Bogus et al., 2014) which enables them to resist physical, chemical and biological destruction and degradation. Thus, cyst records provide a reliable paleoceanographic information where other calcareous and siliceous microfossil taxa, such as foraminifera, diatoms, and radiolarian, are subject to dissolution (Pospelova et al., 2006). In the recent years, various paleoceanographic studies have demonstrated the use of dinoflagellate cyst assemblages to reconstruct paleo-environmental conditions on a centennial as well as millennial time scale (Shaozhi and Harland, 1993; de Vernal and Pedersen, 1997; Marret et al., 2001; Mudie et al., 2002; Matthiessen et al., 2005; Pospelova et al., 2006; Price et al., 2013). Dinoflagellates have species specific differential environmental and growth requirements, thus their cyst distribution in sediments can portray surface water conditions (Dale, 2001; Marret and Zonneveld, 2003; Zonneveld et al., 2013). Higher abundance of autotrophic species in sediments reveals stable water conditions with increased light penetration and ample nutrient supply in water column, whereas

* Corresponding author. Tel.: +91 832 2450 232.
E-mail address: divakar@nio.org (P.D. Naidu).

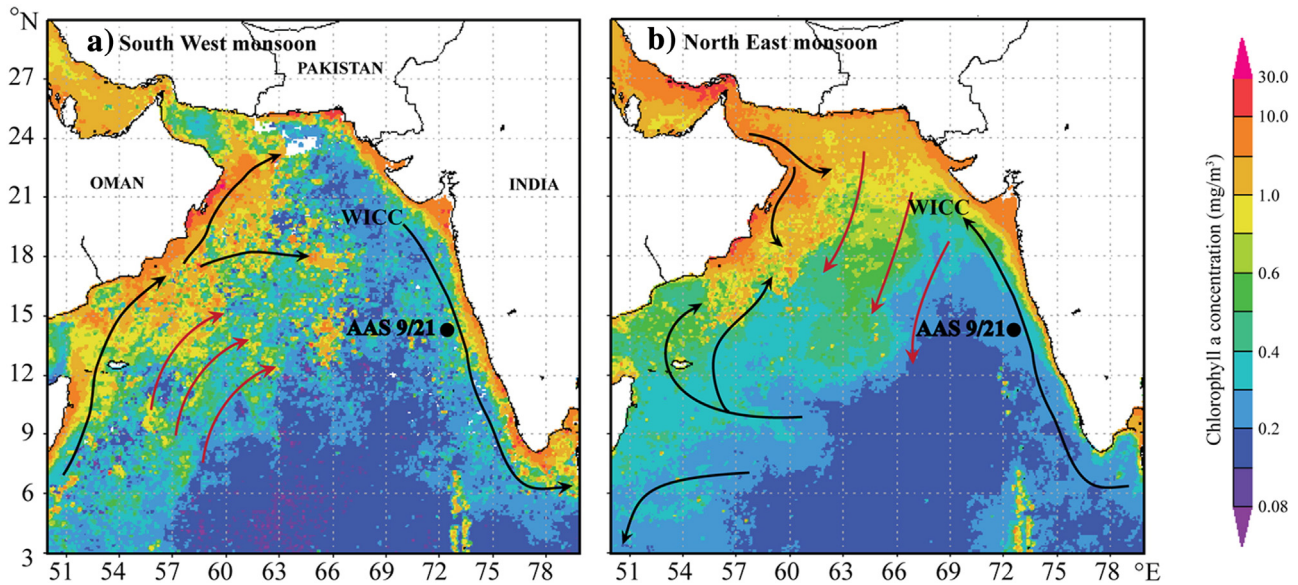


Fig. 1. Core AAS 9/21 sampling site and schematic representation of the ocean circulation (black lines) and dominant wind directions (red lines) in the Arabian Sea during the monsoons (as inferred from Shankar et al., 2002; Schott et al., 2009; Cabarcos et al., 2014). Map indicates chlorophyll concentration (source NASA/Sea WiFS) during a) the South West monsoon and b) the North East monsoons. WICC = West Indian Coastal Current. (For interpretation of the references to colour in this figure legend, the reader is referred to the web version of this article.)

increased abundance of heterotrophic species cysts reveals availability of prey organisms and productivity changes (Zonneveld, 1997a; Marret and Zonneveld, 2003; Kim et al., 2009; Zonneveld et al., 2013). In recent surface sediments, dinoflagellate cyst distribution patterns have shown correlation with regionally varying surface water masses, physico-chemical (temperature, salinity, dissolved oxygen, nutrients) and biological (food availability, productivity) factors (Marret and Zonneveld, 2003; Zonneveld et al., 2013).

Here we present dinoflagellate cyst abundance and assemblage records at a millennial resolution in the EAS over the last 68 ka. The focus of the present study is to better understand the marine primary productivity changes and seasonal monsoonal dynamics in relation to past climatic variability in the EAS over the late Quaternary period.

2. Climatic and oceanographic setting

Semi-annual reversal of the SW and NE monsoon winds divides the year in the SW monsoon and NE monsoon seasons respectively, separated by the two inter-monsoonal periods (spring and fall). The environmental changes induced by the monsoonal variability strongly influence oceanographic and climatic features in the Arabian Sea. Strong SW winds that develop during the SW Monsoon (May–September) as a result of differential heating of the continental and oceanic regions, lead to low atmospheric pressure above the Asian Plateau and high atmospheric pressure over the relatively cool southern Indian Ocean. In response to this, strong wind induces offshore Ekman transport, which results into intense upwelling off Somali and Oman region (Wyrтки, 1973; Clemens et al., 1991; Morrison et al., 1998). During this period the West Indian coastal current (WICC) develops in the NAS and flows towards the equatorward (Shankar et al., 2002; Fig. 1). The offshore divergence (Ekman transport) along shore wind stress component leads to moderate coastal upwelling along the central west coast of India (Shetye et al., 1985). In the EAS, SW Monsoon precipitation from the Western Ghats drains into the Arabian Sea through rivers and streams, which develops low saline plume towards offshore (Sarkar et al., 2000). As a result, increased thermal stratification reduces mixed layer depth (MLD) and nutrient advection to the euphotic layers (Gerson

et al., 2014). Along the coastal regions, the supply of nutrient from upwelled bottom water and terrestrial runoff increases the primary production (Bhattathiri et al., 1996).

During the NE monsoon (November–February), the wind pattern over the basin reverses to northeast due to development of high pressure gradient over the Tibetan Plateau and Central Asia, resulting into flow of cold and dry winds over the Arabian Sea. This change in wind pattern reverses the direction of the WICC northwards (Shankar et al., 2002; Fig. 1). During NE monsoon about 6 Sv of low saline water of the Bay of Bengal intrudes into the Arabian Sea (Shankar et al., 2002). The dry NE winds generally enhance the evaporation in the NAS, subsequently cooling and convective mixing inject nutrients into the surface layers from the thermocline region, which in turn increases productivity (Banse, 1987; Madhupratap et al., 1996), whereas in the EAS also, deep convective winter mixing supports moderate increase in productivity (Bhattathiri et al., 1996; Prasanna Kumar et al., 2000; Gerson et al., 2014) and biogenic particle flux (Haake et al., 1993) in the open ocean region.

3. Material and methods

3.1. Sediment core

A 4.2 m gravity sediment core AAS 9/21 was collected from the continental slope off Goa, in the EAS (14°30.539'N, 72°39.118'E; water depth 1807) during the A.A. Sidorenko cruise 9 (Fig. 1). The sedimentary sequence consists of a mixture of terrigenous and biogenous material. The terrigenous material comprises clay and silt, whereas the biogenous material consists of planktonic and benthic foraminifera and traces of pteropods and diatoms (Govil and Naidu, 2010).

The Chronology of the core AAS 9/21 up to 310 cm depth was established based on six Accelerator Mass Spectrometry (AMS) ^{14}C dates (Table 1). Below, the chronology was established by correlating $\delta^{18}\text{O}$ of *Globigerinoides ruber* record with the low-latitude global isostack curve of Martinson et al. (1987) (refer Govil and Naidu (2010)). Sedimentation rate varies from 4.6 to 13.6 cm ka $^{-1}$ at the core location (Figs. 2 and 3m; Govil and Naidu, 2010).

Table 1
Age model for core AAS 9/21.

Depth (cm)	Radiocarbon age*	Calibrated calendar years BP**
0	850 ± 25	512 ± 9
53	9540 ± 80	10,343 ± 326
110	12,770 ± 80	14,529 ± 326
148	16,070 ± 115	18,965 ± 240
213	21,290 ± 180	24,980 ± 458
310	42,660 ± 2500	46,282 ± 2283

*AMS ^{14}C dating was performed on monospecific samples of the planktonic foraminifera *G. ruber* using the Tandem Accelerator at Leibniz Labor für Altersbestimmung und Isotopenforschung, Christian-Albrechts-Universität, Kiel, Germany. **Measured ^{14}C ages were converted to sediment ages using the online CalPal version QuickCal 2005 version 1.4 (Weninger et al., 2006) [adopted from Govil and Naidu (2010)].

3.2. Palynological sample preparation and analysis

The core was cut into 3 cm-thick slices, out of which samples from alternative sections were used for dinoflagellate cyst analysis. Seventy five samples covering a span of ~68 ka were processed using the palynological method (Matsuoka and Fukuyo, 2000) with some modifications. A known weight of dry sediment (7–8 g) was repeatedly washed with distilled water to remove salts, sonicated (30 s.) and sieved through 120 μm and 10 μm meshes to remove coarse and fine particles. The slurry accumulated on 10 μm was treated with HCl (10%) for 10 h and HF (30%) for 36–48 h to dissolve calcareous and silicate materials. Each chemically treated sample was washed with distilled water to remove acid, sonicated for 30 s. Later, the slurry was sieved through 10 μm to remove fine material. The residue accumulated on the 10 μm mesh was then suspended in 10 ml distilled water and kept in a vial. For

observation, aliquots of processed sample were counted in duplicate or a higher number of replicates, such that a minimum of 250 cysts were counted per sample. However, in some samples (representing ages ~8.3, 1.0, 1.67, 11.11 and 11.92 ka) only 150 to 160 cysts were counted. Dinoflagellate cyst abundance was estimated per gram dry weight sediment (cysts g^{-1}).

Dinoflagellate cysts were identified by using inverted microscope (Olympus IX 71) at 200 \times and 1000 \times magnifications based on published morphological descriptions (Fensome et al., 1993; Zonneveld, 1997b; Lewis et al., 1999; Matsuoka and Fukuyo, 2000; Rochon et al., 2009; Radi et al., 2013) and modern dinoflagellate cyst determination key by Zonneveld and Pospelova, (in press) (on-line version: https://www.marum.de/en/Modern_dinoflagellate_cyst_determination_key.html). The nomenclature used for this study is in accordance with Head (1996), Zonneveld (1997b), Fensome and Williams (2004).

On the basis of morphological similarity some dinoflagellate species have been grouped together prior to statistical analysis. *Spiniferites* species, *S. ramosus* and *S. bulloideus* were grouped together as *S. ramosus* because of very slight interspecific morphological variation in size and processes thickness. Similarly, *S. mirabilis* and *S. hyperacanthus* have morphological similarities with the exception of the absence of crown process in *S. hyperacanthus*, hence grouped together as *S. mirabilis* (Radi and de Vernal, 2008; Rochon et al., 2009). *S. quanta* and cyst of *P. nudum* have similar morphology with some variation in size and number of process, hence considered as *S. quanta*. *Stelladinium* species, *S. stellatum* and *S. reidii* were grouped as *S. stellatum*. *Brigantedinium* spp. represent all smooth walled, spherical brown cysts. In absence of archeopyle intraspecific differentiation is difficult in these morphotypes, whereas sometimes cyst folding also hides the archeopyle structure (Pospelova et al., 2006).

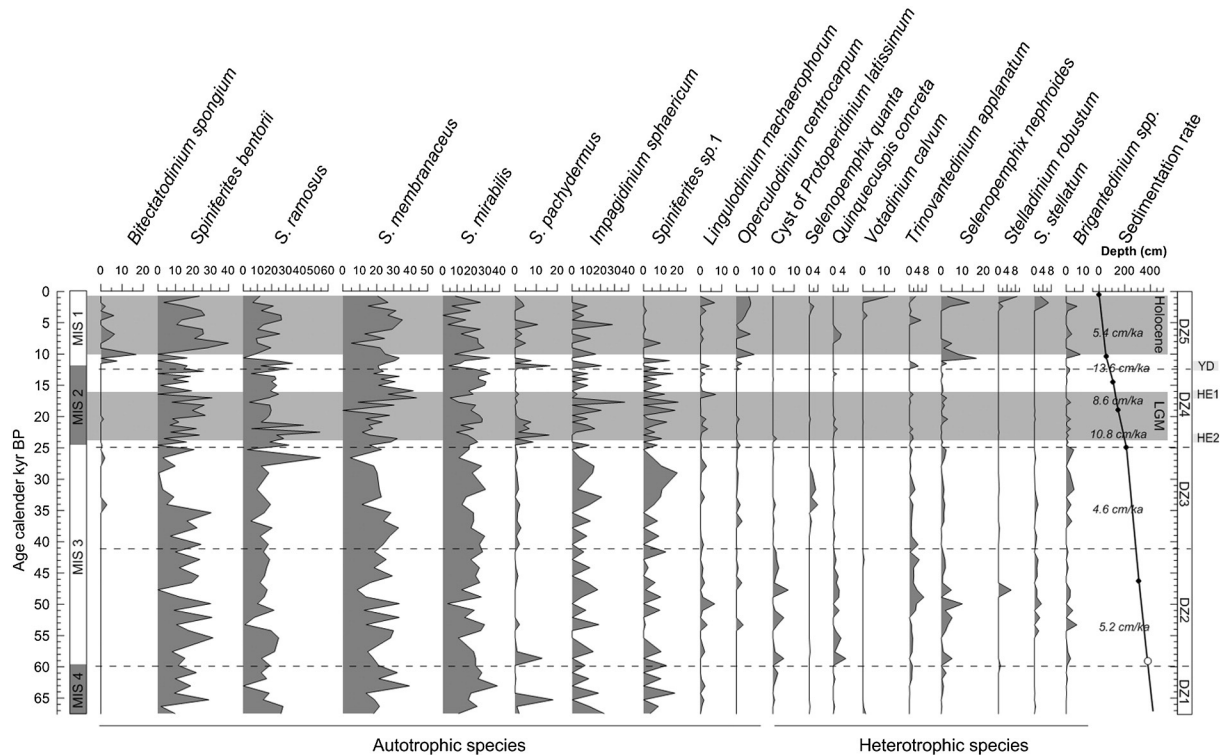


Fig. 2. Relative abundances (%) of selected dinoflagellate cyst taxa and a plot of age–depth along with sedimentation rates (cm ka^{-1}) corresponding between two tie points. AMS ^{14}C dates calibrated to calendar age (filled circles) and isotope stage boundary of MIS 3 and 4 (unfilled circle) [Govil and Naidu, 2010]. Dinoflagellate cyst zones (DZ) are separated by dashed lines. The Holocene and LGM are shown by grey shaded horizontal bars. Heinrich events (HE 2 and HE 1) and the Younger Dryas (YD) are highlighted in grey.

3.3. Statistical analysis

The abundance of dinoflagellate cyst was further subjected to calculate species diversity (Shannon–Wiener diversity index i.e. H'), species richness and evenness using the software PRIMER (version 6).

Further multivariate statistical analysis was performed on relative abundance data of dinoflagellate cyst using CANOCO 4.5 software for Windows (ter Braak and Smilauer, 2002). Prior to statistical analysis, dinoflagellate cyst data were logarithmically transformed ($\log x + 1$) to minimize the dominance of few abundant species and increase the weight of less abundant species, which could thrive in narrow ecological niche. To determine the variability within data set Detrended Correspondence Analysis (DCA) was performed. The length of the first gradient axis was 1.7 standard deviation unit (sd) indicates linear variation (ter Braak and Smilauer, 2002) in cyst assemblage within the core sections. Due to linear character of data set a Principle Component Analysis (PCA) was performed, which can reduce dimensionality of the data set and summarize it by extracting the smallest number components that account for most of the variations in the original multivariate data (Hair et al., 1992).

4. Results

4.1. Dinoflagellate cyst assemblage and abundance

A total of 29 dinoflagellate cyst species were identified from 75 sediment sample intervals analysed in the core AAS 9/21, covering a time

Table 2

List of dinoflagellate cyst species identified in sediment samples from the Core AAS 9/21 with abbreviations and thecate dinoflagellate affinity.

Dinoflagellate cyst (Paleontological name)	Abbreviations	Thecate dinoflagellate affinity (Biological name)
Autotrophic		
<i>Bitectatodinium spongium</i>	Bspo	–
<i>Impagidinium aculeatum</i>	Iacu	<i>Gonyaulax</i> sp.
<i>Impagidinium paradoxum</i>	Ipar	<i>Gonyaulax</i> sp.
<i>Impagidinium sphaericum</i>	Isph	<i>Gonyaulax</i> sp.
<i>Lingulodinium</i>	Lmac	<i>Lingulodinium polyedra</i>
<i>machaerophorum</i>		
<i>Nematosphaeropsis labyrinthus</i>	Nlab	<i>Gonyaulax spinifera</i> complex
<i>Operculodinium centrocarpum</i>	Ocen	<i>Protoceratium reticulatum</i>
<i>Polysphaeridium zoharyi</i>	Pzoh	<i>Pyrodinium bahamense</i>
<i>Spiniferites bentorii</i>	Sben	<i>Gonyaulax digitalis</i> , <i>G. spinifera</i> complex
<i>Spiniferites bulloideus</i>	–	<i>Gonyaulax scrippsae</i> , <i>G. spinifera</i> complex
<i>Spiniferites hyperacanthus</i>	–	<i>Gonyaulax spinifera</i> complex
<i>Spiniferites membranaceus</i>	Smem	<i>Gonyaulax spinifera</i> complex
<i>Spiniferites mirabilis</i>	Smir	<i>Gonyaulax spinifera</i> complex
<i>Spiniferites pachydermus</i>	Spac	<i>Gonyaulax spinifera</i> complex
<i>Spiniferites ramosus</i>	Sram	<i>Gonyaulax scrippsae</i> , <i>G. spinifera</i> complex
<i>Spiniferites</i> sp. 1	Ssp.1	<i>Gonyaulax</i> sp. complex
Heterotrophic		
<i>Brigantedinium</i> spp.	Bsp.	<i>Protoperidinium</i> spp.
–	Pkof	<i>Polykrikos kofoidii</i>
–	Plat	<i>Protoperidinium latissimum</i>
<i>Echinidinium transparantum</i>	Etra	<i>Protoperidinium</i> sp.
<i>Quinquecupis concreta</i>	Qcon	<i>Protoperidinium leonis</i>
<i>Selenopemphix nephroides</i>	Snep	<i>Protoperidinium subinermis</i>
<i>Selenopemphix quanta</i>	Squa	<i>Protoperidinium conicum</i>
–	–	<i>Protoperidinium nudum</i>
<i>Stelladinium robustum</i>	Srob	<i>Protoperidinium</i> sp.
<i>Stelladinium stellatum</i>	Sste	<i>Protoperidinium stellatum</i>
<i>Stelladinium reidii</i>	–	<i>Protoperidinium</i> sp.
<i>Trinovantedinium applanatum</i>	Tapp	<i>Protoperidinium pentagonum</i>
<i>Votadinium calvum</i>	Vcal	<i>Protoperidinium oblongum</i>

span of ~68 ka (MIS 1–4) (Table 2). The number of species varied from 4 to 17. Cysts of autotrophic Gonyaulacoid species were the most dominant and mainly represented by *Spiniferites* group, *Spiniferites ramosus* (up to 54%), *S. membranaceus* (up to 45%), *S. bentorii* (up to 40%), *S. mirabilis* (up to 38%), *Impagidinium sphaericum* (up to 37%) and *Spiniferites* sp. 1 (up to 21%) (Fig. 2). Other dominant autotrophic species were *S. pachydermus* (up to 17%) and *Operculodinium centrocarpum* (up to 8%). Among heterotrophic species, *Selenopemphix nephroides* (up to 13%), *Brigantedinium* spp. (up to 8%) and *Trinovantedinium applanatum* (up to 7%) were dominant.

Dinoflagellate cyst abundance varied down-core from ~140 to 26,000 cysts g^{-1} , averaging 3000 cysts g^{-1} (Fig. 3a). Cyst abundance was higher (~260 to 3390 cysts g^{-1} , avg. 1470 cysts g^{-1}) in MIS 4 than in early MIS 3 (~222 to 2081 cysts g^{-1} , avg. 987 cysts g^{-1}), whereas approximately twofold increase was observed in late MIS 3 (~41.67 to 25.3 ka) (~1030 to 6350 cysts g^{-1} , avg. 3210 cysts g^{-1}). The cyst abundance was twofold higher during MIS 2 (~1500 to 26,000 cysts g^{-1} , avg. 5450 cysts g^{-1}), including the LGM (19 to 21 ka), than in MIS 3. In the Holocene, cyst abundance decreased about threefolds than the preceding LGM (Fig. 3a). Over the last 68 ka autotrophic Gonyaulacoid species were dominant (avg. 2400 cysts g^{-1}), than heterotrophic Protoperidinooid species (avg. 80 cysts g^{-1}) (Fig. 3b and d). Although, absolute abundance of heterotrophic cyst taxa was less, their relative abundance was comparatively more during MIS 3 and in the late Holocene (from ~3 ka onwards) (Fig. 3d). The heterotrophic (H) and autotrophic (A) dinoflagellate cyst ratio (H/A) decreased during MIS 4, MIS 2 and the early Holocene (Fig. 3e). An abrupt increase in H/A ratio towards the late Holocene and large variation during MIS 3 was due to contribution of Protoperidinooid species (Fig. 3d and e).

The Shannon–Wiener, a species diversity index (H') varied from 1.05 to 2.39. It was the highest from ~35 to 25 ka and since ~3 ka, and the lowest was observed during the LGM to early Holocene (Fig. 3f). Species richness also followed similar trends as that of species diversity index (Fig. 3g). However, species evenness varied from 0.59 to 0.95, cyst assemblage was more even in MIS 1 (avg. 0.86) (Fig. 3h).

4.2. Statistical analysis and dinoflagellate cyst zones

A Principle Component Analysis (PCA) performed on the logarithmically transformed relative abundance data of dinoflagellate cyst, reveals four principal components axis (1–4 PCs) accounting 28.4%, 11.5%, 8.8% and 7.3% of variances respectively, with total cumulative variance of 56%. Graphical representation of the same, a PCA biplot, shows ordination of each species and samples along the first two most dominant PCs, PCA1 and PCA2 (Fig. 4). Samples similar in species composition are located close to each other in the PCA biplot. Based on sample score for PCA1, PCA2 and relative abundance of dinoflagellate cyst, five dinoflagellate cyst zones (DZ1–5) were established. All dinoflagellate cyst zones were characterised by dominance of *Spiniferites* species. Apart from this, the characteristic species composition of each zone is presented below.

4.2.1. DZ1 (~67.5 to 58.67 ka)

This zone was dominated by autotrophic *Spiniferites* species, *S. membranaceus* (avg. ~23.2%), *S. mirabilis* (avg. 23.4%), *S. ramosus* (avg. 16.8%) and *S. bentorii* (avg. 13.9%), and relatively less contribution of Protoperidinooid species (avg. 0.03%), which results into lesser Shannon–Wiener diversity index, species richness and evenness (Fig. 2 and 3e, f, g). This zone corresponds to MIS 4 and is characterised by fluctuating values of PCA1 and negative values of PCA2 (Fig. 3i and j).

4.2.2. DZ2 (~58.60 to 42.87 ka)

Approximately twofold decrease in absolute cyst and Gonyaulacoid cyst abundance was observed in DZ2 than the preceding DZ1 (Fig. 3a and b). Increased relative abundance of Protoperidinooid species, *Brigantedinium* spp., *S. nephroides*, *S. stellatum*, *Q. concreta*, cyst of

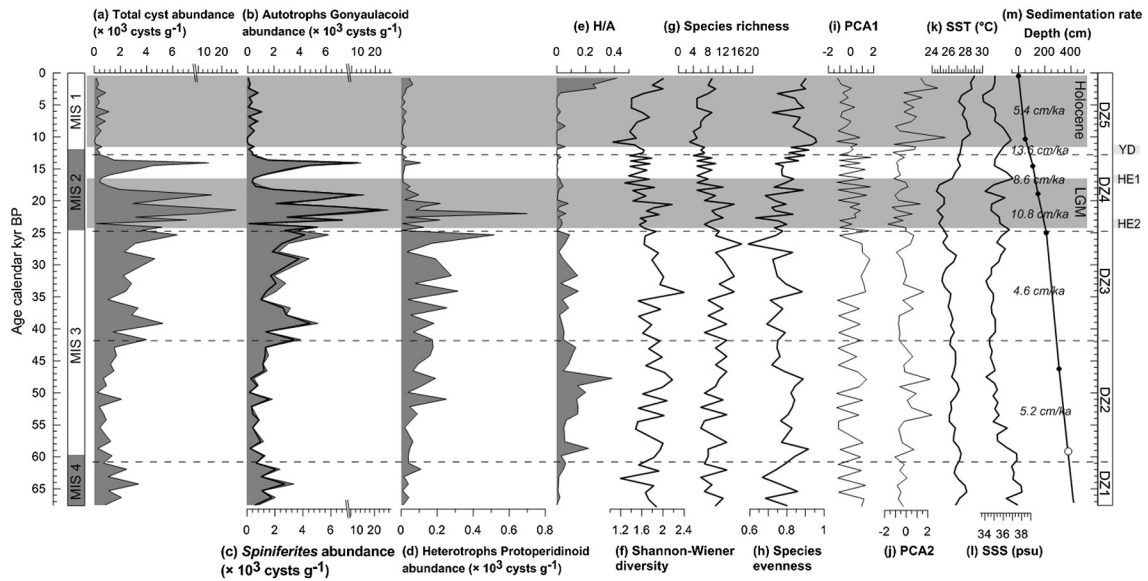


Fig. 3. (a) Total cyst abundance along with (b) Autotrophic Gonyaulacoid (c) *Spiniferites* (dark line) and (d) Heterotrophic Protoperidinoid species abundance; (e) Ratio of heterotrophic to autotrophic cysts (H/A); diversity indices (f) Shannon–Wiener diversity index, (g) Species richness, (h) Species evenness; sample score for (i) PCA 1, (j) PCA 2 and (k) Sea surface temperature (SST) and (l) Salinity (SSS) estimated using Mg/Ca and $\delta^{18}\text{O}$ of *Globigerinoides ruber* respectively (Govil and Naidu, 2010), (m) Plot of age–depth along with sedimentation rates (cm ka^{-1}) corresponding between two tie points. AMS ^{14}C dates calibrated to calendar age (filled circles) and isotope stage boundary of MIS 3 and 4 (unfilled circle) [Govil and Naidu, 2010]. Dinoflagellate cyst zones (DZ) are separated by dashed lines. The Holocene and LGM are shown by grey shaded horizontal bars. Heinrich events (HE 2 and HE1) and the Younger Dryas (YD) are highlighted in grey.

P. latissimum and *T. applanatum* was observed during this period, which could also be responsible for increase in the H/A ratio and Shannon–Wiener diversity index (Fig. 2 and 3e, f).

4.2.3. DZ3 (~41.67 to 25.30 ka)

DZ3 extends from mid to late MIS 3 and is distinguished by mostly positive PCA1 and PCA2 values (Fig. 3i and j). Relative abundance of

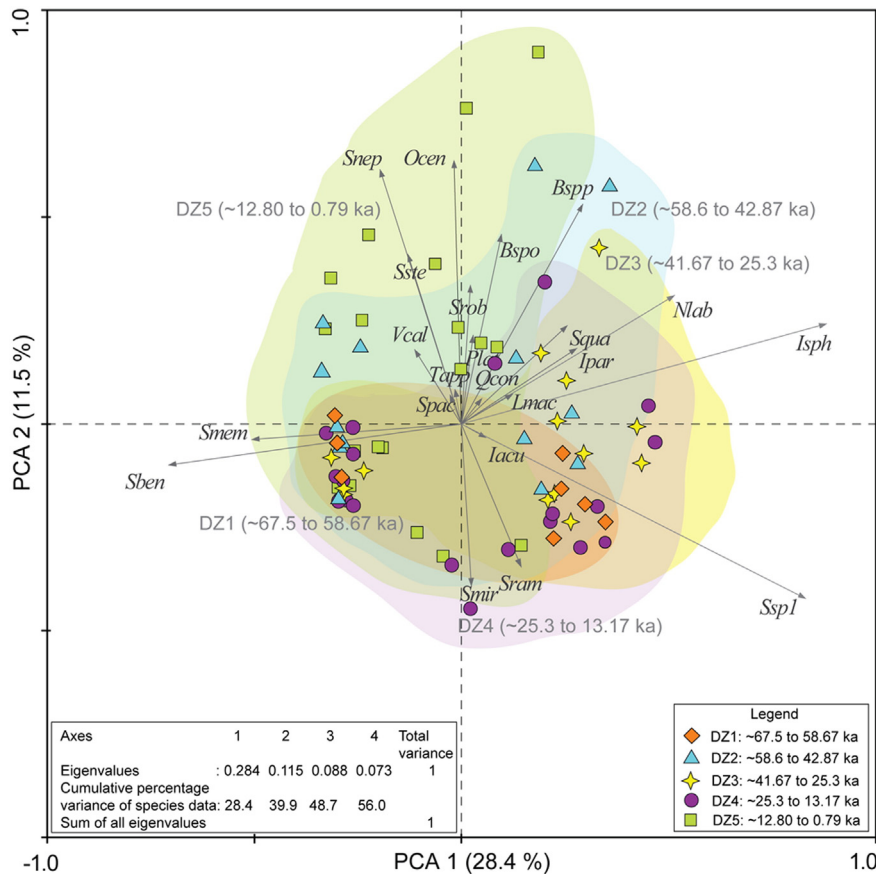


Fig. 4. Principle Component Analysis (PCA) biplot diagram indicate dinoflagellate cyst species (grey arrows) in relation with sediment sample ordination (coloured symbols; diamond, triangle, star, circle, square). Species abbreviations are as given in Table 2.

S. mirabilis (avg. 21.91%), *S. membranaceus* (avg. 21.3%), *S. ramosus* (avg. 16.6%) and *S. bentorii* (avg. 12.09%) increased during this period, whereas heterotrophic taxa *S. quanta* (avg. ~0.8%) appeared during ~34.09 to 29.04 ka (Fig. 2).

4.2.4. DZ4 (~24.6 to 13.17 ka)

DZ4 coincides with MIS 2, including the LGM. Absolute cyst and autotrophic species abundance showed large fluctuation with numerous spikes (Fig. 3a and b), whereas heterotrophic species abundance was the highest during the LGM. An abrupt decrease in absolute cyst, autotrophic and *Spiniferites* species abundance was observed during early MIS2 (23.54 and 20.39 ka) and from 17.03 to 16.45 ka (Fig. 3a, b and c). Changes in cyst assemblage and abundance were also reflected in fluctuating values of PCA1, whereas most of the PCA2 values were negative (Fig. 3i and j). Relative abundance of *S. membranaceus* (avg. ~22%), *S. ramosus* (avg. 21.54%) and *S. mirabilis* (avg. 21.36%) reached its maximum during the LGM whereas it was declined in case of heterotrophic taxa *Brigantedinium* spp. (avg. ~0.7%), *Selenopemphix quanta* (avg. ~0.02%), *Quinquecuspis concreta* (avg. ~0.2%) and *Trinovantedinium applanatum* (avg. ~0.4%) (Fig. 2). Absolute abundance of heterotrophic species was the lowest during this period than the preceding MIS 3 which negatively influenced H/A ratio (Fig. 3e). Fluctuating values of species indices also support the variability in cyst assemblage during this period. Overall decreasing trend in *Protoperidinium* taxa reflected in decreased Shannon–Wiener index, species richness whereas increasing species evenness could be supported by increased abundance of *Gonyaulacoid* species (Fig. 3b, d, f, g and h).

4.2.5. DZ5 (~12.80 to 0.79 ka)

An abrupt increase in cyst of autotrophic taxa, *Bitectatodinium spongium*, *S. pachydermus* and *O. centrocarpum* was the characteristic feature of this zone (Fig. 2). *S. bentorii*, *S. membranaceus* and *S. mirabilis* relatively dominate cyst assemblage especially during 12.36, 9.4, 6.07 and 3.1 ka, in the Holocene (Fig. 2). Relative abundance of heterotrophic species, *S. stellatum*, *S. robustum*, *V. calvum* and *S. nephroides* increased during the late Holocene (~3 ka), which in turn increases H/A ratio, species richness and evenness (Fig. 2 and 3e, f, g). Shannon–Wiener diversity index was the lowest during the entire Holocene, and increased since ~3 ka due to appearance of heterotrophic species. PCA1 values were positive whereas PCA2 values were negative in DZ5 (Fig. 3i and j).

5. Discussion

Dinoflagellate cyst production in the marine environment is mainly influenced by physico-chemical factors such as sea surface temperature (SST), sea surface salinity (SSS) and nutrients, thus cyst abundance and assemblages in sediments have been used to reconstruct climatic and oceanographic variability in the geological past (de vernal et al., 2001; Dale, 2001; Mudie et al., 2002; Morquecho and Lechuga-Deveze, 2004; Pospelova et al., 2008; Zonneveld et al., 2013). Recent sediment trap and cyst distribution studies in the Arabian Sea revealed the monsoon influence on cyst production and assemblage (Zonneveld, 1997a; Zonneveld and Brummer, 2000; D'Costa et al., 2008). Here, we demonstrate the use of dinoflagellate cyst abundance as a paleoceanographic proxy to understand the monsoonal productivity and OMZ variations in the EAS (Table 3).

5.1. Dinoflagellate cyst preservation and OMZ intensity

Dinoflagellate cyst can be affected by oxidative degradation similar to the organic matter, especially cysts of the *Protoperidinium* species, which appear to be more sensitive to oxidative degradation than the *Spiniferites* species (Zonneveld et al., 1997a). Poor preservation of *Protoperidinium* in sediment can be linked to aerobic decay in oxygenated bottom water and weak intensity of the OMZ (Zonneveld et al.,

Table 3

Schematic presentation of variation in productivity, OMZ, monsoon and dinoflagellate cyst assemblage in the EAS during the four Marine Isotopic Stages (MIS 1–4).

MIS 1 Strong summer Monsoon Increased rainfall Increased SST + decreased SSS Stratified water Cloud cover + low light penetration	DZ5 (~12.8 to 0.79 ka) Total cyst abundance (∇) Gonyaulacoid species (∇) Protoperidinium species (∇) Reduced productivity
MIS 2 Strong winter monsoon Reduced SST + fluctuating SSS Less turbulence + deeper light penetration	DZ4 (~24.6 to 13.17 ka) Abrupt changes in total cyst abundance Fluctuation in Gonyaulacoid and Protoperidinium abundance High productivity
MIS 3 Increased strength of winter monsoon Decreasing SST + increasing SSS Increased winter convection Increased light penetration	DZ3 (~41.67 to 25.3 ka) Total cyst abundance (▲) Gonyaulacoid species (▲) Protoperidinium species (▲) Increase in productivity Intense OMZ
Strong summer monsoon Increased rainfall Reduced SST + SSS Stratified water + shallow MLD Cloud cover + reduced light penetration	DZ2 (~58.6 to 42.87 ka) Total cyst abundance (∇) Gonyaulacoid species (∇) Protoperidinium species (▲) Increasing OMZ intensity
MIS 4 Moderate winter monsoon convection High SST + SSS Less turbulence + deeper light penetration	DZ1 (~67.5 to 58.67 ka) Total cyst abundance (▲) Gonyaulacoid species (▲) Protoperidinium species (∇) Increased productivity

1997a, 2007; Reichart and Brinkhuis, 2003), therefore high abundance of *Protoperidinium* species could indicate the increased productivity and good preservation state in the OMZ sediments (Reichart and Brinkhuis, 2003; Zonneveld et al., 2007; Zonneveld et al., 2013). Reichart and Brinkhuis (2003) used *Protoperidinium* cyst as proxy for paleoproductivity in the NAS, where comparison of *Protoperidinium* cyst abundance within and outside the OMZ settings highlighted their degradation during paleo-climatic events where bottom waters were oxic. In the core AAS 9/21, absolute abundance of *Protoperidinium* varies over last 68 ka with maximum abundance in MIS 3 and late Holocene (Fig. 3e). This increase in *Protoperidinium* cyst abundance could be facilitated by their better preservation due to reduced oxygen supply and increased denitrification resultant of intense OMZ, an inference supported by several line of evidences. First, higher $\delta^{15}\text{N}$ and C_{org} value during MIS 3 and late Holocene reveals the increased denitrification and better organic matter preservation in the Core AAS 9/21 sediments (Godad, 2014). Second, increased Mo concentration highlights the low oxygen condition and intensified OMZ during this period (Godad, 2014). Since *Protoperidinium* cysts can be used as productivity proxy, we could expect higher *Protoperidinium* cyst abundance during MIS 4 than in MIS 3, because in the EAS productivity was higher during glacials than interglacials (Ivanochko, 2004; Banakar et al., 2005; Kessarkar et al., 2010; Singh et al., 2011). The sedimentary $\delta^{15}\text{N}$ and Mo records in the core AAS 9/21 reveal weak OMZ due to less denitrification and oxic conditions during the glacials (MIS 4 and MIS 2) (Godad, 2014). This is further supported by other studies in the EAS, which reveal that OMZ was less intense and water column denitrification declined during the glacial periods (Ivanochko et al., 2005; Kessarkar et al., 2010). In this context, the variation in *Protoperidinium* cyst abundance can be used as a biological proxy to reconstruct the OMZ variation (Table 3), similar to other geochemical proxies in the late Quaternary sediments along the EAS, in particular species like *Q. concreta*, *S. stellatum*, *S. nephroides*, *T. applanatum* and *Brigantedinium* sp. which are more susceptible for oxidative

degradation and observed in higher concentrations in anoxic or hypoxic sediments (Zonneveld et al., 1997a, 2007; Zonneveld et al., 2013).

Cyst produced by Gonyaulacoid species, *L. machaerophorum*, *O. centrocarpum* and *Spiniferites* species including *S. bentorii*, *S. mirabilis*, *S. pachydermus* and *S. ramosus* are proven to be moderately sensitive, whereas *Impagidinium* species (*I. aculeatum* and *I. paradoxum*) and *N. labyrinthus* are resistant to the oxidative degradation (Zonneveld et al., 1997a, 2007). Reichart and Brinkhuis (2003) reported that in surface sediments within and outside the OMZ in the WAS, where fluxes in the productive sea-surface layer were identical, concentrations of most Gonyaulacoid species were similar in all sediments, whereas the OMZ samples were relatively enriched in *Protoberidinium* cysts. The effect of post-depositional species-selective oxidative degradation was minimal on preservation of Gonyaulacoid species than *Protoberidinium* (Reichart and Brinkhuis, 2003). In the core AAS 9/21, autotrophic Gonyaulacoid species dominated cyst assemblage, with peaks in MIS 4, late MIS 3 and MIS 2 (Fig. 3b). Increased absolute abundance of Gonyaulacoid species, in particular *Spiniferites* species during these periods reflects the variability in the primary productivity and monsoon in the EAS (Table 3).

5.2. Productivity variations in the EAS

Dinoflagellate cyst assemblage composition reflects surface productivity and their fossil assemblages were used for the reconstruction of the paleoproductivity during the Late Quaternary period in the Santa Barbara Basin (Pospelova et al., 2006), Guaymas Basin (Price et al., 2013), Gulf of Alaska (de Vernal and Pedersen, 1997; Marret et al., 2001), the Arctic region (Matthiessen et al., 2005), the Black sea (Mudie et al., 2002) and the south China Sea (Shaozhi and Harland, 1993). In the WAS, relative abundance of dinoflagellate cyst was used for the reconstruction of the SW monsoon variability during the Late Quaternary (Zonneveld et al., 1997b), whereas in the Bay of Bengal variation in cyst abundance and species assemblage was implicated to study the Late Quaternary productivity and climatic variability (Naidu et al., 2012). In Core AAS 9/21, temporal variation observed in Gonyaulacoid species, *Spiniferites* species in particular, provide valuable information about the millennial time scale productivity variations in the EAS region and is discussed below.

High absolute abundance of Gonyaulacoid species, *Spiniferites* species in particular, during MIS 2 and MIS 4, indicates biological productivity increase during the glacials (Fig. 3c,d and 5). *Spiniferites* cysts belong to autotrophic *Gonyaulax* species, which can sustain in wide range of environmental variables (mainly salinity, temperature and nutrients) (Zonneveld et al., 2013). Higher abundance of *Spiniferites* species during the glacials suggests nutrient supply from deeper waters due to vertical winter convection resultant of the strong NE Monsoons, whereas reduced strength of the SW Monsoon decreases cloud cover and supply of low saline terrestrial runoff. This reduces turbidity and increases light penetration into euphotic layers which in turn favours growth of *Spiniferites* species. Zonneveld and Brummer (2000), also observed high flux of *Spiniferites* species in the sediment trap along the Somalian region during the end of the SW monsoon when water conditions were relatively stable with high nutrient concentrations and reduced turbulence. Furthermore, our interpretation of the NE monsoonal control on glacial productivity in the EAS gets support from CaCO₃ data in the present core (Godad, 2014) and recent planktonic foraminifera, coccolithophore and geochemical productivity proxy data from other core studies in the region (Rostek et al., 1997; Ivanochko, 2004; Singh et al., 2006, 2011; Cabarcos et al., 2014). The planktonic foraminiferal species and geochemical proxy records in the core MD76-131 and SK 17 increased twofold during the glacials and has been attributed to productivity increase due to nutrient enrichment resultant of the NE Monsoon induced winter mixing (Singh et al., 2006, 2011; Naidu et al., 2014). The strong, cold and dry NE winds during the glacial would have resulted in enhanced evaporation, resulting in increase of

SSS (Govil and Naidu, 2010) and convective upward winter mixing in the EAS (Singh et al., 2011; Rostek et al., 1997; Cabarcos et al., 2014). The above-mentioned cores (MD76-131 and SK 17) were from the present OMZ regions. Thus, comparison of cyst abundance records in the core AAS 9/21 with the productivity trends observed in OMZ cores supports that *Spiniferites* species abundance in the present core can be a good indicator of productivity changes during the glacial and interglacial periods in the EAS.

In glacials, *Spiniferites* species abundance was comparatively lower during the MIS 4 than MIS 2 (Fig. 3b), which could reveal the productivity variability during the MIS 4 and MIS 2. This could be attributed to comparatively decreased strength of the NE Monsoon during the MIS 4 than MIS 2 as observed in salinity proxy ($\delta^{18}\text{O}_w$) records in the core AAS/9-21 (Govil and Naidu, 2010). Furthermore, geochemical paleoproductivity proxy records in OMZ also suggest higher productivity during the MIS 2 than MIS 4 due to the strongest NE monsoon (Banakar et al., 2005).

5.3. Relationship between dinoflagellate cyst assemblage and monsoon variability

The MIS 4 was dominated by *Spiniferites* species, mainly *S. bentorii*, *S. ramosus*, *S. membranaceus* and *S. mirabilis* (Fig. 2 and 3b). In modern sediments, these *Spiniferites* species can be found in the eutrophic to oligotrophic waters, whereas their high relative abundance can be observed in the nutrient elevated waters within well-mixed surface waters as well as outside the upwelling cells (Zonneveld et al., 2013). *S. bentorii*, *S. membranaceus* and *S. mirabilis* are warm-water species. In addition *S. bentorii* and *S. mirabilis* can tolerate high SSS as well (Marret and Zonneveld, 2003; Zonneveld et al., 2013). Higher proportion of *Spiniferites* taxa have also been suggested to reflect the warmer water in the southern Californian region (Prauss, 2002). In the EAS increased abundance of *Spiniferites* species during MIS 4 could be attributed to comparatively warm, hypersaline (Fig. 1, 2) and stable water mass. This interpretation could be supported by previous paleo-salinity reconstructions on this Core AAS 9/21 (Govil and Naidu, 2010), which reveals that during MIS 4, variation in SST and SSS was higher (Fig. 3k and l), indicating the warmer and saline water as a result of increased evaporation and decreased precipitation due to the relatively stronger NE monsoon.

Absolute cyst abundance decreased from MIS 4 to early MIS 3 (~58.6 to 42.87 ka). Similar shift has been observed in *Spiniferites* species, whereas *Protoberidinium* cyst abundance increased in MIS 3 compared to MIS 4 (Fig. 3c and d). This interval characterised by *Q. concreta*, *S. nephroides*, cyst of *P. latissimum*, *T. applanatum* and *Brigantedinium* spp. (Fig. 2). This increase in *Protoberidinium* species abundance could be due to their better preservation in the anoxic sediments as discussed in Section 5.1. During most of the deglaciation, the winter monsoon winds were weak, resulting in reduced vertical mixing. However, the strong SW monsoon and associated river discharge in to the EAS enhances nutrients' supply in surface layers, which fuel the growth of primary producers, mainly diatoms. However, reduced light penetration due to increased turbidity and cloud cover during the prevalent SW monsoon as well as competition with diatom for nutrients could be the reasons for the suppressed growth of *Spiniferites* species during early MIS 3.

The upper section of MIS 3 (~41.67 to 25.3 ka) was characterised by increased abundance of autotrophic *Spiniferites* species (Fig. 3b). In the Santa Barbara Basin, elevated relative abundance of *Spiniferites* species was related to the enhanced input of nutrient enriched water (Pospelova et al., 2006). In core AAS 9/21, increasing relative abundance of *Spiniferites* species, especially *S. membranaceus*, *S. mirabilis* and *S. ramosus* during late MIS 3 could be due to elevated nutrient concentrations resultant of the strong winter convection and more availability of light due to less cloud cover, especially from ~34.09 to 26.62 ka. Cysts of other autotrophic species like *I. sphaericum* and *Spiniferites* sp. 1

increased greatly during this period, which highlights elevated SSS (Fig. 2 and 3k), resultant of increased evaporation due to the strong NE monsoon dry and cold winds. This conclusion is in partly supported by the increasing SSS due to lower precipitation during late MIS 3 (Fig. 3l). Increasing abundance of *Protoperidinium* species, especially *S. quanta* reveals a decrease in oxidative degradation due to intense OMZ (refer Section 5.1).

A shift from relatively stable to largely fluctuating dinoflagellate cyst abundance was noticed during the transition from MIS 3 to MIS 2 (Fig. 3a). Abrupt change in total cyst abundance is the characteristic feature of the MIS 2, including LGM period. Samples from DZ4 are more dispersed in the PCA biplot, demonstrating greater variation in cyst assemblages during MIS 2. Since dinoflagellates respond to their surrounding environmental conditions, high variation in cyst abundance during MIS 2 indicates that variability in the climatic and oceanographic conditions was more complex. Absolute abundance of autotrophic species indicates higher productivity, but largely fluctuating cyst abundance values emphasize that the productivity changes were not constant throughout MIS 2. This fluctuation in the cyst abundance could be due to the varying cyst flux, which can be influenced by variation in sedimentation rate during MIS 2 in the present core (Figs. 2 and 3m). The increased abundance of Gonyaulacoid species, especially *S. ramosus*, *S. membranaceus*, *S. mirabilis*, *S. pachydermus* and *Spiniferites* sp. 1 during this period suggests strong winter mixing due to prevalence of the strong NE monsoon winds. Reduced stratification and deeper MLD facilitate vertical advection of nutrients into upper photic layers, which in turn supports growth of autotrophic dinoflagellates.

Our dinoflagellate records showed the sudden decrease in total cyst abundance, *Spiniferites* species abundance and relative abundance of all dominant species during the stadial periods (Northern hemisphere cold periods), the Heinrich events (HE2 and HE1) and Younger Dryas (YD) (Fig. 2 and 3a). The reduction in the NE monsoon wind-flow during the stadials could lead to reducing the winter deep convective mixing and/or upwelling along the EAS, leading to the higher SST (Govil and Naidu, 2010) and decreased production (Anand et al., 2008; Singh et al., 2011). Although the *Spiniferites* species responds well to warmer SST, a rapid switch to stratified, oligotrophic water due to decreased strength of the NE monsoon controls their growth in the EAS region. Similarly, drastic fluctuations in cyst abundance during the deglaciation caused due to rapid SST fluctuations (Govil and Naidu, 2010).

The dinoflagellate cyst abundance and assemblages document an abrupt change during the transition from MIS 2 to MIS 1 (Fig. 2 and 3a). Absolute cyst abundance that declined from about 12.8 to 10 ka, could be a resultant of decreased winter mixing due to the weak NE monsoon winds during deglaciation period. This result coincides with the sharp decrease in foraminiferal records in the Core SK 17, which suggests low productivity during deglaciation in the EAS (Singh et al., 2011). The most important change in cyst assemblage during this period was the presence of *O. centrocarpum*, *B. spongium* and *S. pachydermus* (from about ~11 ka). *O. centrocarpum* reached its maximum abundance during MIS 1 (Fig. 2). This autotrophic cosmopolitan species tolerates a wide range of salinity and temperature (Zonneveld et al., 2013), and commonly associated with unstable waters at the coastal–oceanic boundary (Dale et al., 2002). In recent sediment, *B. spongium* are typical to warmer tropical–subtropical marine settings with salinity range 31.9 to 38.3 psu, whereas higher abundance can be observed in regions where SST > 20 °C (Zonneveld et al., 2013). *S. pachydermus* are strictly restricted to temperate to equatorial regions (Zonneveld et al., 2013) and able to tolerate SSS 27.8 to 39 psu (Zonneveld et al., 2013). This shift in species assemblage along with increased species diversity could support the increased SST and moderate SSS during the early Holocene (Fig. 3k and l). In the WAS, *B. spongium* and *S. pachydermus* are typically dominant during the SW monsoon upwelling (Zonneveld, 1997a; Zonneveld and Brummer, 2000). The presence of these species during the early Holocene in AAS 9/21 strengthens the belief that the SW monsoon evolved during this period in the Holocene. Furthermore,

increase in SST and decreased trend of $\delta^{18}\text{O}_w$ values and SSS represent increased strength of the SW monsoon during ~10.5 to 3 ka in the present core (Fig. 3k and l; Govil and Naidu, 2010).

Since 3 ka, a major shift in the cyst assemblage was observed. Cyst assemblage was characterised by the appearance of *Protoperidinium* species, *S. stellatum*, *S. robustum*, *S. nephroides* and *V. calvum* (Fig. 2). In modern sediments, high relative abundance of *S. robustum* and *S. stellatum* is found in warm, hypersaline waters in mesotrophic to eutrophic regions. Among these *S. robustum* is endemic in the Indian Ocean (Zonneveld et al., 2013). Occurrence of these species suggests increase in SSS and SST around 3 ka (Fig. 3k and l), which could be due to the weak SW monsoon (Govil and Naidu, 2010). Increased abundance of *Protoperidinium* species could be due to their better preservation in sediment. This is further supported by increased $\delta^{15}\text{N}$ values and reduced Mo concentration during this period, suggests increased denitrification and reduced oxidative stress (Godad, 2014). However, moderate increase in productivity has been observed in the fertile foraminiferal species records between ~3 and 1 ka in the core SK 17 (Singh et al., 2011; Cabarcos et al., 2014) which also reveals the presence of food material and organic matter, whereas this increase in productivity was not evidenced in autotrophic coccolithophore (productivity factor) records in the same core (Cabarcos et al., 2014). In our study, productivity increase during this period was not evidenced by autotrophic Gonyaulacoid species. Thus an inference can be drawn that change in the environmental condition (elevated SST) during the late Holocene period was not optimal to support the growth of these autotrophic species (Fig. 3b). Furthermore, most of the *Spiniferites* species can grow in temperature up to 29 °C (Zonneveld et al., 2013), whereas in the WAS their maximum flux was reported at the end of summer monsoon when temperature ranges from 23 to 27 °C (Zonneveld and Brummer, 2000), which could be the optimum range for their proliferation in the Arabian Sea region. Thus, increased SST (28.5 to 29 °C) in the EAS from ~3 to 1 ka (Govil and Naidu, 2010) could be responsible for the decline in abundance of *Spiniferites* species.

Recent modern dinoflagellate cyst distribution studies in the EAS reveal dominance of *Protoperidinium* species in surface sediments (Godhe et al., 2000; D'Costa et al., 2008; D'Silva et al., 2011). The relative shift in dinoflagellate cyst assemblage during ~3–0.7 ka suggests that the increased trend in *Protoperidinium* abundance incited during this time could be due to changing environment conditions initiated by increased SST and SSS. Thus, it can be predicted that the increase in SST due to global warming would lead to different dinoflagellate assemblages which will be dominated by heterotrophic species in the future.

6. Conclusion

This study presents the first detailed investigation of dinoflagellate cyst records over the late Quaternary period in the EAS. The variation observed in dinoflagellate cyst abundance and assemblages suggests that productivity changes over the past 68 ka in the EAS were influenced by seasonal monsoon circulation. The main dinoflagellate cyst signals recorded in the EAS are as follows;

1. The productivity in the EAS was higher during the glacial than the interglacial periods, and was mainly controlled by nutrient supply from subsurface water due to winter convection driven by the NE monsoonal wind. The productivity change was highlighted by increased abundance of Gonyaulacoid species (especially *Spiniferites*). Within the glacials, productivity was higher during MIS 2 than in MIS 4 and characterised by twofold increase in cyst abundance. During the interglacials, reduction in the primary productivity during early MIS 3 (~67.5 to 58.67 ka) and in MIS 1 was highlighted by less abundance of Gonyaulacoid cyst, which could be due to strong summer monsoon, resulting in intense stratification and reduced light penetration.
2. Dinoflagellate cyst abundance and assemblage difference reveal that productivity was higher during the LGM than Holocene. The LGM

was more dynamic with larger fluctuations in cyst abundance and assemblages. This reveals that winter mixing was not consistent throughout the LGM.

- Variation in *Protoperidinium* species abundance over the past 68 ka represents variation in the OMZ intensity. Increased *Protoperidinium* abundance during MIS 3 and late MIS 1 (~3 ka onwards) highlighted their good preservation in sediments due to strong OMZ.
- SST increased during the Holocene was characterised by increased abundance of *B. spongium*, *S. pachydermus* and *O. centrocarpum*.

The present study supports the use of dinoflagellate cyst abundance and assemblages as a proxy of paleoproductivity and paleoceanographic variability in the EAS. Our dinoflagellate cyst proxy demonstrates that, the EAS responds to both regional and global scale climatic variations.

Acknowledgements

We are grateful to the Director, CSIR-National Institute of Oceanography (NIO), India for his support. We thank Dr. Paropakari, CSIR-NIO, India for sharing the core samples; Dr. Kenneth Neil Mertens, Ghent University, Belgium and Dr. Malte Elbrachter, AWI, Germany for the dinoflagellate cyst identification training course and for providing taxonomic literature. D.D.N. is grateful to CSIR for awarding the Senior Research Fellowship (SRF) and DST-SERB for International Travel Support Scheme. This is a NIO contribution (no. 5770).

Appendix A. Supplementary data

Supplementary data associated with this article can be found in the online version, at <http://dx.doi.org/10.1016/j.palaeo.2015.06.006>. These data include Google maps of the most important areas described in this article.

References

- Anand, P., Kroon, D., Singh, A.D., Ganeshram, R., Ganssen, G., Elderfield, H., 2008. Coupled sea surface temperature–seawater $\delta^{18}\text{O}$ reconstructions in the Arabian Sea at the millennial scale for the last 35 ka. *Paleoceanography* 23.
- Banakar, V., Oba, T., Chodankar, A.R., Kuramoto, T., Yamamoto, M., Minagawa, M., 2005. Monsoon related changes in sea surface productivity and water column denitrification in the Eastern Arabian Sea during the last glacial cycle. *Mar. Geol.* 219, 99–108.
- Banse, K., 1987. Seasonality of phytoplankton chlorophyll in the central and northern Arabian Sea. *Deep-Sea Res.* 134, 713–723.
- Bhattachiri, P., Pant, A., Sawant, S., Gauns, M., Matondkar, S., Mahanraju, R., 1996. Phytoplankton production and chlorophyll distribution in the eastern and central Arabian. *Curr. Sci.* 71, 857–862.
- Bogus, K., Mertens, K.N., Lauwaert, J., Harding, I.C., Vrielinck, H., Zonneveld, K.A.F., Versteegh, G.J.M., 2014. Differences in the chemical composition of organic-walled dinoflagellate resting cysts from phototrophic and heterotrophic dinoflagellates. *J. Phycol.* 50, 254–266.
- Cabarcos, E., Flores, J., Singh, A., Sierro, F., 2014. Monsoonal dynamics and evolution of the primary productivity in the eastern Arabian Sea over the past 30 ka. *Palaeogeogr. Palaeoclimatol. Palaeoecol.* 411, 249–256.
- Clemens, S., Prell, W., Murray, D., Shimmield, G., Weedon, G., 1991. Forcing mechanisms of the Indian Ocean monsoon. *Nature* 353, 720–725.
- D'Silva, M.S., Anil, A.C., D'Costa, P.M., 2011. An overview of dinoflagellate cysts in recent sediments along the west coast of India. *Indian J. Geo-Mar. Sci.* 40, 697–709.
- Dale, B., 2001. The sedimentary record of dinoflagellate cysts: looking back into the future of phytoplankton blooms. *Sci. Mar.* 65, 257–272.
- Dale, B., Dale, A.L., Jansen, J.H.F., 2002. Dinoflagellate cysts as environmental indicators in surface sediments from the Congo deep-sea fan and adjacent regions. *Palaeogeogr. Palaeoclimatol. Palaeoecol.* 185, 309–338.
- D'Costa, P.M., Anil, A.C., Patil, J.S., Hegde, S., D'Silva, M.S., Chourasia, M., 2008. Dinoflagellates in a mesotrophic, tropical environment influenced by monsoon. *Estuar. Coast. Shelf Sci.* 77, 77–90.
- de Vernal, A., Pedersen, T.F., 1997. Micropaleontology and palynology of core PAR87A-10: a 23,000 year record of paleoenvironmental changes in the Gulf of Alaska, northeast North Pacific. *Paleoceanography* 12, 821–830.
- de Vernal, A., Henry, M., Matthiessen, J., Mudie, P.J., Rochon, A., Boessenkool, K.P., Eynaud, F., Grosfjeld, K., Guiot, J., Hamel, D., 2001. Dinoflagellate cyst assemblages as tracers of sea-surface conditions in the northern North Atlantic, Arctic and sub-Arctic seas: the new 'n = 677' data base and its application for quantitative paleoceanographic reconstruction. *J. Quat. Sci.* 16, 681–698.
- Fensome, R.A., Williams, G.L., 2004. The Lentin and Williams index of fossil dinoflagellates. *AASP Found. Contrib. Ser.* 42, 909.
- Fensome, R.A., Norris, G., Sarjeant, W., Taylor, F., Wharton, D., Williams, G., 1993. A classification of living and fossil dinoflagellates. *Micropaleontology Press* 7, 351.
- Gerson, V.J., Madhu, N., Jyothibabu, R., Balachandran, K., Nair, M., Revichandran, C., 2014. Oscillating environmental responses of the eastern Arabian Sea. *Ind. J. Geo-Mar. Sci.* 43, 67–75.
- Godad, S.P., 2014. Variability of SST, monsoon productivity and OMZ over last 40 ka in the Arabian Sea (PhD Thesis). Goa University, pp. 1–110.
- Godhe, A., Karunasagar, I., Karlson, B., 2000. Dinoflagellate cysts in recent marine sediments from SW India. *Bot. Mar.* 43, 39–48.
- Govil, P., Naidu, P.D., 2010. Variations of Indian monsoon precipitation during the last 32 kyr reflected in the surface hydrography of the Western Bay of Bengal. *Quat. Sci. Rev.* 30, 3871–3879.
- Haake, B., Ittekkot, V., Rixen, T., Ramaswamy, V., Nair, R., Curry, W., 1993. Seasonality and interannual variability of particle fluxes to the deep Arabian Sea. *Deep-Sea Res.* 140, 1323–1344.
- Hair, J.F., Anderson, R.E., Tatham, R.L., Black, W.C., 1992. *Multivariate Data Analysis with Readings*. MacMillan Publishing Company, New York.
- Head, M., 1996. Modern dinoflagellate cysts and their biological affinities. In: Jansonius, J., McGregor, D.C. (Eds.), *Palynology: Principles and Applications 3*. American Association of Stratigraphic Palynologists Foundation, Dallas, TX, pp. 1197–1248.
- Ivanochko, T.S., 2004. Sub-orbital scale variations in the intensity of the Arabian Sea monsoon (PhD Thesis). University of Edinburgh, pp. 1–229.
- Ivanochko, T.S., Ganeshram, R.S., Brummer, G.-J.A., Ganssen, G., Jung, S.J., Moreton, S.G., Kroon, D., 2005. Variations in tropical convection as an amplifier of global climate change at the millennial scale. *Earth Planet. Sci. Lett.* 235, 302–314.
- Ivanova, E., Schiebel, R., Singh, A.D., Schmiel, G., Niebler, H.S., Hemleben, C., 2003. Primary production in the Arabian Sea during the last 135,000 years. *Palaeogeogr. Palaeoclimatol. Palaeoecol.* 197, 61–82.
- Kessarkar, P.M., Rao, V.P., Naqvi, S.W.A., Chivas, A.R., Saino, T., 2010. Fluctuations in productivity and denitrification in the southeastern Arabian Sea during the Late Quaternary. *Curr. Sci.* 99, 485–491.
- Kim, S.Y., Moon, C.H., Cho, H.J., Lim, D.I., 2009. Dinoflagellate cysts in coastal sediments as indicators of eutrophication: a case of Gwangyang Bay, South Sea of Korea. *Estuar. Coast.* 32, 1225–1233.
- Lewis, J., Rochon, A., Harding, I., 1999. Preliminary observations of cyst-theca relationships in *Spiniferites ramosus* and *Spiniferites membranaceus* (Dinophyceae). *Grana* 38, 113–124.
- Luckge, A., Doose-Rolinski, H., Khan, A.A., Schulz, H., Von Rad, U., 2001. Monsoonal variability in the northeastern Arabian Sea during the past 5000 years: geochemical evidence from laminated sediments. *Palaeogeogr. Palaeoclimatol. Palaeoecol.* 167, 273–286.
- Madhupratap, M., Prasanna Kumar, S., Bhattachiri, P., Kumar, M.D., Raghukumar, S., Nair, K., Ramaiah, N., 1996. Mechanism of the biological response to winter cooling in the northeastern Arabian Sea. *Nature* 384, 549–552.
- Marret, F., Zonneveld, K.A.F., 2003. Atlas of modern organic-walled dinoflagellate cyst distribution. *Rev. Palaeobot. Palynol.* 125, 1–200.
- Marret, F., de Vernal, A., Pedersen, T.F., McDonald, D., 2001. Middle Pleistocene to Holocene palynostratigraphy of ocean drilling program site 887 in the Gulf of Alaska, northeastern North Pacific. *Can. J. Earth Sci.* 38, 373–386.
- Martinson, D.G., Pisias, N.G., Hays, J.D., Imbrie, J., Moore Jr., T.C., Shackleton, N.J., 1987. Age dating and the orbital theory of the ice ages: development of a high-resolution 0 to 300,000-year chronostratigraphy. *Quat. Res.* 27, 1–29.
- Matsuoka, K., Fukuyo, Y., 2000. Technical guide for modern dinoflagellate cyst study. WESTPAC-HAB/WESTPAC/IOC, Japan Soc. Promotion Sci.
- Matthiessen, J., de Vernal, A., Head, M., Okolodkov, Y., Zonneveld, K.A.F., Harland, R., 2005. Modern organic-walled dinoflagellate cysts in arctic marine environments and their (paleo-) environmental significance. *Paläontol. Z.* 79, 3–51.
- Morqucho, L., Lechuga-Deveze, C.H., 2004. Seasonal occurrence of planktonic dinoflagellates and cyst production in relationship to environmental variables in subtropical Bahia Concepcion, Gulf of California. *Bot. Mar.* 47, 313–322.
- Morrison, J., Codispoti, L., Gaurin, S., Jones, B., Manghni, V., Zheng, Z., 1998. Seasonal variation of hydrographic and nutrient fields during the US JGOFS Arabian Sea Process Study. *Deep-Sea Res.* II 45, 2053–2101.
- Mudie, P.J., Rochon, A., Aksu, A.E., Gillespie, H., 2002. Dinoflagellate cysts, freshwater algae and fungal spores as salinity indicators in Late Quaternary cores from Marmara and Black seas. *Mar. Geol.* 190, 203–231.
- Naidu, P.D., Malmgren, B.A., 1996. A high-resolution record of late Quaternary upwelling along the Oman Margin, Arabian Sea based on planktonic foraminifera. *Paleoceanography* 11, 129–140.
- Naidu, P.D., Patil, J.S., Narale, D.D., Anil, A., 2012. A first look at the dinoflagellate cysts abundance in the Bay of Bengal: implications on Late Quaternary productivity and climate change. *Curr. Sci.* 102, 495–498.
- Naidu, P.D., Singh, A.D., Ganeshram, R., Bharti, S.K., 2014. Abrupt climate-induced changes in carbonate burial in the Arabian Sea: causes and consequences. *Geochem. Geophys. Geosyst.* 15, 1398–1406.
- Pospelova, V., Pedersen, T.F., de Vernal, A., 2006. Dinoflagellate cysts as indicators of climatic and oceanographic changes during the past 40 kyr in the Santa Barbara Basin, southern California. *Paleoceanography* 21, 1–16.
- Pospelova, V., de Vernal, A., Pedersen, T.F., 2008. Distribution of dinoflagellate cysts in surface sediments from the northeastern Pacific Ocean (43–25 N) in relation to sea-surface temperature, salinity, productivity and coastal upwelling. *Mar. Micropaleontol.* 68, 21–48.
- Prasanna Kumar, S., Madhupratap, M., Kumar, M.D., Gauns, M., Muralidharan, P., Sarma, V., De Souza, S., 2000. Physical control of primary productivity on a seasonal scale in central and eastern Arabian Sea. *J. Earth Syst. Sci.* 109, 433–441.

- Prauss, M., 2002. Recent global warming and its influence on marine palynology within the central Santa Barbara Basin, offshore southern California, U.S.A. *Palynology* 26, 217–238.
- Price, A.M., Mertens, K.N., Pospelova, V., Pedersen, T.F., Ganeshram, R.S., 2013. Late Quaternary climatic and oceanographic changes in the Northeast Pacific as recorded by dinoflagellate cysts from Guaymas Basin, Gulf of California (Mexico). *Paleoceanography* 28, 200–212.
- Radi, T., de Vernal, A., 2008. Dinocysts as proxy of primary productivity in mid-high latitudes of the Northern Hemisphere. *Mar. Micropaleontol.* 68, 84–114.
- Radi, T., Bonnet, S., Cormier, M.-A., de Vernal, A., Durantou, L., Faubert, E., Head, M.J., Henry, M., Pospelova, V., Rochon, A., 2013. Operational taxonomy and (paleo-) autecology of round, brown, spiny dinoflagellate cysts from the Quaternary of high northern latitudes. *Mar. Micropaleontol.* 98, 41–57.
- Reichart, G.-J., Brinkhuis, H., 2003. Late Quaternary *Protoperidinium* cysts as indicators of paleoproductivity in the northern Arabian Sea. *Mar. Micropaleontol.* 49, 303–315.
- Reichart, G.-J., Lourens, L., Zachariasse, W., 1998. Temporal variability in the northern Arabian Sea Oxygen Minimum Zone (OMZ) during the last 225,000 years. *Paleoceanography* 13, 607–621.
- Rochon, A., Lewis, J., Ellegaard, M., Harding, I.C., 2009. The *Gonyaulax spinifera* (Dinophyceae) “complex”: perpetuating the paradox? *Rev. Palaeobot. Palynol.* 155, 52–60.
- Rostek, F., Bard, E., Beaufort, L., Sonzogni, C., Ganssen, G., 1997. Sea surface temperature and productivity records for the past 240 kyr in the Arabian Sea. *Deep-Sea Res. II* 44, 1461–1480.
- Sarkar, A., Ramesh, R., Somayajulu, B., Agnihotri, R., Jull, A., Burr, G., 2000. High resolution Holocene monsoon record from the Eastern Arabian Sea. *Earth Planet. Sci. Lett.* 177, 209–218.
- Schott, F.A., Xie, S.P., McCreary, J.P., 2009. Indian Ocean circulation and climate variability. *Rev. Geophys.* 47.
- Shankar, D., Vinayachandran, P., Unnikrishnan, A., 2002. The monsoon currents in the north Indian Ocean. *Prog. Oceanogr.* 52, 63–120.
- Shaozhi, M., Harland, R., 1993. Quaternary organic-walled dinoflagellate cysts from the South China Sea and their paleoclimatic significance. *Palynology* 17, 47–65.
- Shetye, S.R., Shenoi, S.S.C., Antony, M., Kumar, V.K., 1985. Monthly-mean wind stress along the coast of the north Indian Ocean. *Proc. Ind. Acad. Sci. Earth Planet. Sci.* 94, 129–137.
- Singh, A.D., Kroon, D., Ganeshram, R., 2006. Millennial scale variations in productivity and OMZ intensity in the eastern Arabian Sea. *J. Geol. Soc. India* 68, 369–377.
- Singh, A.D., Jung, S.J., Darling, K., Ganeshram, R., Ivanochko, T., Kroon, D., 2011. Productivity collapses in the Arabian Sea during glacial cold phases. *Paleoceanography* 26.
- ter Braak, C.J.F., Smilauer, P., 2002. CANOCO reference manual and CanoDraw for Windows user's guide: software for canonical community ordination (version 4.5). Section on Permutation Methods. Microcomputer Power, Ithaca, New York.
- Weninger, B., Joris, O., Danzeglocke, U., 2006. Calpal-Cologne Radiocarbon Calibration and Paleoclimate Research Package. Inst. für Ur-und Frühgeschichte Radiocarbon Lab., Univ. zu Köln, Köln, Germany.
- Wyrtki, K., 1973. *Physical Oceanography of the Indian Ocean, The Biology of the Indian Ocean*. Springer, pp. 18–36.
- Zonneveld, K.A.F., 1997a. Dinoflagellate cyst distribution in surface sediments from the Arabian Sea (northwestern Indian Ocean) in relation to temperature and salinity gradients in the upper water column. *Deep-Sea Res. II* 44, 1411–1443.
- Zonneveld, K.A.F., 1997b. New species of organic walled dinoflagellate cysts from modern sediments of the Arabian Sea (Indian Ocean). *Rev. Palaeobot. Palynol.* 97, 319–337.
- Zonneveld, K.A.F., Brummer, G.A., 2000. (Palaeo-) ecological significance, transport and preservation of organic-walled dinoflagellate cysts in the Somali Basin, NW Arabian Sea. *Deep-Sea Res. II* 47, 2229–2256.
- Zonneveld, K.A.F., Pospelova, V., 2015. A determination key for modern dinoflagellate cysts. *Palynology* <http://dx.doi.org/10.1080/01916122.2014.990115> (in press).
- Zonneveld, K.A.F., Versteegh, G.J.M., de Lange, G.J., 1997a. Preservation of organic-walled dinoflagellate cysts in different oxygen regimes: a 10,000 year natural experiment. *Mar. Micropaleontol.* 29, 393–405.
- Zonneveld, K.A.F., Ganssen, G., Troelstra, S., Versteegh, G.J.M., Visscher, H., 1997b. Mechanisms forcing abrupt fluctuations of the Indian Ocean summer monsoon during the last deglaciation. *Quat. Sci. Rev.* 16, 187–201.
- Zonneveld, K.A.F., Bockelmann, F., Holzwarth, U., 2007. Selective preservation of organic-walled dinoflagellate cysts as a tool to quantify past net primary production and bottom water oxygen concentrations. *Mar. Geol.* 237, 109–126.
- Zonneveld, K.A.F., Marret, F., Versteegh, G.J., Bogus, K., Bonnet, S., Bouimetarhan, I., Crouch, E., de Vernal, A., Elshanawany, R., Edwards, L., 2013. Atlas of modern dinoflagellate cyst distribution based on 2405 data points. *Rev. Palaeobot. Palynol.* 191, 1–197.

**Dinoflagellate cyst
distribution in recent
sediments along the
south-east coast of India***

doi:10.5697/oc.55-4.979
OCEANOLOGIA, 55 (4), 2013.
pp. 979–1003.

© Copyright by
Polish Academy of Sciences,
Institute of Oceanology,
2013.

KEYWORDS

Dinoflagellate cysts
Heterotrophic
Phototrophic
South-east coast of India
Coastal sediments

DHIRAJ DHONDIRAM NARALE
JAGADISH S. PATIL
ARGA CHANDRASHEKAR ANIL*

CSIR – National Institute of Oceanography,
Dona Paula, Goa 403 004, India;

e-mail: acanil@nio.org

*corresponding author

Received 2 January 2013, revised 2 August 2013, accepted 26 September 2013.

Abstract

The spatial variation in the dinoflagellate cyst assemblage from the south-east coast of India is presented along with a comparison of the cyst abundance from other regions of the world. Samples from 8 stations revealed the presence of 24 species from the genera *Protoperidinium*, *Zygabikodinium*, *Gonyaulax*, *Lingulodinium* and *Gyrodinium*. Cyst abundance was comparatively high at northern stations and was well correlated with the fine-grained (silt-clay dominated) sediments. In contrast, low cyst abundance was recorded in sandy sediments at southern stations. Fourteen cyst-forming dinoflagellate species previously unrecorded in planktonic samples were detected in the sediments. The cyst abundance recorded here is low (29–331 cysts g⁻¹ dry sediment) as compared to sub-tropical and temperate regions, but it is on a par with tropical regions, including the west coast of India.

* The financial support for this work was received from the Ministry of Earth Sciences (MoES) under the Indian XBT programme and the Ballast Water Management programme, funded by the Directorate General of Shipping, India.

The complete text of the paper is available at <http://www.iopan.gda.pl/oceanologia/>

Comparison of the cyst assemblage along the Indian coast revealed a smaller number of potentially harmful and red-tide-forming dinoflagellate species on the south-east coast (6 species) than on the west coast (10 species). Calcareous cysts of the genus *Scrippsiella* reported from the west coast and Visakhapatnam harbour (south-east coast) were not observed in this study although their planktonic cells have been reported.

1. Introduction

Dinoflagellates are a major component of the plankton community and play an important role in marine ecosystem dynamics. They are composed of phototrophic (autotrophic, mixotrophic) and heterotrophic species. Many species of dinoflagellates are known to produce toxins and form harmful algal blooms (HABs). As a consequence of the global increase in HAB events, the study of phytoplankton dynamics, including dinoflagellates and their cysts, has gained in importance. Dinoflagellates are amongst the most unwanted marine bioinvasers. Approximately 200 marine dinoflagellate species are known to form resting cysts (Head 1996) as part of their life cycle; these are known to be well preserved in sediments for several years (Dale 1983) and even for up to a century (Ribeiro et al. 2011). These cysts serve as potential seed banks that can be important to phytoplankton bloom dynamics and species dispersal (Anderson et al. 1995). They remain viable in a ship's ballast-tank sediment and biofilms, subsequently transported to different regions by shipping (Drake et al. 2005). Additionally, resting cysts may be introduced to new locations through shellfish transplantation (Anderson & Wall 1978). The sediments store resting stages produced by the planktonic species present in the region, thus providing a historical archive at different temporal resolutions (Dale 2001a). Cyst mapping of harmful dinoflagellate species assemblages can provide information about the mechanism of recurrence and spreading of HAB species. Moreover, by studying the cysts in a specific region, it is possible to record dinoflagellate species whose pelagic stages are rarely observed and difficult to identify (Hesse et al. 1996).

In spite of the importance of dinoflagellate cysts in understanding the population dynamics of vegetative stages, information from the seas around the Indian subcontinent is very limited and mainly restricted to the west coast of India (Godhe et al. 2000, D'Costa et al. 2008, D'Silva et al. 2011). In the Bay of Bengal, reports are available on cyst occurrence from Late Quaternary sediments (Naidu et al. 2012). Recently, a contemporary cyst assemblage has been studied from recent sediments of Visakhapatnam harbour (D'Silva et al. 2013). To date, information on modern cyst assemblages and their distributions from other parts of the western boundary of the Bay of Bengal is lacking.

This study of the dinoflagellate cyst distribution is the first of its kind from the south-east coast of India. Its aims are i) to evaluate the spatial variation of dinoflagellate cyst assemblages in the surface sediments along the south-east coast of India (western boundary of the Bay of Bengal), ii) to compare planktonic dinoflagellate records and dinoflagellate cyst data, iii) to compare the cyst abundance in the present study with that of other regions, and iv) to identify harmful and potentially harmful species.

2. Material and methods

2.1. Description of the study region

The sampling stations are located on the Indian continental shelf, in the vicinity of the western boundary of the Bay of Bengal (BOB). The physical oceanography of the area is controlled by the monsoon current system. Forming part of the seasonally reversing monsoon-current system, the East Indian Coastal Current (EICC) changes direction twice a year (Shankar et al. 2002). The summer monsoon (May–September) begins in May with strong winds blowing towards the south-west. The clockwise surface current develops in summer, flows in a south-westerly direction with a velocity of $\sim 0.2 \text{ m s}^{-1}$. During the winter monsoons (November–February), winds blow north-eastwards. The surface current flows in an anticlockwise (north-easterly) direction. The current velocity reaches 0.5 m s^{-1} .

The south-east continental shelf of India is a river-dominated shelf system characterized by inputs of fresh water, suspended sediment and nutrients from the Rivers Krishna-Godavari, Cauvery, Ponnaiyar and Penner. The surface water tends to be rich in silicate, supporting the predominance of diatoms throughout the year (Madhu et al. 2006). Weak, localized wind-driven upwelling has been reported in this area during the summer monsoon (Shetye et al. 1991). Oceanographic features like sea surface salinity (SSS) and sea surface temperature (SST) are influenced mainly by the reversing EICC and riverine runoff. The average SSS and SST respectively range from 27.3 to 30.0 PSU and from 25.6 to 34.5°C.

The characteristics of the shelf sediments vary from north to south. The south is dominated by silty-sand, whereas clayey-silt and silty-clay are present in the north (Musale & Desai 2010). The sediments along the continental shelf are thought to be fresh owing to the high sedimentation rate from riverine input.

2.2. Sediment sampling

Surface sediments were collected from 8 stations (covering a distance of 463 nautical miles) off the south-east coast of India (Figure 1, Table 1)

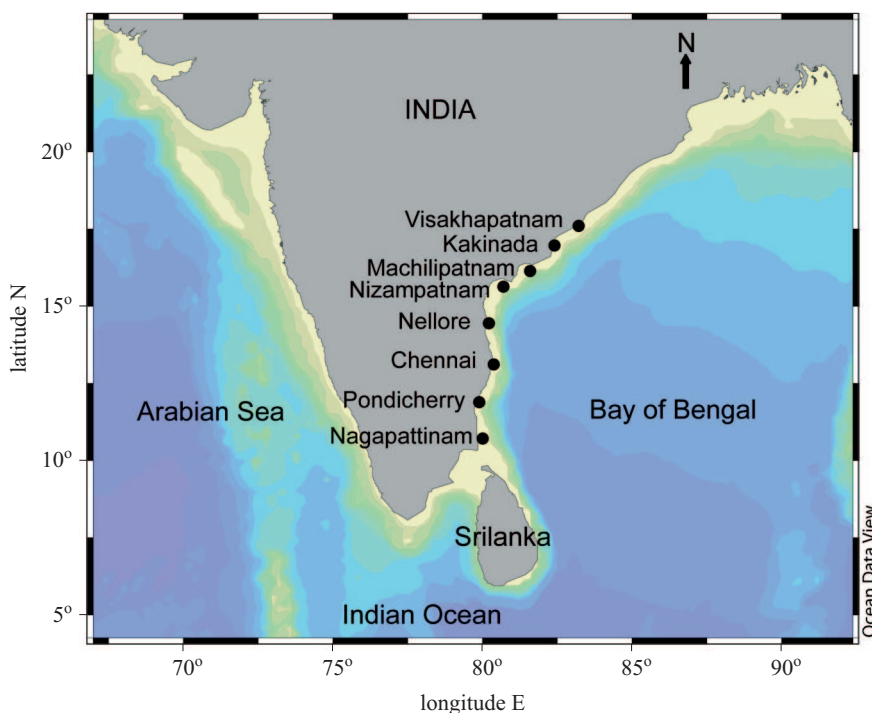


Figure 1. Location of sampling stations along the south-east coast of India

during the Sagar Sukti cruise (SASU 125) in the winter monsoon (December 2006). At each station (except Visakhapatnam) sediment sampling was carried out at 2–3 different sites at intervals of 2 nautical miles. Surface sediment samples were collected using a modified van Veen grab (grabbing area 0.04 m²) equipped with flaps on the top, enabling cores of surface sediments to be collected. Duplicate sediment cores (PVC cores, 25 cm long, inner diameter of 2.5 cm) were obtained with the grab. At Visakhapatnam, a sample was collected at only one position with a gravity corer (1 m length, inner diameter 5 cm). All sediment cores (PVC and gravity) were sectioned at 2 cm intervals, mixed well and stored in airtight plastic bags at 4°C in the dark.

2.3. Sediment preparation, processing and analysis

Sediment samples from the upper 0–2 cm sections of each sediment core were treated using a palynological method (Matsuoka & Fukuyo 2000) with some modifications (D'Costa et al. 2008). A known weight (2–3 g) of wet sediment was repeatedly washed with distilled water to remove salts. The salt-free sample was treated with 7 ml 10% HCl to dissolve calcareous minerals and then with 30% HF to dissolve silicate materials.

Table 1. Geographical coordinates and cyst abundance [cysts g⁻¹ dry sediment] at the sampling stations along the south-east coast of India. Note: data on sediment characteristics for the stations marked with an asterisk was obtained from Musale & Desai (2010)

Station Name	Latitude [°N]	Longitude [°E]	Water depth [m]	Samples analysed	Cyst abundance	Sediment characteristics [%]		
						Sand	Silt	Clay
Visakhapatnam	17.58	83.23	31	6	331	0.7	41.2	58.1
Kakinada*	16.95	82.41	30	10	128	0.8	42.5	56.7
Machilipatnam*	16.15	81.58	27	12	89	1.4	50.0	48.6
Nizampatnam*	15.61	80.66	20	10	59	1.6	67.5	30.9
Nellore*	14.45	80.23	24	8	83	61.5	19.3	19.1
Chennai	13.10	80.40	30	8	45	80.5	13.3	6.2
Pondicherry*	11.91	79.91	27	8	29	79.8	12.4	7.8
Nagapattinam*	10.70	80.03	25	4	63	81.8	11.7	6.5

Each chemically treated sample was rinsed 3–4 times with distilled water to remove acid. Subsequently, the acid-free slurry was sieved through a tier of two different meshes (120 and 20 μm) to remove coarse and fine material. The residue accumulated on the 20 μm mesh was then suspended in 10 ml distilled water and stored in a vial. For the quantification of calcareous cysts, 2–3 g of wet sediment samples were rinsed with distilled water only and sieved through 120 and 20 μm meshes without any acid treatment. The sieved sample (10 ml) was then stored in a vial until further analysis.

For the microscopic identification of dinoflagellate cysts, an aliquot of the processed sample was diluted to a total volume of 2 ml in a transparent Petri dish (3.8 cm diameter), mixed well and placed on the microscope stage. After the sample had settled, the entire Petri dish was scanned under an inverted microscope (Olympus IX 71) equipped with a digital camera (Olympus CAMEDIA C-4040ZOOM) at 100 and 400x magnifications. Depending on the volume of the aliquot, the processed sample was counted in duplicate or a higher number of replicates, such that a total of 2 ml was analysed. Dinoflagellate cysts were identified on the basis of the published literature (Wall & Dale 1968, Sonneman & Hill 1997, Matsuoka & Fukuyo 2000).

A known weight (1 g) of wet sediment sample was dried at 70°C for 24 h to estimate the water content (Matsuoka & Fukuyo 2000). Cyst concentration was calculated as the number of cysts per gram of dry sediment [cysts g^{-1} dry sediment] using the formula $N/W(1 - R)$, where N – number of cysts, W – weight of sediment and R – proportion of water in the sediment.

The percentage grain size composition of the sediment (sand, silt and clay) was determined by standard wet sieving (for sand) and pipette analysis (for silt and clay) (Buchanan 1984). In this study, sediment samples from three stations (Visakhapatnam, Chennai, Nagapattinam) were analysed for grain size composition, while data from other stations and the same period were obtained from Musale & Desai (2010). The size classification used was sand ($> 62 \mu\text{m}$), silt (62–3.9 μm) and clay ($< 3.9 \mu\text{m}$).

To assess the distribution of cyst-producing dinoflagellate species in the study area, the information collected from previous studies (Madhav & Kondalarao 2004) on the distribution of dinoflagellate planktonic cells during different seasons from the same study region is presented together with cyst data (present study; Table 2). Although several reports on phytoplankton distribution are available, we selected for comparison only those in which dinoflagellates from the sampling region (south-east coast of India) were identified down to species level.

Table 2. List of cyst-forming dinoflagellates from the south-east coast of India compiled from earlier published planktonic data (PSEC) and dinoflagellate cysts recorded previously along the west coast (DWC) and the south-east coast (DSEC) i.e. the present study (Pre Stu) and Visakhapatnam harbour (Vizag Har) (*continued on next page*)

Biological name	Palaeontological name	Species code	Planktonic dinoflagellate (PSEC)	Dinoflagellate cyst		
				DWC	DSEC	
					Pre Stu	Vizag Har ⁶
Phototrophic						
<i>Alexandrium affine</i> ^{††}	—			● ⁵		●
<i>Alexandrium cf. affine</i>	—			● ⁴		
<i>Alexandrium minutum</i> [†]	—			● ⁵		●
<i>Alexandrium cf. minutum</i>	—			● ^{3,4}		
<i>Alexandrium tamarense</i> [†]	—			● ⁵		
<i>Alexandrium cf. tamarense</i>	—			● ^{3,4}		
<i>Alexandrium cf. tamiyavanichi</i> [†]	—			● ³		
<i>Alexandrium</i> sp.	—			● ⁵		
<i>Cochlodinium cf. polykrikoides</i>	—			● ^{4,5}		
<i>Cochlodinium</i> sp.	—			● ⁵		●
<i>Gonyaulax diacantha</i>			● ¹			
<i>Gonyaulax digitalis</i>	<i>Spiniferites bentori</i>	GnxD	● ²	● ^{3,4,5}	●	●
<i>Gonyaulax scrippsae</i>	<i>Spiniferites bulloideus</i>	GnxS		● ^{3,4,5}	●	●
<i>Gonyaulax verior</i>	—			● ³		
<i>Gonyaulax spinifera</i> complex [†]	<i>Spiniferites miribilis</i>	GnxSp		● ^{3,4,5}	●	●
	<i>Spiniferites membranaceus</i>			● ^{3,4,5}	●	●
	<i>Spiniferites ramosus</i>			● ^{3,4,5}		
<i>Gonyaulax</i> sp.						●
<i>Gymnodinium catenatum</i> [†]	—			● ³		
<i>Gymnodinium cf. catenatum</i>	—			● ^{4,5}		
<i>Gyrodinium impudicum</i>	—	Gyrl		● ⁵	●	●
<i>Lingulodinium polyedrum</i> [†]	<i>Lingulodinium machaerophorum</i>	LngP		● ^{3,4,5}	●	●
<i>Pentapharsodinium dalei</i>	—			● ^{3,4,5}		●

Table 2. (continued)

Biological name	Palaeontological name	Species code	Planktonic dinoflagellate (PSEC)	Dinoflagellate cyst		
				DWC	DSEC	
					Pre	Stu
<i>Pheopolykrikos hartmannii</i>	–			• ^{3,4,5}		
<i>Protoceratium reticulatum</i> [†]	<i>Operculodinium centrocarpum</i>	PcerR		• ^{3,4,5}	•	•
<i>Pyrodinium</i> cf. <i>bahamense</i>	–			• ⁴		
<i>Pyrodinium bahamense</i> var. <i>compressum</i> [†]	<i>Polysphaeridium zoharyi</i>			• ⁵		
<i>Pyrophacus steinii</i>	<i>Tuberculodinium vancampoae</i>		• ¹	• ^{4,5}		•
<i>Pyrophacus</i> sp.	–			• ⁵		
<i>Scrippsiella trifida</i> [#]	–			• ⁵		
<i>Scrippsiella trochoidea</i> ^{††, #}	–		• ¹	• ^{3,4,5}		•
<i>Scrippsiella</i> sp.	–			• ⁵	•	
Heterotrophic						
<i>Diplopelta parva</i>	–			• ^{3,5}		•
<i>Diplopsalis lenticula</i>	–		• ²	• ^{3,4,5}		
<i>Lebouraia minuta</i>	–			• ⁵		
<i>Lebouraia</i> cf. <i>minuta</i>	–			• ⁴		
<i>Polykrikos kofoidii</i>	–			• ⁵		
<i>Polykrikos</i> cf. <i>kofoidii</i>	–			• ⁴		
<i>Polykrikos schwartzii</i>	–			• ^{3,5}		
<i>Polykrikos</i> cf. <i>schwartzii</i>	–			• ⁴		
<i>Polykrikos</i> sp.	–			• ⁵		
<i>Protoperidinium americanum</i>	–			• ³		
<i>Protoperidinium avellana</i>	<i>Brigantedinium cariacense</i>	PpA		• ³	•	
<i>Protoperidinium</i> cf. <i>avellana</i>	–	PpAva		• ³	•	
<i>Protoperidinium brochii</i>	–		• ²			
<i>Protoperidinium claudicans</i>	<i>Votadinium spinosum</i>	PpCla	• ²	• ^{3,4,5}	•	•
<i>Protoperidinium compressum</i>	<i>Stelladinium stellatum</i>	PpCom		• ^{4,5}	•	•

Table 2. (continued)

Biological name	Palaeontological name	Species code	Planktonic dinoflagellate (PSEC)	Dinoflagellate cyst		
				DWC	DSEC	
					Pre	Stu
<i>Protoperidinium conicoides</i>	<i>Brigantedinium simplex</i>			● ^{4,5}		
<i>Protoperidinium conicum</i>	<i>Selenopemphix quanta</i>	PpC	● ²	● ^{4,5}	●	●
<i>Protoperidinium denticulatum</i>	<i>Brigantedinium irregulare</i>			● ⁵		●
<i>Protoperidinium divaricatum</i>	<i>Xandarodinium variable</i>			● ^{4,5}		
<i>Protoperidinium excentricum</i>	–		● ²	● ³		
<i>Protoperidinium grandii</i>			● ²			
<i>Protoperidinium latissimum</i>	–	PpLa		● ^{3,4,5}	●	
<i>Protoperidinium leonis</i>	<i>Quinquecuspis concreta</i>	PpL	● ²	● ^{4,5}	●	●
<i>Protoperidinium minutum</i>	–			● ³		
<i>Protoperidinium cf. minutum</i>	–			● ³		
<i>Protoperidinium nudum</i>	–	PpNu		● ³	●	
<i>Protoperidinium oblongum</i>	<i>Votadinium calvum</i>	PpO	● ²	● ^{3,5}	●	●
<i>Protoperidinium pentagonum</i>	<i>Trinovantedinium applanatum</i>	PpPn	● ²	● ^{4,5}	●	
<i>Protoperidinium cf. pentagonum</i>	<i>Trinovantedinium capitatum</i>			● ^{3,4,5}		●
	<i>Brigantedinium majusculum</i>			● ³		
<i>Protoperidinium stellatum</i>	–			● ³		
<i>Protoperidinium subinerme</i>	<i>Selenopemphix nephroides</i>		● ²	● ^{3,4,5}		●
<i>Protoperidinium thorianum</i>	–	PpThr			●	
<i>Protoperidinium sp.</i>	<i>Lejeunecysta sp.</i>	PpsLe		● ⁵	●	
<i>Protoperidinium sp.</i>	<i>Lejeunecysta concreta</i>					●
<i>Protoperidinium sp.</i>	<i>Stelladinium robustum</i>	PpSr		● ^{4,5}	●	
<i>Protoperidinium sp.</i>	<i>Peridinium cf. stellatum</i>					●
<i>Protoperidinium sp.</i>	<i>Trinovantedinium palidifluvium</i>			● ^{4,5}		
<i>Protoperidinium sp.</i>	<i>Brigantedinium sp.</i>					●
<i>Zygabikodinium lenticulatum</i>	<i>Dubridinium caperatum</i>	ZyLen		● ^{4,5}	●	●
<i>Protoperidinium sp. Type 1[§]</i>	–	PpS1			●	

Table 2. (*continued*)

Biological name	Palaeontological name	Species code	Planktonic dinoflagellate (PSEC)	Dinoflagellate cyst		
				DWC	DSEC	
					Pre Stu	Vizag Har ⁶
<i>Protoperidinium</i> sp. Type 2 ^s	–	PpS2		•		
Dinoflagellate cyst type 1 ^s	–	DS1		•		
Dinoflagellate cyst type 2 ^s	–	DS2		•		

References indicated as superscript numbers:

¹unpublished data,

²Madhav & Kondalarao 2004,

³Godhe et al. 2000,

⁴D'Costa et al. 2009,

⁵D'Silva et al. 2011,

⁶D'Silva et al. 2013;

†potentially harmful species;

††red-tide-forming species;

#calcareous cyst;

^sunidentified cyst recorded during present study. As they are not identified down to species level, they have not been considered in the comparison.

In order to evaluate the dinoflagellate cyst composition and identify the harmful and potentially harmful species in the Indian region, the cyst assemblage of the south-east coast of India (D'Silva et al. 2013, present study) is compared with that of the west coast of India (Godhe et al. 2000, D'Costa et al. 2008, D'Silva et al. 2011) and presented in Table 2. The dinoflagellate cyst species identified to species level are only considered for comparison.

2.4. Data analysis

The abundance of dinoflagellate cysts was converted into a lower triangular similarity matrix using the Bray-Curtis coefficient. This similarity matrix was then subjected to cluster analysis by the group average method to evaluate the spatial variation. All the analyses were carried using PRIMER software (version 5).

3. Results

3.1. Dinoflagellate cyst assemblage

A total of 24 dinoflagellate cyst morphotypes were recorded in the sediment samples collected along the south-east coast of India (Table 2; Figure 2). 20 of these 24 cyst types were identified to species level and 2 to genus level (*Protoperidinium* sp. type 1 (PpS1) and *Protoperidinium* sp. type 2 (PpS2); Table 2, Figures 3m–n). The remaining two cyst morphotypes (Figures 3o–p) could not be identified as they lacked identifying structures and germination efforts were not successful.

Hence, depending on their morphology, they are characterized as dinoflagellate cyst type 1 (DC1) or dinoflagellate cyst type 2 (DC2). Furthermore, cysts belonging to the *Gonyaulax spinifera* species complex, i.e. *Spiniferites mirabilis* and *S. membranaceus*, are recorded as *Gonyaulax*

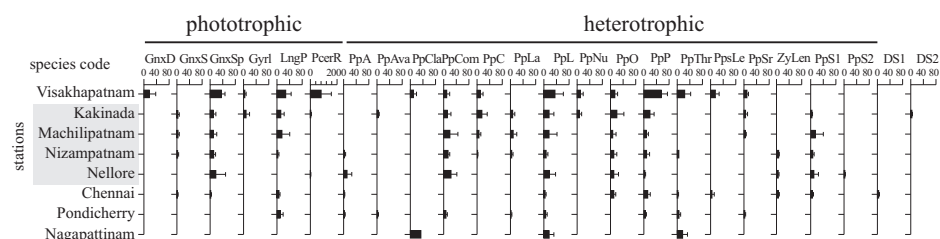


Figure 2. Dinoflagellate cyst abundance [cyst g^{-1} of dry sediment] of each species in the surface sediments at 8 sampling stations along the south-east coast of India. The error bar represents the standard deviation from the mean (for the species code, please refer to Table 2)

spinifera complex in this study. The light microscopy photomicrographs of the dinoflagellate cysts recorded are provided in Figure 3.

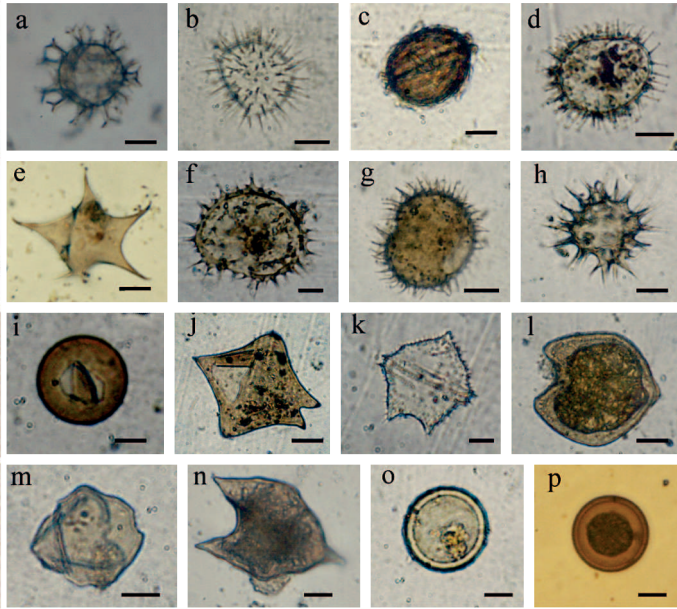


Figure 3. Photomicrographs of dinoflagellate cysts recorded from the recent sediments along the south-east coast of India: *Gonyaulax spinifera* complex (a), *Lingulodinium polyedrum* (b), *Zygabikodinium lenticulatum* (c), *Protoceratium reticulatum* (d), *Protoperidinium compressum* (e), *P. conicum* (f), *P. claudicans* (g), *P. nudum* (h), *P. avellana* (i), *P. latissimum* (j), *P. pentagonum* (k), *P. oblongum* (l), *Protoperidinium* sp. 1 (m), *Protoperidinium* sp. 2 (n), Dinoflagellate cyst type 1 (o), Dinoflagellate cyst type 2 (p). All scale bars 20 μm

The dinoflagellate cyst assemblage was dominated by heterotrophic dinoflagellates (Figures 4a,b,c) represented by 16 species (Figure 2) belonging to the genera *Protoperidinium* (15 species) and *Zygabikodinium* (1 species). Phototrophic dinoflagellates consisted of 6 species (Figure 2) representing four genera: *Gonyaulax* (3 species), *Lingulodinium* (1 species), *Protoceratium* (1 species) and *Gyrodinium* (1 species).

3.2. Dinoflagellate cyst distribution

The dinoflagellate cyst abundance ranged from 29 to 331 cysts g^{-1} dry sediment, and their numbers increased from southern (Nagapattinam) to northern (Visakhapatnam) stations (Figure 4a, Table 1). Cyst abundance

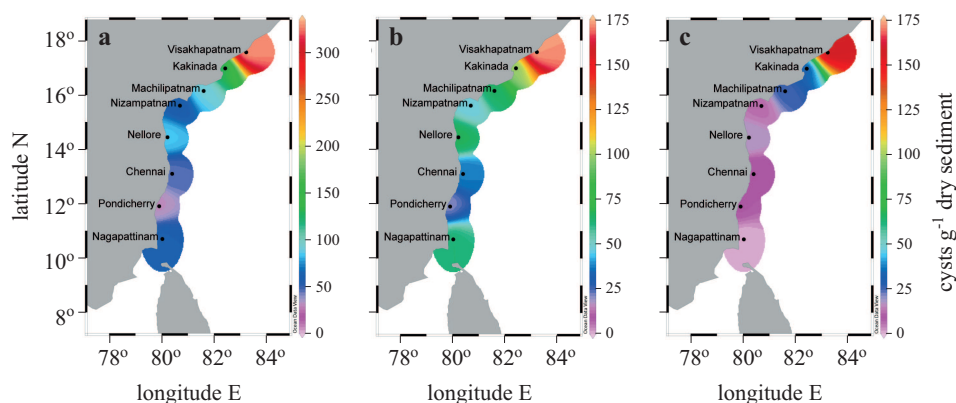


Figure 4. Spatial distribution of total dinoflagellate cysts (a), heterotrophic dinoflagellate cysts (b) and phototrophic dinoflagellate cysts (c)

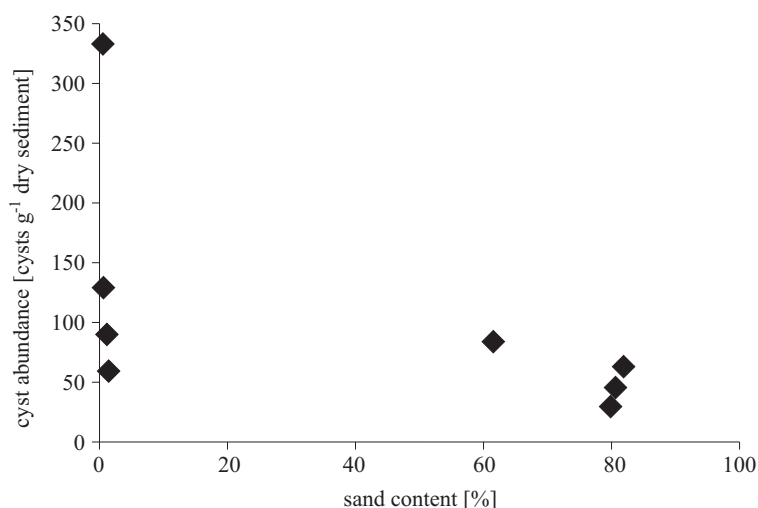


Figure 5. Dinoflagellate cyst abundance [cyst g⁻¹ dry sediment] versus sand content [%] in the surface sediment along the south-east coast of India

was influenced by the sediment characteristics. Cyst abundance was higher in the fine grained (silt-clay dominated) sediments than in the sandy sediments (Table 1, Figure 5). Cluster analysis of the sampling stations based on the dinoflagellate cyst assemblage at the 50% similarity level revealed one group of four stations (Machilipatnam, Kakinada, Nellore and Nizampatnam) and four ungrouped stations (Figure 6). The grouped stations had a higher cyst abundance (59 to 128 cysts g⁻¹ dry sediment). Among the four ungrouped stations, the cyst abundance (331 cysts g⁻¹ dry

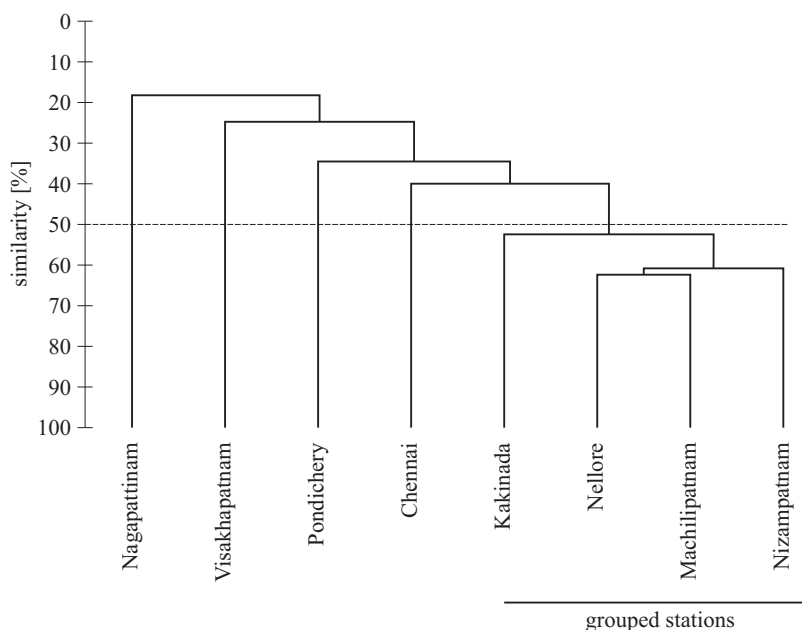


Figure 6. Cluster dendrogram of sampling stations relationship using the Bay-Curtis similarity coefficient and group average method

sediment) was the highest at Visakhapatnam and lower at the other three stations (Nagapattinam, Chennai and Pondicherry; Figure 4a, Table 1).

3.3. Comparison of dinoflagellate cysts and planktonic dinoflagellates

Comparison of the present data with the collated information on the cyst-forming species revealed that 14 cyst-producing dinoflagellate species present in the sediments (cysts) had not been previously identified in planktonic samples (Table 2). Among these, the *Gonyaulax spinifera* complex (2 subspecies), *Lingulodinium polyedrum* and *Protoperidinium compressum* dominated the cyst assemblage and had not been previously recorded in planktonic form. Furthermore, 8 cyst-producing dinoflagellate species previously recorded in the planktonic samples were not observed in their cyst forms (Table 2). Cysts of calcareous cyst-producing species were not observed in the sediment sample treated without acid.

3.4. Comparison of dinoflagellate cysts assemblage between the west and the south-east coasts of India

Taxonomic comparison of the dinoflagellate cyst data between the west and south-east coasts of India showed that although the cyst abundance

was comparable, the species composition was different (Table 2). Along both coasts, cysts belonging to the heterotrophic *Protoperidinium* species dominated the cyst assemblage over phototrophic species. However, the number of phototrophic species was higher along the west coast (26 species) than along the south-east coast (12 species). The number of cysts of potentially harmful and red-tide-forming dinoflagellates along the west coast (10 species) was also comparatively higher than along the south-east coast (6 species). A similar trend was also observed in the case of calcareous cysts between the two coasts. Calcareous cysts reported from the west coast were represented by 3 species belonging to the genus *Scrippsiella*, whereas a cyst of only one species (*S. trochoidea*) was reported from Visakhapatnam harbour on the south-east coast (Table 2). During the present study no calcareous cysts were observed along the south-east coast of India.

4. Discussion

4.1. Comparison of dinoflagellate cyst abundance with different regions

Zonneveld et al. (2013) summarized the global distribution of dinoflagellate cysts from recent sediments and their relationship with environmental conditions. The compilation presented here includes data sets on the dinoflagellate cyst distribution from this study region that were not published in any earlier compilation. The global distribution of dinoflagellate cyst abundance as collated from the literature and the present study is given in Table 3. For this comparison, studies that used similar sample processing (acid treatment) and cyst abundance presentation [cysts g⁻¹ dry sediment] methods are considered. The present compilation revealed that the cyst abundance recorded in this study was low (29 to 331 cysts g⁻¹ dry sediment) as compared to sub-tropical and temperate coastal regions (Table 3). However, the cyst abundance recorded is on a par with that of other tropical regions (Table 3), such as the coasts of south-east Asia (Furio et al. 2012) and the west coast of India (Godhe et al. 2000, D'Costa et al. 2008, D'Silva et al. 2011).

The abundance of dinoflagellate cysts (139 to 75 000 cysts g⁻¹ dry sediment) along the western boundaries of the African subcontinent (Table 3), has been related to intensive upwelling (Targarona et al. 1999, Sprangers et al. 2004, Holzwarth et al. 2007). A high dinoflagellate cyst abundance (100 to 25 000 cysts g⁻¹ dry sediment) is also recorded in the Arctic and Atlantic confluence (Table 3). In sub-polar regions with highly variable nutrient supplies and environmental conditions (Solignac et al. 2009), opportunistic species with higher growth rates are favoured, resulting in

Table 3. Records of dinoflagellate cysts abundance from different parts of the world

Study areas	Cyst abundances	References
a) off south-east Greenland	102–7920	Boessenkool et al. 2001
b) Mediterranean Sea	177–929	Elshanawany et al. 2010
Izmir Bay (Aegean Sea, Eastern Mediterranean)	41–3292	Aydin et al. 2011
c) North Canary Basin, NW Africa	192–13147	Targarona et al. 1999
Benguela upwelling, off SE Africa	139–38580	Holzwarth et al. 2007
Offshore NW Iberia	15000–>75000	Sprangers et al. 2004
d) Chinese Coastal waters	154–113483	Wang et al. 2004
Yellow China Sea	114–20828	Hwang et al. 2011
Geoje Island, Korea	528–2834	Shin et al. 2007
Tokyo Bay, Japan	240–8380	Matsuoka et al. 2003
e) Southern Ocean (eastern Atlantic sector)	74–8714	Esper & Zonneveld 2002
f) Eastern Australia	100–20000	McMinn 1990
g) Sabah, Malaysia	2–411	Furio et al. 2006*
North-western and central Philippines	30–580	Furio et al. (in press)*
North-western Philippines	43–1940	Baula et al. 2008*
h) MPT and JNPT Mumbai, India	36–262	D'Costa et al. 2008
Zuari estuary, India	150–750	Patil (unpublished)
West coast of India	6–1076	D'Silva et al. 2011
i) Visakhapatnam harbour, India	15–1218	D'Silva et al. 2012
South-east coast of India	29–331	present study

*obtained from Furio et al. 2012.

a lower species richness (Barton et al. 2010). In the Mediterranean Sea (Table 3) the high cyst abundance is influenced mainly by river plumes and eutrophic waters in coastal regions (Elshanawany et al. 2010, Aydin et al. 2011). Another region where high cyst numbers are reported embraces the waters around China, Korea and Japan (Table 3); this has been related to eutrophication (Matsuoka et al. 2003, Shin et al. 2007). Furthermore, a high abundance (in thousands) of dinoflagellate cysts has been recorded in sediment traps in the western Arabian Sea upwelling region (Zonneveld & Brummer 2000). Compared to these numbers, the dinoflagellate cyst

abundance reported along the coasts of India is low (Table 3), even though the west coast of this subcontinent is influenced by upwelling and the south-west monsoon. However, further intensive studies are needed to investigate the reason for the small numbers of dinoflagellate cysts in the region.

4.2. Cyst assemblages along the south-east coast of India

Along the south-east coast of India, the cyst abundance decreases from north to south (Figure 4a). It has been observed that the differences in cyst abundance and assemblage composition between areas are caused primarily by differences in the abundance of vegetative cells and their cyst production efficiencies, and/or by differences in the hydrology and the sedimentary regime (Dale 1983, Anderson et al. 1995, Joyce et al. 2005). Dinoflagellate cysts are believed to have the hydrodynamic characteristics of fine silt-sized particles (Dale 1983, Kawamura 2004) and can be transported by water currents. In the study area, the abundance of dinoflagellate cysts can be correlated with the texture of the sediment, i.e. silt and clayey sediment. A high cyst abundance was encountered in the fine-grained (silt and clayey) sediments as compared to the sandy sediments (Table 1, Figure 5). The southern stations (Chennai, Pondicherry and Nagapattinam, 3 ungrouped stations, Figure 6) contain a high percentage of sand, which is not suitable for cyst deposition (Dale 1983), while the sediments at the northern stations (Nellore, Nizampatnam, Machilipatnam, Kakinada and Visakhapatnam) are characterized by high percentage of silt-clay and a high cyst abundance (Table 1, Figure 5). These results indicate that sediment grain size plays a major role in determining the cyst distribution in this area.

Apart from this, other processes, like bio- and oxidative degradation, benthic predation and bioturbation, also influence the cyst assemblage and distribution in the sediments (Zonneveld et al. 1997, Persson & Rosenberg 2003). A contemporaneous study investigating the macrobenthic community along the south-east coast of India (Musale & Desai 2010) indicated the dominance of burrowing and subsurface deposit-feeding polychaetes (e.g. *Magelona cincta*, *Cirratulus* sp., *Capitella capitata* etc.), and bivalves in the silty-clayey sediments at the northern stations (Nellore, Nizampatnam, Machilipatnam and Kakinada), where cyst abundance was comparatively higher. At Pondicherry, the loose sandy sediment harboured only a few surface feeding polychaetes (*Prionospio* spp., *Amphiarete* sp.) and the cyst abundance was low. It has been reported that *Protooperidinium* cysts are more susceptible to degradation by the activity of deposit-feeding animals than the cysts of phototrophic species such as *P. reticulatum*, *L. polyedrum* and *Spiniferites* spp. (Persson & Rosenberg 2003). However, in this study, *Protooperidinium* cysts were dominant, indicating that bioturbation and

predation by benthic fauna are unlikely to be the major factors determining the composition of the cyst assemblages.

Another contemporaneous study from the west coast of India (D'Silva et al. 2011) reported the dominance of heterotrophic forms (*Protooperidinium* spp.). Their dominance is generally attributed to i) elevated nutrient concentrations and high productivity (Harland et al. 2006), ii) the availability of prey organisms such as diatoms (Matsuoka et al. 2003, Godhe & McQuoid 2003), iii) reduced light intensity (Dale 2001b) and iv) the smaller production of phototrophic dinoflagellates (Dale 2001b). As in any other tropical coastal environment, the high nutrient supply through riverine material, the dominance of diatoms (Madhu et al. 2006) and the low light penetration due to suspended riverine loads could be the governing factors ensuring the dominance of heterotrophic dinoflagellates over phototrophic dinoflagellates in this coastal region.

At Visakhapatnam station, phototrophic species (*P. reticulatum*, *L. polyedrum* and *Gonyaulax* spp.) contributed significantly to the total cyst abundance (Figure 2). Earlier studies indicated that the dominance of phototrophic forms can be influenced by variable salinity regimes, nutrient inputs and sediment texture (Dale 2000, Godhe & McQuoid 2003, Kawamura 2004). The dominance of *P. reticulatum* in Visakhapatnam harbour has also been correlated with elevated nutrient inputs (D'Silva et al. 2013). The present sampling station at Visakhapatnam is part of the mesotrophic environment (Tripathy et al. 2005) in the vicinity of Visakhapatnam harbour and is influenced by a varying salinity (range 17 to 35 PSU) that is due to terrestrial runoff and the current circulation pattern (Vijaykumaran 2005). It is possible that a high nutrient input and varying salinity regimes could be the reason for the dominance of phototrophic forms. Cysts of *Alexandrium affine*, *A. minutum*, *Cochlodinium* sp., *Pentaparsodinium dalei*, *Pyrophacus steinii*, *Diplopelta parva*, *Protooperidinium denticulatum* and *P. subinermis*, reported from Visakhapatnam harbour (D'Silva et al. 2013), were not observed at this station, which is located approximately 4 km away from the harbour.

4.3. Comparison of dinoflagellate cysts and planktonic dinoflagellates

Analysis of planktonic and sediment samples enables identification of both motile and cyst stages, thus providing the best information on the dinoflagellate species composition (Dale 1983). Generally, the number of dinoflagellate species in a study area increases when information on cysts is included in the study (Persson & Rosenberg 2003, Orlova et al. 2004, Satta et al. 2010).

Fourteen cyst-forming dinoflagellate species not previously identified in planktonic samples were detected in the sediments analysed in this study (Table 2). This may be due to the sample preservation technique, which sometimes alters the morphology of planktonic cells. Particularly, the light microscopic identification of naked/unarmoured vegetative dinoflagellates is more difficult in the preserved state than of their cyst forms. The small size thecate *Gonyaulax* species like *G. spinifera*, *G. scrippsae* are very difficult to differentiate in poorly preserved samples. Apart from this, the identification of small thecate dinoflagellates is difficult without an exhaustive thecal plate analysis (Orlova et al. 2004). Consequently, some taxa of the genera *Protoperidinium*, *Gonyaulax*, *Gymnodinium* and *Gyrodinium* are usually identified only to generic level. These identification difficulties affect the comparative taxonomic analysis.

Seasonal cycles in the occurrence of vegetative cells and benthic cysts could be another factor for the mismatch.

On the other hand, the eight cyst-forming dinoflagellate species observed in planktonic form were previously not recorded in the recent sediments (Table 2). This may be attributed to i) the low production of cysts in the water column, which is insufficient to produce a detectable quantity of cysts; ii) the acids used in the palynological method of sediment preparation, which dissolve the calcareous cyst wall and/or cyst. Hence calcareous cyst-forming *S. trochoidea* and other *Scripsiella* spp. may be overlooked in such samples (Montresor et al. 1998). This could result in an underestimation of the total dinoflagellate cyst abundance. To resolve this, microscopic analysis of untreated, distilled water cleaned and sieved sediment samples was carried out. The absence of these species in an untreated sediment sample highlights the undetectable quantity of cyst production rather than the methodology used for sediment preparation.

4.4. Comparison of the dinoflagellate cyst assemblages along the west and the south-east coasts of India

Taxonomic comparison of the present data with the dinoflagellate cyst studies from the west coast of India (Godhe et al. 2000, D'Costa et al. 2008, D'Silva et al. 2011) indicates that the total number of cyst-forming species (26 phototrophic species and 33 heterotrophic species) is higher along the west coast than the south-east coast (12 phototrophs and 21 heterotrophs). Comparison of the data sets also showed that calcareous cysts of the genera *Scripsiella* reported from the west coast were not observed along the south-east coast in this study, even though their vegetative cells were reported in the planktonic samples (Table 2). However, the occurrence of these cysts has been reported from Visakhapatnam harbour (D'Silva et al. 2013).

The reason for the absence of calcareous cysts in the present sediment samples is not known and needs detailed investigation. Apart from that, cysts of eight potentially harmful dinoflagellate species, i.e. *A. minutum*, *A. tamarense*, *A. cf. tamiyavanichii*, *G. spinifera*, *Gymnodinium catenatum*, *L. polyedrum*, *P. reticulatum*, *Pyrodinium bahamense* var. *compressum* (IOC-UNESCO Taxonomic reference list of harmful micro algae, web: <http://www.marinespecies.org/HAB./dinoflag.php>, accessed 28 June 2013), and two red-tide-forming species, i.e. *A. affine* and *S. trochoidea* (Garate-Lizarraga et al. 2001, Su-Myat & Koike 2013) have been recorded from the surface sediments of the west coast of India (Table 2). Sediment core analyses from the west coast of India have reported the presence of *A. affine*, *A. minutum*, *G. spinifera*, *L. polyedrum*, *P. reticulatum* and *S. trochoidea* since the early 1900s (D'Silva et al. 2012). Incidences of HABs and outbreaks of paralytic shellfish poisoning (PSP) have also occurred along the west coast of India (Godhe et al. 2000). Compared to this, only three potentially toxic yessotoxin (YTX)-producing species *G. spinifera*, *P. reticulatum* and *L. polyedrum* have been reported from the surface sediments of the south-east coast of India. Moreover, the red-tide-forming species *A. affine* and *S. trochoidea*, as well as the potentially PSP producing species *A. minutum* have been reported from Visakhapatnam harbour (D'Silva et al. 2013). Oceanographic features like intensive coastal upwelling and anthropogenic input influence the dinoflagellate cyst composition along the west coast of India (D'Silva et al. 2011). Furthermore, D'Costa et al. (2008) observed the potential of the south-west monsoon to influence the seasonal cycling between planktonic dinoflagellates in the water column and cysts in the sediment.

In view of the influence of the south-west and north-east monsoons along the south-east coast of India, it is possible that the changes brought about by these events could affect the dinoflagellate cyst composition. This needs further elucidation.

5. Conclusion

The present study of the dinoflagellate cyst distribution along the south-east coast of India recorded a southward decrease in cyst abundance that was influenced mainly by sediment texture (a high cyst abundance in silt-clay and a low one in sandy sediments). Fourteen cyst-forming dinoflagellate species including three potentially harmful ones (*G. spinifera*, *P. reticulatum* and *L. polyedrum*), not previously reported in planktonic samples, were recorded for the first time. Cyst abundance along the south-east coast of India is low compared to subtropical and temperate coastal regions, but is similar to that in other tropical regions, including the west coast of India.

Comparatively, the number of potentially harmful cyst-forming species is less than that reported from the west coast.

Acknowledgements

We are grateful to Dr S.R. Shetye, Director, National Institute of Oceanography, Goa for his support. We acknowledge the crew and participants of the CRV *Sagar Sukti* for their valuable assistance. We thank Dr Ravidas Naik, Dr Shamina D'Silva, Mr Vinayak Kulkarni and Mr Rajath Chitari for their help. DDN is grateful to CSIR for being awarded the senior research fellowship (SRF). This is an NIO contribution (No. 5478).

References

- Anderson D.M., Fukuyo Y., Matsuoka K., 1995, *Cyst methodologies*, [in:] *Manual on harmful marine microalgae*, G.M. Hallegraeff, D.M. Anderson & A.D. Cembella (eds.), IOC Manuals and Guides, Vol. 33, UNESCO, Paris, 229–245.
- Anderson D.M., Wall D., 1978, *The potential importance of benthic cysts of Gonyaulax tamarensis and Gonyaulax excavata in initiating toxic dinoflagellate blooms*, J. Phycol., 14 (2), 224–234, <http://dx.doi.org/10.1111/j.1529-8817.1978.tb02452.x>.
- Aydin H., Matsuoka K., Minareci E., 2011, *Distribution of dinoflagellate cysts in recent sediments from Izmir Bay (Aegean Sea, Eastern Mediterranean)*, Mar. Micropaleontol., 80 (1–2), 44–52, <http://dx.doi.org/10.1016/j.marmicro.2011.03.004>.
- Barton A.D., Dutkiewicz S., Flierl G., Bragg J., Follows M.J., 2010, *Patterns of diversity in marine phytoplankton*, Science, 327, 1509–1511, <http://dx.doi.org/10.1126/science.1184961>.
- Boessenkool K. P., Gelder M. V., Brinkhuis H., Troelstra S. R., 2001, *Distribution of organic-walled dinoflagellate cysts in surface sediments from transects across the Polar Front offshore southeast Greenland*, J. Quaternary Sci., 16 (7), 661–666, <http://dx.doi.org/10.1002/jqs.654>.
- Buchanan J.B., 1984, *Sediment analysis*, [in:] *Methods for the study of marine benthos*, N.A. Holme & A.D. McIntyre (eds.), Blackwell Sci. Publ., Oxford, 45–65.
- Dale B., 1983, *Dinoflagellate resting cysts: 'Benthic plankton'*, [in:] *Survival strategies of the algae*, G. A. Fryxell (ed.), Cambridge Univ. Press, Cambridge, 69–136.
- Dale B., 2000, *Dinoflagellate cysts as indicators of cultural eutrophication and industrial pollution in coastal sediments*, [in:] *The application of microfossils to environmental geology*, R.E. Martin (ed.), Kluwer Acad., Plenum Publ., New York, 305–321.
- Dale B., 2001a, *The sedimentary records of dinoflagellate cysts: Looking back into the future of phytoplankton blooms*, Sci. Mar., 65 (2), 257–272.

- Dale B., 2001b, *Marine dinoflagellate cysts as indicators of eutrophication and industrial pollution: A discussion*, *Sci. Total Environ.*, 264 (3), 235–240, [http://dx.doi.org/10.1016/S0048-9697\(00\)00719-1](http://dx.doi.org/10.1016/S0048-9697(00)00719-1).
- D'Costa P. M., Anil A. C., Patil J. S., Hegde S., D'Silva M. S., Chourasia M., 2008, *Dinoflagellates in a mesotrophic, tropical environment influenced by monsoon*, *Estuar. Coast. Shelf Sci.*, 77 (1), 77–90, <http://dx.doi.org/10.1016/j.ecss.2007.09.002>.
- Drake L. A., Meyer A. E., Forsberg R. L., Baier R. E., Doblin M. A., Heinemann S., Johnson W. P., Koch M., Rublee P. A., Dobbs F. C., 2005, *Potential invasion of microorganisms and pathogens via 'interior hull fouling': Biofilms inside ballast-water tanks*, *Biol. Invasions*, 7 (6), 969–982, <http://dx.doi.org/10.1007/s10530-004-3001-8>.
- D'Silva M. S., Anil A. C., D'Costa P. M., 2011, *An overview of dinoflagellate cysts in recent sediments along the west coast of India*, *Indian J. Geo.-Mar. Sci.*, 40 (5), 697–709.
- D'Silva M. S., Anil A. C., Borole D. V., Nath B. N., Singhal R. K., 2012, *Tracking the history of dinoflagellate cyst assemblages in sediments from the west coast of India*, *J. Sea Res.*, 73, 86–100, <http://dx.doi.org/10.1016/j.seares.2012.06.013>.
- D'Silva S. M., Anil A. C., Savant S. S., 2013, *Dinoflagellate cyst assemblages in recent sediments of Visakhapatnam harbour, east coast of India: Influence of environmental characteristics*, *Mar. Pollut. Bull.*, 66 (1–2), 59–72, <http://dx.doi.org/10.1016/j.marpolbul.2012.11.012>.
- Elshaniwany R., Zonneveld K., Ibrahim M. I., Kholeif S. E. A., 2010, *Distribution patterns of recent organic-walled dinoflagellate cysts in relation to environmental parameters in the Mediterranean Sea*, *Palynology*, 34 (2), 233–260, <http://dx.doi.org/10.1080/01916121003711665>.
- Esper O., Zonneveld K. A. F., 2002, *Distribution of organic-walled dinoflagellate cysts in surface sediments of the Southern Ocean (eastern Atlantic sector) between the Subtropical Front and the Weddell Gyre*, *Mar. Micropaleontol.*, 46 (1–2), 177–208, [http://dx.doi.org/10.1016/S0377-8398\(02\)00041-5](http://dx.doi.org/10.1016/S0377-8398(02)00041-5).
- Furio E. F., Azanza R. V., Fukuyo Y., Matsuoka K., 2012, *Review of geographical distribution of dinoflagellate cysts in Southeast Asian coasts*, *Coast. Mar. Sci.*, 35 (1), 20–33.
- Garate-Lizarraga I., Hernandez-Orozco M. L., Band-Schmidt C. J., Serrano-Casillas G., 2001, *Red tides along the coasts of the Baja California Sur, Mexico (1984 to 1999)*, *Oceanides*, 16 (2), 127–134.
- Godhe A., Karunasagar I., Karlson B., 2000, *Dinoflagellate cysts in recent marine sediments from SW India*, *Bot. Mar.*, 43 (1), 39–48, <http://dx.doi.org/10.1515/BOT.2000.004>.
- Godhe A., McQuoid M. R., 2003, *Influence of benthic and pelagic environmental factors on the distribution of dinoflagellate cysts in surface sediments along the Swedish west coast*, *Aquat. Microb. Ecol.*, 32, 185–201, <http://dx.doi.org/10.3354/ame032185>.

- Harland R., Nordberg K., Filipsson H.L., 2006, *Dinoflagellate cysts and hydrographical change in Gullmar Fjord, west coast of Sweden*, *Sci. Total Environ.*, 355(1–3), 204–231, <http://dx.doi.org/10.1016/j.scitotenv.2005.02.030>.
- Head M.J., 1996, *Modern dinoflagellate cysts and their biological affinities*, [in:] *Palynology principles and applications*, J. Janosnius & D.C. McGregor (eds.), AASP Foundation, Dallas, 1197–1248.
- Hesse K.J., Tillmann U., Nehring S., Brockmann U., 1996, *Factors controlling phytoplankton distribution in coastal waters of the German Bight North Sea*, [in:] *Biology and ecology of shallow Coastal waters*, A. Eleftheriou, A.D. Ansell & C.J. Smith (eds.), Olsen and Olsen, Fredensborg, 11–22.
- Holzwarth U., Esper O., Zonneveld K., 2007, *Distribution of organic-walled dinoflagellate cysts in shelf surface sediments of the Benguela upwelling system in relationship to environmental conditions*, *Mar. Micropaleontol.*, 64(1–2), 91–119, <http://dx.doi.org/10.1016/j.marmicro.2007.04.001>.
- Hwang C.-H., Kim K.-Y., Lee Y., Kim C.-H., 2011, *Spatial distribution of dinoflagellate resting cysts in Yellow Sea surface sediments*, *Algae*, 26(1), 41–50, <http://dx.doi.org/10.4490/algae.2011.26.1.041>.
- Joyce L.B., Pitcher G.C., du Randt A., Monteiro P.M.S., 2005, *Dinoflagellate cysts from surface sediments of Saldanha Bay, South Africa: an indication of the potential risk of harmful algal blooms*, *Harmful Algae*, 4(2), 309–318, <http://dx.doi.org/10.1016/j.hal.2004.08.001>.
- Kawamura H., 2004, *Dinoflagellate cyst distribution along a shelf to slope transect of an oligotrophic tropical sea (Sunda Shelf, South China Sea)*, *Phycol. Res.*, 52(4), 355–375, <http://dx.doi.org/10.1111/j.1440-1835.2004.tb00345.x>.
- Madhav V.G., Kondalarao B., 2004, *Distribution of phytoplankton in the coastal waters of east coast of India*, *Indian J. Geo.-Mar. Sci.*, 33(3), 262–268.
- Madhu N.V., Jyothibabu R., Maheswaran P.A., Gerson V.J., Gopalakrishnan T.C., Nair K.K.C., 2006, *Lack of seasonality in phytoplankton standing stock (chlorophyll a) and production in the western Bay of Bengal*, *Cont. Shelf Res.*, 26(16), 1868–1883, <http://dx.doi.org/10.1016/j.csr.2006.06.004>.
- Matsuoka K., Fukuyo Y., 2000, *Technical guide for modern dinoflagellate cyst study*, WESTPAC-HAB/WESTPAC/IOC, Japan Soc. Promotion Sci.
- Matsuoka K., Joyce L.B., Kotani Y., Matsuyama Y., 2003, *Modern dinoflagellate cysts in hypertrophic coastal waters of Tokyo Bay, Japan*, *J. Plankton Res.*, 25(12), 1461–1470, <http://dx.doi.org/10.1093/plankt/fbg111>.
- McMinn A., 1990, *Recent dinoflagellate cyst distribution in eastern Australia*, *Rev. Palaeobot. Palyno.*, 65(1–4), 305–310, [http://dx.doi.org/10.1016/0034-6667\(90\)90080-3](http://dx.doi.org/10.1016/0034-6667(90)90080-3).
- Moestrup Ø., Akselman R., Cronberg G., Elbraechter M., Fraga S., Halim Y., Hansen G., Hoppenrath M., Larsen J., Lundholm N., Nguyen L.N., Zingone A., (eds.), 2009 onwards, *IOC-UNESCO taxonomic reference list of harmful micro algae*, [available online at <http://www.marinespecies.org/HAB>], (accessed on 2013-6-28).

- Montresor M., Zingone A., Sarno D., 1998, *Dinoflagellate cyst production at a coastal Mediterranean site*, J. Plankton Res., 20(12), 2291–2312, <http://dx.doi.org/10.1093/plankt/20.12.2291>.
- Musale A.S., Desai D.V., 2010, *Distribution and abundance of macrobenthic polychaetes along the South Indian coast*, Environ. Monit. Assess., 178(1–4), 423–436, <http://dx.doi.org/10.1007/s10661-010-1701-3>.
- Naidu P.D., Patil J.S., Narale D.D., Anil A.C., 2012, *A first look at the dinoflagellate cysts abundance in the Bay of Bengal: Implications on late quaternary productivity and climate change*, Curr. Sci., 102(3), 495–498.
- Orlova T.Y., Morozova T.V., Gribble K.E., Kulis D.M., Anderson D.M., 2004, *Dinoflagellate cysts in recent marine sediments from the east coast of Russia*, Bot. Mar., 47(3), 184–201, <http://dx.doi.org/10.1515/BOT.2004.019>.
- Persson A., Rosenberg R., 2003, *Impact of grazing and bioturbation of marine benthic deposit feeders on dinoflagellate cysts*, Harmful Algae, 2(1), 43–50, [http://dx.doi.org/10.1016/S1568-9883\(03\)00003-9](http://dx.doi.org/10.1016/S1568-9883(03)00003-9).
- Ribeiro S., Berge T., Lundholm N., Andersen T.J., Abrantes F., Ellegaard M., 2011, *Phytoplankton growth after a century of dormancy illuminates past resilience to catastrophic darkness*, Nat. Commun., 2, 311, <http://dx.doi.org/10.1038/ncomms1314>.
- Satta C.T., Angles S., Garce E., Lugli A., Padedda B.M., Sechi N., 2010, *Dinoflagellate cysts in recent sediments from two semi-enclosed areas of the Western Mediterranean Sea subject to high human impact*, Deep-Sea Res. Pt. II, 57(3–4), 256–267, <http://dx.doi.org/10.1016/j.dsr2.2009.09.013>.
- Shankar D., Vinayachandran P.N., Unnikrishnan A.S., 2002, *The monsoon currents in the north Indian Ocean*, Prog. Oceanogr., 52(1), 63–120, [http://dx.doi.org/10.1016/S0079-6611\(02\)00024-1](http://dx.doi.org/10.1016/S0079-6611(02)00024-1).
- Shetye S.R., Shenoi S.S.C., Gouveia A.D., Michael G.S., Sundar D., Nampoothiri G., 1991, *Wind-driven coastal upwelling along the eastern boundary of Bay of Bengal during southwest monsoon*, Cont. Shelf Res., 11(11), 1397–1408, [http://dx.doi.org/10.1016/0278-4343\(91\)90042-5](http://dx.doi.org/10.1016/0278-4343(91)90042-5).
- Shin H.H., Yoon Y.H., Matsuoka K., 2007, *Modern dinoflagellate cysts distribution off the eastern part of Geoje Island, Korea*, Ocean Sci. J., 42(1), 31–39, <http://dx.doi.org/10.1007/BF03020908>.
- Solignac S., Grosfeld K., Giraudeau J., de Vernal A., 2009, *Distribution of recent dinocyst assemblages in the western Barents Sea*, Norw. J. Geol., 89, 109–119.
- Sonneman J.A., Hill D.R.A., 1997, *A taxonomic survey of cyst-producing dinoflagellates from recent sediments of Victorian coastal waters, Australia*, Bot. Mar., 40(1–6), 149–178.
- Sprangers M., Dammers N., Brinkhuis H., van Weering T.C.E., Lotter A.F., 2004, *Modern organic-walled dinoflagellate cyst distribution offshore NW Iberia, tracing the upwelling system*, Rev. Palaeobot. Palyno., 128(1–2), 97–106, [http://dx.doi.org/10.1016/S0034-6667\(03\)00114-3](http://dx.doi.org/10.1016/S0034-6667(03)00114-3).

- Su-Myat, Koike K., 2013, *A red tide off the Myanmar coast: Morphological and genetic identification of the dinoflagellate composition*, *Harmful Algae*, 27 (7), 149–158, <http://dx.doi.org/10.1016/j.hal.2013.05.010>.
- Targarona J., Warnaar J., Boessenkool K. P., Brinkhuis H., Canals M., 1999, *Recent dinoflagellate cyst distribution in the North Canary Basin, NW Africa*, *Grana*, 38 (2–3), 170–178, <http://dx.doi.org/10.1080/00173139908559225>.
- Tripathy S. C., Kusumakimari B. A. V. L., Sarma V. V., Murty T. V. R., 2005, *Evaluation of trophic state and plankton abundance from the environmental parameters of Visakhapatnam Harbour and near-shore waters, east coast of India*, *Asian J. Microbiol. Biotech. Env. Sc.*, 7 (4), 831–838.
- Vijaykumaran K., 2005, *Productivity parameters in relation to hydrography of the inshore surface waters off Visakhapatnam*, *J. Mar. Biol. Ass. India*, 47 (2), 115–120.
- Wall D., Dale B., 1968, *Modern dinoflagellate cysts and evolution of the Peridiniales*, *Micropaleontology*, 14 (3), 265–304, <http://dx.doi.org/10.2307/1484690>.
- Wang Z. H., Matsuoka K., Qi Y. Z., Chen J. F., Lu S. H., 2004, *Dinoflagellate cyst records in recent sediments from Daya Bay, South China Sea*, *Phycol. Res.*, 52 (4), 396–407, <http://dx.doi.org/10.1111/j.1440-1835.2004.tb00348.x>.
- Zonneveld K. A. F., Versteegh G. J. M., deLange G. J., 1997, *Preservation of organic-walled dinoflagellate cysts in different oxygen regimes: A 10 000 year natural experiment*, *Mar. Micropaleontol.*, 29 (3–4), 393–405, [http://dx.doi.org/10.1016/S0377-8398\(96\)00032-1](http://dx.doi.org/10.1016/S0377-8398(96)00032-1).
- Zonneveld K. A. F., Brummer G. J. A., 2000, *Palaeo-ecological significance, transport and preservation of organic walled dinoflagellate cysts in the Somali Basin, NW Arabian Sea*, *Deep-Sea Res. Pt. II*, 47 (9–11), 2229–2256, [http://dx.doi.org/10.1016/S0967-0645\(00\)00023-0](http://dx.doi.org/10.1016/S0967-0645(00)00023-0).
- Zonneveld K. A. F., Marret F., Versteegh G. J. M., Bogus K., Bouimetarhana I., Crouch E., de Vernal A., Elshaniwany R., Esper O., Forke S., Grøsfjeld K., Henry M., Holzwarth U., Bonnet S., Edwards L., Kieft J.-F., Kim S.-Y., Ladouceur S., Ledu D., Chen L., Limoges A., Lu S.-H., Mahmoud M. S., Marino G., Matsuoka K., Londeix L., Matthiessen J., Mildenhall D. C., Mudie P., Neil H. L., Pospelova V., Qi Y., Radi T., Rochon A., Sangiorgi F., Solignac S., Turon J.-L., Wang Y., Wang Z., Young M., Richerol T., Verleye T., 2013, *Atlas of modern dinoflagellate cyst distribution based on 2405 datapoints*, *Rev. Palaeobot. Palyno.*, 191, 1–198, <http://dx.doi.org/10.1016/j.revpalbo.2012.08.003>.

A first look at the dinoflagellate cysts abundance in the Bay of Bengal: implications on Late Quaternary productivity and climate change

P. Divakar Naidu*, Jagadish S. Patil, Dhiraj D. Narale and A. C. Anil

National Institute of Oceanography (CSIR), Dona Paula, Goa 403 004, India

Abundance and composition of dinoflagellate cysts in a sediment core (SK218/1) from the Bay of Bengal were examined for the last 23 kyr. Cyst abundance at this site varied from 20 to 153 cysts/g dry wt, which is far less than that reported from other oceans. The Holocene harboured higher number of cysts (74–153 cysts/g dry wt) than the last glacial period (up to 67 cysts/g dry wt). Although cyst abundance is low at this site, the cyst composition and its abundance between Holocene and last glacial period reflect the affinity to climate change between these two periods, like other regions. Greater abundance of heterotroph and autotroph cysts and higher species diversity were noticed during Holocene than in the last glacial period, which supports earlier observations depicting higher productivity during the Holocene than in the last glacial period in the southwest monsoon-influenced regions of the Indian Ocean.

Keywords: Climate change, Cyst abundance and composition, dinoflagellates, geological past.

DINOFLAGELLATES are one of the principal groups of marine phytoplankton which has a life cycle that includes a cyst stage in most of the species. Several researchers have shown that the distribution of dinoflagellate cysts corresponds with the physical characteristics of overlying water masses¹. Hence cysts have been used for reconstruction of paleoenvironmental conditions, such as productivity variations in the Santa Barbara Basin sea level², nutrient changes in the South China Sea³ and palaeoecological and palaeoclimatological conditions in the Mediterranean Sea⁴. The spatial distribution of dinoflagellate cysts has been used to interpret the local environmental conditions and the role of seasonal upwelling intensity on cyst export to the underlying sediments in the Gulf of Alaska⁵. Furthermore, dinoflagellate cyst abundance was also used in quantitative reconstruction of the sea surface temperature (SST) using modern analogue techniques in the Gulf of Alaska^{6,7}. Thus, dinoflagellate cysts are a reliable proxy to reconstruct the paleoceanographic changes in the geological past.

Though cyst abundance studies have been carried out in the Arabian Sea using sediment traps⁸ and in sediment

cores^{9–11}, so far no study has attempted an analysis of cyst abundance in the sediment traps or in the sediment cores from the Bay of Bengal. This study reports cyst assemblage in a sediment core that depicts Holocene and the last glacial period in the Bay of Bengal.

The northern Indian Ocean has two different surface water masses. A low-salinity water mass is formed in the Bay of Bengal by excess precipitation and abundant river run-off. A high-salinity water mass is formed in the Arabian Sea. Although both the Arabian Sea and the Bay of Bengal are highly influenced by monsoon reversals, the hydrography and biology differ widely. In most oceanic areas variations in temperature are large compared to salinity, but in the Bay of Bengal temperature gradient throughout the year is less compared to salinity¹². During the SW monsoon high precipitation in the Bay of Bengal and freshwater discharge from the Ganges, Brahmaputra, Irrawadi and Godavari lead to strong stratification preventing the entrainment of nutrients into the surface waters all through the year, resulting in low primary productivity. Biological features such as chlorophyll, primary productivity, phytoplankton abundance and mesozooplankton are lower in the Bay of Bengal compared to the Arabian Sea¹³. The prevalence of stratified and oligotrophic conditions in the Bay of Bengal almost throughout the year is among the causative factors that facilitate the preponderance of diazotrophs¹⁴. However, information regarding the extent to which the nitrogen fixed by diazotrophs in supporting primary production is not yet available for the Bay of Bengal.

Core SK218/1 was collected at a water depth of 3000 m from the Bay of Bengal (Figure 1). The chronology of the core was established using AMS carbon-14

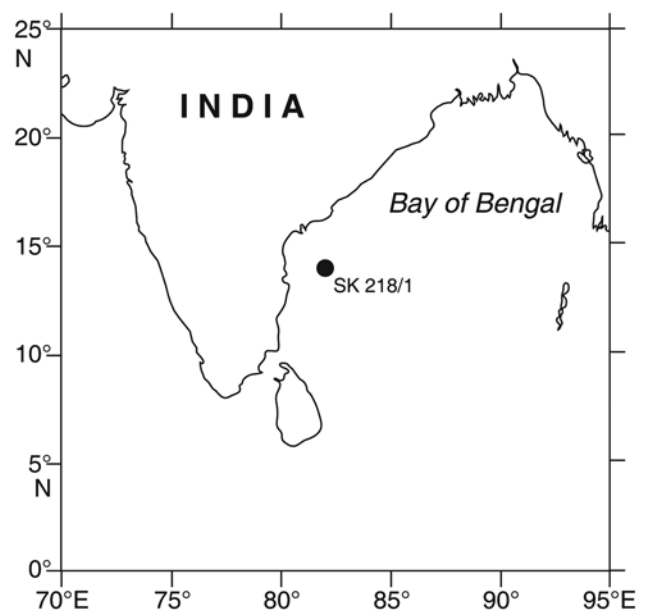


Figure 1. Location of the core in the Bay of Bengal.

*For correspondence. (e-mail: divakar@nio.org)

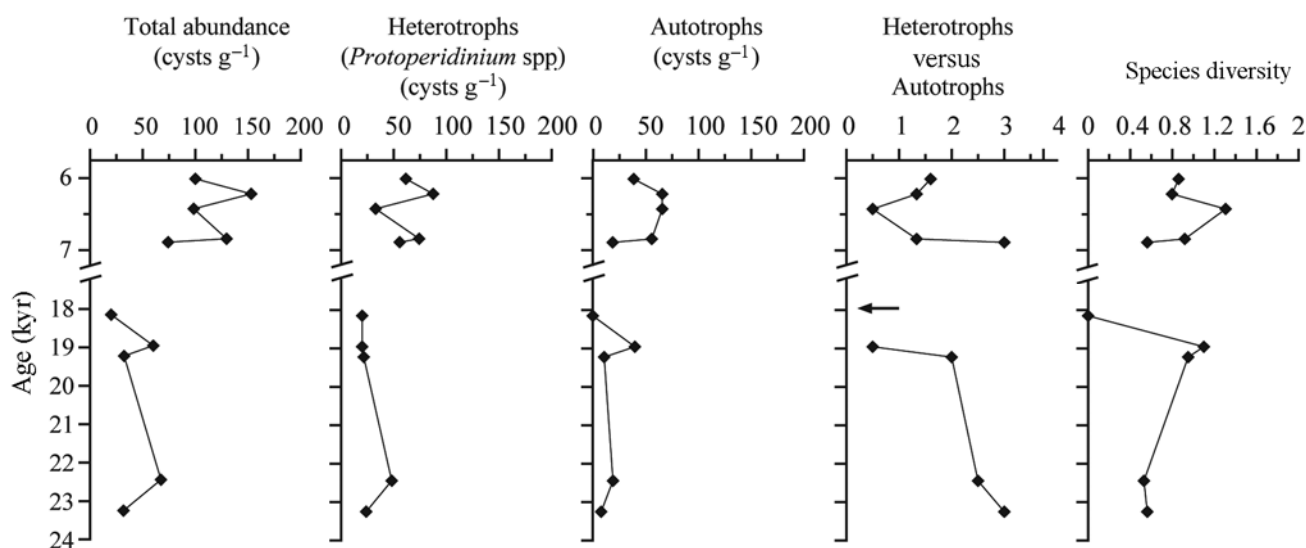


Figure 2. Fluctuations of total dinoflagellates, heterotrophs, autotrophs, ratios of heterotrophs and autotrophs, and species diversity.

dates¹⁵. Five samples from the Holocene covering a time-span from 6 to 6.89 kyr and five samples from last glacial period from 18 to 23 kyr were processed for the study of dinoflagellate cysts using palynological technique^{16,17}, with some modification⁹. A known weight of the sediment was repeatedly washed with distilled water to remove salts followed by acid treatment, i.e. HCL (10%) and HF (30%) to dissolve calcareous and silicate materials. Each chemically treated sample was washed with distilled water to remove the acid and then placed in a 10 ml beaker with distilled water to make a slurry. Later, the slurry was sieved through a tier of two different meshes (120 and 20 μm) to remove coarse and fine materials. The residue accumulated on the 20 μm mesh was then suspended in 10 ml distilled water and kept in a vial. For observation, a 0.5–1.0 ml aliquot of the processed sample was used. Observations were carried out under an inverted microscope (Olympus IX 71) at 100 and 400 \times magnification. Dinoflagellate cysts were identified based on published literature^{4,18–21} and cysts abundance was estimated per gram dry weight sediment (cysts/g dry wt). The abundance of dinoflagellate cyst was further used to calculate species diversity (Shannon–Weaver diversity index, i.e. H') using the software PIMER (version 5).

In core SK218/1 autotrophic and heterotrophic forms of dinoflagellate cysts were present during the last glacial period and the Holocene. Heterotrophic forms were dominant during both the periods (Figure 2 and Table 1). High abundance of cysts was observed during the Holocene compared to the last glacial period (Figure 2), and this difference in the distribution of cysts was significant between both the periods (t test: $df=20$, $P \leq 0.003$, $n = 11$). This is also evident from the t test, which shows a significant difference in the distribution of autotrophic

(t test: $df=8$, $P \leq 0.019$, $n = 5$) and heterotrophic cysts (t test: $df=8$, $P \leq 0.01$, $n = 5$) between the last glacial period and the Holocene. Species diversity was higher during the Holocene than the last glacial period at this site (Figure 2).

In the present study a total of 19 dinoflagellate cysts belonging to autotrophs (five species) and heterotrophs (14 species) have been reported and presented along with their palynological and modern names (thecate dinoflagellate) in Table 1. Autotrophic cyst assemblages are represented by four Gonyaulacoid (*Spiniferites*, *Polysphaeridium*, *Lingulodinium*, *Operculodinium*) species and *Tuberculodinium vancampoeae* (*Pyrophacus steinii*), whereas heterotrophs are represented by the cysts belonging to genera *Proto-peridinium* with the following palynological names: *Brigantedinium*, *Selenopemphix*, *Votadinium*, *Stelladinium*, *Quinquecuspis*, *Trinovantedinium* and *Lejeunecysta*. Among the autotrophs, *Spiniferites* cysts were dominant in both the Holocene and the last glacial period. The abundance of *Spiniferites* cysts, however, was high during the Holocene compared to the last glacial period. Cysts of autotrophic dinoflagellates *Polysphaeridium* and *Tuberculodinium* were found only in the Holocene, whereas cysts of *Lingulodinium* were encountered only in the samples representing the last glacial period (Table 1). Ratio of heterotrophs to autotrophs showed a slight decrease in the Holocene (1.3) compared to the last glacial period (1.7; Figure 2).

Abundance of dinoflagellate cysts varied from 20 to 158 cysts/g dry wt sediment (Figure 2). The abundance observed in this site is comparatively lower than that observed in other regions, for example, the Santa Barbara Basin², South China Sea³, Black Sea²² and Arabian Sea^{8,11}. This raises a doubt on whether the cysts represent

Table 1. Dinoflagellate cysts and their abundance (cysts g⁻¹ dry wt) documented in core SK218/1 in the Bay of Bengal

Palaeontological name	Modern name	Holocene (kyr)					Glacial (kyr)				
		6.0	6.2	6.4	6.8	6.9	18.2	19.0	19.2	22.4	23.3
Autotrophic											
<i>Spiniferites</i> spp.	<i>Gonyaulax</i> spp.	31	60	33	46	0	0	20	5	0	8
<i>Polysphaeridium zoharyi</i>	<i>Pyrodinium bahamense</i>	8	0	0	0	19	0	0	0	0	0
<i>Lingulodinium machaerophorum</i>	<i>Lingulodinium polyedrum</i>	0	0	0	0	0	0	20	0	0	0
<i>Operculodinium centrocarpum</i>	<i>Protoceratium reticulatum</i>	0	5	16	9	0	0	0	0	19	0
<i>Tuberculodinium vancampoeae</i>	<i>Pyrophacus steinii</i>	0	0	16	0	0	0	0	0	0	0
Heterotrophic											
<i>Trinovantedinium applanatum</i>	<i>Peridinium</i> sp. cf. <i>P. pentagonum</i>	0	0	0	0	9	0	0	0	10	0
<i>Stelladinium robustum</i>	<i>P. sp. (Stelladinium robustum)</i>	8	0	0	0	0	0	0	0	0	0
	<i>Protoperidinium</i> sp. <i>Type 1</i>	38	11	8	0	9	10	0	0	19	8
	<i>P. sp. Type 4</i>	0	5	0	19	0	0	0	0	0	0
<i>Brigantedinium cariacensis</i>	<i>P. sp. (P. avellanum)</i>	0	0	8	28	0	0	0	8	0	0
<i>Stelladinium stellatum</i>	<i>P. compressum</i>	0	0	0	0	0	0	10	0	0	0
<i>Quinquecuspidata concreta</i>	<i>P. leonis</i>	0	22	8	19	9	0	0	8	0	8
	<i>P. thrianum</i>	0	0	8	0	0	0	0	0	10	0
<i>Lejeunecysta concreta</i>	<i>P. sp. (Lejeunecysta concreta)</i>	8	0	0	0	0	0	0	0	0	0
<i>Selenopemphix nephroides</i>	<i>P. subinermis</i>	8	27	0	9	9	10	10	0	10	8
<i>S. quanta</i>	<i>P. conicum</i>	0	5	0	0	9	0	0	0	0	0
<i>S. quanta</i>	<i>P. nudum</i>	0	5	0	0	0	0	0	0	0	0
<i>Votadinium spinosum</i>	<i>P. claudicans</i>	0	0	0	0	9	0	0	8	0	0
<i>V. calvum</i>	<i>P. oblongum</i>	0	11	0	0	0	0	0	0	0	0

genuine signals of export productivity or an artifact of poor cyst preservation caused due to well-oxidized conditions in the sediment water interface. However, no visible cyst degradation was noticed in samples from both the Holocene and the last glacial period. Moreover, the maximum cyst density observed in recent sediments along the west coast of India is also low compared to the other regions⁹. Hence we presume that cyst preservation changes might not have contributed to less abundance of cysts at this site. Further, greater abundance of dinoflagellate cysts was reported from the sediment traps and sediment cores in the Arabian Sea from the regions of upwelling^{8,11}. Therefore, the most possible reason for the less abundance of cysts at this site in Bay of Bengal could be due to: (i) low salinity and freshwater influx due to river discharge into the Bay of Bengal and the changes brought in by these events (reduced light availability due to cloud cover and increased turbidity); (ii) the present studied core location is not influenced by upwelling, and (iii) the seasonal SST changes are not significant as seen in the temperate regions. Therefore, the less abundance of dinoflagellate cysts is attributable to the lower productivity in the present studied location. Even though abundance was less, the cyst composition and variation in abundance between the Holocene and the last glacial period indicate the similar climatic changes in the past, as observed elsewhere.

The Bay of Bengal was 4°C warmer during the Holocene than in the last glacial period¹⁵, the warmer SST during the Holocene may have been congenial for the

thriving of dinoflagellates in this region (corresponds to higher cyst abundance). Similarly, in the Santa Barbara Basin also greater abundance of cysts was noticed during the Holocene than in the last glacial period². In addition, the lower ratio of heterotrophs to autotrophs during the Holocene than in the last glacial period lends support to the distinct SST difference between these two periods. This encourages us to suggest that the ratio of autotroph and heterotroph cysts can be used as a proxy of sea-water temperature in the Bay of Bengal, as lower ratios correspond to warm temperature and vice versa. Cysts of autotrophic dinoflagellates *Polysphaeridium* and *Tuberculodinium* were found only in the Holocene, whereas cysts of *Lingulodinium* were encountered only in the samples representing the last glacial period. This reveals genera preference and/or sensitivity to temperature changes.

Various proxies have been used to determine palaeo-productivity in different regions of the Oceans. For example, the number planktonic foraminiferal species has been identified as an indicator of productivity²³. Similarly, the fluxes of organic matter, opal, calcium carbonate and benthic foraminifera have been used extensively to study the palaeo-productivity of the ocean basins²⁴.

Sediment trap experiments have demonstrated that the biological productivity and foraminiferal flux and terrigenous supply in the Arabian Sea are strongly linked to the intensity of the SW monsoon²⁵. It is generally understood that the summer monsoon was stronger during the interglacials than in the glacial²³. Detailed studies have

been carried out in the Arabian Sea to understand the influence of monsoon on the biological productivity and terrigenous supply during the Late Quaternary^{26–29}. However, the debate regarding whether productivity in the Arabian Sea was higher during the Holocene or in the last glacial period is ongoing.

Earlier findings from the eastern³⁰ and western Arabian Sea^{26,31} also revealed high productivity during interglacials as a result of strong SW monsoon, and low productivity during glacials due to weak SW monsoon. On the contrary, based on the accumulation rates of organic carbon and alkenones, it was suggested that high productivity during the Last Glacial Maximum than in the Holocene was driven by strong NE monsoons³². It is argued here that if the strong NE monsoon had influenced the productivity changes along the eastern Arabian Sea, one would expect high productivity in the Bay of Bengal, because the NE monsoon activity is much stronger in the Bay of Bengal than in the eastern Arabian Sea.

The influence of SW monsoon on the community structure of dinoflagellates has been highlighted based on the recent sediment studies from the west coast of India⁹. Abundance of *Protoperidinium* has been used a proxy in the Arabian Sea¹¹ and in Santa Barbara Basin². Thus, we use the same proxy to discuss the productivity changes in the Bay of Bengal. In this study higher abundance of *Protoperidinium* was documented during the Holocene than in the last glacial period (Figure 2), reflecting higher productivity during the former period. This in turn supports the growing body of evidence that the strong SW monsoon during the Holocene fuelled productivity in the Bay of Bengal and vice versa during the last glacial period. Consequently, weak SW monsoon during last glacial period resulted in less productivity. Though the NE monsoon was stronger during the last glacial period³³, productivity was relatively lower than in the Holocene, which suggests that overall the SW monsoon has a strong bearing on the productivity of the northern Indian Ocean in general and the Arabian Sea and Bay of Bengal in particular.

The study of dinoflagellate cyst abundance in the Bay of Bengal reveals lowest cyst abundance (20–153 cysts/g dry wt) compared to the other regions. The changes in composition of both autotroph and heterotroph cyst assemblages exhibited clear distinction between the Holocene and the last glacial period at this site. Higher abundance of dinoflagellate cysts, their diversity and the dominance of heterotroph and autotroph cysts during the Holocene than in the last glacial period indicate that productivity was higher during the Holocene than in last glacial period in the Bay of Bengal.

1. Rochon, A., de Vernal, A., Turon, J. L., Matthiessen, J. and Head, J., Distribution of recent dinoflagellate cysts in surface sediments from the North Atlantic Ocean and adjacent seas in relation to sea surface parameters. *American Association of Stratigraphic Palynologists Ser.* 35, 1999, p. 150.

2. Pospelova, V., Pedersen, T. and de Vernal, A., Dinoflagellate cysts as indicators of climatic and oceanographic changes during the past 40 kyr in the Santa Barbara Basin. *Paleoceanography*, 2006, **21**, PA2010 (1–16); doi:10.1029/2005PA001251.
3. Shaozhi, M. and Harland, R., Quaternary organic-walled dinoflagellate cysts from the south China Sea and their paleoclimatic significance. *Palynology*, 1993, **17**, 47–65.
4. Zonneveld, K. A. F. and Brummer, G. A., Paleoclimatic and palaeo-ecological changes during the last deglaciation in the Eastern Mediterranean – implication for dinoflagellate ecology. *Rev. Palaeobot. Palynol.*, 1995, **84**, 221–253.
5. Radi, T. and de Vernal, A., Dinocyst distribution in surface sediments from the northeastern Pacific margin (40–60°N) in relation to hydrographic conditions, productivity and upwelling. *Rev. Palaeobot. Palynol.*, 2004, **128**, 163–193.
6. de Vernal, A. and Pedersen, T. F., Micropaleontology and palynology of core PAR87A-10: a 23000 year record of paleoenvironmental North Pacific. *Paleoceanography*, 1997, **12**, 821–830.
7. Marret, F., de Vernal, A., McDonald, D. and Pederson, T., Middle Pleistocene to Holocene palynostratigraphy of ODP Site 887 in the Gulf of Alaska, northeast North Pacific. *Can. J. Earth Sci.*, 2001, **38**, 373–386.
8. Zonneveld, K. A. F. and Brummer, G. A., Ecological significance, transport and preservation of organic walled dinoflagellate cysts in the Somali Basin, NW Arabian Sea. *Deep Sea Res. II*, 2000, **47**, 2229–2256.
9. D’Costa, P. M., Anil, A. C., Patil, J. S., Hegde, S., D’Silva, M. S. and Chourasia, M., Dinoflagellates in a mesotrophic, tropical environment influenced by monsoon. *Estuar. Coastal Shelf Sci.*, 2008, **77**, 77–90.
10. Godhe, A., Karunasagar, I., Karunasagar, I. and Karlson, B., Dinoflagellate cysts in recent marine sediments from SW India. *Bot. Mar.*, 2000, **43**, 39–48.
11. Reichart, G. J. and Brinkhuis, H., Late Quaternary *Protoperidinium* cysts as indicators of paleoproductivity in the northern Arabian Sea. *Mar. Micropaleontol.*, 2003, **49**, 303–315.
12. Wyrki, K., Physical oceanography of the Indian Ocean. In *The Biology of the Indian Ocean* (ed. Zeitzschel, B.), Springer, New York, 1973, pp. 18–36.
13. Gauns, M., Madhupratapa, M., Ramaiah, N., Jyothibabu, R., Fernandes, V., Paul, J. T. and Prasanna Kumar, S., Comparative accounts of biological productivity characteristics and estimates of carbon fluxes in the Arabian Sea and the Bay of Bengal. *Deep-Sea Res. II*, 2005, **52**, 2003–2017.
14. Hegde, S., Anil, A. C., Patil, J. S., Mitbavkar, S., Krishnamurthy, V. and Gopalakrishna, V. V., Influence of environmental settings on the prevalence of *Trichodesmium* spp. in the Bay of Bengal. *Mar. Ecol. Prog. Ser.*, 2008, **356**, 93–101.
15. Naidu, P. D. and Govil, P., New evidence on the sequence of deglacial warming in the tropical Indian Ocean. *J. Quaternary Sci.*, 2010, **25**, 1138–1143.
16. Matsuoka, K., Fukuyo, Y. and Anderson, D. M., Method for modern dinoflagellate cyst studies. In *Red Tides: Biology, Environmental Science, and Toxicology* (eds Okaichi, T., Anderson, D. M. and Nemoto, K.), Elsevier, Now York, 1989, pp. 461–479.
17. Matsuoka, K. and Fukuyo, Y., *Technical Guide for Modern Dinoflagellate Cyst Study*, WESTPAC-HAB/WESTPAC/IOC, Japan Society for the Promotion of Science, Japan, 2000, pp. 1–29.
18. Marret, F., Mudie, P., Aksu, A., Richard, N. and Hiscott, R. N., A Holocene dinocyst record of a two-step transformation of the Neoeuxinian brackish water lake into the Black Sea. *Quaternary Int.*, 2009, **197**, 72–86.
19. Sonneman, J. A. and Hill, D. R. A., A taxonomic survey of cyst-producing dinoflagellates from recent sediments of Victorian coastal waters, Australia. *Bot. Mar.*, 1997, **40**, 149–177.
20. Wall, D. and Dale, B., Modern dinoflagellate cysts and evolution of the Peridinales. *Micropaleontology*, 1968, **14**, 265–304.

21. Harland, R., Nordberg, K. and Filipsson, H. L., A high-resolution dinoflagellate cyst record from latest Holocene sediments in Koljö Fjord, Sweden. *Rev. Palaeobot. Palynol.*, 2004, **128**, 119–141.
22. Mudie, P. J., Rochon, A., Aksu, A. E. and Gillespie, H., Dinoflagellate cyst, freshwater algae and faunal spores as salinity indicators in late Quaternary cores from Marmara and Black seas. *Mar. Geol.*, 2002, **190**, 203–231.
23. Prell, W. L., Murray, D. W., Clemens, S. C. and Anderson, D. M., Evolution and variability of the Indian Ocean summer monsoon: evidence from western Arabian Sea drilling program. *Geophys. Monogr.*, 1992, **70**, 447–469.
24. Herguera, J. C. and Berger, W. H., Paleoproductivity from benthic foraminifera abundance: glacial to post glacial changes in the west-equatorial Pacific. *Geology*, 1991, **19**, 1173–1176.
25. Curry, W. B., Ostermann, D. R., Guptha, M. V. S. and Ittekkot, V., Foraminiferal production and monsoonal upwelling in the Arabian Sea: evidence from sediment traps. In *Upwelling Systems: Evolution Since the Early Miocene* (eds Summerhayes, C. P., Prell, W. L. and Emies, K. C.), Geological Society of Special Publication, Geological Society, London, 1992, pp. 93–106.
26. Murray, D. W. and Prell, W. L., Late Pliocene and Pleistocene oscillations and monsoon upwelling recorded in sediments from the Owen Ridge, northwestern Arabian Sea. In *Upwelling Systems: Evolution Since the Early Miocene* (eds Summerhayes, C. P., Prell, W. L. and Emies, K. C.), Geological Society of Special Publication 64, Geological Society, London, 1992, pp. 301–321.
27. Naidu, P. D., Glacial to interglacial contrasts in the calcium carbonate content and influence of Indus discharge in two eastern Arabian sea cores. *Palaeogeogr., Palaeoclimatol., Palaeoecol.*, 1991, **86**, 255–263.
28. Naidu, P. D., Malmgren, B. A. and Bornmalm, L., Quaternary history of calcium carbonate fluctuations in the western equatorial Indian Ocean (Somali Basin). *Palaeogeogr., Palaeoclimatol., Palaeoecol.*, 1993, **103**, 21–30.
29. Bhusan, R., Dutta, K. and Somayajulu, B. L. K., Concentrations and burial fluxes of organic and inorganic carbon on the eastern margins of the Arabian Sea. *Mar. Geol.*, 2001, **178**, 95–113.
30. Pattan, J. N., Masuzawa, T., Naidu, P. D., Parthiban, G. and Yamamoto, M., Productivity fluctuations in the southeastern Arabian Sea during the last 140 ka. *Palaeogeogr., Palaeoclimatol., Palaeoecol.*, 2003, **193**, 575–590.
31. Naidu, P. D. and Malmgren, B. A., A high-resolution record of late Quaternary upwelling along the Oman Margin, Arabian Sea based on planktonic foraminifera. *Paleoceanography*, 1996, **11**, 129–140.
32. Rostek, F., Bard, E., Beaufort, L., Sonzogni, C. and Ganssen, G., Sea surface temperature and productivity records for the past 240 kyr in the Arabian Sea. *Deep Sea Res. II*, 1997, **44**, 1461–1480.
33. Duplessy, J. C., Glacial to interglacial contrast in the northern Indian Ocean. *Nature*, 1982, **295**, 494–498.

ACKNOWLEDGEMENTS. We thank Dr Shetye, Director, National Institute of Oceanography, Goa for providing the necessary facilities and encouragement, and the anonymous reviewer for constructive comments. This work is financially supported by ISRO-GBP and Ministry of Earth Sciences, Government of India. This is National Institute of Oceanography Contribution No. 5107.

Received 6 June 2011; revised accepted 22 December 2011

Correction

Historical and future seismicity near Jaitapur, India

Roger Bilham and Vinod K. Gaur

[[Curr. Sci.](#), 2011, **101**, 1275–1281]

On page 1275, para 2, line 24, we inadvertently summarize our findings as:

‘Indeed Jaitapur has frequently experienced intensity VII shaking from such earthquakes.’

The sentence should read as:

‘Indeed, Jaitapur has frequently experienced intensity V and occasional intensity VI shaking from such earthquakes.’

